SELF-ACTION EFFECTS OF LASER BEAMS IN NONLINEAR MEDIA AND THEIR EFFECTS ON THz AND HIGHER HARMONIC GENERATION

Thesis Submitted For the Award of the Degree of

DOCTOR OF PHILOSOPHY

in

PHYSICS

by

SANDEEP KUMAR

(Registration Number: 11720099)

Supervised By

DR. NAVEEN GUPTA

LOVELY PROFESSIONAL UNIVERSITY
PUNJAB
2022

Declaration

I hereby declare that the thesis entitled "**Self-Action Effects of Laser Beams in Nonlinear Media and their Effects on THz and Higher Harmonic Generation"** being submitted to the Lovely Professional University, Phagwara (Punjab) in the fulfillment of the requirement for the award of the degree of **DOCTOR OF PHILOSOPHY** in physics is the original research work of mine and has not formed the basis for the award of any degree, diploma or any other title or recognition previously.

(Sandeep Kumar)

Date:

Place:Lovely Professional University,

Phagwara (Punjab)

CERTIFICATE

This is to certify that the thesis entitled **" Self-Action Effects of Laser Beams in Nonlinear Media and their Effects on THz and Higher Harmonic Generation"** being submitted by ***Mr.Sandeep Kumar*** to the ***Lovely Professional University***, **Phagwara (Punjab)** is worthy of consideration for the award of the degree of ***Doctor of Philosophy*** and is a record of bonafide research work carried out by him under my guidance and supervision and that the results contained in it have not been submitted in part or full to any other university or institute for award of any degree/diploma.

I certify that he has pursued the prescribed course of research. I approve the thesis for the award of the aforesaid degree.

Date m

Dr. Naveen Gupta
(Supervisor)
Department of Physics
Lovely Professional University
Phagwara, Punjab-144001

Abstract

This thesis focuses on nonlinear dynamics of different laser beams (q-Gaussian, Cosh-Gaussian (ChG), Quadruple-Gaussian (Q.G.) laser beams) in different nonlinear media such as plasmas and narrow band gap semiconductors. Further, the impacts of self-action effects that are self focusing, self defocusing, self trapping, self phase modulation etc. have been studied on higher harmonics and THz generation. Additionally, a scheme of THz generation by self focused surface plasma wave (SPW) at free space-semiconductor interface is developed in this thesis.

The nonlinear propagation of laser beams in different plasmas and narrow band gap semiconductors has been investigated analytically and numerically. Among different semi-analytical approaches, variational approach has been opted to study the propagation of laser beams in nonlinear media under nonlinear regime. The nonlinear propagation of elliptical q-Gaussian laser beam in plasma with ramp density is affected by deviation parameter $'q'$ and ellipticity of the laser beam. It has been observed that self focusing for $q = 3$ is maximum, whereas the self focusing is decreased along the transverse direction along which the beam is more elliptic. In the case of Cosh-Gaussian laser beam, it has been found in collisional plasma that the uniform irradiance over cross section of laser beam helps to increase the efficiency of laser plasma coupling. It is observed that for $b = 1$, the beam width is minimum because beam get equal contribution from off-axial rays. Whereas, the nonlinear characteristics of Q.G. laser beam have been observed in relativistic plasma. The comparisons between linear and nonlinear propagation of Q.G. and Gaussian laser beam have been made. It has been investigated that the extent of self focusing is enhanced at $\frac{x_0}{r_0} = 1.5$ for Q.G. laser beam as compare to the Gaussian laser beam.

In this work, theoretical model has been developed for the generation of sub-millimeter radiations in relativistic plasma and narrow band gap semiconductor. It has been derived on the basis of beating of two laser beams. It has been observed that yield of resonant THz radiations is affected significantly by cross focusing of q-Gaussian laser beams. As the q value is increased that means q-Gaussian laser beam shifts towards

Gaussian distribution, the cross focusing is decreased. In this case, the contribution of off-axial rays is obviated, the intensity of the pump laser beam is decreased, and therefore yield of the generation of THz radiation is decreased. The off-axial rays helps to enhance the intensity of laser beam which further increases the yield of THz radiation. A special treatment for generation of THz radiations by surface plasma wave (SPW) and filamentation of laser beam has been incorporated theoretically and numerically.

In addition, the generation of second harmonics of q-Gaussian and Q.G. laser beams has been developed in collisional plasma with upward density ramp. It has been found that the conversion efficiency of SHG is enhanced where the beam width is minimum. The density ramp of plasma is utilized to increase the density of plasma along the propagation direction. On propagation of two laser beams, the nonlinearity of the plasma is increased which increases the cross focusing of laser beam. In the results of which the yield of SHG is enhanced.

Dedication

Every challenging work need self-efforts as well as guidance of elders

those who were very close to our heart .

My humble effort I dedicate to my Lovely and caring

Mother (Mrs. Bimla Devi)

And

Father (Mr. Gurpal Singh)

Along with hard working and respected

Teachers

Acknowledgment

I wouldn't miss this opportunity to thank those special people of my life who have brought best out of me and helped me directly or indirectly to pursue and complete this degree awarded in physics.

First and foremost, I would like to express my gratitude and thanks to my research supervisor and mentor ***Dr. Naveen Gupta*** *for his irreplaceable guidance, care, consistent encouragement, critical review through this work. His mastery of scientific questioning, imaginations, interpretations and suggestions enhanced my cognitive awareness and have helped remarkably in the fulfillment of my proposed objectives. My sincere thanks are due to his unconditional help and keen observations throughout my degree. I am unable to measure and express the support and care that I have received from him. His devotion towards research and teaching has always inspired me a lot.*

*From the bottom of my heart, I thank my family for all their unlimited love and remarkable support of my pursuit of a scientific career even, I had initiated after six years of my master's degree. They had encouraged me to follow my passion. Especially, this thesis is for the lovely memories of my elder brother (****Mr. Avtar Singh****), who was so proud of his brother. My siblings* ***Mrs. Amarjeet Kaur, Mrs. Balvir Kaur*** *and* ***Mr. Gurdial Singh*** *had become my backbone during these years. I value their faith and patience for such a long period. The love and affection, faith, sacrifices of my all family members always strengthen me.*

I would like to express my sincere thanks to organizing committees of ***DST-SERB school*** *(India) and* ***15th Kudowa School*** *(Poland) who considered me as a part of their schools. I am thankful to all the professors of these schools for the unforgettable experiences that I have learnt from them. I would like to mention here that Dr. Ajit Upadhya (RRCAT, Indore) and Dr. Ewa Pawelec (Opole University, Poland) has a great impacts on my research work. It's my pleasure to thank* ***department of physics*** *and* ***Department of research and development of Lovely Professional University*** *for their general support due to which I had participated in conference/workshop/summer school nationally/internationally. Consequently, among these scientific programs I have been*

*awarded by **best young scientist, excellent talk and best poster awards**. Especially, I am grateful to Dr. Kailash Chandra Juglan, Dr. Niti Kant,,Dr. Mukesh Kumar, Dr. Rekha, Dr. Ramesh Thakur, Mr. Parshant kumar, Ms. Harpreet Kaur for their invaluable support and encouragement during these years.*

*I think this is the time where I could mention my sincere thanks to my postgraduate/graduate/school teachers who had made my base strong and ignite the spark for doctorate degree. From postgraduate university (**NIT Jalandhar**), Dr. Harleen Dhahiya, Dr. H.M.Mittle, Dr. Arvinder Singh, Dr. Rohit Mehra are the eminent teachers whose impacts had directed me for Ph.D degree. From my graduate college (**ASSM College, GNDU Regional Campus**), Mr. Manjit Singh and Dr. Sangeeta are the teachers who have created my power of imaginations in physics and mathematics respectively. I would like to convey my special thanks to my school teachers Mr. Bakhtabar Singh, Mr. Harblass Singh, and Mrs. Jagdish Kaur for making my base strong due to which I am able to survive in education field.*

*It is my pleasure to acknowledge my companion Mr. Aman Sharma, Ms. Divya Bhagat, Mrs. Pallavi Sharma, Ms. Durdana Sadaf, Mr. Karan Singh Maan, Ms. Manpreet Kaur Somal, Ms. Shaista Manzoor, Ms. Ruby Angurana, Ms. Vaidehi Katoch, Ms. Agrataben Vadhel and Mr. Dipesh Dalal for their immeasurable support during this period. All my friends have also patiently answered many questions which I raised. I thank in particular Dr. Syed Mufassir and Ms. Shaista Manzoor for his generous help in computer software and many useful discussions for thesis writing. Among my friends, **Mr.Aman Kumar, Ms.Divya Bhagat** and **Mrs. Pallavi Sharma** have always supported me emotionally in my rough time and I owe them a deep sense of gratitude.*

Debts being various, are not easy to remember, hence I convey my heartiest thanks to all those who helped me or blessed me in making this milestone. I deeply regret here for not mentioning these individuals.

Date:15/04/2022 ***Sandeep Kumar***

Preface

The present thesis focuses especially on the self-action effects of laser beams, THz generation, and higher harmonics generation in plasmas and narrow band gap semiconductors. The present work has been divided into twelve. Mostly, emphasis is given to investigating the effects of self-focusing on THz and second harmonics generation.

In particular, **chapter 3 to chapter 6** incorporate the different self-action effects of different laser beams in different plasmas. C**hapter 3** involves the description of the amplitude structures of q-Gaussian, cosh-Gaussian, and quadruple-Gaussian laser beams. In this chapter, different parameters of the laser beam have been described in detail which are useful for the next chapters. In **chapter 4**, emphasis is put on investigating the dynamics of beam width and axial phase of elliptical q-Gaussian laser beams using variational theory. The differential equations so obtained have been solved numerically to envision the effect of laser-plasma parameters on the propagation dynamics of the laser beam. **Chapter 5** includes the investigation of self focusing phenomenon of cosh-Gaussian laser beams in underdense plasmas. The effect of nonlinear absorption of laser energy in plasma also has been incorporated. The formulation is based on finding a semi-analytical solution of the nonlinear Schrodinger wave equation for the slowly varying beam envelope. In **chapter 6**, a theoretical investigation on linear and nonlinear propagation characteristics of a new class of laser beams known as multi Gaussian (M.G) laser beams have been presented. The optical nonlinearity of the plasma has been modeled by relativistic mass nonlinearity of the plasma electrons in the field of laser beam which causes self focusing.

In this thesis **chapter 7** and **chapter 8** is about the methods for the generation of THz radiation by q-Gaussian laser beam. **Chapter 7** incorporates a method of generation of coherent terahertz (THz) radiations by nonlinear interaction of a pair of coaxial q-Gaussian laser beams with underdense plasma. It explains the production of nonlinear current density due to propagation of two laser beams acts as the source of THz radiation. In **chapter 8** is a theoretical investigation on THz generation by filmentation of two q-Gaussian laser beams in narrow band gap semiconductors. The nonlinear dynamics of both beams have been studied by solving the nonlinear Schrodinger wave equation with

variational approach. The filamentations and their effects on THz generation have been studied numerically.

Chapter 9 and **chapter 10** are focused on second harmonics generation of q-Gaussian and quadruple-Gaussian (Q.G) laser beam in collisional plasma. **Chapter 9** represent an investigation of frequency up-conversion of a laser beam through the phenomenon of second harmonic generation (SHG) in collisional plasma with an upward density ramp is presented. By using a hydrodynamic fluid model of plasma, the source term for the SHG has been obtained. Emphasis is put on the investigation of the effect of various laser and plasma parameters on the propagation dynamics of the pump beam and the conversion efficiency of second harmonics. In **Chapter-10,** a scheme for the generation of second harmonics of intense quadruple Gaussian (Q.G) laser beams propagating through collisional plasmas has been presented. Variational theory has been adopted to find the semi-analytical solution of the wave equation for the slowly varying envelope of the laser beam.

In **chapter 11**, introduction to surface plasma waves (SPWs) and a method of generation of THz radiation with SPWs propagating over the semiconductor-free space interface are incorporated. Firstly the cross focusing of SPWs has been investigated. Then the investigation has been extended to see the effect of self focusing of the SPW on THz generations. **Chapter 12** summarizes the obtained results on the basis of analytical and numerical investigations on the self-action effects, THz and higher harmonics generation in different nonlinear media.

TABLE OF CONTENTS

List of Figures

Chapter 1

Laser Plasma Interactions: Introduction

1.1 Introduction

Light has always fascinated man and investigation of interaction of light with matter is as old as human civilization. Ancient people used glass made lenses to focus light to burn pieces of papers. However, the debut of LASER in 1960s [1] revealed the true beauty of light matter interactions. The unique characteristics of laser light are significantly applicable in different fields of science and technology [2-5] (fig.1.1). Laser has reserved a special place in scientific community due to its demand in daily life such as from CD player to medical imaging. Even high end applications such as inertial confinement fusion (ICF) [3, 6], laser driven particle accelerator [7], coherent radiation source [8] etc. are also abound. Over the last few decades, the Q-switching, mode locking and chirped pulse amplification techniques (CPA) [9, 10] have enabled researchers to obtain laser beams up to zettawatt of peak power [11-13]. The giant leap in laser technology during past few decades has led to a renaissance in the field of light matter interactions by giving birth to two entirely new areas of research known as "nonlinear optics" and "laser-plasma interactions (LPI)".

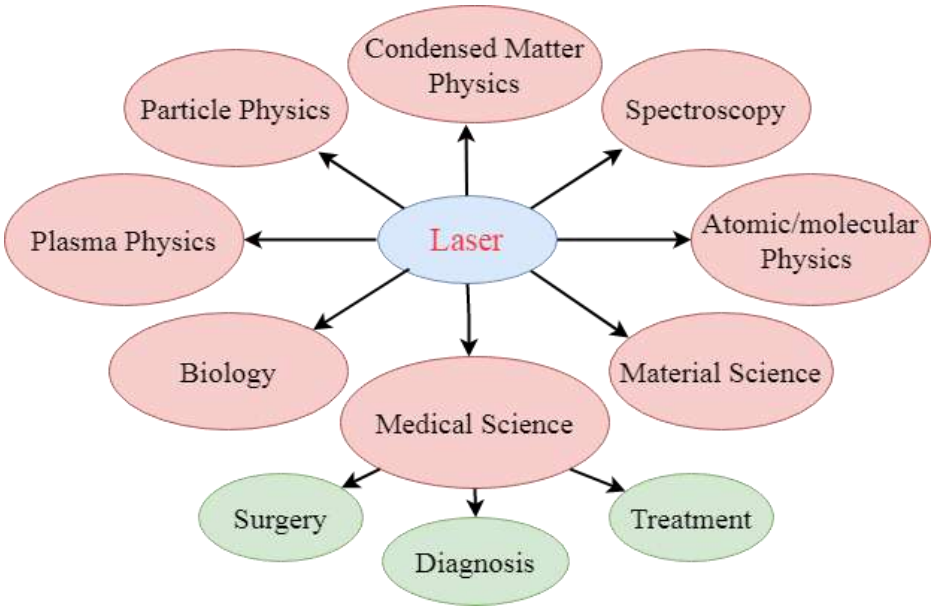

Fig.1.1: Laser in different fields of science and technology

The interactions of intense coherent beams of light produced by modern laser systems with plasmas are rich in copious nonlinear phenomena [14,15] (fig.1.2) those were not possible before the invention of laser. The field of LPI is fascinating researchers because of its promising applications like compact particle accelerator [16], X-ray laser [17], THz generations [18], ICF [6] etc. The nonlinear phenomenon like higher harmonics generation (HHG) [19], sum frequency generation (SFG) [20], difference frequency generation (DFG) [21] etc. can be used to obtain laser beams at new frequencies those are not achievable from direct laser systems.

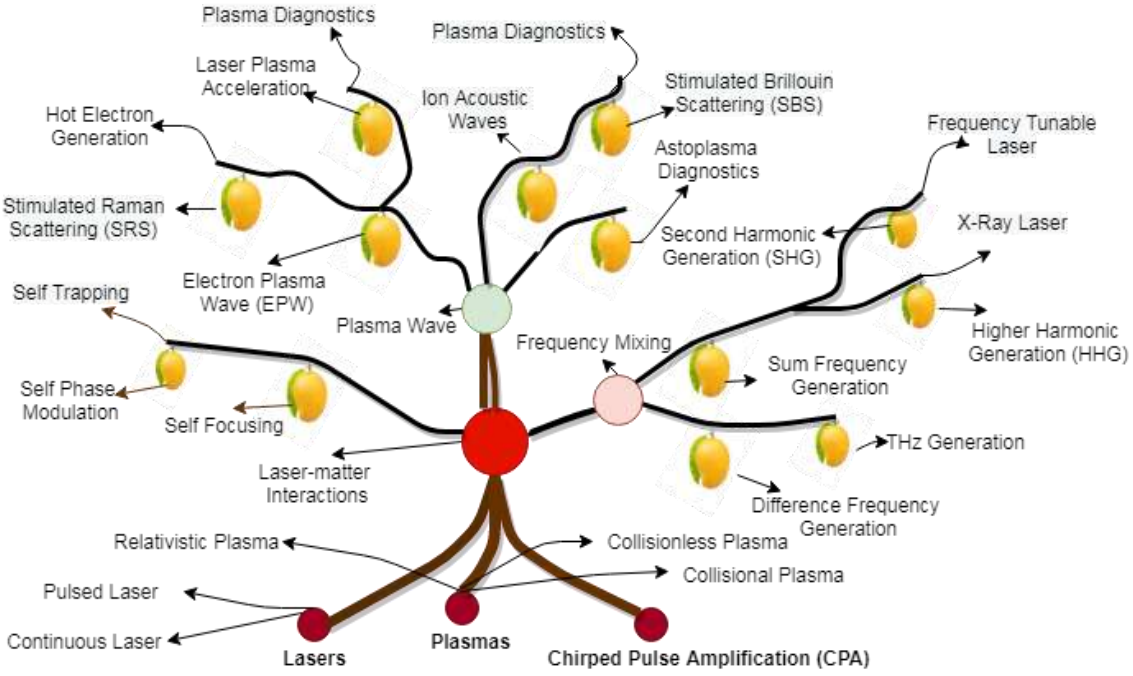

Fig.1.2: Tree diagram for laser plasma interactions

In present research work, I have investigated some of nonlinear phenomena like self focusing, self trapping, second harmonics generation (SHG), terahertz (THz) generation [19,22, 23] occurring during LPI. As a special case of nonlinear interactions of laser beams with narrowband gap semiconductors also have been investigated. The effects of self focusing of laser beams on SHG and THz generation has been investigated in detail.

1.2 Mechanisms of Optical Nonlinearity in Plasma

In the linear regime, a highly collimated optical beam starts spreading along the transverse axes due to diffraction property of light. More tightly we try to confine the beam more it will spread. Before the invention of laser it was thought that diffraction broadening of optical beam is unavoidable as it arises at a fundamental level from uncertainty principle of quantum mechanics. Conventionally, the diffraction of an electromagnetic beam can be obviated by using optical fibers or waveguides. But, in applications involving laser plasma interactions, laser beams of intensities of the order of $10^{16} W/cm^2$ are being used. However, a glass fiber gets damaged only at intensity of $10^{12} W/cm^2$. Hence, for ultrahigh intensity laser beams optical fibers are not an appropriate solution for optical guiding. In 1964, it was shown by Chiao et al. [24] that the spreading of an optical beam passing through a material medium could in principle be avoided if the medium start responding nonlinearly (i.e., if the index of refraction of the medium becomes a function of the intensity of light) to the incident beam. The electric breakdown strength of the normal materials limits the use of high intensity lasers. But, plasma have shown possibility to use these high intensity lasers. A plasma by definition is a quasineutral gas of charged particles that possess collective behaviour. However, being already ionized, plasmas (fig. 1.3) show almost infinite immunity against such kind of damages. Due to their inherent properties of quasi-neutrality and collective behaviour they also respond nonlinearly to intense optical beams.

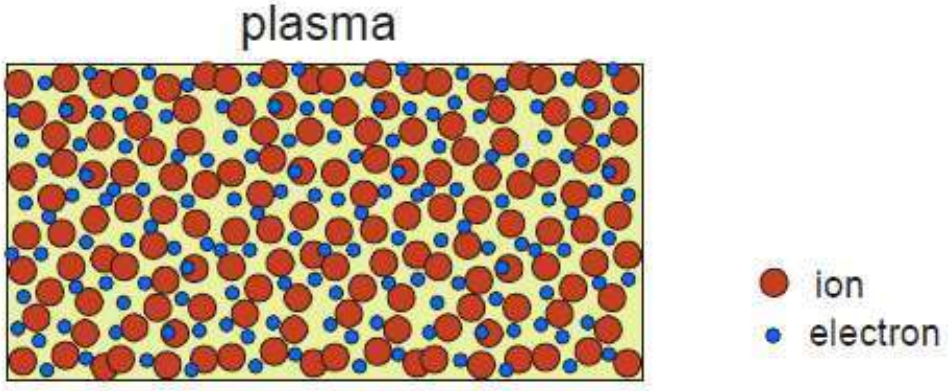

Fig.1.3: Plasma

The dielectric response of plasma to an incident optical beam of frequency ω_0 is given by

$$\varepsilon = 1 - \frac{\omega_p^2}{\omega_0^2} \tag{1.1}$$

where,

$$\omega_p = \sqrt{\frac{4\pi e^2}{m_e} n_e} \tag{1.2}$$

Is the characteristic frequency of plasma which is known as plasma frequency. It is the natural frequency of oscillations of plasma electrons when they are perturbed from their equilibrium positions. Here, e, m_e, n_e are the electronic charge, mass and density, respectively. Thus any mechanism by which laser beam can modify n_e or m_e will result in nonlinear response of plasma to the incident optical beam.

There are mainly three mechanisms (fig.1.4) by which plasma can interact nonlinearly with laser. These mechanisms are:

1. Ponderomotive Force
2. Ohmic Heating
3. Relativistic increase in electron mass

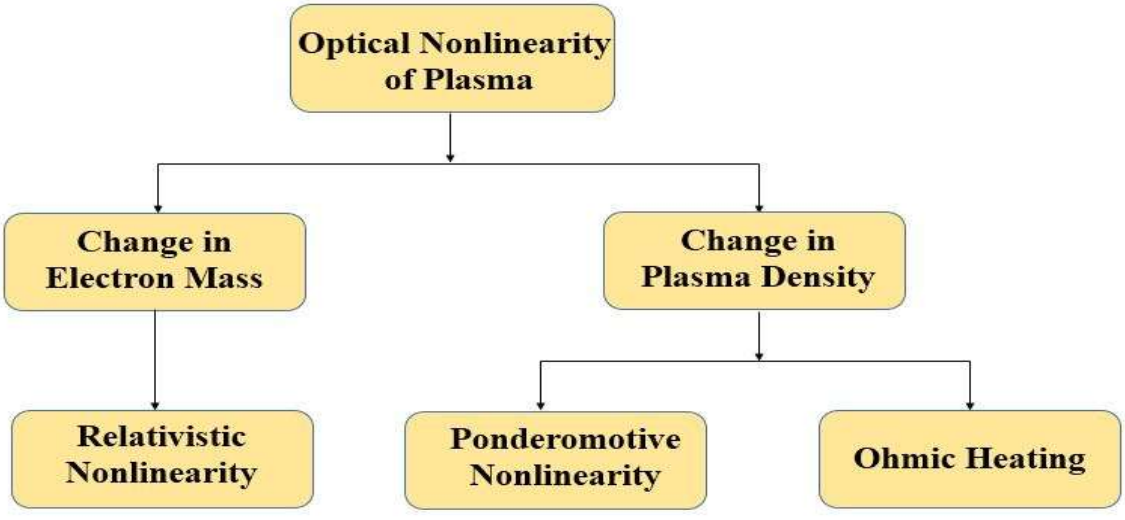

Fig.1.4:Various optical nonlinearities of plasma

First two mechanisms involve the modification of electron density due to the physical movement of the plasma electrons under the effect of laser beam and thus show transient behaviour. Whereas, the third mechanism does not involve any modification of electron density and thus does not show any transient behaviour. It comes into picture alsmost instantaneously as soon as the intensity of the beam crosses the threshold intensity.

1.2.1 Ponderomotive Nonlinearity

Generally the laser beams do not possess uniform amplitude structure over the cross sections. Due to their finite cross section laser beams are having some amplitude structure over their cross sections. The amplitude profiles of the laser beams depend upon the mode of laser cavity. At the lowest mode of the cavity operation i.e., TEM_{00} the amplitudue structure over the cross section of resulting beam of light is described by Gaussian distribution of the form

$$E_0(r) = E_{00} e^{-\frac{r^2}{2r_0^2}} \tag{1.3}$$

where, r_0 is the waist size of the beam and E_{00} is the axial amplitude. Thus, there exists a radial intensity gradient over the cross section of the laser beam. When such a laser beam propagates through plasma, the radial density gradient over its cross section results in a nonlinear force called as Ponderomotive force [25, 26, 27]. The magnitude of this ponderomotive force is directly proportional to the intensity gradient over the beam cross section i.e.,

$$F_{Pond} \propto -\nabla E_0 E_0^{\star} \tag{1.4}$$

The DC component of this ponderomotive force results in the migration of plasma electrons in the illuminated portion of plasma from high intensity regions to low intensity regions (fig.1.5). Thus, the laser dugs a density channel into the plasma for its propagation. If n_0 is the equilibrium electron density of the plasma, then its modified density in the presence of laser beam is given by [25]

$$n_e = n_0 e^{-\frac{e^2}{8m_e\omega_0^2 K_0 T_0} E_0 E_0^{\star}} \tag{1.5}$$

where, K_0 is the Boltzmann cosntant, T_0 is the temperture of plasma electrons. This modification of electron density of plasma due to the ponderomotive force makes the index of refraction of plasma a fuction of laser beam intensity as

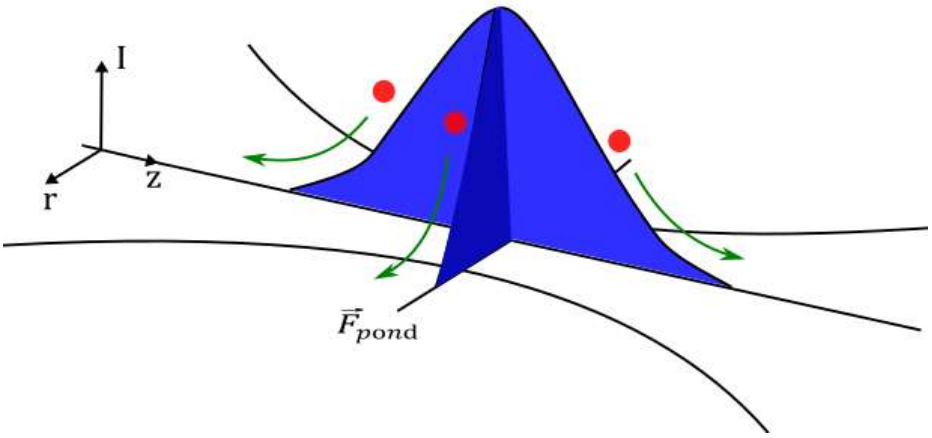

Fig.1.5: Ponderomotive force acting on plasma electrons

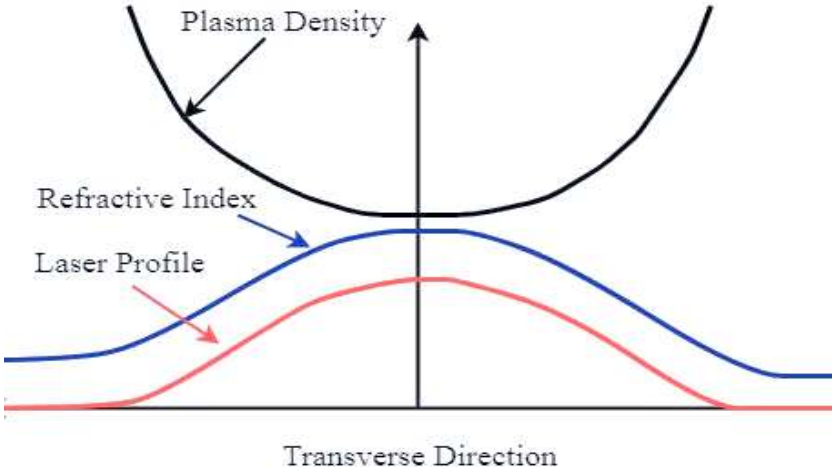

Fig.1.6: Variation of index of refraction of plasma with radial distance from beam axis

$$\epsilon = 1 - \frac{\omega_{p0}^2}{\omega_0^2} e^{-\frac{e^2}{8m_e\omega_0^2 K_0 T_0} E_0 E_0^*} \tag{1.6}$$

Here, $\omega_{p0} = \sqrt{\frac{4\pi e^2}{m_e} n_0}$ is the equilibrium plasma frequency of the ecetrons i.e., plasma frequency in the absence of laser beam. The resulting transverse variation of index of

refraction of plasma is shown in fig.(1.6). Such an index of refraction resembles to that of graded index optical fiber.

1.2.2 Ohmic Heating

During the propagation of intense laser beam through plasma, the nonuniform intensity distribution over its cross section produces the nonuniform Ohmic heating of plasma electrons [28, 29, 30] along the transverse axes. Due to the bell shape intensity distribution over the cross section of laser beam, the temperature of electrons in the illuminated portion of plasma becomes maximum at the beam center and it decreases radially towards the beam edges. This results in migration of plasma electrons from the center of beam towards its edges. The redistribution of plasma electrons in the presence of intense laser beam changes index of refraction of medium a function of laser intensity and thus plasma starts behaving nonlinearly to the incident beam.

Therefore, in this mechanism the nonuniform amplitude structure over the cross section of an optical beam results in nonuniform heating of plasma electrons due to their other species like ions and neutral particles. The resulting temperature of plasma electrons is given by

$$T_e = T_0 \left(1 + \frac{e^2 M}{6K_0 T_0 m_e^2 \omega_0^2} E_0 E_0^{\star}\right) \tag{1.7}$$

where, T_0 is the equilibrium plasma temperature, M is the mass of ions. This nonuniform heating of plasma electrons results in their evacuation from high intensity regions of the illuminated portion of plasma. These migrating electrons move towards the low intensity regions of plasma. The resulting electron density of plasma is given by

$$n_e = n_0 \left(\frac{2T_0}{T_0 + T_e}\right)^{1-\frac{s}{2}} \tag{1.8}$$

where, the phenominological parameter s describes the nature of collisions of plasma electrons. $s = -3$ corresponds to electron ion collisions, $s = 2$ corresponds to collisions of plasma electrons with diatomic molecules and $s = 0$ corresponds to velocity

independent collisions of plasma electrons. Thus, using eq.(1.1), the resulting intensity dependent dielctric function of plasma can be written as

$$\epsilon = 1 - \frac{\omega_{p0}^2}{\omega_0^2}\left(1 + \frac{e^2 M}{6K_0 T_0 m_e^2 \omega_0^2} E_0 E_0^\star\right)^{\frac{s}{2}-1} \tag{1.9}$$

1.2.3 Relativistic Nonlinearity

If under the effect of intense laser beam the quiver velocity of plasma electrons become comparable to that of light in vacuum, then the electrons of plasma attain relativistic mass. The effective mass of plasma electrons in eq.(1.2) need to be replaced by $m_0\gamma$, where, m_0 is the rest mass of electron and γ is the relativistic Lorentz factor which is related to laser beam intensity as [31,32,33]

$$\gamma = \left(1 + \frac{e^2}{m_0^2 c^2 \omega_0^2} E_0 E_0^\star\right)^{\frac{1}{2}} \tag{1.10}$$

Thus, using eqs.(1.1) and (1.2) the intensity dependent dielectric function of plasma can be written as

$$\epsilon = 1 - \frac{\omega_{p0}^2}{\omega_0^2}\left(1 + \frac{e^2}{m_0^2 c^2 \omega_0^2} E_0 E_0^\star\right)^{-\frac{1}{2}} \tag{1.11}$$

It can be seen from eq.(1.11) that similar to the case of ponderomotive nonlinearity or thermal nonlinearity, in the case of relativistic nonlinearity also, the laser beam experiences maximum index of refraction where the intensity is maximum and vice versa. This gradient in the case of refraction of plasma again results in the self focusing of the laser beam known as relativistic self focusing.

1.3 Self-Action Effects of Laser Beams in Nonlinear Media

In conventional optics, the geometric structure and propagation characteristics of an optical beam are generally controlled with the help of various optical elements such as lenses, prisms, mirrors, diffraction gratings etc. These elements are made by high-quality optical materials, i.e., materials having uniform index of refraction distribution. The

function of such an optical element is ensured by a regular variation of thickness, or equivalently, by the regular variation of optical path. For example, a convex lens can be used to converge an incident optical beam, whereas a concave lens is used to diverge the incident optical beam. If an ordinary quasi-parallel optical beam passes through a glass slab, the beam structure will not be changed because the thickness or optical path of the slab is the same over different sections of the incident beam.

In nonlinear optics, however, even the medium is equivalent to a parallel slab; the spatial structure of an intense laser beam may get changed due to the nonlinear interaction between the medium and the laser beam. These effects come into frame when an intense laser beam induces a change in refractive index of medium through which it is propagating. Indirectly, the self-action effects are occurred due to the dependence of complex dielectric function on the intensity of electromagnetic radiations. The change in medium properties reacts back to the laser beam in results of which the characteristics of the beam get altered. Thus, propagation characteristics of beam undergo different self-actions such as self focusing, self trapping, self defocusing, self phase modulation (Gouy phase) etc.

Consider the propagation of a linearly polarized, quasi parallel optical beam with electric field vector

$$\boldsymbol{E} = E_0(x,y)e^{\iota(kz-\omega_0 t)}\hat{\boldsymbol{x}} \tag{1.12}$$

through an isotropic nonlinear medium characterized by third order nonlinear susceptibility $\chi^{(3)}(\omega,-\omega,\omega)$. The third order change in the index of refraction of the medium produced by the optical beam is given by

$$\Delta n(x,y) = n_2|E_0(x,y)|^2 \tag{1.13}$$

where,

$$n_2 = \frac{1}{2n_0}\chi^{(3)}(\omega,-\omega,\omega) \tag{1.14}$$

Usually the intensity of optical beams decreases with radial distance from the axis of the beam. Thus, depending on the values of n_2 there are four different possibilities [22, 24, 31]

1.3.1 Linear Divergence: $n_2 = 0$

If the induced index of refraction change is negligible then the beam size increases gradually with the propagation distance owing to the diffraction-divergence of the incident beam. This is due to the fact that a laser beam with finite cross section can be considered as a superposition of plane waves, all having the same wave number, but with different angle with respect to the beam axis. Therefore, each component propagates at different phase velocity with respect to the longitudinal direction. Thus, each plane wave acquires a different phase and thus the beam broadens along the transverse directions.

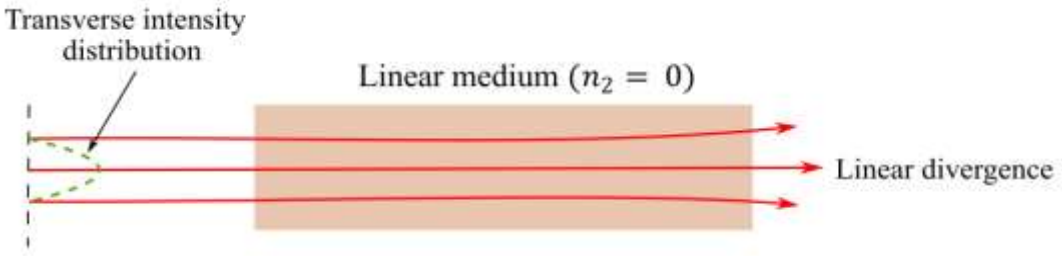

Fig.1.7: Linear divergence of an optical beam

1.3.2 Self Focusing: $n_2 > 0$

If the change in the index of refraction of the medium produced by optical beam is positive, then the laser beam focuses towards its axis by its own and this mode of propagation is known as self focusing.

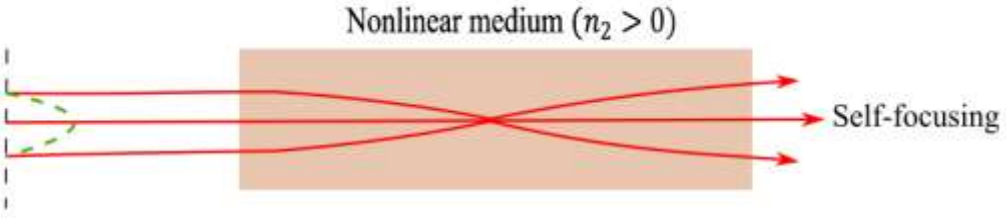

Fig.1.8: Self focusing of an optical beam

This is due to the fact that being most intense, the axial part of optical beam gets maximum opposition from the medium for its propagation and this opposition

decreases with radial distance from the axis of beam. Hence the beam develops a velocity gradient over its cross section and thus the phase fronts of the beam bend as if the beam is passing through a converging lens.

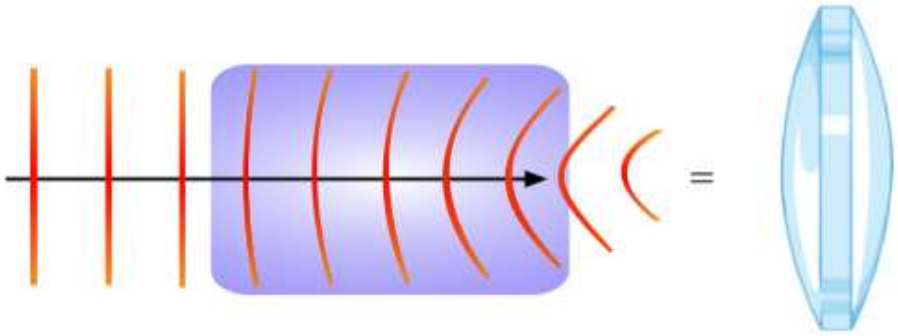

Fig. 1.9: Induced lens due to self focusing

This fact can be understood with the help of following analogy: consider a family consisting of children, parents and grand parents going for walk. When they are leaving home grandparents are at center, then parents on each side and then children as shown in fig.(1.10). As they move parents lag behind children and grandparents lag behind parents. In this way respective positions of the family members develop a curvature as shown.

Fig.1.10: Analogy for self focusing

Similarly the velocity gradient over the cross section of optical beam results in its self focusing.

1.3.3 Self Trapping: $n_2 > 0$

The Kerr nonlinearity [24] causes self trapping of laser beam. If n_2 is positive and once the propagating beam is focused onto a small spot, the beam size remains unchanged over a longer propagation distance within the nonlinear medium, then the beam is said to be self trapped. In other words, the beam is finally confined in a waveguide channel formed by the induced refractive-index change; here we term this phenomenon the self trapping effect or uniform waveguide propagation and beam is said to constitute a spatial soliton [34].

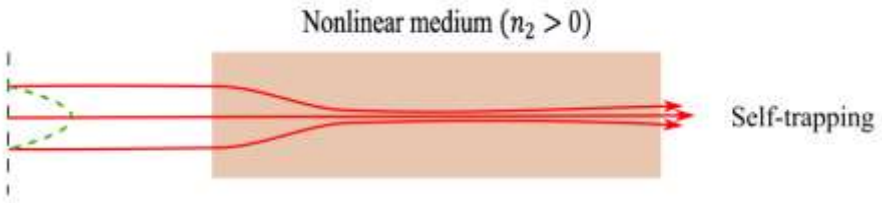

Fig.1.11: Self trapping of an optical beam

To understand intuitively soliton formation in nonlinear optical media, consider a group of cyclists travelling into the wind and drafting off one another (that is, riding close together to cut wind resistance for those behind the leader) as depicted in fig.(1.12). In the absence of wind the cyclists would spread apart because of their different cycling speeds. However, the wind resistance impedes the stronger cyclists, who break the headwind for the weaker cyclists. Consequently they all travel together as a packet. The different cycling speeds are like the diffraction effect of optical beam, and the wind resistance is like the nonlinearity.

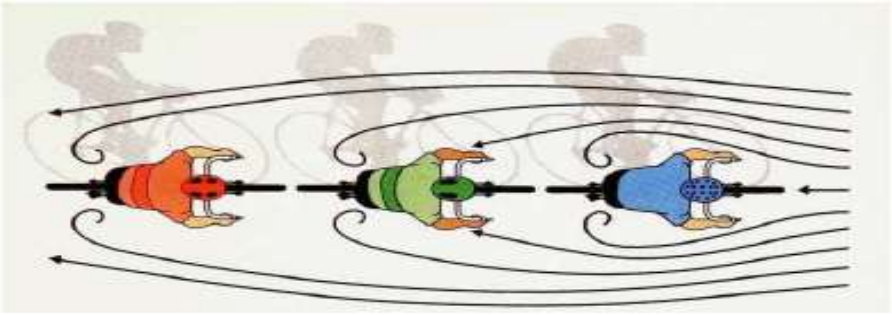

Fig.1.12: Analogy for self trapping

1.3.4 Self Defocusing: $n_2 < 0$

This aspect of nonlinear dynamic of laser beam comes into picture due to Kerr nonlinearity [24]. If n_2 is negative, then the nonlinear medium behaves like a concave lens to the incident optical beam and hence, the beam spread into the transverse directions.

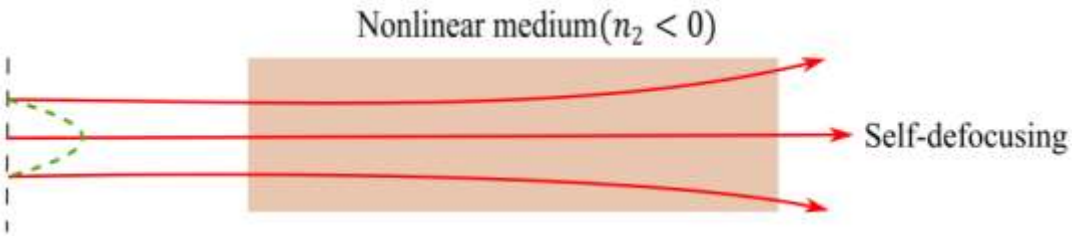

Fig.1.13: Self defocusing of an optical beam

Variation of the axial intensity of the optical beam with distance of propagation through the nonlinear medium for above mentioned self-action effects has been shown in fig.1.14.

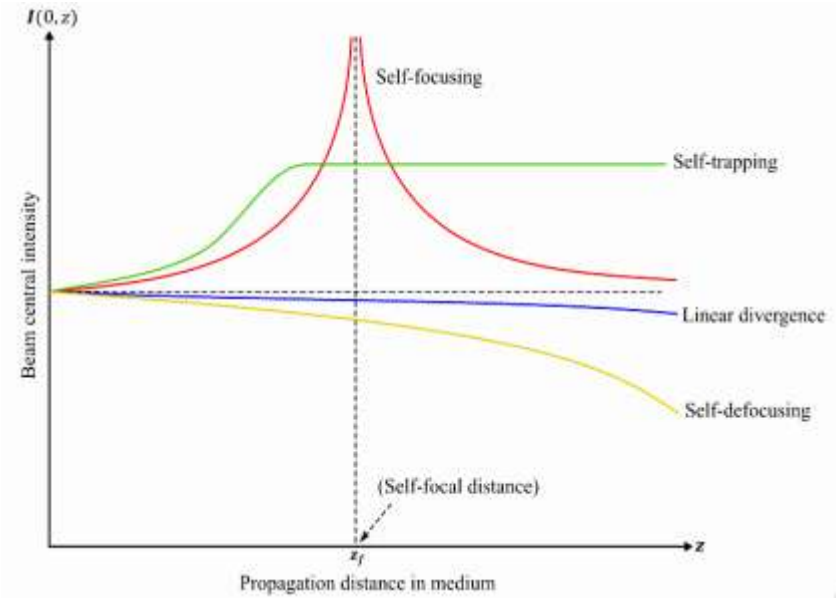

Fig.1.14: Variation of axial intensity of an optical beam during self-action effects

1.4 Variational Theory

Literature review reveals that almost the base of the nonlinear dynamics of laser beams have built on the paraxial theory [35]. Paraxial theory only takes into account the axial portion of the laser beam means it does not involve the effect off-axial part of laser beam. This approach is not properly suitable when we need to deal with situations related to non-Gaussian beams such as *q*-Gaussian, Cosh-Gaussian , super-Gaussian , Quadruple beams in which off-axial fields play a crucial role in propagation dynamics. In present work, I have proposed the application of variational theory which remove the shortcomings of paraxial theory. This methodology is obtained by examining some integral relations derived from the nonlinear Schrodinger equation (NLSE).This method is more acceptable from the elementary point of view, since the whole wavefront of the beam is examined in the interaction procedure.

Variational theory is based on variational calculus. It is a semi analytical technique to obtain approximate solutions to partial differential equations which cannot be solved analytically [36, 37, 38]. This technique replaces a set of partial differential equations with a set of coupled ordinary differential equations those can be solved either analytically or by using simple numerical techniques like Runge Kutta fourth-order method etc. It can be used successfully to have physical insight into number of nonlinear systems like propagation of waves in various nonlinear media, super conductors, Bose Einstein condensates etc. In present investigation, variational technique has been used to investigate nonlinear interactions of intense laser beams with plasmas and narrow band gap semiconductors. A detailed description of this technique is as follows:

$$\nabla_{\perp}^{2} E_0 + \frac{\omega_0^2}{c^2} \Phi(E_0 E_0^*) E_0 - 2ik_0 \frac{\partial E_0}{\partial z} = 0 \tag{1.15}$$

where, $\nabla_{\perp}^{2} = \frac{\partial^2}{\partial r^2} + \frac{1}{r}\frac{\partial}{\partial r}$ is the transverse Laplacian and $\Phi(E_0 E_0^*) = \varepsilon(E_0 E_0^*) - \varepsilon_0$ is the intensity dependent nonlinear dielectric function of the medium.

Being nonlinear in nature superposition principle does not apply to eq. (1.15) i.e., linear combination of two solutions will not be a solution of this equation. Hence, traditional methods of solving partial differential equations are not applicable for this

equation. Although there exist a number of numerical methods to solve this equation, but these methods suffer from major difficulties due to dependence of accuracy and speed on the functional form and number of the nonlinear terms included in eq. (1.15). Careful selection of step sizes is an important issue in order to achieve the desired accuracy. All these difficulties can pose serious convergence problems for beam propagation algorithm. In contrast to this explicit analytical or semi-analytical solutions to eq. (1.15) are more advantageous rather than numerical methods, since they give an overall insight into the behavior of the system.

There are different semi analytical techniques for solving eq. (1.15) among which variational approach is one which is providing results very close to numerical results and in many cases it provides qualitative as well as quantitative results. This technique is based on Ritz's optimization method and has been widely used when studying NLSE that appears not only in nonlinear optics, but also in many other physical problems where NLSE is encountered. It reduces the infinite-dimensional problem of the partial differential equations to a Newton-like second order ordinary differential equation for the parameters characterizing the solution. In other cases, however, the validity of the variational results is only qualitative i.e. if the shape of the actual solution is close to the trial function, the results obtained with the variational technique will be in good agreement with the real solutions, but in other cases the method can be very rough or even fail.

We first write the Nonlinear Schordinger Wave Equation in the form:

$$\hat{F}[\Psi] = 0$$

We then define a Lagragian density $\pounds\,[\Psi, \Psi^*]$, such that:

$$\frac{\partial \pounds}{\partial \Psi^*} = \hat{F}[\Psi]$$

According to variational Method, we need to solve the following set of extended Euler-Lagrange equation for the variational parameter $g_i(z)$ with i=1, 2, 3…..N:

$$\frac{d}{dz}\left(\frac{\partial L}{\partial\left(\frac{\partial q_i}{\partial z}\right)}\right)-\frac{dL}{dz}=0 \tag{1.16}$$

Here, L is the average Lagrangian obtained by integration of £ over the transverse coordinates x and y.

$$L=\iint £\ dxdy$$

For our particular problem, the Lagrangian density corresponding to eq.(1.15) is

$$£=ik_0\left(\Psi\frac{\partial\Psi^*}{\partial z}-\Psi^*\frac{\partial\Psi}{\partial z}\right)+\left|\frac{\partial\Psi}{\partial x}\right|^2+\left|\frac{\partial\Psi}{\partial y}\right|^2-\frac{\omega_0^2}{c^2}\int_0^{E_0E_0^*}\Phi(E_0E_0^*)d(E_0E_0^*) \tag{1.17}$$

The variational method investigates the dynamic characteristics of the laser beam through medium under nonlinear regime by using different trial functions for laser beam.

1.5 Second Harmonic Generation

Second-harmonic generation (SHG) or frequency doubling is a nonlinear optical effect [39, 40] that converts monochromatic coherent light of frequency ω_0 to another coherent light wave of frequency $2\omega_0$ (fig.1.15) when it interacts with a second-order nonlinear medium. The invention of laser made it possible to treat light waves like radio waves, in other words, it extended the art of electronics to visual portion of the electromagnetic spectrum. One of the first successful experiments in optical electronics (now known as nonlinear optics) has been reported by Franken et al in 1961 who produced first overtone of laser light: the phenomenon which now a days is called as second harmonic generation [41, 42].

In ordinary electronic devices the production of harmonics, or overtones, is almost unavoidable. Unless a circuit element, such as an amplifier, is absolutely linear, (i.e., unless its output is exactly proportional to its input), the output will always contain harmonics of the input wave. For example, take the case of a full wave rectifier, whose actual motive is to eliminate the time variations of the signal, but along with that it generates multiple new frequency components. Although the amplitudes of these new frequency components are very small but still they are useful in number of applications. The only way to avoid

harmonics is to limit the input energy to a narrow range of frequencies over which the operation of the device is virtually linear.

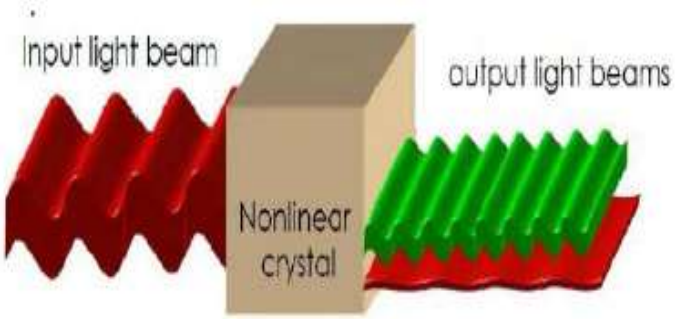

Fig.1.15: Second harmonic generation in nonlinear media

In ordinary electronic devices the production of harmonics, or overtones, is almost unavoidable. Unless a circuit element, such as an amplifier, is absolutely linear, (i.e., unless its output is exactly proportional to its input), the output will always contain harmonics of the input wave. For example, take the case of a full wave rectifier, whose actual motive is to eliminate the time variations of the signal, but along with that it generates multiple new frequency components. Although the amplitudes of these new frequency components are very small but still they are useful in number of applications. The only way to avoid harmonics is to limit the input energy to a narrow range of frequencies over which the operation of the device is virtually linear.

Optical circuit elements e.g., quartz are linear over a much wider range of energies. In fact, before the invention of laser it was impossible to concentrate enough energy to drive them into nonlinear regime. With ultra-intense lasers, this can be done. E.g., optical beams from commercially available Ruby laser can be focused so sharply as to produce in a small volume of quartz an electric field of some $10^5 Vcm^{-1}$, at the accurately defined wave length of 6943Å in red region of the electromagnetic spectrum. Franken and his co-workers exposed a quartz crystal to the intense illumination and analyzed the emitted light with a spectroscope. They found a faint, though sharp, blue light close to 3472Å which was exactly the half of the fundamental wave. This is called as wavelength of the second harmonic or first overtone.

In Franken's experiment the interaction between the optical field and the crystal was not phase matched. Hence, ultraviolet output power was so small that the editors at Physical Review Letters mistook for a blemish the spot on Franken's spectrograph plate that demonstrated the new effect. They airbrushed it out of the published version (fig.1.16), rendering the first evidence of nonlinear frequency conversion truly invisible. Subsequent progress in the field was rapid. By the end of 1962 the classic paper had appeared in which Nicolaas Bloembergen and co-workers gave the theoretical [43] underpinnings for both the microscopic origins of the nonlinear susceptibilities and the propagation effects governing macroscopic nonlinear interactions between electromagnetic waves.

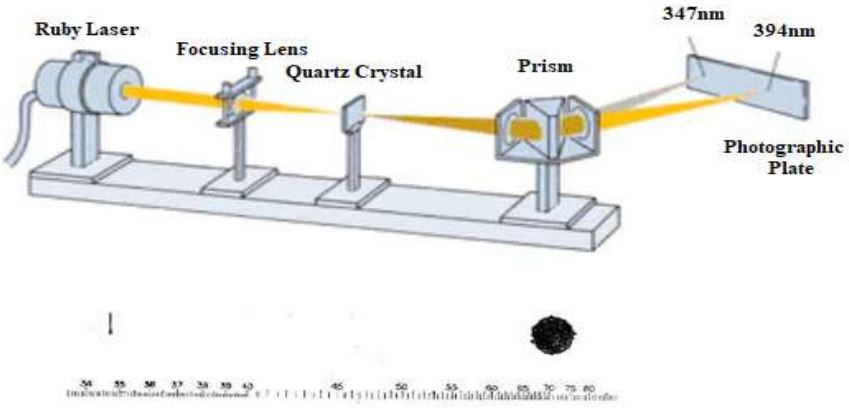

Fig.1.16: SHG by Franken

1.5.1 Second Harmonics Generation in Plasma

Although second harmonics of intense laser beams can be produced in a number of nonlinear media like solids, liquids or gases. However, ionization threshold of these media limits the power of generated harmonics. By contrast being already in ionized states plasmas are entirely immune to ionization induced damages. Hence, second harmonics of any power can be produced in plasmas [44-46]. In case of plasmas second harmonic radiation of the pump beam produced by the excitation of an electron plasma wave at pump frequency as follows:

Due to its quasi neutrality and collective behaviour plasma can support a number of modes of oscillations. Thus, an imbalance between the charge densities of electrons and

ions can be created by an intense laser beam propagating through plasma. The laser beam throws the electrons out of its way however, due to their large inertia the ions remain at rest. This redistribution of carriers results in the creation of the regions of excess positive and negative charges. The resulting electric field pulls the electrons towards the positive region of ions. As the electrons start moving towards the positive regions, they steadily gain momentum. This increased momentum causes the electrons to overshoot the positive region and thus reverses the direction of electric field [47]. This reversed field pulls back the electrons and thus slow down their motion. The process repeats itself and thus the electrons start oscillating with a frequency equal to that of pump beam. The process repeats itself, establishing an electron oscillator (fig.1.17).

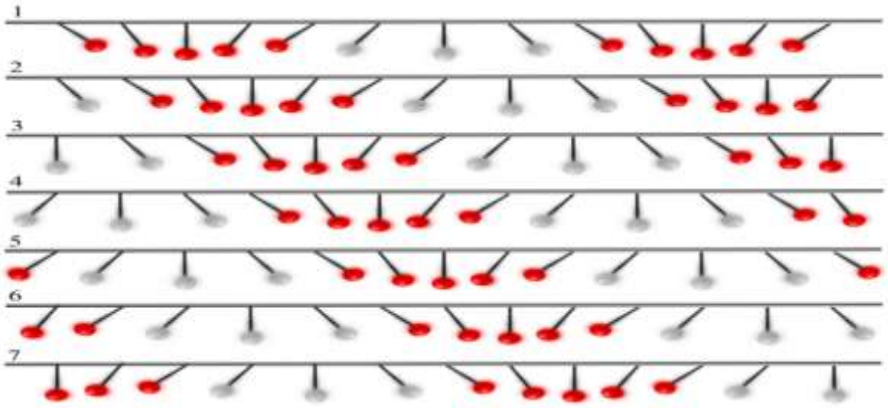

Fig.1.17: Analogy of electron oscillations with motion of simple pendulum

Imagine thin cylinder of plasma, it long axis horizontal. Every electron oscillator is centered at different point in the cylinder and oscillates left and right, parallel to the axis. Suppose the oscillators are made to oscillate in the sequence. Suppose an oscillator at left end of plasma cylinder occupies it's left most position. A small distance along the plasma cylinder another electron oscillator is in its center position and it is followed by an oscillator in its rightmost position. Next comes an oscillator at its center position and then one at its leftmost position. If all these electron oscillators were to start oscillating at the same frequency and achieve the same maximum amplitude, regions of negative or positive charge would appear to move along the cylinder in a travelling wave. The effect would resemble to light on a theatre marquee: although each bulb switches on and off in sequence, waves of light seem to move across the sign. In this way the combined motion of the

electron oscillators form a longitudinal wave of positive and negative regions travelling through the plasma (fig.1.18).

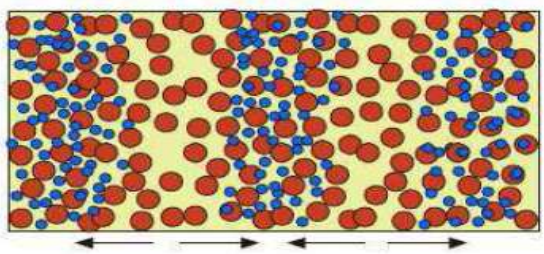

Fig.1.18: Electron plasma wave

The electron oscillators can be set into motion by intense laser beams. As the laser beam enters into the plasma region, it exerts pressure on plasma electrons and hence the plasma electrons move out of the way. As the laser beam exits, leaving a region deficient of electrons, the plasma electrons rush back to re-establish equilibrium. This movement of plasma electrons initiates the oscillations of plasma electrons and results in plasma wave. The oscillations of these plasma electrons contain a frequency component twice of that of the pump beam and thus result in emission of coherent second harmonic radiation

1.6 Terahertz (THz) Generation

THz radiations are also known as submillimeter radiations, terahertz waves, terahertz light, T-rays, T-waves, T-light, T-lux, or THz, consist of electromagnetic waves at frequencies from 0.3 to 10 terahertz (THz). The term applies to electromagnetic radiation with frequencies between the high-frequency edge of the millimeter wave band, 300 GHz and the low frequency edge of the far-infrared light band, 3000 GHz as shown in fig.(1.19). Corresponding wavelengths of radiation in this band range from 1 mm to 0.1 mm (or 100 μm). The terahertz radiation begins at a wavelength of 1 mm and proceeds into shorter wavelengths hence, it is sometimes known as the submillimeter band and its radiation as submillimeter waves, especially in astronomy. These radiations possess following unique characteristics:

I. They can penetrate through many non-metallic and non-polar substances such as cloths, woods, papers and plastic. But it has restricted penetration through clouds and fog [48].

II. They are s phase sensitive to polar substances. It interacts with some molecules having rotational and vibrational absorption energy in the range of THz radiation such as water, carbon monoxide, oxygen etc. [49].

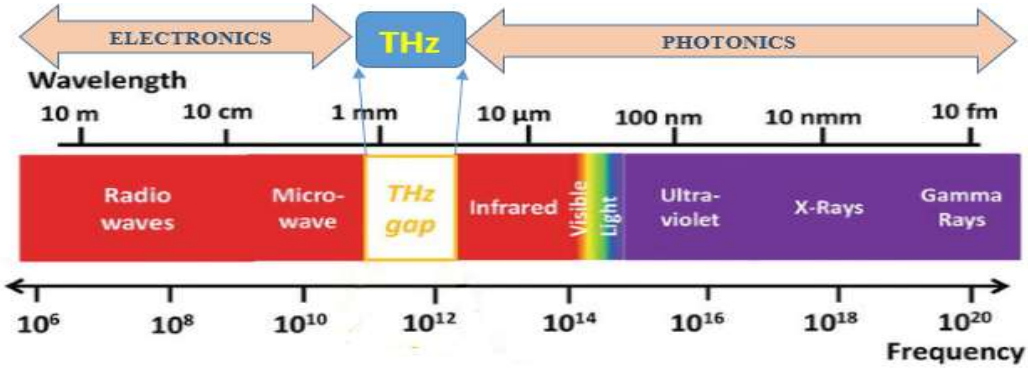

Fig.1.19: Electromagnetic spectra based on frequency and wavelength

III. They cannot penetrate through metal, so it get reflected back from the surface of metal.

IV. Their photon energy lies between 0.4meV to 41meV [50, 51]. Thus, they are non-invasive and non-ionizing in nature. Hence, THz radiations are not harmful for living cells and tissues.

Due to these unique features of THz radiation, THz radiation has made remarkable place in electromagnetic spectrum. It is widely applicable in distinct fields such as biological imaging, remote sensing, explosive detection, medicines, broadband wireless communication technology etc. Due to their optical nonlinearity plasmas offer themselves as a promising medium [52, 53] to convert optical frequencies to THz frequency through the phenomenon of difference frequency generation (DFG). When two intense laser beams with frequencies ω_1 and ω_2 propagate simultaneously through plasmas, the oscillations of plasma electrons under the fields of these laser beams contain frequencies $\omega_1, \omega_2, \omega_1 + \omega_2$ and $\omega_1 - \omega_2$ [54]. As an oscillating charge behaves as a tiny dipole antenna and emits the

electromagnetic radiation at the frequency of its oscillations, the oscillations of plasma electrons at frequency component $\omega_1 - \omega_2$ leads to generation of THz radiations (fig.1.20).

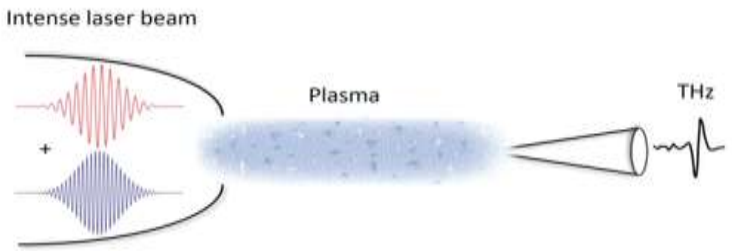

Fig.1.20: Generation of THz radiation by beating of two laser beams in plasma.

Now a days, in laser plasma based experiments, THz radiations are generating with the use solid state devices. But with the proposed scheme THz intensity can be achieved efficiently. To make the results more realistic the irradiance profile has been modeled by q-Gaussian laser beam.

1.7 Research Objectives

In the present research work, it is proposed to investigate the following problems theoretically as well as through numerical simulations.

1. Self-focusing and Self-phase modulation of laser beams (q-Gaussian, Cosh-Gaussian, Quadruple-Gaussian) in nonlinear media.

2. Self-focusing of laser beams in nonlinear media and its effect on Terahertz generation.

3. Terahertz generation by self-focused surface plasma waves at free space-semiconductor interface.

4. Terahertz generation by self-focused laser beams in semiconductor plasmas.

5. Higher harmonic generation of self-focused intense laser beams in nonlinear media.

6. Effect of laser beam filamentation on Terahertz and Higher Harmonic generation in nonlinear media.

Chapter 2

Literature Review

2.1 Introduction

This chapter unravels the contribution of different researchers in the field of laser-matter interactions. They are trying to enhance the efficiency of inertial confinement fusion (ICF). Besides, theoretical and experimental work on self-action effects, the yield of THz, and higher harmonics generation are hot topics. I have incorporated previous investigations of self-action effects, HHG, THz generation, filamentation, and surface plasma waves to support the different aspects of laser-matter interactions which are explained in chapter-1. Moreover, I have tried to explain briefly the different parameters which were used to enhance self-focusing, higher harmonics, and THz generations.

2.2 Self-Action Effects

After the investigation of self-trapping of light by *Chiao* [24], *Kelley* [55] has reported first time the calculations of stationary self focusing of light which can enhance intensity of light. He has explored the regime where the self focusing is not balanced by the inherent diffraction phenomenon. *Piekara et al.* [56] have extended the study of *Chiao* [24]. They have reported the theoretical investigation on self-trapping for higher order of electric field that is up to sixth power of electric field. *Hora* [57] has reported the self focusing characteristic of laser beam under the effect of nonuniform distribution of intensity of laser beam. He has reported that the ponderomotove force arises due to intensity gradient which further causes self focusing. *Sodha et al*. [58] have observed the self focusing and self trapping in magneto-plasmas by moment theory approach. They have observed that the qualitative results are in good agreement with paraxial theory results. *Mori et al.* [59] have studied the self action effects with the help of 2D PIC (particle in cell) simulation code wave. They have studied three effects, relativistic self focusing, ponderomotive and the filamentation of the laser in plasma. *Anderson and Bonnedal* [60] have analyzed the self-focusing and self-trapping of Gaussian laser beam in plasma by using variational approach. They have claimed the difference between the paraxial and

variational theory. He has also observed that the results obtained for beam width by variational theory exactly follow the moment theory. *Anderson et al.* [61, 62] have found solutions for self-trapping of laser beam when it propagates through nonlinear medium. By using Gaussian beam as a trial function, it has been revealed that variational approach shows good results as compare to paraxial theory which are in good agreement with numerical outcomes. *Chen* [63] has observed the self-trapping of laser beam in a saturable nonlinear medium. He has disclosed that the self trapping power is highly dependent on the effective propagation constant. *Desaix* [64] has first time explained the collapsing mechanism of laser beam by variational theory. It has been observed the variational theory can abolish the inaccuracy in results obtained by paraxial ray theory. *Karlsson and Anderson* [65, 66], have applied variational approach to study the nonlinear dynamics of super-Gaussian beam through nonlinear parabolic-index optical fiber. The full explanation about longitudinal phase and amplitude of field of laser beam has been conveyed. Further, the comparison between Gaussian and super-Gaussian laser beam profiles has been incorporated. *Dimitrevski et al.* [67] have applied the variational method for achieving the stationary solution for super-Gaussian laser beam propagating through cubic quintic medium. The outcomes by variational theory are well satisfied with the numerical results. *Chen and Wang* [68] have investigated the nonlinear dynamics of Laguerre-Gaussian (LG) laser in cubic quintic medium with the help of variational theory. They have represented that the nonlinear dynamics results by variational theory match with the simulation results. *Nanda et al.* [69] have studied the relativistic self –focusing of Hermite-cosh-Gaussian beam in collision-less plasmas by applying paraxial ray approximation. It has been investigated that relativistic self-focusing can be stronger for mode $m = 0$ and 1. *Ianetz et al.* [70] have predicted the propagation of asymmetric Gaussian beam through absorbing medium. The NLSE has been solved by using variational method for self-focusing of laser beam. They have introduced new phenomenon 'beats' during observing the self-focusing and self-defocusing behavior of laser beam. *Wani and Kant* [71] have analyzed self-action effects of chirped Guassian laser beam in collisionless plasma with linear absorption by paraxial approach. They have reported that self-focusing and de-focusing can be controlled

by the chirp parameter of the laser beam. *Gupta and Singh* [72, 73] have studied first time the propagation of quadruple laser beam through collisionless plasmas and cubic quintic nonlinear medium by using moment theory. They have reported that the self-focusing can be increased by controlling the ratio of position coordinate to the initial spot size of laser beams. *Purohit et al.* [74] have reported the impacts of two Cosh-Gaussian laser beams on each other during propagation in collisionless plasma. They have studied the nonlinear dynamics of both beams by taking relativistic and Ponderomotive nonlinearity into consideration. Further, the comparison study of Cosh-Gaussian and Gaussian laser beam has been also presented in this work. *Kaur et al.* [75] have used paraxial ray approximations for the investigation of self-action effects of Hermite-cosh-Gaussian laser beam in a non-uniform rippled plasmas. Under the effect of relativistic nonlinearity the self focusing and defocusing is studied and it has been reported that for mode 0 and 1, with increase in de-centered parameter of beam the self-focusing is enhanced up-to several Rayleigh length. Whereas for $m = 2$ the diffraction of beam is dominated. *Yadav et al.* [76] have investigated the phenomenon of self-focusing of q-Gaussian laser beam. They have observed that self focusing of q-Gaussian laser beam in stronger than the Gaussian laser beam. They have also mentioned that q-Gaussian laser beam can generate EPW with high amplitude which can be used to accelerate electron with high energy. *Walia and Singh* [77] has studied nonlinear dynamics of laser beam in plasma under the effects of relativistic and Ponderomotive nonlinearities. They have reported the comparison of Cosh-Gaussian laser beam in quantum and relativistic plasma. *Kant and Thakur* [78] have presented a theoretical study on LG laser beam in relativistic plasma. They have applied the exponential ramp to enhance the self focusing of laser beam. They have promised that their study may be applied in laser-driven fusion.

2.3 Higher Harmonics Generation

Bobin et al. [79] have explained that the harmonics generation are due to nonlinear electron current and density gradient of plasma which are produced when intense laser light passes through plasma. They have reported $2\omega_0, \frac{3}{2}\omega_0, \frac{1}{2}\omega_0$ (ω_0 is the laser frequency)

and further observed the parametric excitation of longitudinal plasma wave. *Burnett et al*. [80] have shown experimentally that interaction of CO_2 laser beam with solid generates harmonics. They have reported a series of first six harmonics generation in the line of backscattered radiations when laser interacts with solid target. *Sprangle et al*. [81] have investigated an optical guiding, nonlinear plasma wake field and coherent harmonics generation of intense laser beam in plasma. It has been explained that harmonics generation are most efficient in case of short laser pulse and harmonics amplitude can be increased by high amplitude of wake-field. *Rax and Fisch* [82] have disclosed the method of generation of third harmonics by the ultrahigh laser pulse and plasma. It has been observed that plasma is efficient media for harmonics generation. *Parashar and Pandey* [83] have predicted the generation of second harmonics by propagating high power laser through plasma. They have explained that phase matching condition can be achieved by ripple density which further enhances the yield of second harmonics generation. *Esarey et al.* [84] have revealed that the relativistic harmonics amplitude is high when the laser plasma interaction length is an integral multiple of phase detuning length. *Malka et al.* [85] have observed first time the second harmonics in forward direction. It has been further reported stokes and anti-stokes lines which are named as forward Raman scattering. This is produced due to nonlinear interactions between SHG and the relativistic plasma electrons wave. *Jha et al.* [86], have studied the propagation of laser pulse through uniformly magnetized plasma and found a scheme for SHG. It has been reported that the conversion efficiency is increased as the magnetic field is increased. *Rajput et al.* [87] have investigated the generation of resonant third harmonics by laser pulse and plasma under the effect of wiggler magnetic field. It has been observed that amplitude of third harmonics generation can be increased by applying the wiggler field. This field provides the additional angular momentum to the photon of third harmonics. *Singh and Walia* [88] have observed the self-focusing of Gaussian laser beam through collision-less plasma. The density gradient produced by Ponderomotive force generates electron plasma wave (EPW). The EPW interacts with laser beam which leads to second harmonics generation. Whereas, *Singh and Walia* [89] have further reported the method for second harmonics generation by Gaussian laser beam and

collisional plasma. In collisional plasma, the electrons are heated non-uniformly which results in plasma wave. The second harmonics are generated due to the laser and plasma interactions. *Singh and Gupta* [90] have studied theoretically that the propagation dynamics of q-Gaussian laser beam through preformed collision-less plasma channel by using the moment theory. It has been predicted that self-focusing of q-Gaussian laser beam increases with decrease in q value. It has been reported that the harmonics yield becomes maximum for q-Gaussian laser beam as compare to the Gaussian laser beam. *Singh and Gupta* [91] have studied the impact of relativistic self-focusing on second harmonic generation. They have considered that when a q-Gaussian beam passes through the preformed parabolic plasma the electrons density perturbation of plasma results in second harmonic generations. They have observed that the yield of harmonic generation is maximum for q-Gaussian as compare to the Gaussian beam and q-Gaussian is more suitable laser beam for SHG. *Singh and Gupta* [92] have utilized moment theory for investigation of relativistic self-focusing effect of cosh-Gaussian beam in under-dense plasma. The impact of relativistic self-focusing on second harmonics generation has also been studied. They have revealed that the self focusing and second harmonics are increased when decentered parameter of laser beam lies between zero and one. *Gupta et al.* [93] have reported a method for SHG in collisional plasma. They have studied the effects of a preformed parabolic plasma channel and nonlinear absorption on SHG. They have revealed that the nonuniform intensity distribution of the q-Gaussian laser beam excites an EPW. The second harmonic of the pump beam is generated when EPW interacts with the pump beam. It has been reported that a preformed channel can be used to control the effect of nonlinear absorption. *Singh et al.* [94] have investigated theoretically with moment theory the generation of second harmonics of Cosh-Gaussian laser beam in collisional plasma. The authors have taken nonlinear absorption into account. They have studied the self-focusing of the laser beam and its effects on SHG in detail. They have observed that a Cosh-Gaussian laser beam is more suitable than a Gaussian laser beam for suppressing nonlinear absorption and increasing the efficiency of SHG. Recently, *Bhatia et al.* [95] have studied the SHG of LG laser beam in plasma. They have incorporated relativistic

nonlinearity and density transition for their analytical study. They have reported that self focused LG laser interacts with the induced EPW wave and generate second harmonics of the laser beam. *Pathak et al.* [96] have revealed the SHG by using relativistic and Ponderomotive nonlinearity of the plasma. They have used the rippled density plasma to obtain the phase matching condition for generation of second harmonics of laser beam. They have disclosed that instead the ripple density the yield of SHG can be enhanced by increasing the self focusing of laser beam.

2.4 Generation of THz Radiations

Ample investigations have been performed for generation of THz radiation. In 1990s, *Hamster et al.* [97] have observed THz generation due by the interactions of two laser pulses with solids and gases experimentally. On comparing with gas target, they have reported that the interaction of TW laser pulses with solid target produces more intense THz radiation along with X-rays and electrons of MeV energies. Onwards, *Hamester et al.* [98] have followed wake field method and generated THz radiation by the interactions of femtosecond laser pulse with solid. It has been observed that MeV X-rays and electrons of 0.6 MeV are associated with $0.5\mu J$ THz radiations. *W.P. Leemans et al.* [99] have revealed, generation of THz from high density solid-targets under relativistic regime has been investigated. It has been found that the relativistic effects come into picture when the laser of intensity is more than 10^{18}W/cm^2 is used to generate THz radiation. The relativistic electrons beams from laser-plasma based accelerators have been utilized to generate coherent THz radiation. *Thomas et al*. [100] have investigated that excitation of THz radiation by ponderomotive force with uniform plasma can be enhanced by using inhomogeneous (corrugated) plasma channel. Further, it has been revealed that the external electric field increases the oscillations of electrons which increase the amplitude of THz radiations linearly. *Bhasin et al.* [101] have explained the THz generation by propagating two collinear laser beams which induce ponderomotive force on the electrons of magnetized clustered plasma. *Malik et al.* [102] have revealed the method of generating THz radiation by two spatial-Gaussian beams in periodic ripple density plasma. They have

explained that large amplitude of normalized ripple density can be utilized for obtaining intense THz radiation. It is further extended by *Malik et al.* [103] *by* applying perpendicular magnetic field on the rippled plasma. The applied magnetic field indirectly produces the perturbation in electron density of the plasma which helps to increase the nonlinear current. The ripples of plasma help to obtain the phase matching condition in results of which the efficiency for THz generation is enhanced. *Malik and Malik* [104] have shown work which improves THz radiations up to efficiency of the order of 0.006. It can be obtained by propagating two super Gaussian laser beams of higher beam index and smaller beam width through rippled plasma. *Varshney et al.* [105] have revealed the THz generation of 0.015 efficiency by beating of extraordinary mode lasers in periodic rippled plasma under the effect of external magnetic field. *Sharma and Singh* [106] have observed the nonlinear dynamics of two Gaussian laser beams in plasma in collisional plasma. They have investigated the effects of self-action effects and applied electric field on THz generation. In collisional plasma where electron-ion collision is operative, the THz yield can be enhanced by two to three times. *Singh and Malik* [107] have found scheme for THz generation by propagating two super-Gaussian laser beams through collisional plasma where electron-neutral collision has been taken into account. It has mentioned that THz generation can be controlled by index of super-Gaussian laser beam. The effect of transverse magnetic field on THz radiation has been further evaluated by *Singh et al*. [108]. They have reported that the negative effect of electron-neutral collisions can be recovered by higher value of index of laser. *Hussain et al.* [109] have investigated THz generation by beating of dark hollow laser beams in magnetized collisionless plasma. They have considered a pre-excited electron plasma wave (EPW) for the enhancement of THz radiation. It has been reported that small beam width and density perturbation can enhance the conversion efficiency. Moreover, with increase in the width of the central shadow region the extent of self-focusing as well as the intensity of THz radiation is increased. *Hussain et al.* [110] have explained method for THz generation by beating of two super Gaussian beams in collisional plasma under the effect of dc electric field. It has been revealed in detail about the dependence of THz radiation on density of plasma, transverse

static electric field, index of super Gaussian beam and length of plasma column. *Sobhani et al.* [111] have reported the effect of pump depletion and cross focused Laguerre-Gaussian (LG) lasers on twisted THz radiations. They have found that the presence of pump depletion reduces the ponderomotive force on the electrons of plasma. Hence, THz field is saturated along the propagation distance. *Varaki and Jafari* [112], have reported generation of THz radiation by propagating two cosh-Gaussian laser beams through collisional plasma. It has been revealed that under the effect of decentered parameter and wiggler field the THz power can be enhanced and the peak of the laser can be controlled. *Varshney et al.* [113] have found THz generation by two co-axial cosh-Gaussian laser beams and collisional plasma under the effect of magnetic field. It has been found that decentred parameter of cosh-Gaussian laser beam, ripples of plasma and the applied axial magnetic field can be used to enhance the THz field. *Safari et al.* [114], have come with new method of THz generation in which propagation of two different laser beams that are HG (Hermite-Gaussian) and LG (Laguerre-Gaussian) through magnetized collisional plasma is taken into account. It has been claimed that the generation of THz radiation can be enhanced by 4.5% by using different beam profiles. *Ayoob et al.* [115] have revealed the method for THz generation by propagating cosh-Gaussian and top-hat laser beams in an underdense plasma. They have investigated the impacts of laser profiles, frequency of collisions and magnetic field on THz generation. They have represented the comparison between the yield of cosh-Gaussian and top-hat laser beam and reported that top-hat laser profile can produce higher pondermotive nonlinearity, hence higher yield of THz radiation. *Motahareh et al.* [116] have developed a scheme for THz generation by the propagation of laser beams in warm collisional plasma under the effect of magnetic field. The have produced the resonant THz field by optimizing the values of magnetic field, collisional frequency, plasma density and chirp-ness of laser beams.

2.5 Generation of Surface Plasma Waves

In 1902, after the diffraction grating experiment performed by *Wood* [117], the step was taken towards surface plasma wave (SPW). He found the bright and dark bands of

reflected light. *Rayleigh* [118] had theoretically represented these in 1907 and reported that this pattern of dark and bright bands as new spectral lines. *Fano* [119] had suggested theoretically that the pattern observed by Wood are the surface plasma waves produced at grating surface. These SPWs are similar to electromagnetic oscillations that excited at the dielectric-medium interface where relative permittivity switches sign. *Stern and Ferrell* [120] have examined the dispersion relation of surface plasma wave at metal-dielectric interface. *Ritchie* [121] have studied the interactions of fast electrons and the conduction electrons of the metal. The author has shown that incident fast electrons cause the plasma oscillations in an infinite foil. In 1968, *Otto* [122] had used prism metal configuration for attenuated total reflection (ATR) for production of SPW which was further modified by *Kretschmann and Raether* [123] by depositing metallic layer of 50nm at the base of prism. *Raether* [124] have reported that the incident electromagnetic wave on the base generate SPW along the metal-free space interface with approximately hundred percent efficiency. It has been reported by *Lee* [125] that the resonant surface plasma waves can be excited by falling the light at the metal surface. The phase matching condition can be achieved by the laser parameters for the excitation of SPW. *Yasumoto* [126] has analyzed theoretically the shining p-polarized light obliquely on the vacuum- unmagnetised plasma interface. He has found the light decays into two surface plasma waves. *Singh and Tripathi* [127] have revealed the beating method for the generation of SPW and ablation of material. They have explained that the both lasers impose the pondermotive force on the electrons of metal and generate SPW at frequency difference in skin layer. Then it heats the electrons and ablation of material is taken place. *Aliev and Brodin* [128] have observed the generation of SPW in an inhomogeneous solid state plasma. They have investigated the interactions of p-polarized wave and plasma boundaries. The growth of SPW due to p-polarized light is enhanced by taking thermal effects into account. *Macchi et al.* [129] have investigated the surface electrons oscillations by impinging the laser pulse on over-dense plasma. They have developed a new parametric instability that depends upon the decay of 1D oscillations into two electrons surface waves. *Parashar et al.* [130] have revealed that as the laser pulse strikes the metallic target the overdense plasma is created. The excitation of SPW for the

planar surface has been studied by stimulated Compton scattering. They have reported that the perturbation in density due to Ponderomotive force and the oscillatory oscillation of the electrons due to laser pulse couple together and produce nonlinear current. Hence, the surface wave if generated. *Raynaud et al*. [131] have presented the significance of pulse duration and spectral width of the laser pulse for the generation of SPW and emitted fast electrons from over-dense plasma under relativistic regime. With the help of 2D-particle-in-cell (PIC) simulations, it has been reported that the energy and charge of the emitted electron bunched are more dependent on energy of laser instead of profile of laser pulse. *Kaur et al*. [132] have studied the excitation of SPW by using femtosecond laser and metal sheet. They have reported that the generated SPW decays exponentially and is helpful to accelerate the electron. *Marini et al.* [133] have studied generation of SPW in over-dense plasma with intensity 10^{20} W/cm^2. They have used the PIC simulation for explaining that the electron acceleration at ultra-high intensity can be possible with SPW. They have shown that the density of plasma and shape of plasma surface play vital role in excitation of SPW.

2.6 Filamentation of Laser Beams

Kaw et al. [134] have presented theoretically the formation of filaments in collisionless plasma. They have explained filamentation and self-trapping of laser beam can be achieved by pondermotive nonlinearity of plasma. *Salimullah et al.* in 1987 [135] have explained about the filamentation of a circularly polarized Alfven wave by using compensated semiconductor (Ge). They have explained the differences of semiconductor plasma and gases plasma. They have revealed that holes produce higher nonlinearity as compare to the electrons of compensated semiconductor plasma. *Stenflo and Shukla* [136] have investigated filamentation of em waves in narrow band gap semiconductors under the effect of magnetic field. They have explained that the nonparabolicity of conduction band and magnetic field perturbation arise due to the radiation pressure which further produce filamentation. *Young* [137] has revealed the filamentation can be created by propagation of a laser beam of nonuniform intensity through plasma and filamentation can further

produce density perturbation. He has disclosed experiment technique for detecting filaments and intensities of filaments and he explained that these can be detected by identifying the density perturbation caused by filamentation of laser beam. *Shukla* [138] has reported analytically the filamentation of two coupled em waves plasmas. He has taken into account the relativistic effect and density perturbation due to Ponderomotive force. He has predicted that the instability is larger for two coupled em waves rather than single pump wave. *Braun et al.* [139] have revealed experimentally by using Ti: $Al_2 O_3$ CPA laser that due to the balance between the plasma refraction and natural diffraction the laser pulse get self-channeled into filaments. They have reported the filaments of intensity $7 \times 10^{13}\ W/cm^2$ can propagate to 20 meter distance. *Vidal and Johnston* [140] have used nonlinear Schrodinger wave equation for understanding multiple filaments of electromagnetic wave. They have reported, self focusing of whole beam is known as multiple filaments. They have introduced a parameter with which one can control the number of filaments. *Johnston et al.* [141] have further implemented nonlinear Schordinger wave equation for investigating different aspects of laser plasma filmentation due to Ponderomotive nonlinearity. They have explained about one dimensional and two dimensional geometry of the filamentation and have told that filaments retain their properties once it is formed. They have followed the variational theory for understanding the filamenatation. *Brodeur et al.* [142] have reported that the filament in air is end at diffraction length of the laser when ionization of medium is taken into account. They have mentioned that obtained results are similar to the moving focus model of self-focusing in which the filaments are formed from the continuous focal points of self-focusing. It has been observed that experimental and simulation results are in geed agreement with the moving focus model rather than self-channeling model. *Berge et al.* [143] have investigated experimentally and numerically the filamentation of TW laser pulse in air. The randomly emitted filaments helps to propagate laser pulse to more distance. Further, they have explained that the defects in spatial distribution of high intense laser beam results in filaments. *Singh et al.* [144] have investigated filamentation of laser beam in magnetized plasma by using the extended paraxial ray theory. Further they have reported that THz

radiation is induced at the frequency difference of laser beam and the ripple of plasma. They have further investigated filamentation impacts on the generation of THz radiation. *Hassan et al.* [145] have studied the filmentation of laser (CO_2) beam when it passes through a collisionless plasma. They have considered non-paraxial theory and relativistic nonlinearity to investigate filamentation. They have also shown that in paraxial region the self focusing is greater than non-paraxial region.

Chapter 3

Amplitude Structures of Laser Beams

3.1 Introduction

One of the important characteristic parameter of the laser beam is its spatial amplitude structure over its cross section [146], as laser beams with different spatial amplitude profiles behave differently in nonlinear media [38, 55, 67-79, 147]. From review of literature it has been observed that most of the earlier theoretical investigations revealing the effect of self-action phenomena (i.e., self focusing/defocusing, self trapping) of intense laser beams on generation of their new frequency components in nonlinear media have carried out for ideal Gaussian amplitude structure of the laser beam [22, 24]. However, the experimental investigations carried out to measure the amplitude structures of laser beams (e.g., Vulcan petawatt laser at Rutherford Appleton laboratory) indicate that even the laser system is operating in its fundamental TEM_{00} mode, the amplitude structure over the cross section of the laser beam is not having ideal Gaussian profile [148]. A significant amount of laser energy has been found to be present outside the full width half maximum (FWHM) of the distribution i.e., compared to the Gaussian profile, the wings of the intensity profile of the laser system have been found to be expanded. By fitting into experimental data, it has been suggested by Nakatsutsumi et al. [149] that the actual amplitude structure over the cross section of the laser beam can be modeled by q-Gaussian distribution [150]. Hence, in the present investigation to get more realistic results on the effects of self focusing of laser beams on HHG and THz generation in nonlinear media, the amplitude structure over the cross section of the laser beam has been considered to be q-Gaussian.

In contrast to ideal Gaussian and q-Gaussian laser beams, now a days a new class of laser beams known as flat top laser beams [65, 72, 73, 92] are gaining significant interest among researchers. These beams possess uniform irradiance over their cross section and thus possess more power and lesser divergence compared to the Gaussian and q-Gaussian beams. Thus, such laser beams may help to enhance the power of the generated harmonics

as well as THz radiations [90-92, 150, 152]. Mathematically the amplitude structure over the cross section of such beams is described by supper Gaussian function. But again supper Gaussian approximation is an ideal concept. The laser beams with flat top irradiance [153, 154] produced in laboratory, have a uniform irradiance only up to some finite extent, after which the irradiance starts decreasing radially, as in case of Gaussian or q-Gaussian irradiance. The amplitude structure of such beams can be modeled by Cosh-Gaussian (ChG) function or Quadruple-Gaussian (Q.G) functions.

Thus, in the present investigation three types of amplitude profiles for the laser beams have been investigated:

1. q-Gaussian
2. Cosh-Gaussian (ChG)
3. Quadruple-Gaussian (Q.G)

Following sections describe the physical characteristics (amplitude profile, effective beam width, spectral width etc.) of these laser beams.

3.2 q-Gaussian Laser Beams

The transverse amplitude structure over the cross section of q-Gaussian laser beam [148-151] at the plane of incidence into the medium is given by

$$E_0(r) = E_{00}\left(1 + \frac{r^2}{qr_0^2}\right)^{-\frac{q}{2}} \tag{3.1}$$

where, $r = (x, y)$ is the radial distance from the beam axis, r_0 is the radius of the beam at the plane of incidence and E_{00} is the axial amplitude of the electric field of beam. The key parameter q is related to the deviation of amplitude structure of the beam from ideal Gaussian beam. Thus, the parameter q is termed as deviation parameter. Its value varies from laser system to system and for a given laser system it can be obtained by fitting into the experimental data. The amplitude structure of the laser beam deviates from ideal Gaussian profile due to cavity imperfections like misalignment of the end mirrors, nonuniform reflectivity of the mirrors and inclusion of impurities into the gain medium.

Using L Hospital rule of limits it can be seen that $q = \infty$ corresponds to ideal Gaussian profile i.e.

$$\lim_{q\to\infty} E_0(r) = E_{00}e^{-\frac{r^2}{2r_0^2}} \tag{3.2}$$

In order to see the effect of deviation parameter q on the irradiance over the cross section of the beam, I have shown the variation of irradiance over the cross section of the beam with radial distance from its axis for different values of q in fig.(3.1).

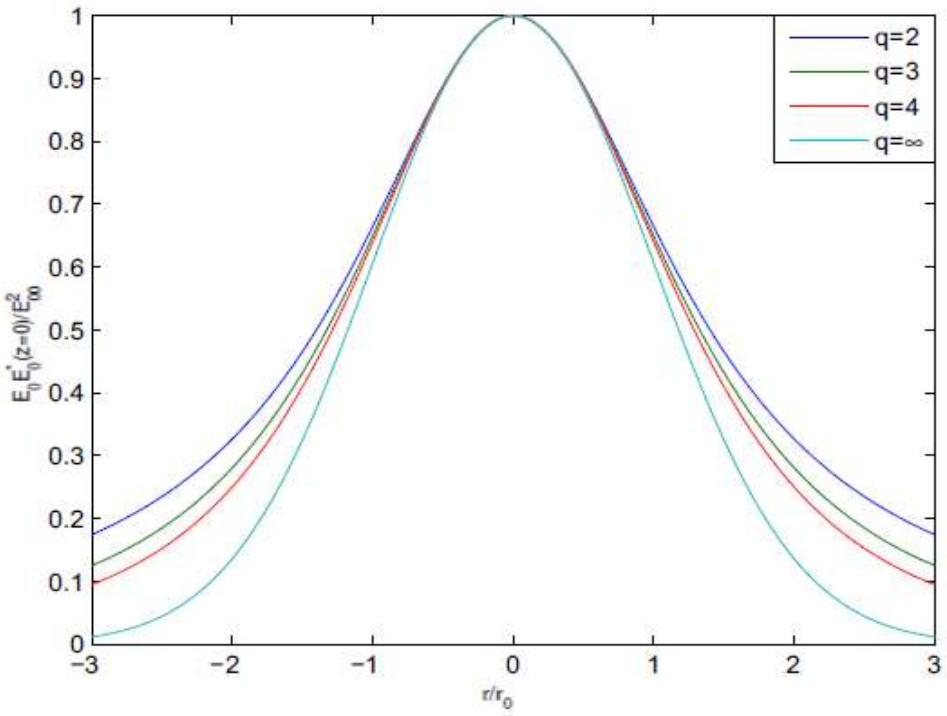

Fig. 3.1: Impact of deviation parameter q on irradiance over the cross section of the laser beam

It can be seen that the deviation parameter q does not affect the irradiance in the axial region of the beam, it only affects the irradiance in the off axial regions as the beams with lower value of q are characterized by expanded wings. These expanded wings correspond to the additional beam energy that gets shifted to the off axial parts of the beam.

Since, during the propagation of the beam through the medium, its beam width does not necessarily remains constant, we can write the instantaneous amplitude structure of the beam at a given point inside the medium as

$$E_0(r,\, z) = \frac{E_{00}}{f(z)}\left(1 + \frac{r^2}{q r_0^2 f^2(z)}\right)^{-\frac{q}{2}} \tag{3.3}$$

where, the function $f(z)$ is currently undetermined parameter and is termed as a dimensionless beam width parameter. Its significance is two-fold: (1) upon multiplication with equilibrium beam width r_0 it gives the instantaneous spot size of the beam at a given location inside the medium. (2) upon division with amplitude it gives the measure of instantaneous intensity of the beam.

3.2.1 Effective Beam Width of q-Gaussian Laser Beams

Any laser beam is not having a sharp boundary i.e., its intensity extends up to infinity; however after some finite distance from the beam axis it becomes insignificant. Hence, the effective beam width of a laser beam is defined in root mean square sense as

$$\langle a^2 \rangle = \frac{1}{I_0}\iint E_0\, r^2 E_0^* d^2 r \tag{3.4}$$

where,

$$I_0 = \iint E_0\, E_0^* d^2 r \tag{3.5}$$

$$d^2 r = r dr d\theta$$

Hence, the effective laser beam width of q-Gaussian beam is obtained as

$$\langle a^2 \rangle = r_0^2 f^2 \left(1 - \frac{1}{q}\right)^{-q} \tag{3.6}$$

The r.m.s beam width of a similar Gaussian beam is $r_0 f$. Thus, the ratio of r.m.s beam widths of q-Gaussian and Gaussian beam can be written as

$$\Sigma = \left(1 - \frac{1}{q}\right)^{-q} \tag{3.7}$$

In order to see the effect of deviation parameter q on effective beam width of the laser beam, the variation of Σ with q has been shown in fig.(3.2). It can be seen that with increase in the value of deviation parameter q the effective beam width of the beam decreases. This is due to the shifting of intensity of the beam towards in off axial parts with increase in the value of q. Thus, it can be seen that ideal Gaussian laser beams possess minimum beam width. As, the diffraction broadening of the laser beam varies inversely with its effective beam width, it can be predicted that compared to the beams with lower value of deviation parameter q, ideal Gaussian beams suffer more diffraction broadening while passing through vacuum or through a linear medium.

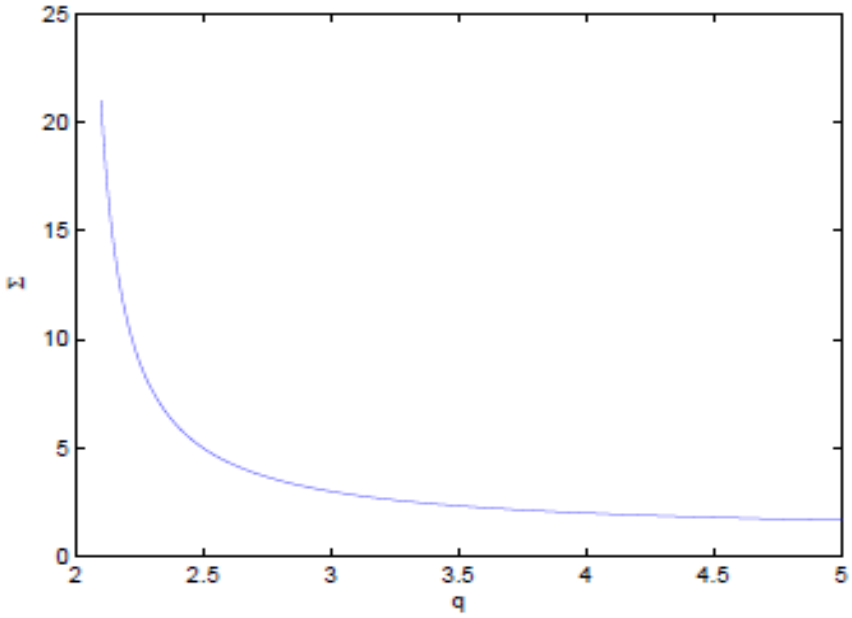

Fig. 3.2: Variation of effective beam width of the laser beam with q

3.3 Cosh-Gaussian (ChG) Laser Beams

The amplitude structure over the cross section of ChG laser beam is given by [153]

$$E_0(r,\, z) = \frac{E_{00}}{f} e^{-\frac{r^2}{2r_0^2 f^2}} \cosh\left(\frac{b}{r_0 f} r\right) \tag{3.8}$$

Here, the parameter b associated with cosh function is known as cosh factor. Eq.(3.8) can also be written as

$$E_0(r,\, z) = \frac{E_{00}}{2f} e^{b^2} \left[e^{-\left(\frac{r}{r_0 f} - b\right)^2} + e^{-\left(\frac{r}{r_0 f} + b\right)^2} + 2e^{-\left(\frac{r^2}{r_0^2 f^2} + b^2\right)} \right]^{\frac{1}{2}} \tag{3.9}$$

From this equation it can be seen that ChG laser beams can be realized experimentally by the in-phase superposition of two otherwise identical Gaussian beams whose intensity maxima instead of lying at beam axes lie at coordinates $(\pm\frac{b}{2}, 0)$, respectively. Thus, the factor b is associated with the displacement of the intensity maxima of the constituting beams from their axes. Thus, the parameter b is also known as decentered parameter.

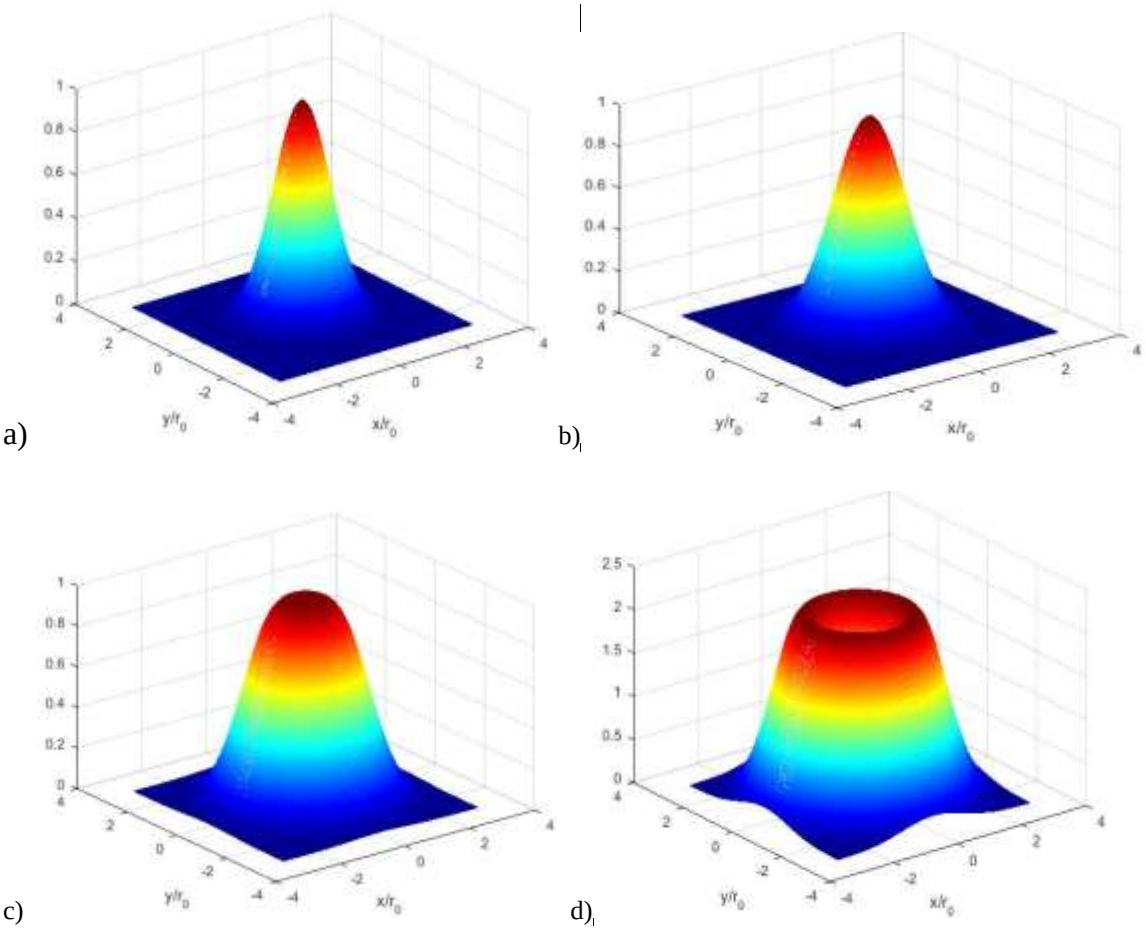

Fig 3.3: 3D intensity profile of ChG laser beam for a) *b*=0 b) *b*=0.5 c) *b*=1.0 d) *b*=1.45

In order to see the effect of decentered parameter b on the irradiance over the cross section of the beam (i.e., its intensity profile) I have plotted 3-D intensity profile of the

ChG laser beam for different values of b in fig.(3.3). The corresponding projections of the intensity profile along the transverse beam axes are shown in fig.(3.4).

It can be seen that for $0 \leq b \leq 1$, with increase in the value of decentered parameter b the irradiance over the beam cross section becomes more and more uniform. However, for $b > 1$, a central dark region appears in the beam profile. Thus, the parameter b acts as a control over the beam profile i.e., by optimizing this decentered parameter b one can obtain desired irradiance over the beam cross section [92, 112,155].

a)

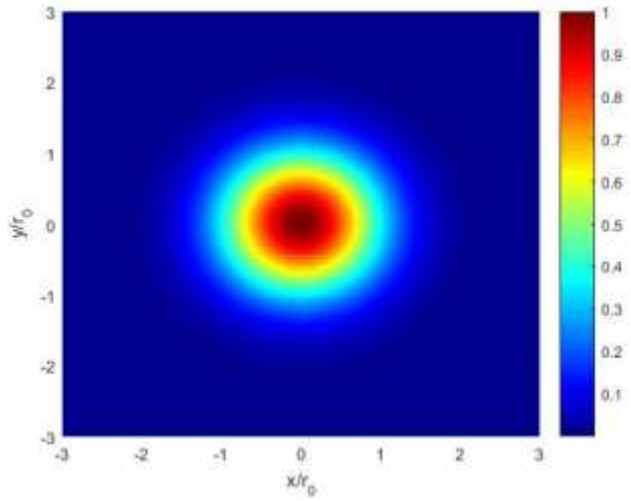

b)

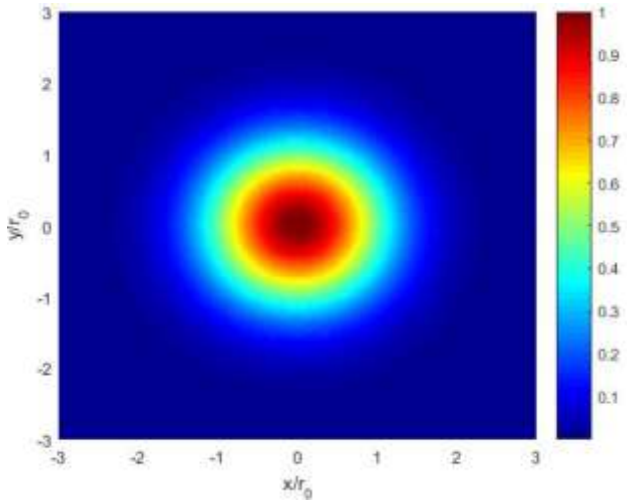

c)

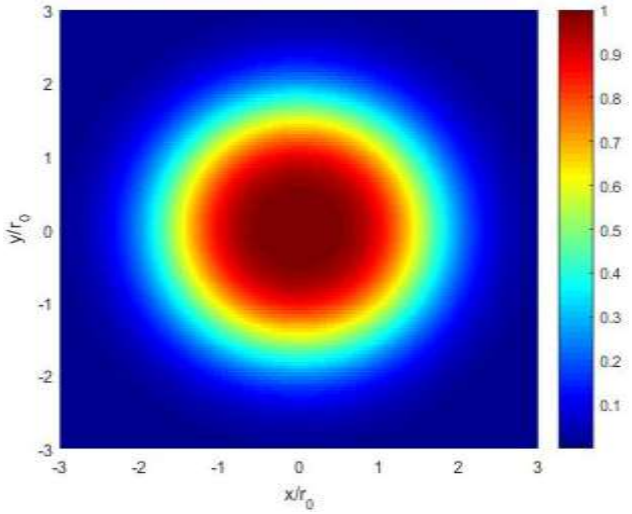

d)

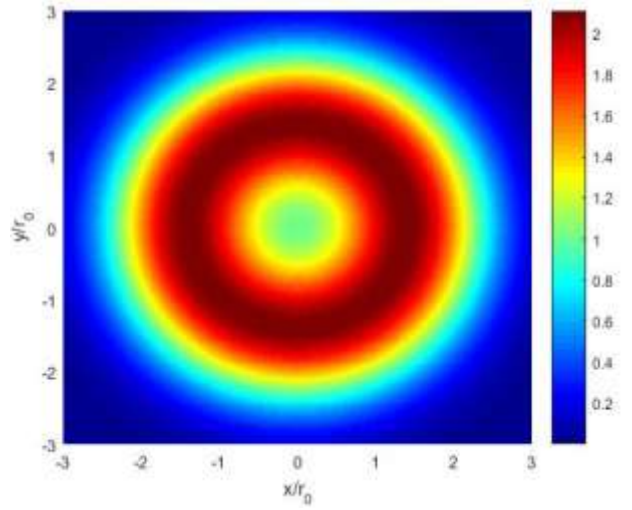

Fig.3.4: The transverse view of ChG laser beam for a) b=0 b) b=0.5 c) b=1.0 d) b=1.45

3.3.1 Effective Beam Width of ChG Laser Beams

Using eq.(3.8) in eq.(3.4) and (3.5) the effective beam width of ChG laser beam has been obtained as

$$< a^2 \geq r_0^2 f^2 (1 + b^2) \tag{3.10}$$

Thus, the ratio of effective beam width of ChG beam to that of Gaussian beam can be written as

$$\Sigma = (1 + b^2) \tag{3.11}$$

Variation of effective beam width of ChG laser beam with decentered parameter has been depicted in fig.(3.5). It can be seen that effect of decentered parameter b of ChG laser beam is to increase its effective beam width. This is due to the shifting of axial intensity of the laser beam to the off axial regions with increase in the value of b. As, the ChG laser beams possess larger beam widths compared to corresponding Gaussian laser beams, it can be predicted that these beams may help to reduce the beam divergence. This, built the impetus behind selecting ChG laser beams for the generation of coherent radiations with new frequencies.

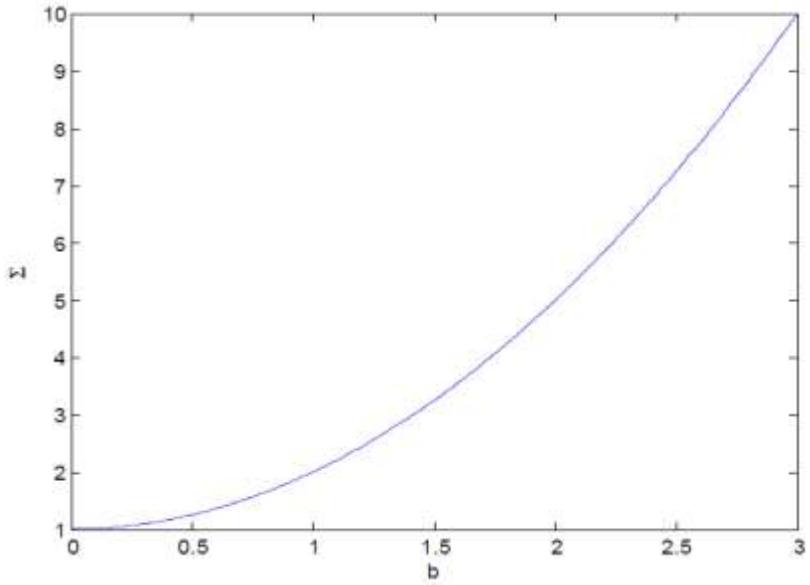

Fig.3.5: Variation of effective beam width of ChG laser beam with decentered parameter

3.4 Quadruple-Gaussian (Q.G.) Laser Beams

Quadruple-Gaussian laser beams also named as multi-Gaussian laser beams and these are produced with the help of four decentered Gaussian laser beam [156, 157]. The intensity maxima of these Gaussian beams are located at coordinates $(x_0, 0), (-x_0, 0), (0, x_0), (0, -x_0)$. The decentered laser beams can be produced in the laboratory by the

reflection of Gaussian laser beams from a spherical mirror whose center is offset from the beam axis. An in phase superposition of these four decentered beams results in Q.G laser beam. The amplitude structure of such laser beams is expressed as

$$A_0(r,\,z) = \frac{E_{00}}{f}\left\{e^{-\frac{(x-x_0f)^2+y^2}{2r_0^2f^2}} + e^{-\frac{(x+x_0f)^2+y^2}{2r_0^2f^2}} + e^{-\frac{x^2+(y-x_0f)^2}{2r_0^2f^2}} + e^{-\frac{x^2+(y-x_0f)^2}{2r_0^2f^2}}\right\} \tag{3.12}$$

The plots in fig.3.6 illustrate that the laser beams for which the value of $\frac{x_0}{r_0}$ lies in the range $0 \leq \frac{x_0}{r_0} \leq 1.5$ possess uniform irradiance over a wider area of their cross section and the area of this uniform illumination region increases with increase in the value of $\frac{x_0}{r_0}$. For $\frac{x_0}{r_0} > 1.50$ the peaks of intensity profile appear in off axial parts of the cross section of the laser beam. Here, surrounded by four off axial peaks, a valley of intensity appears in the axial region of the laser beam.

3.4.1 Effective Beam Width of Q.G Beams

Using the definition of effective beam width given by eq.(3.4), the effective beam width of Q.G laser beam at its focal spot has been obtained as

$$< a_{Q.G}^2 > |_{z=0} = \frac{\sqrt{2}r_0}{\left(1+3e^{-\frac{x_0^2}{2r_0^2}}\right)^{\frac{1}{2}}}\left\{\left(2+2\frac{x_0^2}{r_0^2}\right)+\left(2+\frac{x_0^2}{r_0^2}\right)e^{-\frac{x_0^2}{2r_0^2}}+2e^{-\frac{x_0^2}{2r_0^2}}\right\}^{\frac{1}{2}} \tag{3.13}$$

In deriving Eq. (3.13) use of following standard integrals has been made

$$\int_0^\infty e^{-\frac{(x\mp x_0f)}{2r_0^2f^2}}dx = \frac{\sqrt{\pi}}{2}r_0f\left(1 \pm erf\left(\frac{x_0}{r_0}\right)\right),$$

$$\int_0^\infty e^{-\frac{x^2}{r_0^2f^2}}dx = \frac{\sqrt{\pi}}{2}r_0f$$

$$\int_0^\infty e^{-\frac{((x-x_0f)^2+(x+x_0f)^2)}{2r_0^2f^2}}dx = \frac{\sqrt{\pi}}{2}r_0fe^{-\frac{x^2}{r_0^2}}$$

$$\int_0^\infty x^2e^{-\frac{(x\mp x_0f)^2}{r_0^2f^2}}dx = \frac{1}{4}r_0fe^{-\frac{x_0^2}{r_0^2}}\left\{\pm 2r_0x_0f^2 + (2x_0^2f^2+r_0^2f^2)e^{-\frac{x_0^2}{2r_0^2}}\sqrt{\pi}\left(1 \pm erf\left(\frac{x_0}{r_0}\right)\right)\right\}$$

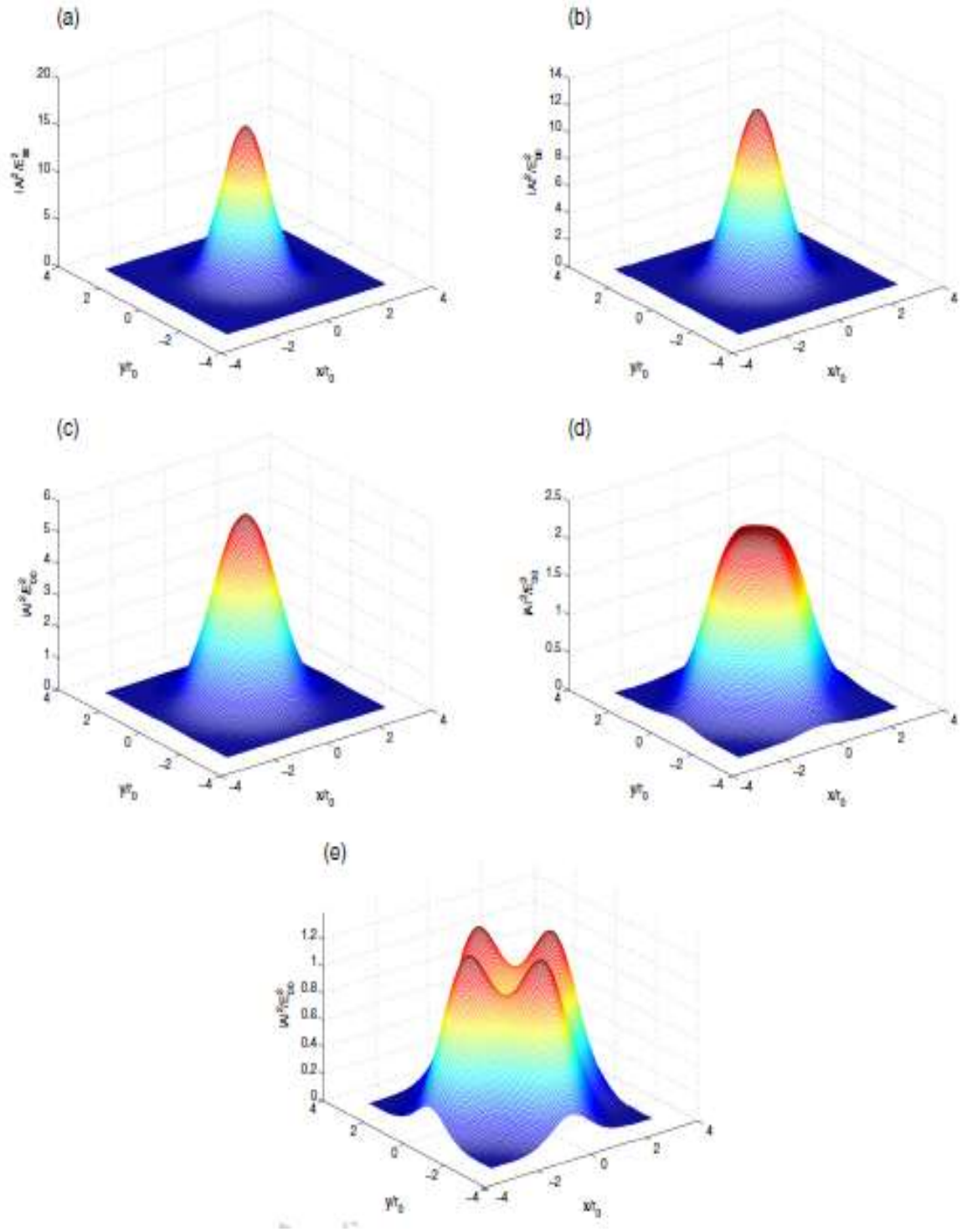

Fig.3.6: 3D intensity profiles of the quadruple laser beam for $\frac{x_0}{r_0}$ =a) 0, b) 0.50, c) 1, d) 1.50 and e) 1.75

The ratio Σ(0) of the r.m.s. beam widths of a Q.G beam to that of a Gaussian beam can be written as

$$\sum(0) = \frac{\sqrt{2}}{\left(1+3e^{-\frac{x_0^2}{2r_0^2}}\right)^{\frac{1}{2}}}\left\{\left(2+2\frac{x_0^2}{r_0^2}\right)+\left(2+\frac{x_0^2}{r_0^2}\right)e^{-\frac{x_0^2}{2r_0^2}}+2e^{-\frac{x_0^2}{2r_0^2}}\right\}^{\frac{1}{2}} \tag{3.14}$$

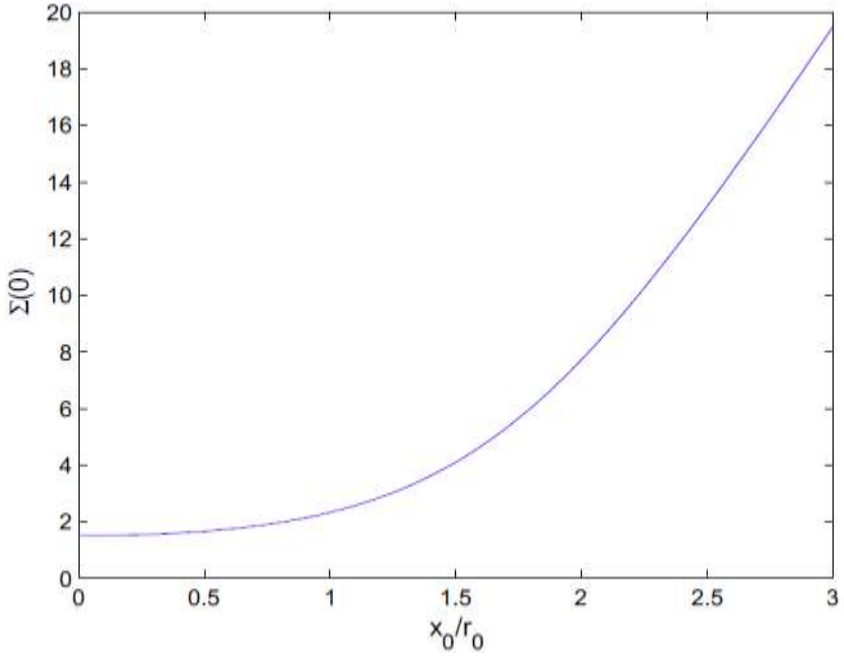

Fig.3.7: Variation of the ration Σ(0) of the r.m.s beam widths of an input Q.G beam to Gaussian beam with $\frac{x_0}{r_0}$

The effect of the parameter $\frac{x_0}{r_0}$ on ratio Σ(0) has been depicted in Fig.3.7. Evidently, compared to the constituent Gaussian beams, Q.G beams with higher values of $\frac{x_0}{r_0}$ are characterized by larger effective beam width. This is due to the fact that with increase in $\frac{x_0}{r_0}$ the intensities of the constituting Gaussian beam get more shifted towards the transverse directions. As a result the Q.G beams with larger values of $\frac{x_0}{r_0}$ possess larger beam widths.

3.4.2 Spectral Width of Q.G Beams

Due to its finite effective beam width, the laser beam behaves as if it is passing through a narrow slit and thus through position-momentum uncertainty ($\Delta x \Delta p_x$=constant)

experiences a spread in its transverse momenta and hence a shift in expectation values of the propagation constant. The r.m.s. spectral width σ_k of the laser beam can be obtained by the Fourier transform of the irradiance profile of the laser beam from coordinate space (x, y) to k space (k_x, k_y) as

$$S(k_x, k_y) = \frac{1}{2\pi}\int_{-\infty}^{\infty}\int_{-\infty}^{\infty} A_0(x, y)e^{-i(k_x x + k_y y)}dxdy \tag{3.15}$$

Using eq.(3.12) in (3.15), one can obtain

$$S(k_x, k_y) = \frac{1}{2\pi}E_{00}r_0^2 f^2 e^{-\frac{r_0^2 f^2\left(k_x^2 + k_y^2\right)}{2}}\left(e^{ix_0 f k_x} + e^{-ix_0 f k_x} + e^{ix_0 f k_y} + e^{-ix_0 f k_x}\right) \tag{3.16}$$

The r.m.s. spectral width of the laser beam in k-space is defined as

$$\sigma_{k,Q.G.} = \sqrt{< k_x^2 > + < k_y^2 >} \tag{3.17}$$

where

$$< k_x^2 > = \frac{\int_{-\infty}^{\infty}\int_{-\infty}^{\infty} k_x^2 S(k_x, k_y)S^*(k_x, k_y)dk_x dk_y}{\int_{-\infty}^{\infty}\int_{-\infty}^{\infty} S(k_x, k_y)S^*(k_x, k_y)dk_x dk_y} \tag{3.18}$$

$$< k_y^2 > = \frac{\int_{-\infty}^{\infty}\int_{-\infty}^{\infty} k_y^2 S(k_x, k_y)S^*(k_x, k_y)dk_x dk_y}{\int_{-\infty}^{\infty}\int_{-\infty}^{\infty} S(k_x, k_y)S^*(k_x, k_y)dk_x dk_y} \tag{3.19}$$

The ratio Σ_k of the spectral widths of two otherwise identical beams with Q.G. and Gaussian irradiance profiles can be written as

$$\Sigma_k = \frac{\sigma_{k,Q.G}}{\sigma_k, G} = \left\{\frac{1 + e^{-\frac{x_0^2}{2r_0^2}}\left(1 + \frac{x_0^2}{r_0^2}\right)}{1 + e^{-\frac{x_0^2}{2r_0^2}}}\right\}^{\frac{1}{2}} \tag{3.20}$$

The variation of Σ_k with $\frac{x_0}{r_0}$ is shown in fig.3.8. It is evident that as a function of $\frac{x_0}{r_0}$ this ratio Σ_k first decreases and then start increasing with a transition occurring at $\frac{x_0}{r_0} = 1.50$. This is due to the fact that the spectral width of an optical beam in (k_x, k_y) space is inversely proportional to the effective area over its cross section (i.e., in (x, y) plane) where

its most of the intensity is concentrated. It can be seen from the surface plots of the laser beam for different values of $\frac{x_0}{r_0}$ (fig.3.6) that the effective area where the most of the laser intensity is concentrated increases with $\frac{x_0}{r_0}$ in the range $0 \leq \frac{x_0}{r_0} \leq 1.50$ and the same decreases with $\frac{x_0}{r_0}$ for $\frac{x_0}{r_0} > 1.50$. Thus, the behaviour of the spectral width of the laser beam in $(k_x;\ k_y)$ shows a transitional dip at $\frac{x_0}{r_0} = 1.50$.

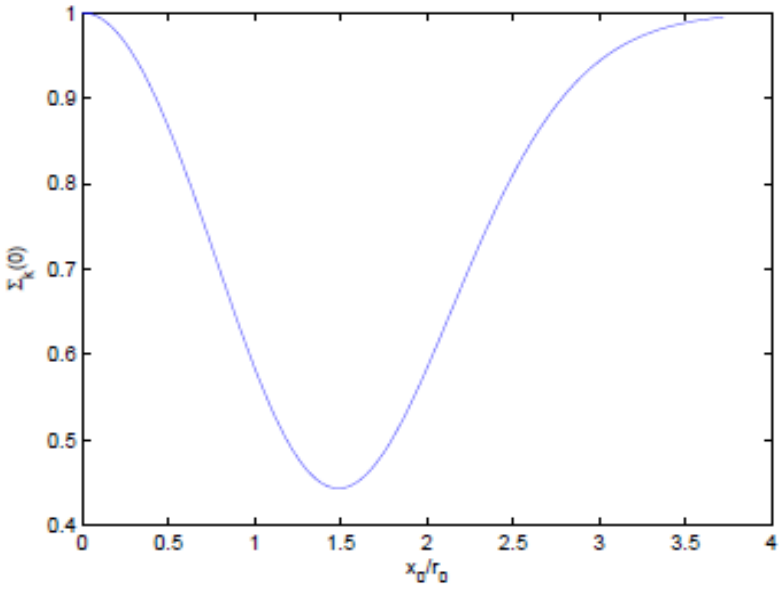

Fig.3.8: Variation of spectral width of Q.G laser beam with $\frac{x_0}{r_0}$

Chapter-4

Nonlinear Interaction of Elliptical q-Gaussian Laser Beams with Plasmas with Axial Density Ramp: Effect of Ponderomotive Force

4.1 Introduction

Laser is one of the most important scientific inventions of the 20th century. When laser made its debut, it was referred to as solution in search of a problem. Today laser has become ubiquitous in consumer technology, from CD players to supermarket checkout scanners. Higher end applications of lasers are also abound. It includes medical diagnostics and treatment [158], nuclear fusion [159], particle accelerators [7], decommissioning of explosives [160] etc. The diversity in the applications of lasers can be felt from the fact that currently this instrument is being used for heating as well as for ultra-intense cooling. The same instrument can produce extremely hot state of matter (plasma) [161] as well as extremely cold state of matter (Bose Einstein Condensate) [162]. The impact of laser on society has changed over time, and is still changing. Already, lasers have provided the preferred solution to an impressive variety of real world situations, and it is expected that in coming years it will keep on enhancing quality of life and will contribute wealth to the world economy.

In most of the applications the laser intensity is the key parameter that decides their ultimate breath. Currently, due to the light's inherent wave property to diffract, the laser power has gotten into bottleneck at the order of few petawatts. Initially it was believed that diffraction of the laser beam cannot be avoided during its propagation neither through vacuum nor through material media. However, *Chiao et al* [24]. showed that in media whose index of refraction depends on the intensity of light, the spreading of an optical beam in principle can be obviated. Hence, the expansion of optical beam due to diffraction is neither inevitable nor irreducible.

Self focusing and self trapping are two examples of nonlinear optical effects which may arise from one of many physical mechanisms. Self focusing describes the formation of a light induced channel in an illuminated material which confines the optical beam. This channel serves as a lens. Self trapping occurs when self focusing substantially exactly

counteracts beam spreading due to diffraction. When this happens, the cross section of the light induced channel remains substantially constant with propagation distance over the distance of the self trapping. There are another similar mechanisms exist under nonlinear regime. For example, a modified self trapping effect occurs when self focusing is somewhat larger than beam spreading due to diffraction. In that case the cross section of the beam vary in an oscillatory way i.e., it remains constant on average. In general, the diameter of a trapped beam may be slightly modulated along the propagation direction, as if wave guiding by the medium were due to a periodic sequence of convex lenses. This results in a channel with diameter variations. In this case, self focusing does not exactly balance diffraction point-by-point along the longitudinal direction. Nevertheless, on average, the beam is trapped.

Self focusing of the laser beams in different nonlinear media has been a hot topic of research since its discovery by Askaryan [22]. In past few years a vast literature has been reported by researchers from all over the globe on various aspects of this phenomenon [60-66]. Early seminal work of Sodha et al. [25], gave a gravest blow to the investigation of this phenomenon for intense laser beams interacting with plasmas in different environments and regimes. Especially in context of inertial confinement fusion this phenomenon is at the vanguard of theoretical as well as experimental investigations [164, 166]. Laser beams differing in irradiance over their cross sections behave differently in plasmas [72]. However, from literature review it has been seen that in previous investigations on self-action effects of elliptical laser beams in plasmas, the laser system operating in lowest order mode i.e., TEM_{00} mode the output beam is ideally Gaussian [164, 165]. However, as discussed in chapter 3, the actual amplitude structure of the laser beam for a laser cavity operating in TEM_{00} mode is described by q-Gaussian distribution [148, 149]. Since, no experimental or theoretical investigation on self focusing of elliptical q-Gaussian laser beams in collisionless plasmas has been reported till date, this gave me a strong motivation to investigate the same.

4.2 Ponderomotive Nonlinearity of Plasma with Density Ramp

Consider the propagation of a laser beam with electric filed vector

$$\boldsymbol{E}(\boldsymbol{r},\boldsymbol{t}) = A_0(x,y,z)e^{-i(k_0 z-\omega_0 t)}e_x \tag{4.1a}$$

$$A_0(x,y,z) = \frac{E_{00}}{\sqrt{f_x f_y}}\left(1+\frac{1}{q}\left(\frac{x^2}{a^2 f_x^2}+\frac{y^2}{b^2 f_y^2}\right)\right)^{-\frac{q}{2}} \tag{4.1b}$$

through a collisionless plasma whose equilibrium electron density is having an upward ramp shaped profile [172] i.e., it increases along longitudinal direction as $n_0(z) = n_0(1 + tan(dz))$. Here, (k_0, ω_0) are the vacuum wave number and angular frequency of the laser beam, respectively,$n_0$is the electron density at $z = 0$, the constant d is associated with the rate of increase of electron density with distance and hence is termed as slope of the density ramp. a and b are the initial widths of the laser beam along the transverse directions and f_x, f_y are the corresponding dimensionless beam width parameters, respectively. Due to the amplitude structure over the cross section of the laser beam given by Eq. (4.1b) the plasma electrons experience a Ponderomotive force that modifies the electron density of the plasma as [25]

$$n = n_0(z)e^{-\frac{e^2}{8m\omega_0^2 T_0 K_0}A_0 A_0^*} \tag{4.2}$$

where, T_0 is the equilibrium electron temperature of plasma and K_0 is the Boltzmann constant. This modified electron density in turn alters the dielectric function $\left(\varepsilon = 1-\frac{4\pi e^2 n}{m\omega_0^2}\right)$ of plasma as

$$\varepsilon = 1-\frac{\omega_{p0}^2}{\omega_0^2}(1+\tan(dz))e^{-\frac{e^2}{8m\omega_0^2 T_0 K_0}A_0 A_0^*} \tag{4.3}$$

Where, $\omega_{p0}^2 = \frac{4\pi e^2 n_0}{m}$ is the unperturbed plasma frequency i.e., the plasma frequency in the absence of laser beam.

Thus, the ponderomotive force on the plasma electrons produced by the laser beam, makes the index of refraction of plasma intensity dependent which in turn due to the spatial dependence of the amplitude structure of the laser beam, resembles to that of graded index fiber. Separating the dielectric function of plasma into linear $(\varepsilon_0)$and nonlinear (ϕ) parts as

$$\varepsilon = \varepsilon_0 + \phi(A_0 A_0^*) \tag{4.4}$$

One can get

$$\varepsilon_0 = 1 - \frac{\omega_{p0}^2}{\omega_0^2} \tag{4.5}$$

and

$$\phi(A_0 A_0^*) = \frac{\omega_{p0}^2}{\omega_0^2}(1 + \tan(dz))\left(1 - e^{-\frac{e^2}{8m\omega_0^2 T_0 K_0} A_0 A_0^*}\right) \tag{4.6}$$

4.3 Evolution of Beam Width of Laser Beam

The propagation of an optical beam through a nonlinear medium characterized by nonlinear dielectric function $\phi(A_0 A_0^*)$is governed by wave equation

$$2ik_0 \frac{\partial A_0}{\partial z} = \nabla_\perp^2 A_0 + \frac{\omega_0^2}{c^2}\phi(A_0 A_0^*) A_0 \tag{4.7}$$

In the present study variational method [30, 60-62] has been used to obtain a semi analytical solution of above NLSE [166, 167] for the nonlinear dielectric function given by eq.(4.6). According to this method the Lagrangian density corresponding to eq.(4.7) is given by

$$£ = i\left(A_0 \frac{\partial A_0^*}{\partial z} - A_0^* \frac{\partial A_0}{\partial z}\right) + |\nabla_\perp A_0|^2 - \frac{\omega_0^2}{c^2}\int^{A_0 A_0^*} \phi(A_0 A_0^*)\, d(A_0 A_0^*) \tag{4.8}$$

Substituting the trial function given by Eq. (4.1b) in Lagrangian density and integrating over the entire cross section of the laser beam and one can get the reduced Lagrangian as $L = \int £\, d^2 r$. The corresponding Euler-Lagrange equations

$$\frac{d}{dz}\left(\frac{\partial L}{\partial\left(\frac{\partial f_{x,y}}{\partial z}\right)}\right) - \frac{\partial L}{\partial f_{x,y}} = 0 \tag{4.9}$$

give

$$\frac{d^2 f_x}{dz^2} = \frac{1}{2k_0^2 a^4}\frac{1}{f_x^3}\left(1 - \frac{1}{q}\right)\left(1 - \frac{2}{q}\right)\left[\left(1 + \frac{1}{q}\right)^{-1} + \left(\frac{\langle L_1\rangle}{E_{00}^2} f_x f_y + \frac{2E_{00}^2}{f_x^2 f_y}\frac{\partial\langle L_1\rangle}{\partial f_x}\right)\right] \tag{4.10a}$$

$$\frac{d^2 f_y}{dz^2} = \frac{1}{2k_0^2 b^4}\frac{1}{f_y^3}\left(1 - \frac{1}{q}\right)\left(1 - \frac{2}{q}\right)\left[\left(1 + \frac{1}{q}\right)^{-1} + \left(\frac{\langle L_1\rangle}{E_{00}^2} f_x f_y + \frac{2E_{00}^2}{f_x f_y^2}\frac{\partial\langle L_1\rangle}{\partial f_y}\right)\right] \tag{4.10b}$$

where

$$\langle L_1\rangle = \frac{\omega_0^2}{c^2}\int\left(\int^{A_0 A_0^*} \phi(A_0 A_0^*) d(A_0 A_0^*)\right) d^2 r$$

The set of eqs.(4.10) can be reduced to

$$\frac{d^2 f_x}{dz^2} = \frac{1}{2k_0^2 a^4}\frac{1}{f_x^3}\frac{\left(1-\frac{1}{q}\right)\left(1-\frac{2}{q}\right)}{\left(1+\frac{1}{q}\right)} + \frac{1}{2}\frac{\left(1-\frac{2}{q}\right)}{a^2\varepsilon_0 I_0}\int x A_0 A_0^* \frac{\partial \phi}{\partial x} d^2 r \qquad (4.11a)$$

$$\frac{d^2 f_y}{dz^2} = \frac{1}{2k_0^2 b^4}\frac{1}{f_y^3}\frac{\left(1-\frac{1}{q}\right)\left(1-\frac{2}{q}\right)}{\left(1+\frac{1}{q}\right)} + \frac{1}{2}\frac{\left(1-\frac{2}{q}\right)}{b^2\varepsilon_0 I_0}\int y A_0 A_0^* \frac{\partial \phi}{\partial x} d^2 r \qquad (4.11b)$$

Using eqs. (4.1b) and (4.6) in eqs. (4.11) one can get

$$\frac{d^2 f_x}{d\xi^2} = \frac{\left(1-\frac{1}{q}\right)\left(1-\frac{2}{q}\right)}{\left(1+\frac{1}{q}\right)}\frac{1}{f_x^3} + \left(1-\frac{1}{q}\right)\left(1-\frac{2}{q}\right)\left(\frac{\omega_{p0}^2 a^2}{c^2}\right)(1+\tan(d'\xi))\frac{\beta E_{00}^2}{f_x^2 f_y} I \qquad (4.12a)$$

$$\frac{d^2 f_y}{d\xi^2} = \left(\frac{a}{b}\right)^4 \frac{\left(1-\frac{1}{q}\right)\left(1-\frac{2}{q}\right)}{\left(1+\frac{1}{q}\right)}\frac{1}{f_x^3} + \left(\frac{a}{b}\right)^2 \left(1-\frac{1}{q}\right)\left(1-\frac{2}{q}\right)\left(\frac{\omega_{p0}^2 a^2}{c^2}\right) \times (1+\tan(d'\xi))\frac{\beta E_{00}^2}{f_x f_y^2} I \quad (4.12b)$$

Where

$$\beta = \frac{e^2}{8m\omega_0^2 T_0 K_0}$$

$$d' = dk_0 a^2$$

$$\xi = \frac{z}{k_0 a^2}$$

$$I = \int_0^\infty t\left(1+\frac{t}{q}\right)^{-2q-1} e^{-\frac{\beta E_{00}^2}{f_x f_y}\left(1+\frac{t}{q}\right)^{-q}} dt$$

The set of eqs. (4.12) is the set of nonlinearly coupled differential equations governing the evolution of beam widths of the elliptical q-Gaussian laser beams along x and y directions with longitudinal distance of propagation through collisionless plasmas. It can be seen that each of the eqs. (4.12) contains two terms on the right hand side. First term models the propagation of laser beams in linear media i.e., in vacuum and second term models the propagation of laser beams in nonlinear media. It can be seen that the although in linearly media (i.e., in the absence of second terms on the R.H.S of eqs.(4.12) the beam widths of the laser beam along the two transverse directions evolve independently, however due the laser induced ponderomotive force they get coupled to each other. The set of eqs. (4.12) also indicate that variational theory has reduced the original problem of solving a nonlinear partial differential equation to a set of coupled ordinary differential equations. Also, this reduced set of coupled differential equations is also lacking from an exact closed

form solution, its approximate solution can be easily obtained by simple numerical techniques.

4.4 Evolution of Axial Phase of Laser Beam

During the propagation of a laser beam through a nonlinear medium its axial phase changes due to its transverse spatial confinement resulting as a consequence of its nonlinear refraction. The transverse spatial confinement through the position momentum uncertainty gives an additional transverse momentum to the photons of the beam and thus changes the longitudinal momentum the photons and hence the axial phase of the beam. The overall wave number of the beam is related to its components through [168, 169]

$$k_0^2 = k_x^2 + k_y^2 + k_z^2 \tag{4.13}$$

Defining the effective axial propagation constant for the laser beam weighted average as

$$\bar{k}_z = k_0 - \frac{\langle k_x^2 \rangle}{k_0} - \frac{\langle k_y^2 \rangle}{k_0} \tag{4.14}$$

This effective propagation constant is associated with overall phase (θ_p) of the beam as

$$\frac{\partial \theta_p}{\partial z} = k_0 - \frac{\langle k_x^2 \rangle}{k_0} - \frac{\langle k_y^2 \rangle}{k_0} \tag{4.15}$$

The first term in this equation gives the phase $k_0 z$ of an infinite plane wave propagating along $z$axis. However, the second term gives the axial phase shift

$$\frac{\partial \theta}{\partial z} = -a^2\left(\langle k_x^2 \rangle + \langle k_y^2 \rangle\right) \tag{4.16}$$

Where

$$\langle k_{x,y}^2 \rangle = \frac{1}{I_k} \int_{-\infty}^{\infty} \int_{-\infty}^{\infty} k_{x,y}^2 \, \tilde{A}_0 \tilde{A}_0^* dk_x dk_y \tag{4.17}$$

$$I_k = \int_{-\infty}^{\infty} \int_{-\infty}^{\infty} \tilde{A}_0 \tilde{A}_0^* dk_x dk_y \tag{4.18}$$

$$\tilde{A}_0(k_x, k_y) = \frac{1}{2\pi} \int_{-\infty}^{\infty} \int_{-\infty}^{\infty} A_0(x, y, z) e^{-i(k_x x + k_y y)} dx dy \tag{4.19}$$

4.5 Results and Discussion

In the present investigation, the coupled differential eqs.(4.12) have been solved with the help of Runge Kutta fourth order method for following set of laser-plasma parameters:

$$\omega_0 = 1.78 \times 10^{15} rad\ sec^{-1}, \qquad a = 10\mu m,$$
$$\beta E_{00}^2 = 3 \text{ (Laser intensity} = 4.5 \times 10^{16} W/cm^2),$$
$$\frac{\omega_{p0}^2 a^2}{c^2} = 9 \text{ (Plasma density} = 3 \times 10^{16} c\ c^{-3})$$

and for different values of $q, d', \text{and}\ \frac{a}{b}$ viz.,

$$q = (3,4,\infty), \qquad d' = (0.25, 0.35, 0.45) \text{ and } \frac{a}{b} = (1, 1.1, 1.2)$$

under the boundary condition that at the plane of incidence the laser beam is having plane wavefront. Mathematically this condition means that at $\xi = 0$:

$$f_{x,y} = 1$$
$$\frac{df_{x,y}}{d\xi} = 0$$

Firstly, in order to see the linear propagation of q-Gaussian laser beam, eqs. (4.12) have been solved in the absence of plasma medium for different values of deviation parameter q and the corresponding variations of the beam width have been sown in figs. 4.1 and 4.2. It can be seen that irrespective of the ellipticity of the beam or deviation parameter q, the beam widths of the laser beam along both the transverse directions broaden with distance of propagation. This is due to the fact that a laser beam with finite cross section can be considered as a superposition of plane waves, all having the same wave number, but with different angle with respect to the beam axis. Therefore, each component propagates at different phase velocity with respect to the longitudinal direction. Thus, each plane wave acquires a different phase and thus the beam broadens along the transverse directions.

It can also be seen in fig. 4.1 that although in vacuum the beam widths along x and y directions broaden independently of each other, the beam width along y direction broaden at a faster rate compared to that along x direction. This is due to the fact that diffraction effect of the laser beam varies inversely as the square of the transverse spread

of the laser beam and in fig.4.2, I have taken $\frac{a}{b} = 1.1$which means $a > b$. As, a result the diffraction effect is more prominent along y direction compared to that along x direction.

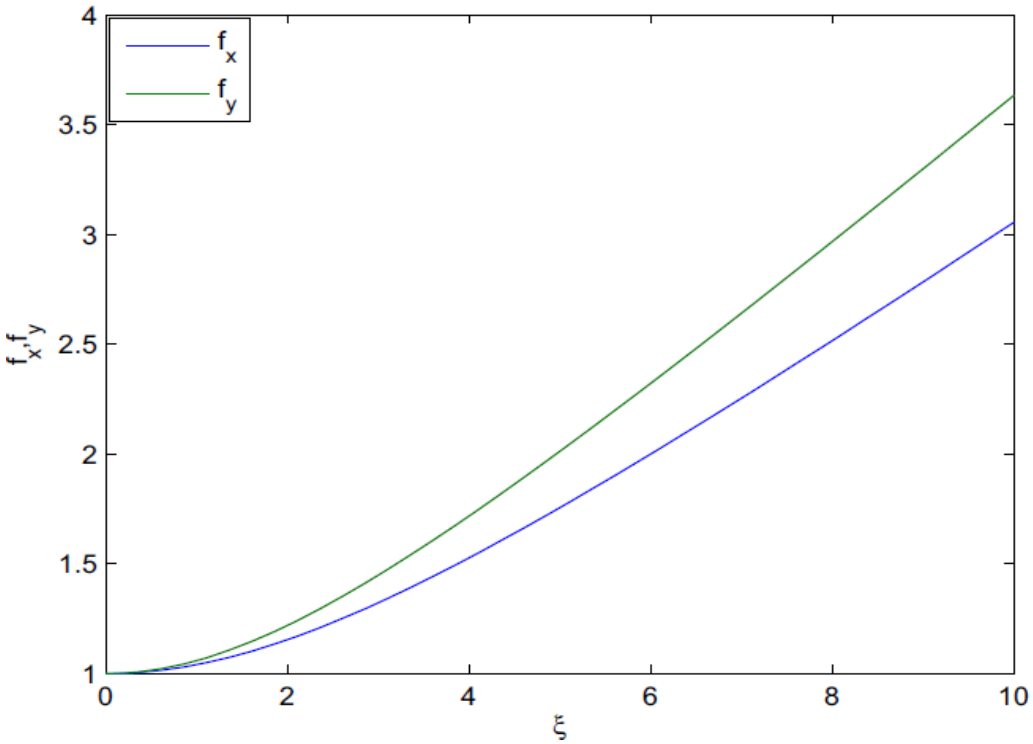

Fig. 4.1: Variation of beam width parameters f_x, f_y with distance of propagation in vacuum for fixed ellipticity $\frac{a}{b} = 1.1$

The plots in fig. 4.2 depict that with increase in the value of deviation parameter q the diffraction broadening of the laser beam along both the transverse direction increases. This is due to the fact that as the value of deviation parameter increases the over whole cross section of the laser beam gets shrinked. Decrease in the effective spot size of the laser beam results in its enhanced diffraction with increase in deviation parameter q. Thus, it can be concluded that although the amplitude structure of the laser beam deviates from ideal Gaussian profile due to cavity imperfections, but it helps to obviate the diffraction broadening of the beam i.e., q-Gaussian beams are more directional compared to ideal Gaussian beams.

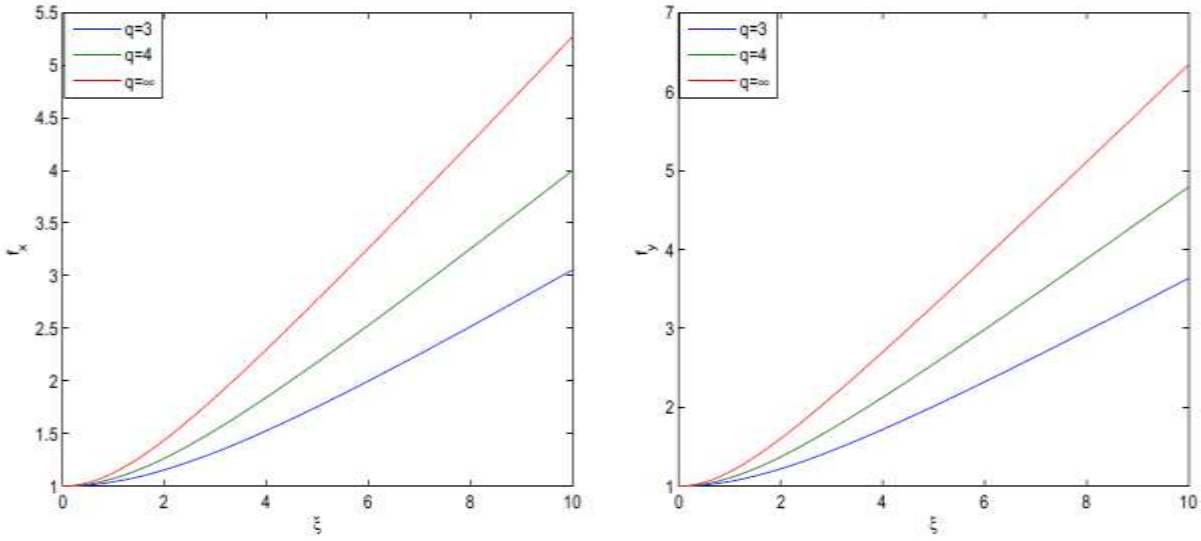

Fig. 4.2: Variation of beam width parameters f_x, f_y with distance of propagation in vacuum for different values deviation parameter q and at fixed ellipticity $\frac{a}{b} = 1.1$

Now in order to see the effect of deviation parameter q on the evolution of beam widths of the laser beam in plasma medium, the set of eqs. (4.12) has been solved for different values of q in the presence of plasma medium and the corresponding evolutions of the beam widths along x and y directions with longitudinal distance are sown in Figs. 4.3 and 4.4. It can be seen that inside the plasma medium the beam widths of the laser beam along both the transverse directions show oscillatory behaviour over the longitudinal direction. This behaviour of the laser beam can be explained by analyzing the role and origin of various terms contained in the evolution equations for the beam widths i.e., eqs. (4.12). The first terms on the right hand side (R.H.S) of these equations that vary inversely as the cube of corresponding beam width (i.e., as $f_{x,y}^{-3}$) are the spatial dispersive term that models the spreading of the laser beam in transverse x and y directions as a consequence of the diffraction divergence. The second terms on the R.H.S of these equations that have complex dependence on beam widths $f_{x,y}$ originate as a consequence of ponderomotive force exerted by the laser beam on plasma electrons. These terms model the nonlinear refraction of the laser beam and the nonlinear coupling of the beam widths along transverse directions.

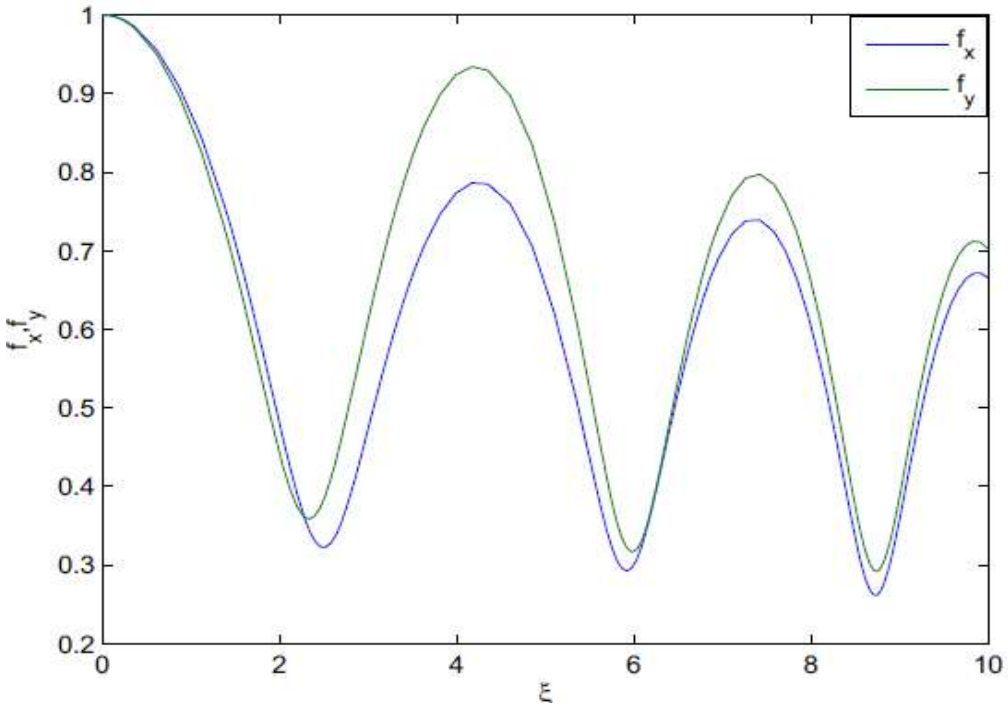

Fig. 4.3: Variation of beam width parameters f_x, f_y with distance of propagation in plasma for $q = 3, d' = 0.25$ and $\frac{a}{b} = 1.1$

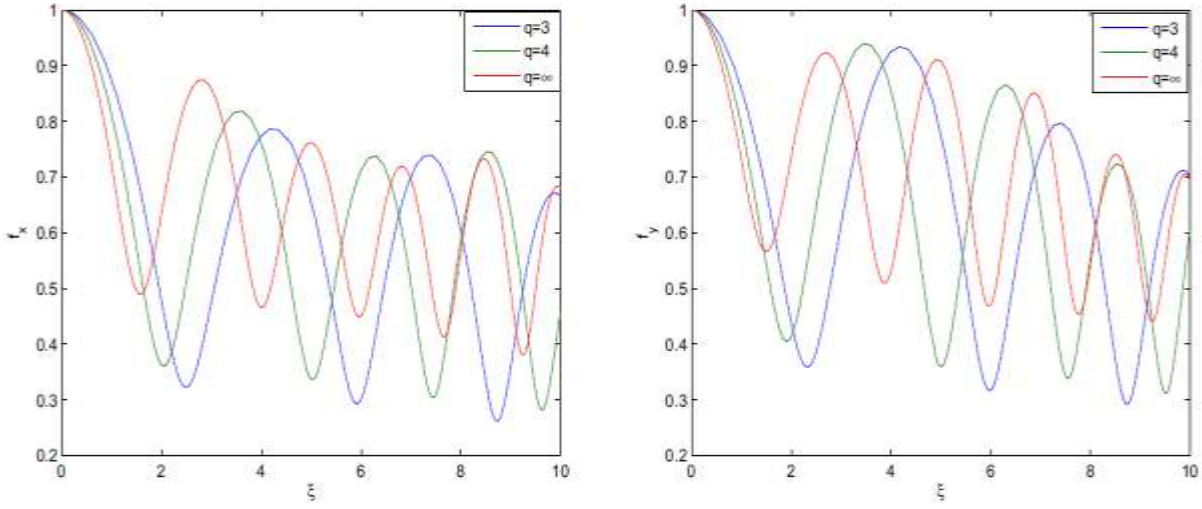

Fig. 4.4: Variation of beam width parameters f_x, f_y with distance of propagation in plasma for $q = (3, 4, \infty), d' = 0.25$ and $\frac{a}{b} = 1.1$

As a result of laser induced nonlinearity of plasma the resulting nonlinear refraction of the laser beam tends to counter balance the effect of diffraction along both the transverse directions. Thus, during the propagation of laser beam through the plasma, there starts a

competition between the two phenomena of diffraction and nonlinear refraction. The winning phenomenon decides the ultimate behaviour of the laser beam i.e., whether the beam will converge or diverge. Thus, there exists a critical value of beam intensity (that can be obtained by balancing the two terms on the R.H.S of eqs. 4.12) above which the beam converges along both the transverse directions. In the present investigation the initial beam intensity has been taken to be greater than the critical intensity. That is why the beam widths of the laser beam along both the transverse directions converging initially. As the cross section of the laser beam shrinks, its intensity increases. When the intensity of the laser beam becomes too high, the illuminated portion of the plasma gets almost evacuated from the electrons. Hence, the beam now propagates as if it is propagating through vacuum. As an optical beam propagating through vacuum undergoes diffraction, the beam width of a laser beam propagating through plasma, after attaining possible minimum value, the beam bounces back towards its original value. As the widths of the laser beam along both the transverse directions start expanding, the competition between diffraction broadening and nonlinear refraction starts again. Now this competition lasts till $f_{x,y}$ obtain their maximum possible values. These, processes keep on repeating themselves and thus give oscillatory behaviour to the beam widths of the laser beam along the two transverse directions.

Further it has been observed that after every focal spot, the maximum as well as the minimum of the beam width shift downwards. This is owing to the fact that the equilibrium electron density is an increasing function of longitudinal distance. Hence, the plasma index of refraction keep on decreasing with the penetration of laser beam into the plasma. Consequently, the self focusing effect gets enhanced and the maximum as well as minimum of the beam width go on shifting downwards after every focal spot. It is also seen that the frequency of oscillations of beam with increases with distance. The physics behind this fact is that denser is the plasma, higher will be the phase velocity of laser beam through it. Hence, in denser plasma laser beam takes less duration to get self focused.

It can be also be seen that initially the beam widths of the laser beam along the two transverse directions vary in phase with each other but over some distance of propagation

their oscillations establish a phase mismatch. This phase mismatch in the oscillations of beam widths along x and y directions is due to the fact that due its ellipticity the laser beam experience different indices of refraction along x and y directions i.e., for the elliptical beam the plasma behaves as an anisotropic medium.

It can also be seen that the extent of self focusing of the laser beam along x direction is more compared to that along y direction. This is due to the fact that initial width of the beam along x direction is more compared to that along y direction $\left(\frac{a}{b} = 1.1\right)$. Thus, the opposition offered by diffraction effect to the nonlinear refraction is more along x direction. This results in reduced self focusing along y direction.

The plots in Fig. 4.4 depict that with increase in the value of deviation parameter q, the extent of self focusing along both the transverse directions gets reduced. This is due to the fact for laser beams with larger value of q, most of the beam energy is concentrated around a narrow region around the beam axis. Hence, these beams get a little contribution from the off axial rays towards the nonlinear refraction. As the phenomenon of self focusing is a homeostasis of nonlinear refraction of the optical beam due to optical nonlinearity of the medium, increase in the value of deviation parameter q reduces the extent of self focusing of the laser beam. Thus, compared to q-Gaussian laser beams, ideal Gaussian laser beams possess minimum focusing character.

It can also be seen that instead of their reduced focusing, laser beams with higher values of deviation parameter q possess faster focusing along both the transverse directions. This is due to the faster focusing character of the rays closer to beam axis. Being away from the beam axis, off axial rays take more duration to get self focused. As there are more number of off axial rays in laser beams with lower values of deviation parameter q, these beams possess slower focusing character.

Figure 4.5 illustrates the effect of beam ellipticity along y direction on self focusing of the laser beam. It can be seen that with increase in the beam ellipticity along y direction there is reduction in extent of self focusing of the laser beam along y direction. This is due to the fact that, at fixed value of a increase in beam ellipticity (i.e.,$\frac{a}{b}$) means the reduction

in initial width of the beam along y direction. Hence, with increase in beam ellipticity along y direction makes the diffraction effect stronger along y direction. This results in the reduced focusing of the laser beam along y direction

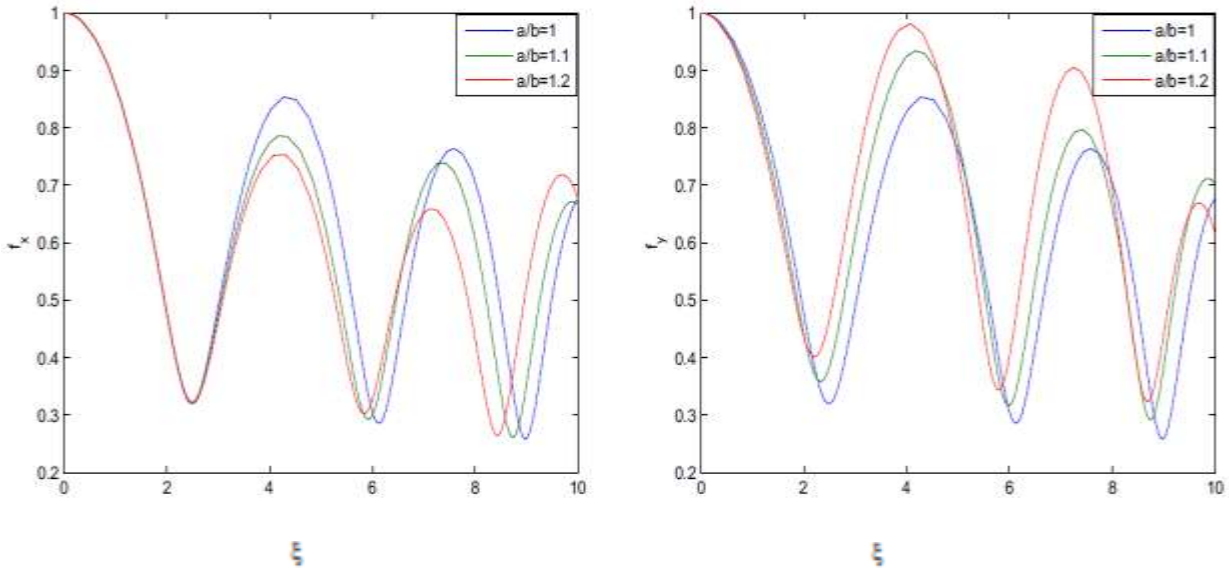

Fig. 4.5: Variation of beam width parameters f_x, f_y with distance of propagation in plasma for $q = 3, d' = 0.25$ and $\frac{a}{b} = (1, 1.1, 1.2)$

It can also be seen that initially the increase in beam ellipticity does not produce any significant effect on self focusing of the beam along x direction. However, as the beam penetrates deeper into the plasma the focusing along x direction also decreases. This is due to the fact that as the beam penetrates deeper and deeper into the plasma, the nonlinear coupling between the two beam widths becomes stronger and stronger.

Fig.4.6 illustrates the effect of slope of density ramp on self focusing of the laser beam along the two transverse directions. It can be seen that with increase in the slope of density ramp the extent of self focusing of the laser beam along both the transverse directions increases. This is due to the fact that with increase in slope density of ramp, the number of electrons contributing to the ponderomotive nonlinearity increases along the direction of propagation. This results in enhanced transverse as well as longitudinal gradient in the index of refraction of plasma that in turn increases the extent of self focusing of the laser beam along the two transverse directions.

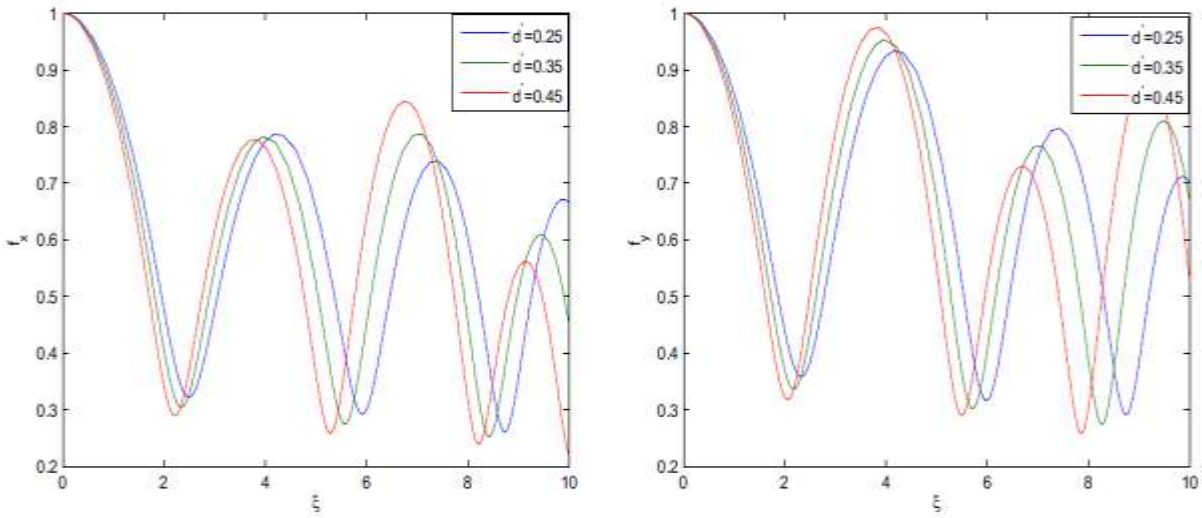

Fig.4.6: Variation of beam width parameters f_x, f_y with distance of propagation in plasma for $q = 3, d' = (0.25, 0.35, 0.45)$ and $\frac{a}{b} = 1.1$

Further, eq. (4.16) gives the evolution of axial phase of the laser beam during its propagation through the plasma. This equation has been solved in association with the set of eqs. (4.12a) and (4.12b), and the corresponding dynamics of the axial phase for different laser-plasma parameters has been depicted in figs. 4.7, 4.8 and 4.9.

It is observed that axial phase θ decreases monotonically with distance of propagation, showing abrupt jumps at the periodic positions of the minimum beam widths. These jumps of axial phase at the focal positions of the laser beam give it a step like behaviour. The monotonic decrease in axial phase with distance is due to the fact that the self focusing of the laser beams with distance of propagation leads to reduction in volume of space available for its propagation. This in turn through position momentum uncertainty along the transverse directions

$$\Delta x \Delta p_x = \text{constant}$$

$$\Delta y \Delta p_y = \text{constant}$$

results in increase in the transverse momentum of the photons of the laser beam. This situation is similar to that observed for a quantum particle trapped in a tube or a photon confined in a waveguide. However, the interesting fact is that in the present case there is no physical boundary to confine the photons. Now, as the overall momentum should remain conserved, the increase transverse momentum results in reduction in the longitudinal

momentum of the photons. This reduction in the longitudinal momentum is the consequence of monotonic decrease in the axial phase of the laser beam.

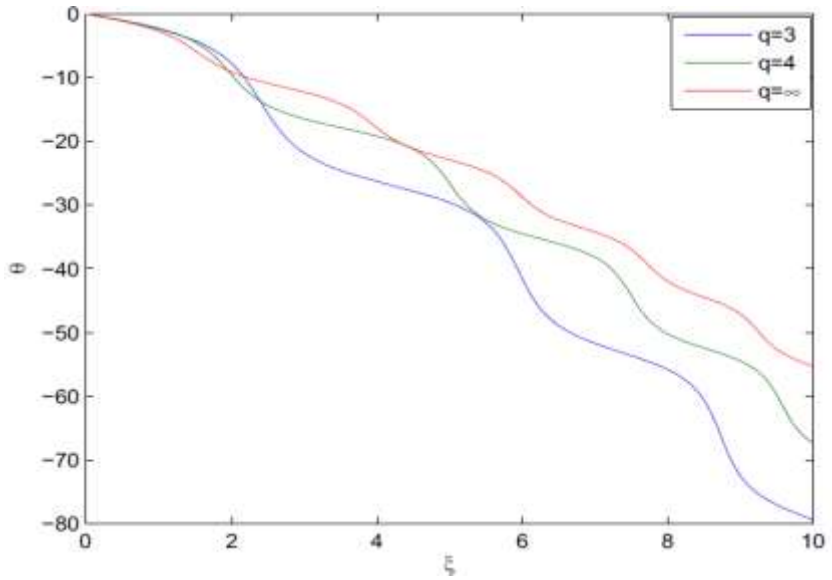

Fig. 4.7: Variation of axial phase θ with distance of propagation in plasma for $q = (3, 4, \infty), d' = 0.25$ and $\frac{a}{b} = 1.1$

Step like behaviour of the axial phase, with each step occurring at positions of minimum beam width indicates that there is slowest decrement in θ at points of minimum beam width. This is opposite to the behaviour of phase in graded index fibers, where phase decreases slowest in the positions of minimum intensity i.e., maximum beam width. This difference in the behaviour of axial phase in plasmas and that in graded index fibers is due to the fact that due to their optical nonlinearity, plasmas behave as oscillating linear wave guides. In linear wave guides, the growth rate of axial phase is inversely proportional to the square of beam width.

Fig. 4.7 depicts that with increase in the value of deviation parameter q there is decrease in the rate of change of axial phase with distance. This is due to the fact that as the spatial profile of the laser beam converges towards ideal Gaussian profile the transverse confinement of the laser beam due to self focusing decreases. As spatial confinement of the laser beam is homeostasis for the axial phase shift, the reduction of self focusing with increase in deviation parameter q results in reduction in the rate of change of axial phase

with distance. Thus, axial phase of the ideal Gaussian beams changes at slowest rate during their propagation through nonlinear media.

Fig. 4.8 illustrates the effect of beam ellipticity on the evolution of axial phase of the laser beam. It can be seen that with increase in the ellipticity of the laser beam its axial phase changes at a slower rate. This is due to the reduction in overall focusing of the laser beam with increase in its ellipticity.

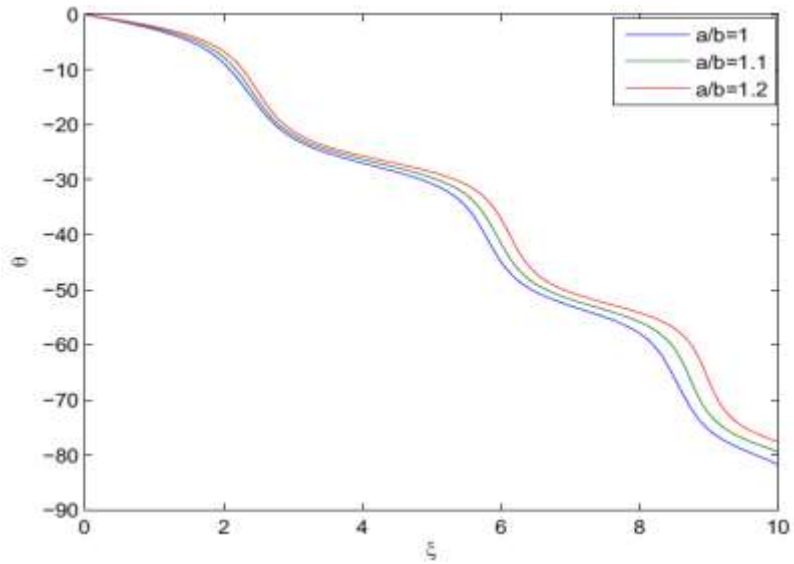

Fig. 4.8: Variation of axial θ phase with distance of propagation in plasma for $q = 3, d' = 0.25$ and $\frac{a}{b} = (1, 1.1, 1.2)$

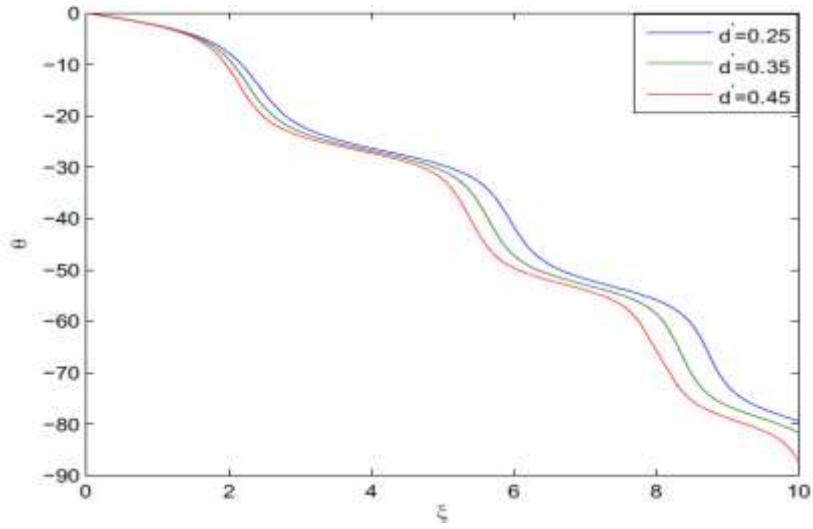

Fig. 4.9: Variation of axial phase θ with distance of propagation in plasma for $q = 3, d' = (0.25,\ 0.35, 0.45)$and $\frac{a}{b} = 1.1$

Fig. 4.9 depicts the effect of slope of plasma density ramp on the axial phase of the laser beam. It can be seen that in denser plasmas the axial phase of the laser beam changes at a faster rate. This is due to the fact that denser is the plasma, higher is the spatial confinement of the laser beam due to self focusing. As a result the axial phase of the beam changes at a faster rate in denser plasmas.

4.6 Conclusions

In conclusion I have presented the effects of both ellipticity of the cross section of the laser beam as well as the deviation of amplitude structure from ideal Gaussian profile on its nonlinear propagation characteristics. It has been observed that although the deviation of amplitude structure from ideal Gaussian profile arises due to cavity imperfections, it helps to enhance the self focusing of the laser beam in nonlinear media. But along with enhancing the extent of self focusing it delays the self focusing of the laser beam. It is also observed that initial ellipticity of the beam also plays a significant role in determining the propagation characteristics of the beam. Self focusing of the laser beam is lesser along the transverse direction along which it is initially more elliptical. The results of present investigation may serve as a guide for the experimentalists working in the area of laser-plasma interactions and nonlinear optics.

Chapter-5

Self Focusing of Cosh-Gaussian Laser Beam in Collisional Plasma: Effect of Nonlinear Absorption

5.1 Introduction

Amelioration in laser technology fuelled by the advent of chirp pulse amplification (CPA) technique [9, 10] has led to a resurgence in the field of light matter interactions by giving birth to two entirely new areas of science i.e., nonlinear optics and laser plasma interactions. Interactions of intense coherent beams of light produced by modern laser systems with plasmas are rich in copious nonlinear phenomena those were not possible before the invention of laser. This includes a gamut from optical self-action effects like (self focusing, self guiding, self phase modulation etc.) to several frequency mixing processes like sum frequency generation, difference frequency generation, second harmonic generation (SHG) [19] etc. Being extremely complex but rich in physics, these nonlinear effects have the potential to keep researchers busy for several upcoming years. Over past few years veteran physicists are attempting to improve on the understanding of laser plasma interactions by carrying out experimental as well as theoretical investigations. The major impetus behind these investigations on laser-plasma interactions was built by the proposal of initiating controlled nuclear fusion reaction by using ultra intense laser beams. Fusion is considered to be the cleanest source of energy that bears the promise to quench means endless thirst for energy, without giving any harm to global climate change. Apart from fusion, several other applications have emerged as a consequence of laser plasma interactions. This include laser driven plasma accelerators [16], X-ray lasers [17], HHG [19] etc. The ultimate breath of all these applications is decided by the efficiency of laser plasma coupling. As, during the coupling of laser energy with plasmas, above mentioned processes play a significant role, therefore, it becomes essential to investigate some of these nonlinear phenomena in order to optimize the efficiency of laser plasma coupling.

Self focusing of the laser beam is such a nonlinear phenomenon that significantly affects the propagation of an intense laser beam through plasma. The propagation of an

intense laser beam through plasma modifies the index of refraction of plasma in such a way that the illuminated region of plasma behaves like a graded index fiber. Thus, the axial part of optical beam gets maximum opposition from the plasma for its propagation and this opposition decreases with radial distance from the axis of beam. Hence the beam develops a velocity gradient over its cross section and thus the phase fronts of the beam bend as if the beam is passing through a converging lens.

Self focusing of the laser beams in different nonlinear media has been a hot topic of research since its discovery by *Askaryan* [22]. In past few years a vast literature has been reported by researchers from all over the globe on various aspects of this phenomenon. Early seminal work of *Sodha et al* [25]. gave a gravest blow to the investigation of this phenomenon for intense laser beams interacting with plasmas in different environments and regimes. Especially in context of inertial confinement fusion this phenomenon is at the vanguard of theoretical as well as experimental investigations.

Laser beams differing in irradiance over their cross sections behave differently in plasmas. However, from literature review it has been observed that most of the earlier theoretical investigations on self focusing of laser beams in plasmas have been carried out for Gaussian laser beams. Only a few investigations on self focusing of laser beams with other irradiance profiles like Cosh-Gaussian, q-Gaussian, Quadruple-Gaussian etc. have been reported in the past. But all these investigations suffer from the limitation that they have been carried out under the assumption that there is no absorption of laser energy by plasma. However, in actual during its propagation through plasma the laser beam gets attenuated due to absorption of laser energy by plasma. If the index of plasma is a function of laser intensity, then the attenuation function of plasma is also a function of laser intensity, i.e., attenuation of the beam is also nonlinear in nature. Thus, the aim of present study to investigate self focusing of a ChG laser beam in collisional plasma under the effect of its nonlinear attenuation.

5.2 Optical Nonlinearity of Plasma

The dielectric function of the plasma can be written as

$$\varepsilon = \varepsilon_r + \varepsilon_i \tag{5.1}$$

where, ε_r and ε_i are the real and imaginary parts of the dielectric function respectively. The real part is responsible for the nonlinear refraction of the laser beam whereas; imaginary part is responsible for its attenuation. The real part of dielectric function of plasma can be written as:

$$\varepsilon_r = 1 - \frac{\omega_p^2}{\omega_0^2} \tag{5.2}$$

Where

$$\omega_p^2 = \frac{4\pi e^2}{m} n_e \tag{5.3}$$

is the plasma frequency in the presence of laser beam, and e, m are electronic charge and mass respectively. Here, the propagation of a laser beam with amplitude structure modeled by Cosh-Gaussian function defined as

$$E_0 = \frac{E_{00}}{f} e^{-\frac{r^2}{2r_0^2 f^2}} Cosh\left(\frac{b}{r_0 f} r\right) e^{-k_{ae} z} \tag{5.4}$$

has been considered. Here, $k_{ae}$is the attenuation coefficient of plasma. The nonuniform irradiance over the cross section of the laser beam leads to nonuniform heating of the plasma electrons. The resulting electron temperature of plasma is related to laser field amplitude as [25]

$$\frac{T_e}{T_0} = 1 + \frac{\beta E_{00}^2}{f^2} e^{-\frac{r^2}{r_0^2 f^2}} \cosh^2\left(\frac{b}{r_0 f} r\right) e^{-2k_{ab} z} \tag{5.5}$$

where, T_0 is the equilibrium electron temperature of the plasma i.e., the temperature of plasma electrons in the absence of laser beam. The parameter $\beta = \frac{e^2 M}{6K_0 T_0 m^2 \omega_0^2}$ is the coefficient of collisional nonlinearity [93, 94]. From eq.(5.5) it can be seen that the transverse variation of electron temperature of plasma exactly follows the amplitude structure over the cross section of the laser beam. Thus, temperature of plasma electrons in the irradiated portion of plasma is maximum where intensity of the laser beam is maximum and vice versa. This results in the migration of plasma electrons from high intensity regions towards the low intensity regions. The resulting distribution of electrons is given by

$$n_e = n_0 \left(\frac{2T_0}{T_0 + T_e}\right)^{1-\frac{s}{2}} \tag{5.6}$$

Using eqs. (5.3)-(5.6) in (5.2), the real part of dielectric function of plasma has been obtained as

$$\varepsilon_r = 1 - \frac{\omega_{p0}^2}{\omega_0^2}\left\{1 + \frac{1}{2}\frac{\beta E_{00}^2}{f^2} e^{-\frac{r^2}{r_0^2 f^2}} \cosh^2\left(\frac{b}{r_0 f} r\right) e^{-2K_{ab} z}\right\}^{\frac{s}{2}-1} \tag{5.7}$$

where, $\omega_{p0}^2 = \frac{4\pi e^2}{m} n_0$ is the plasma frequency in the absence of the laser beam. The parameter s describes the nature of collisions and can be defined through the dependence of collision frequency ν on electron's random velocity v and temperature T_e as $\nu\alpha\left(\frac{v^2}{T_e}\right)^s$. For velocity independent collisions $s = 0$, for collisions between electrons and diatomic molecules $s = 2$, and for electron-ion collisions $s = -3$.

Taking

$$\varepsilon_r = \varepsilon_0 + \varphi(E_0 E_0^*) \tag{5.8}$$

where, ε_0 and $\varphi(E_0 E_0^*)$ are the linear and nonlinear parts of the dielectric function of the channel, respectively, one can obtain

$$\varepsilon_0 = 1 - \frac{\omega_{p0}^2}{\omega_0^2} \tag{5.9}$$

And

$$\varphi(E_0 E_0^*) = \frac{\omega_{p0}^2}{\omega_0^2}\left\{1 - \left(1 + \frac{1}{2}\frac{\beta E_{00}^2}{f^2} e^{-\frac{r^2}{r_0^2 f^2}} cosh^2\left(\frac{b}{r_0 f} r\right) e^{-2K_{ab} z}\right)^{\frac{s}{2}-1}\right\} \tag{5.10}$$

5.3 Attenuation Function of the Plasma

Following *Sodha et al* [25], the imaginary part of the dielectric function of the plasma can be written as

$$\varepsilon_i = \frac{4}{3}\sqrt{\pi}\Gamma\frac{(s+5)}{2}\left[\frac{\omega_{p0}^2}{\omega_0^2}\frac{\nu_0}{\omega_0}\left(1 + \frac{\beta E_{00}^2}{f^2} e^{-\frac{r^2}{r_0^2 f^2}} \cosh^2\left(\frac{b}{r_0 f} r\right)\right)\right]^{\frac{s}{2}} \tag{5.11}$$

The nonlinear attenuation function of the plasma can be obtained by averaging the imaginary part of the dielectric function over the cross section of the laser beam as

$$K_{ab} = \frac{\omega_0^2}{k_0 c^2}\frac{\int_0^\infty \varepsilon_i \frac{E_{00}^2}{f^2} e^{-\frac{r^2}{r_0^2 f^2}} \cosh^2\left(\frac{b}{r_0 f} r\right) r dr}{\int_0^\infty \frac{E_{00}^2}{f^2} e^{-\frac{r^2}{r_0^2 f^2}} \cosh^2\left(\frac{b}{r_0 f} r\right) r dr} \tag{5.12}$$

Using eq.(5.11) in (5.12), one can get

$$K_{ab} = \frac{4}{3}\sqrt{\pi}\frac{\Gamma\frac{(s+5)}{2}}{e^{b^2}}\frac{1}{k_0 r_0^2} I_{ab} \tag{5.13}$$

Where

$$I_{ab} = \int_0^\infty \left\{1 + \frac{\beta E_{00}^2}{f^2} e^{-x^2}\, cosh^2(bx)\right\}^{\frac{s}{2}} e^{-x^2}\, cosh^2(bx)\, x dx \tag{5.14}$$

$$x = \frac{r}{r_0 f}$$

5.4 Beam Width Evolution of Laser Beam

The nonlinear propagation of a laser beam through an absorptive medium is governed by the wave equation

$$\nabla_\perp^2 E_0 + \frac{\omega_0^2}{c^2}\, \varphi(E_0 E_0^*) E_0 - iK_{ab} E_0 - 2ik_0 \frac{\partial E_0}{\partial z} = 0 \tag{5.15}$$

Using the same procedure as in chapter-4 i.e., variational analysis, the equation governing the evolution of beam width of the laser beam has been obtained as

$$\frac{d^2 f}{d\xi^2} + \frac{1}{f}\left(\frac{df}{d\xi}\right)^2 = \frac{1+e^{-b^2}(1-b^2)}{2(1+b^2)}\frac{1}{f^3} + \frac{\omega_{p0}^2 r_0^2}{c^2}\left(\frac{s}{2} - 1\right)\frac{\beta E_{00}^2}{f^3} e^{-K'_{ab}\xi}\left(\frac{e^{-b^2}}{1+b^2}\right)(T_1 - bT_2) \tag{5.16}$$

Where, $\xi = \frac{z}{k_0 r_0^2}$ is the dimensionless distance of propagation,

$$T_1 = \int_0^\infty x^3 \left\{1 + \frac{1}{2}\frac{\beta E_{00}^2}{f^2} e^{-x^2}\, cosh^2(bx) e^{-2K'_{ab}\xi}\right\}^{\frac{s}{2}-2} e^{-2x^2} cosh^4(bx) dx$$

$$T_2 = \int_0^\infty x^2 \left\{1 + \frac{1}{2}\frac{\beta E_{00}^2}{f^2} e^{-x^2}\, cosh^2(bx) e^{-2K'_{ab}\xi}\right\}^{\frac{s}{2}-2} e^{-2x^2} cosh^3(bx) \sinh(bx) dx$$

and

$$K'_{ab} = \frac{4}{3}\sqrt{\pi}\frac{\Gamma\frac{(s+5)}{2}}{e^{b^2}} I_{ab}$$

is the dimensionless attenuation function of the plasma. For an initially plane wavefront, eq.(5.16) is subjected to boundary conditions $f = 1, \frac{df}{d\xi} = 0\ at\ \xi = 0$.

5.5. Results and Discussion

The evolution of spot size of ChG laser beam through collisional plasma with nonlinear absorption is governed by eq. (5.16). This equation has been solved numerically for the following set of laser as well as plasma parameters

$$\omega_0 = 1.78 \times 10^{15} rad/sec$$

$$\lambda = 1.06\mu m$$

$$r_0 = 15\mu m$$

$$T_0 = 10^6 K$$

to investigate the propagation dynamics of ChG laser beam.

Fig.5.1 illustrates the effect of decentered parameter of the ChG laser beam on its focusing/defocusing behavior. It is observed that initially the spot size of the laser beam decreases monotonically with distance of propagation and then after attaining a minimum value the spot size of the laser beam starts increasing monotonically. In other initially the self focusing of the laser beam is the dominant phenomenon and beyond the focus diffraction broadening becomes dominant. It can be seen that inside the plasma medium the beam widths of the laser beam along both the transverse directions show oscillatory behavior over the longitudinal direction.

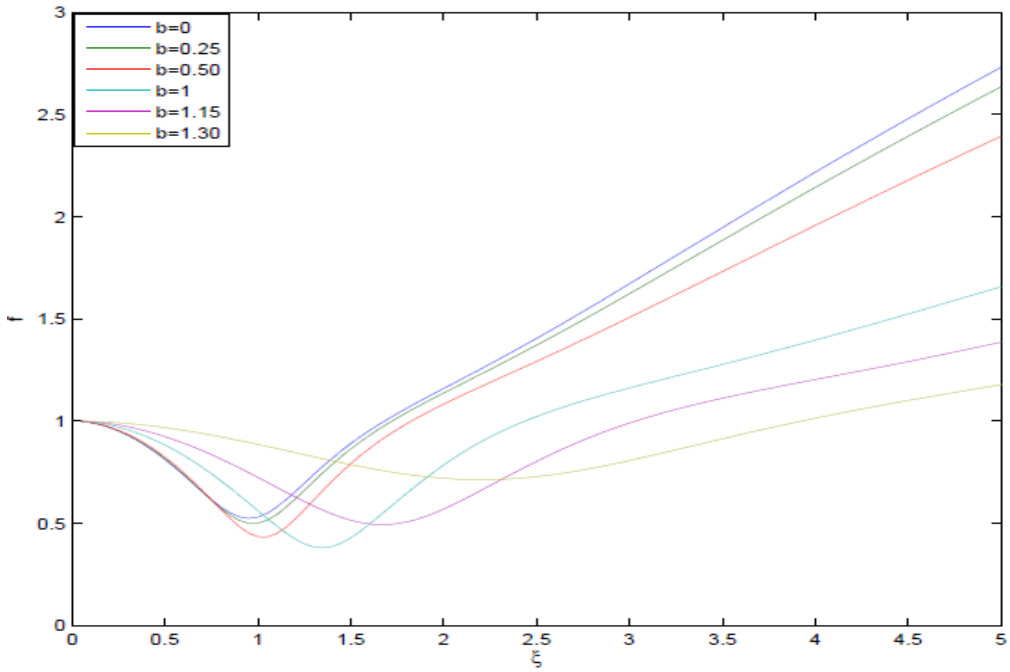

Fig. 5.1: Variation of beam width parameter f with normalized distance of propagation ξ for different values of decentered parameter b viz., $b = 0,\ 0.25,\ 0.50,\ 1.0,\ 1.15,\ 1.30$ and at fixed values of $\beta E_{00}^2 = 3.0, \left(\frac{\omega_{p0} r_0}{c}\right)^2 = 12, \frac{\nu_0}{\omega_0} = 0.05, s = -3$

This behavior of the laser beam can be explained by analyzing the role and origin of various terms contained in the evolution equation for the beam width i.e., eq.(5.16). The first terms on the right hand side (R.H.S) of this equation that vary inversely as the cube of

corresponding beam width (i.e., as f^{-3}) is the spatial dispersive term that models the spreading of the laser beam in transverse directions as a consequence of the diffraction divergence. The second terms on the R.H.S of this equation that has complex dependence on beam width f originates as a consequence of optical nonlinearity of plasma under the effect of intense field of the laser beam. This term models the nonlinear refraction of the laser beam. As a result of laser induced nonlinearity of plasma the resulting nonlinear refraction of the laser beam tends to counter balance the effect of diffraction along the transverse directions. Thus, during the propagation of laser beam through the plasma, there starts a competition between the two phenomena of diffraction and nonlinear refraction. The winning phenomenon decides the ultimate behavior of the laser beam i.e., whether the beam will converge or diverge. Thus, there exists a critical value of beam intensity (that can be obtained by balancing the two terms on the R.H.S of eq.(5.16) above which the beam converges along the transverse directions. In the present investigation the initial beam intensity has been taken to be greater than the critical intensity. That is why the beam width of the laser beam along the transverse directions converges initially. As the cross section of the laser beam shrinks, its intensity increases. When the intensity of the laser beam becomes too high, the illuminated portion of the plasma becomes almost evacuated from plasma electrons and thus the laser beam propagates as if it is propagating through vacuum. As an optical beam propagating through vacuum undergo diffraction, the beam width of a laser beam propagating through plasma, after attaining possible minimum value bounces back towards its original value. Now, as along with the distance of propagation the intensity of the laser beam is getting attenuated to collisional absorption, after a certain distance the intensity of the beam becomes lesser than the critical intensity for self focusing. Hence, beyond the focal spot, the laser beam keep on diffracting continuously.

The plots in fig.5.1 also depict that there is increase in the extent of self focusing of the laser beam with increase in the value of decentered parameter of the laser beam for $0 \leq b \leq 1$. This is due to the fact that the intensity profile of the ChG laser beam resembles with that of at topped laser beams for $0 \leq b \leq 1$, and the degree of flatness increases with the increase in the value of b. Hence, for $0 \leq b \leq 1$, the ChG laser beam gets equal

contribution from off axial rays towards the nonlinear refraction as provided by the axial rays.

Also, it can be seen from fig.5.2 that with increase in the value of b for $0 \leq b \leq 1$ there is decrease in the attenuation of the beam. As a result, there is increase in the extent of self focusing of the laser beam with increase in the value of b for $0 \leq b \leq 1$.

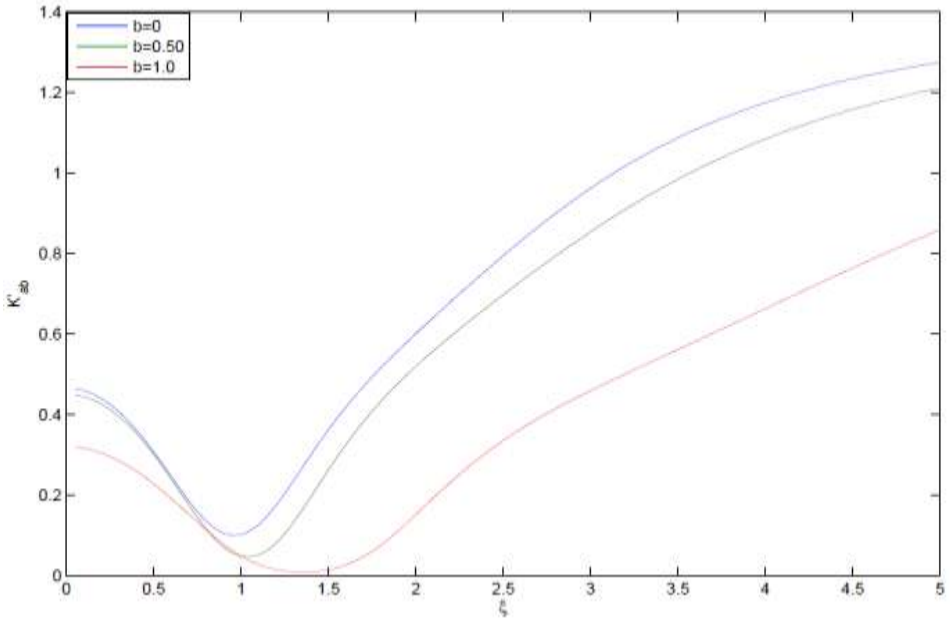

Fig. 5.2 Variation of attenuation function K'_{ab} with normalized distance of propagation ξ for different values of decentered parameter b viz., $b = 0, 0.50, 1.0$ and at fixed values, $\beta E_{00}^2 = 3.0$, $\left(\frac{\omega_{p0} r_0}{c}\right)^2 = 12, \frac{\nu_0}{\omega_0} = 0.05, s = -3$

It is also observed from fig.5.1 that there is decrease in the extent of self focusing of the laser beam with increase in the value of decentered parameter of the laser beam for $b > 1$. This is due to the fact that the intensity maxima of the laser beam for $b > 1$ appears in the off axial part of the laser beam rather than on axial part. As a result, the axial part of the laser beam becomes weaker as compared to the off axial part with increase in the value of b beyond 1. Thus, for $b > 1$ ChG laser beam gets a little contribution from axial rays for nonlinear refraction. The reduced nonlinear refraction of the laser beam with increase in the value of b for $b > 1$ results in decreased focusing of the laser beam.

It can also be seen from the plots in fig.5.1 that with increase in the value of b the focal spot of the laser beam gets shifted longitudinally in the forward direction i.e., ChG

laser beams with higher value of b show delayed focusing. This is due to the fact that with increase in the value of b the intensity of the laser beam shifts from axial region to the off axial region of the laser beam and being away from the axis, off axial rays take more duration to get self focused.

Fig.5.3 illustrates the effect of initial beam intensity on focusing/defocusing characteristics of the laser beam. It is observed that there is decrease in the extent of rate of increase of the spot size of the laser beam beyond the focus with increase in its intensity. This is due to the fact that increase in the intensity of the laser beam leads to weakening of its nonlinear absorption.

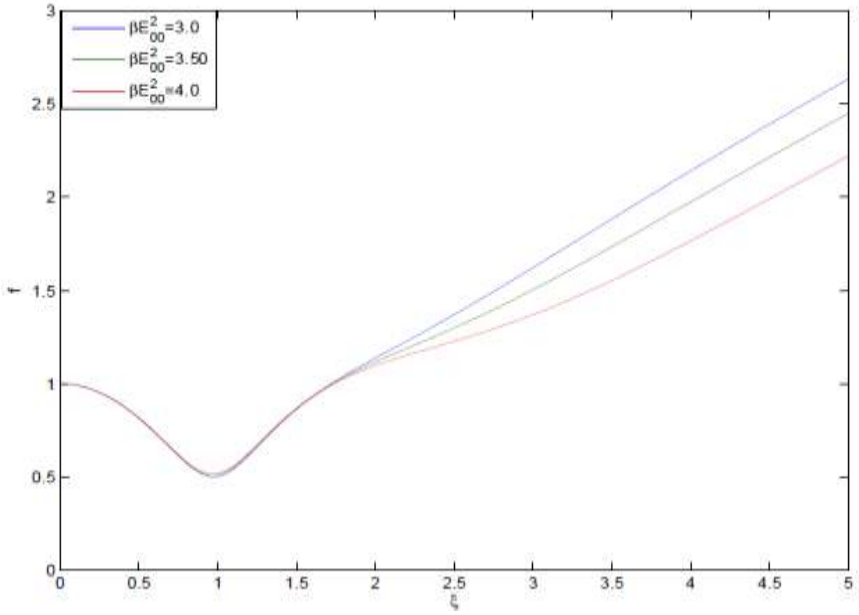

Fig. 5.3: Variation of beam width parameter f with normalized distance of propagation ξ for different values of laser intensity βE_{00}^2 viz., $\beta E_{00}^2 = 3.0, 3.50, 4.0$ and at fixed values of $b = 0.25, \left(\frac{\omega_{p0} r_0}{c}\right)^2 = 12, \frac{\nu_0}{\omega_0} = 0.05, s = -3$

Fig.5.4 illustrates the effect of plasma density on the focusing/defocusing of the laser beam. The stronger focusing of the laser beam is observed with increase in the density of the plasma. The stronger focusing of the laser beam is due to the fact that the number of electrons contributing to the collisional nonlinearity also increases with increase in the density of plasma. Also, with increase in electron density of plasma the mean free path of electrons gets reduced and hence, the collisions of plasma electrons with other species

become more frequent. This results in enhanced optical nonlinearity of the plasma that in turn increases the self focusing of the laser beam.

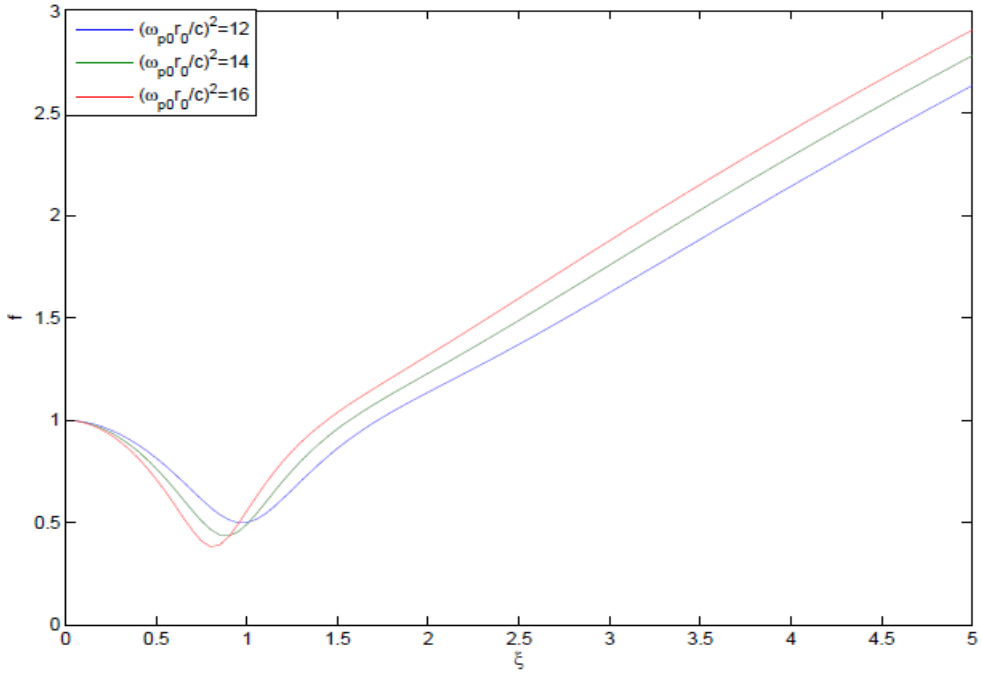

Fig. 5.4: Variation of beam width parameter f with normalized distance of propagation ξ for different values of normalized plasma density $\left(\frac{\omega_{p0}r_0}{c}\right)^2$ viz., $\left(\frac{\omega_{p0}r_0}{c}\right)^2 = 12, 14, 16$ and at fixed values of $b = 0.25, \beta E_{00}^2 = 3.0, \frac{\nu_0}{\omega_0} = 0.05, s = -3$

Fig.5.5 illustrates the effect of collisional frequency on focusing/defocusing of the laser beam. It is observed that there is decrease in the extent of self focusing of the laser beam with increase in the collisional frequency. This is due to the fact that increase in collisional frequency leads to enhanced damping of the laser energy. As a result, the nonlinear refraction of the laser beam becomes weaker. Hence, increase in collisional frequency leads to reduced focusing of the laser beam.

Fig.5.6 illustrates the effect of nature of collisions on self focusing/defocusing of the laser beam. It is observed that no self focusing of the laser beam takes place in plasmas dominant with collisions between electrons and diatomic molecules. This is due to the fact that $s = 2$ corresponds to the situation, where $n_e = n_0 = n_{0i}$ and hence, no redistribution of electrons takes place. Thus, the magnitude of nonlinear refractive term in eq.(5.16) becomes zero. The diffraction divergence is a dominating mechanism in this case.

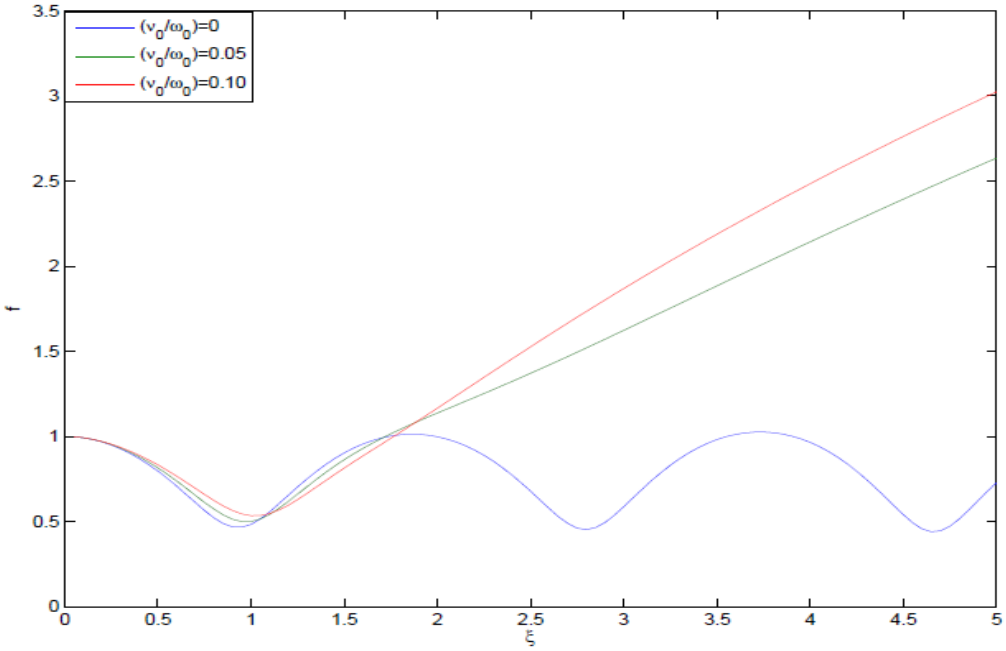

Fig. 5.5: Variation of beam width parameter f with normalized distance of propagation ξ For different values of collisional frequency $\frac{\nu_0}{\omega_0}$ viz., $\frac{\nu_0}{\omega_0} = 0, 0.05, 0.10$ and at fixed values of $b = 0.25, \beta E_{00}^2 = 3.0, \left(\frac{\omega_{p0} r_0}{c}\right)^2 = 12, s = -3$

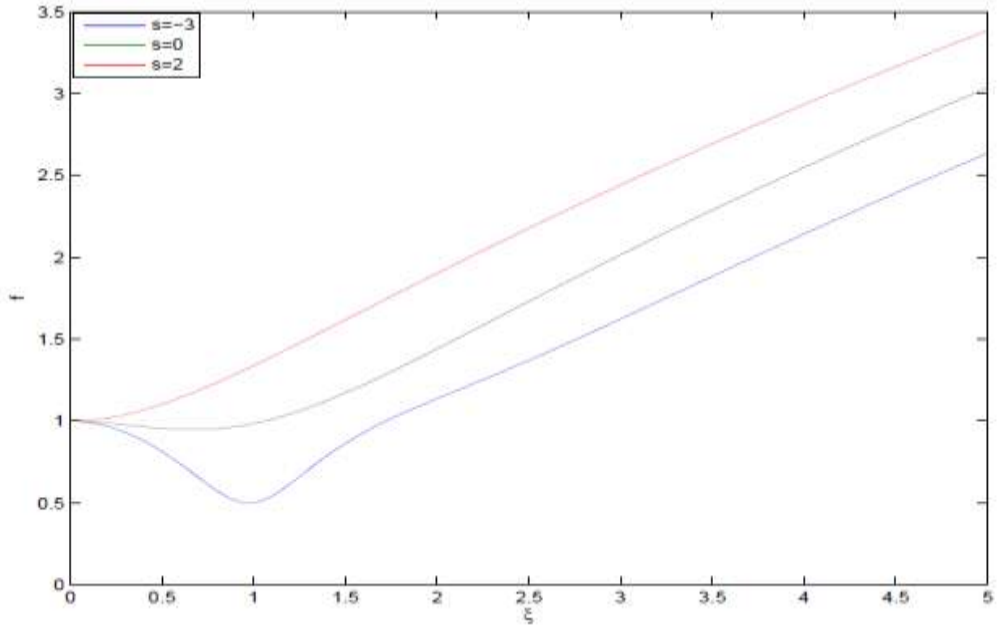

Fig. 5.6: Variation of beam width parameter f with normalized distance of propagation ξ For different values of s viz., $s = -3, 0, 2$ and at fixed values of $b = 0.25, \beta E_{00}^2 = 3.0, \left(\frac{\omega_{p0} r_0}{c}\right)^2 = 12, \frac{\nu_0}{\omega_0} = 0.05$

5.6 Conclusions

I have investigated, the nonlinear propagation of ChG laser beams through collisional plasma by incorporating the effect of intensity dependent absorption of the laser beam. It has been observed that ChG laser beams can play a significant role in enhancing the efficiency of laser plasma coupling. The uniform irradiance over the cross section of the laser beam results in its enhanced self focusing in plasma by reducing the nonlinear attenuation. Further it has been observed that for a given laser beam the self focusing of the laser beam can be increased by increasing the electron density of plasma. The results of present investigation may serve as a guide for the experimentalists working in the field of laser plasma interactions.

Chapter-6

Linear and Nonlinear Propagation Characteristics of Multi-Gaussian Laser Beams

6.1 Introduction

The expansion of the transverse dimensions of a propagating beam is ubiquitous for all kinds of waves including electro-magnetic waves and even matter waves. It would seem that this kind of spreading is inevitable and therefore irreducible, since it originates at a fundamental level from light's natural wave property of diffraction. However, *Chiao et al*. [24] showed that in media whose index of refraction depends on the intensity of light, and the spreading of an optical beam in principle can be obviated. Hence, the expansion of optical beam due to diffraction is neither inevitable nor irreducible. In nonlinear media, the presence of an optical beam modifies their optical properties like index of refraction, absorption, or conversion to higher frequencies. The resulting change in index of refraction resembles to that of a graded index fiber and thus the beam automatically becomes accumulated towards its axis. This phenomena is known as self focusing. When self focusing exactly balances the diffraction of the laser beam, the beam propagates in a stable self trapped mode. Since its discovery by *Askaryan* [22], the phenomenon of self focusing is at the vanguard of experimental as well as theoretical investigations due to its relevance in number of applications.

In the design of ultra intense laser systems such as those being used in laser driven nuclear fusion, the phenomenon of self focusing plays an important role. By producing intra cavity losses, it can limit the cavity intensity or can slow down the release of optical energy. It can also alter the transverse profile of the laser beam by producing wavefront distortions. It is well known fact that with respect to a reference on axis plane wave, a converging/diverging electromagnetic beam undergoes modulation of its longitudinal phase. This self phase modulation of the longitudinal phase of a laser beam is also known as Gouy phase shift, which is a matter of debate over past few years. Since this discovery, various theories (ranging from classical [170] to quantum [162]) have been used to explain

its origin. Classically, self phase modulation of the laser beam arises due to the contribution of an additional phase per unit length in the neighbourhood of beam focal spot arising from the second order derivative of field amplitude with respect to transverse coordinates. However, in quantum mechanical terms, the longitudinal phase shift is considered as a purely geometrical effect, resulting as a consequence of modification of volume of space available for the propagation of the beam. The consequent change in the transverse momentum of the photon changes the longitudinal momentum as well that in turn modifies the longitudinal phase of the laser beam. Precise knowledge of the behaviour of the overall phase of the laser beam is important to control and understand laser driven processes. In laser cavities, it plays a significant role in determining the resonant frequencies of the transverse modes. By increasing the frequency degeneracy of the resonant modes of the cavity, longitudinal phase shift [171] can influence the beam quality achieved in the laser resonator.

Since the seminal works of Chiao et al [24]., Kelley [55], Gupta et al. [172] and Gustafson et al. [173], extensive literature has been reported by several researchers highlighting various aspects of propagation characteristics of laser beams in various nonlinear media. Laser beams differing in intensity profile behave differently in nonlinear media. The reported review reveals the fact that most of the earlier theoretical investigations on nonlinear optical phenomena of laser beams have been directed towards revealing the propagation characteristics of laser beams with ideal Gaussian profile. However, in context of the ICF, there is growing interest in class of laser beams those are having uniform irradiance over wider area of their cross sections. In comparison to Gaussian beams, laser beams with uniform irradiance possess low divergence and thus can improve the efficiency of laser plasma coupling during the ICF. Also, these beams can deliver high power densities to the target while keeping power density below the threshold for other parametric instabilities. Mathematically such beam profiles are modeled by super Gaussian or the multi-Gaussian (M.G.) beam profiles [157]. Most of the earlier investigations on propagation characteristics of the M.G. laser beams in plasmas have been carried out in the framework of paraxial theory. Paraxial theory oversimplifies the analysis

by taking into consideration the effect of only the paraxial region of the cross section of the laser beam towards the optical nonlinearity of the medium. This approximation is valid up to some extent for Gaussian laser beams. But for the M.G laser beams those possess uniform irradiance over their cross section, this approximation is not valid.

The aim of the present study is to give more detailed analysis of the propagation characteristics of the M.G laser beams with the help of variational theory approach which is free from the limitations of paraxial theory.

6.2 Intensity Profile of M.G. Laser Beam

The intensity profile of M.G. laser beams is modeled by the function

$$AA^*|_{z>0} = \frac{E_{00}^2}{f^2}\left[e^{-\frac{(x-x_0f)^2+y^2}{2r_0^2f^2}} + e^{-\frac{(x+x_0f)^2+y^2}{2r_0^2f^2}} + e^{-\frac{x^2+(y-x_0f)^2}{2r_0^2f^2}} + e^{-\frac{x^2+(y+x_0f)^2}{2r_0^2f^2}}\right]^2 \tag{6.1}$$

where $A(x, y, z)$ is the slowly varying beam envelope, r_0 is the beam width at focal plane and E_{00} is the axial amplitude of the electric field, i.e. amplitude at the center $(x = 0, y = 0)$ of the focal plane. The parameter $f(z)$ is currently undetermined and upon multiplication with initial beam width r_0 and gives the instantaneous beam width of the laser beam. Hence, $f(z)$ is termed as dimensionless beam width parameter. The M.G. laser beam provides a uniform irradiance over the cross section of spot size. It further improves the propagation of laser beam in a nonlinear media.

6.3 Relativistic Nonlinearity of Plasma

The dielectric function of plasma can be written as

$$\varepsilon_0 = 1 - \frac{\omega_p^2}{\omega_0^2} \tag{6.2}$$

where

$$\omega_p^2 = \frac{4\pi e^2 n_0}{m_e} \tag{6.3}$$

$e, m_e,$ and n are electronic charge, mass and density, respectively. The electric field vector

$$\boldsymbol{E} = A(r, z)e^{i(\omega_0 t - k_0 z)}\left(e_x + ie_y\right) \tag{6.4}$$

imparts oscillatory velocity

$$v = \frac{eE}{im\omega_0^2} \tag{6.5}$$

to the plasma electrons. When this quiver velocity of the carriers approaches to that of light in vacuum under the effect of ultra-intense laser beam, the effective mass m_e of the electrons in eq. (4) needs to be replaced by $m_0\gamma$, where m_0 is the rest mass of electron and γ is the relativistic Lorentz factor. Following Akhiezer and Polovin, the relativistic Lorentz factor γ is related to laser field amplitude as [31]

$$\gamma = (1 + \beta A A^*)^{\frac{1}{2}} \tag{6.6}$$

where the coefficient $\beta = \frac{e^2}{m_0^2 c^2 \omega_0^2}$ gives the strength of relativistic nonlinearity. Using eqs. (2), (4) and (7) in Eq. (3), the effective dielectric function of plasma for the M.G laser beams can be written as

$$\varepsilon = 1 - \frac{\omega_{p0}^2}{\omega_0^2}\left\{1 + \frac{\beta E_{00}^2}{f^2}\left(e^{-\frac{(x-x_0 f)^2+y^2}{2r_0^2 f^2}} + e^{-\frac{(x+x_0 f)^2+y^2}{2r_0^2 f^2}} + e^{-\frac{x^2+(y-x_0 f)^2}{2r_0^2 f^2}} + e^{-\frac{x^2+(y+x_0 f)^2}{2r_0^2 f^2}}\right)\right\}^{-\frac{1}{2}} \tag{6.7}$$

where $\omega_{p0}^2 = \frac{4\pi e^2 n}{m_0}$ is the equilibrium plasma frequency, i.e. the plasma frequency in the absence of laser beam. For linearly polarized laser beam the relativistic Lorentz factor is given by

$$\gamma = \left(1 + \frac{1}{2}\beta A A^*\right)^{\frac{1}{2}}$$

Thus it can be predicted that for a given intensity circularly polarized laser beam produces more nonlinearity compared to that by linearly polarized laser beam. This is due to the fact that in case of circularly polarized laser beam propagating through relativistic plasma, a quasi-stationary magnetic field is produced. The pinching effect of this produced magnetic field gets added to plasma nonlinearity. Thus, due to this additional contribution of the pinching effect of the magnetic field, circularly polarized laser beam produces larger nonlinearity in the index of refraction of plasma compared to that by linearly polarized beam.

Separating effective dielectric function of plasma into linear ε_0 and nonlinear $\phi(A_0 A_0^*)$ parts as

$$\varepsilon = \varepsilon_0 + \phi(A_0 A_0^*) \tag{6.8}$$

$$\varepsilon_0 = 1 - \frac{\omega_{p0}^2}{\omega_0^2} \tag{6.9}$$

$$\phi(AA^*) = \frac{\omega_{p0}^2}{\omega_0^2}\left[1 - \left\{1 + \frac{\beta E_{00}^2}{f^2}\left(e^{-\frac{(x-x_0 f)^2+y^2}{2r_0^2 f^2}} + e^{-\frac{(x+x_0 f)^2+y^2}{2r_0^2 f^2}} + e^{-\frac{x^2+(y-x_0 f)^2}{2r_0^2 f^2}} + e^{-\frac{x^2+(y+x_0 f)^2}{2r_0^2 f^2}}\right)\right\}\right] \quad (6.10)$$

6.4 Evolution of Beam Width

The propagation of the laser beams in nonlinear media is governed by nonlinear Schrodinger wave equation (NLSE)

$$i\frac{\partial A}{\partial z} = \frac{1}{2k_0}\nabla_\perp^2 A + \frac{k_0}{2\varepsilon_0}\phi(AA^*)A \quad (6.11)$$

where, $\nabla_\perp^2 = \frac{\partial^2}{\partial x^2} + \frac{\partial^2}{\partial y^2}$ is the Laplacian along the transverse direction. Using the same analysis as that of chapter-4, one can get equation of motion of beam width of the laser beam as

$$\frac{d^2 f}{d\xi^2} + \frac{1}{f^2}\left(\frac{df}{d\xi}\right)^2 = \frac{1}{4f^3}\left(\frac{1 + e^{-\frac{x_0^2}{r_0^2}}\left(1 - \frac{x_0^2}{r_0^2}\right) + e^{-\frac{x_0^2}{2r_0^2}}\left(2 - \frac{x_0^2}{r_0^2}\right)}{\left(2 + 2\frac{x_0^2}{r_0^2}\right) + \left(2 + 2\frac{x_0^2}{r_0^2}\right)e^{-\frac{x_0^2}{r_0^2}} + 2e^{-\frac{x_0^2}{r_0^2}}}\right) - \left(\frac{\frac{3}{2\pi}\left(\frac{\omega_{p0} r_0}{c}\right)^2 \frac{\beta E_{00}^2}{f^3}(K_1 + K_2 + K_3 + K_4)}{\left(2 + 2\frac{x_0^2}{r_0^2}\right) + \left(2 + 2\frac{x_0^2}{r_0^2}\right)e^{-\frac{x_0^2}{2r_0^2}} + 2e^{-\frac{x_0^2}{r_0^2}}}\right) \quad (6.12)$$

Where

$$K_1 = \int_0^\infty \int_0^\infty t_1\left(t_1 - \frac{x_0}{r_0}\right)e^{-\frac{\left(t_1 - \frac{x_0}{r_0}\right)^2 + t_2^2}{2}} \times G_1^3(t_1, t_2)G_2(t_1, t_2)dt_1 dt_2$$

$$K_2 = \int_0^\infty \int_0^\infty t_1\left(t_1 + \frac{x_0}{r_0}\right)e^{-\frac{\left(t_1 + \frac{x_0}{r_0}\right)^2 + t_2^2}{2}} \times G_1^3(t_1, t_2)G_2(t_1, t_2)dt_1 dt_2$$

$$K_3 = \int_0^\infty \int_0^\infty t_1^2 e^{-\frac{t_1^2 + \left(t_2 - \frac{x_0}{r_0}\right)^2}{2}} \times G_1^3(t_1, t_2)G_2(t_1, t_2)dt_1 dt_2$$

$$K_4 = \int_0^\infty \int_0^\infty t_1^2 e^{-\frac{t_1^2 + \left(t_2 + \frac{x_0}{r_0}\right)^2}{2}} \times G_1^3(t_1, t_2)G_2(t_1, t_2)dt_1 dt_2$$

$$G_1(t_1, t_2) = e^{-\frac{\left(t_1 - \frac{x_0}{r_0}\right)^2 + t_2^2}{2}} + e^{-\frac{\left(t_1 + \frac{x_0}{r_0}\right)^2 + t_2^2}{2}} + e^{-\frac{t_1^2 + \left(t_2 - \frac{x_0}{r_0}\right)^2}{2}} + e^{-\frac{t_2^2 + \left(t_2 + \frac{x_0}{r_0}\right)^2}{2}}$$

$$G_2(t_1, t_2) = \left[1 + \frac{\beta AA^*}{f^2}G_1^2(t_1, t_2)\right]^{-\frac{3}{2}}$$

$$t_1 = \frac{x}{r_0 f}, \quad t_2 = \frac{y}{r_0 f}, \quad \xi = \frac{z}{k_0 r_0^2}$$

Thus, it follows from eq. (6.12) that the problem of solving a partial differential equation, i.e., the NLSE (eq. (6.11)) has reduced to that of solving an ordinary differential

equation. Although this reduced equation is also lacking form exact analytical solution due to its non integrability, its approximate solution can be easily obtained with the help of simple numerical techniques by assuming that initially the beam is collimated, i.e. it satisfies the initial conditions $f = 1$ and $\frac{df}{d\xi} = 0$ at $x = 0$.

6.5 Potential Well for Self Focusing

Equation (6.12) resembles to the equation of motion of a forced harmonic oscillator of unit mass and can be written as

$$\frac{d^2f}{d\xi^2} + \frac{\partial V(f)}{\partial f} = 0 \tag{6.13}$$

$$V(f) = -\int^{f} F(f)df \tag{6.14}$$

$$F(f) = \frac{1}{4f^3}\left[\frac{1 + e^{-\frac{x_0^2}{r_0^2}}\left(1 - \frac{x_0^2}{r_0^2}\right) + e^{-\frac{x_0^2}{2r_0^2}}\left(2 - \frac{x_0^2}{r_0^2}\right)}{\left(2 + 2\frac{x_0^2}{r_0^2}\right) + \left(2 + 2\frac{x_0^2}{r_0^2}\right)e^{-\frac{x_0^2}{r_0^2}} + 2e^{-\frac{x_0^2}{r_0^2}}}\right] + \left(\frac{\frac{1}{2\pi}\left(\frac{s}{2} - 1\right)\left(\frac{\omega_{p0}r_0}{c}\right)^2 \frac{\beta E_{00}^2}{f^3}(K_1 + K_2 + K_3 + K_4)}{\left(2 + 2\frac{x_0^2}{r_0^2}\right) + \left(2 + 2\frac{x_0^2}{r_0^2}\right)e^{-\frac{x_0^2}{2r_0^2}} + 2e^{-\frac{x_0^2}{r_0^2}}}\right) - \frac{1}{f}\left(\frac{df}{d\xi}\right)^2 \tag{6.15}$$

From Eqs.(6.12)–(6.15), it is clear that with the help of variational theory, the problem of nonlinear wave propagation has reduced to a simple mechanical problem with potential $V(f)$, where the particle's coordinate is related to the beam width parameter f, particle velocity to the wavefront curvature $\frac{df}{d\xi}$, and the time to axial distance ξ.

As $V(f) \to \infty$ for $f \to 0$ and $V(f) \to 0$ for $f \to \infty$, the potential function $V(f)$ for self focusing resembles to that for Kepler's attractive central force problem. Hence f can be treated as radial coordinate of polar coordinate system (f, θ_f). The lagrangian L for a particle of unit mass in (f, θ_f) plane is given by

$$L = \frac{1}{2}\left[\left(\frac{df}{d\xi}\right)^2 + f^2\left(\frac{d\theta_f}{d\xi}\right)^2\right] - U(f) \tag{6.16}$$

Multiplying Eq. (6.13) by $\frac{df}{d\xi}$ and integrating both sides and we can get

$$\frac{1}{2}\left(\frac{df}{d\xi}\right)^2 + V(f) = E \tag{6.17}$$

where E is the constant of integration and is known as energy function. The canonical momentum associated with polar angle θ_f

$$p_{\theta_f} = \frac{dL}{d\dot{\theta}_f} = f^2\dot{\theta}_f \tag{6.18}$$

where $\dot{\theta}_f = \frac{d\theta_f}{d\xi}$. The corresponding Lagrange equation

$$\frac{d}{d\xi}\left(\frac{\partial L}{\partial \dot{\theta}_f}\right) - \frac{\partial L}{\partial \theta_f} = 0$$

gives

$$\frac{d}{d\xi}\left(f^2\dot{\theta}_f\right) = 0$$

Which implies that

$$f^2\dot{\theta}_f = l \tag{6.19}$$

Hence, angular momentum corresponding to polar coordinate θ_f is conserved. The Lagrange equation for radial coordinate f is

$$\frac{d}{d\xi}\left(\frac{\partial L}{\partial \dot{f}}\right) - \frac{\partial L}{\partial f} = 0$$

Using eq. (6.16) we can obtain

$$\frac{d^2 f}{d\xi^2} = -\frac{d}{df}\left(U(f) + \frac{l^2}{2f^2}\right)$$

Integrating this equation after multiplying with $\frac{df}{d\xi}$, we can get

$$\frac{1}{2}\left(\dot{f}^2 + \frac{l^2}{f^2}\right) + U(f) = E \tag{6.20}$$

Comparing Eq. (6.17) with eq. (6.20)

$$V(f) = U(f) + \frac{l^2}{2f^2} \tag{6.21}$$

Comparing this Kepler's potential with potential function (Eq. (6.14)) for self focusing we can obtain

$$l = \left[\frac{1 + e^{-\frac{x_0^2}{r_0^2}}\left(1 - \frac{x_0^2}{r_0^2}\right) + e^{-\frac{x_0^2}{2r_0^2}}\left(2 - \frac{x_0^2}{r_0^2}\right)}{\left(2 + 2\frac{x_0^2}{r_0^2}\right) + \left(2 + 2\frac{x_0^2}{r_0^2}\right)e^{-\frac{x_0^2}{2r_0^2}} + 2e^{-\frac{x_0^2}{r_0^2}}}\right]$$

This is an interesting and curious result since it explains the dependence of divergence of laser beam on $\frac{x_0}{r_0}$, as the angular momentum of the beam in (f, θ_f) plane is dependent on $\frac{x_0}{r_0}$. Since, with increase in the value of $\frac{x_0}{r_0}$, the magnitude of angular

momentum l decreases (fig.6.1), hence with increase in the value of $\frac{x_0}{r_0}$, the divergence of the laser beam decreases.

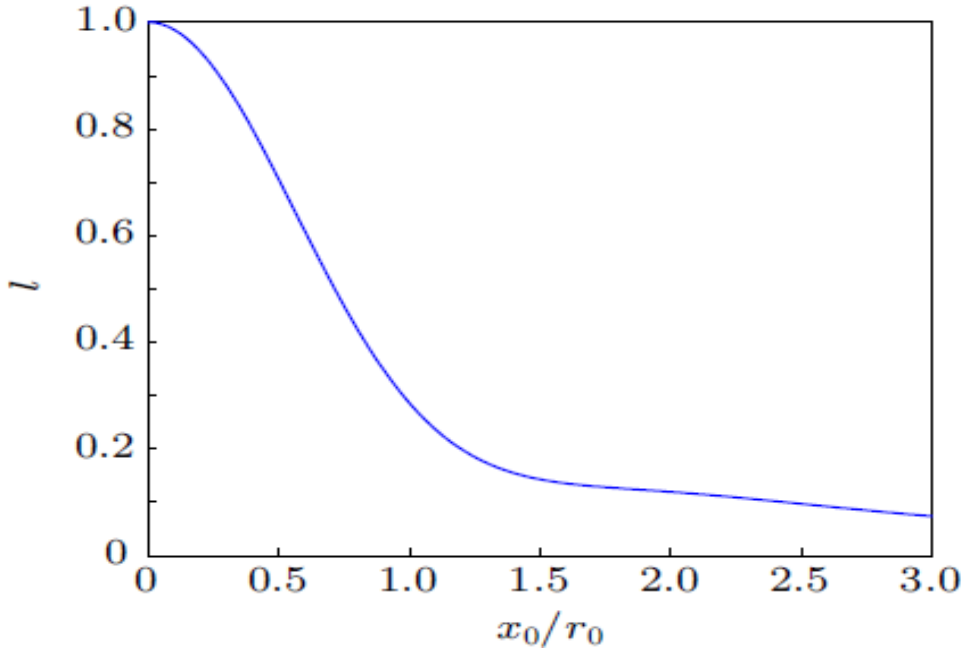

Fig.6.1: Variation of angular momentum l of M.G beam in (f, θ_f) plane with $\frac{x_0}{r_0}$

6.6 Self Channeling of Laser Beam

If while entering into the medium, the beam possesses at plane wavefront, i.e. if $f = 1$, and $\frac{df}{d\xi} = 0$, at $\xi = 0$, then the condition $\frac{d^2f}{d\xi^2} = 0$ will maintain their values throughout the journey of the beam through the medium. Such a mode of propagation, when there is no change in the beam width of the laser beam, is called self trapped mode or spatial optical soliton [34]. Hence, for $\frac{df}{d\xi} = \frac{d^2f}{d\xi^2} = 0$, eq. (6.12) gives the relation between dimensionless beam width $\left(\frac{\omega_{p0} r_0}{c}\right)$ and the critical beam intensity βE_{00}^2 as

$$r_e^2 = \frac{\pi}{2\beta E_{00}^2}\left[\frac{1 + e^{-\frac{x_0^2}{r_0^2}}\left(1 - \frac{x_0^2}{r_0^2}\right) + e^{-\frac{x_0^2}{2r_0^2}}\left(2 - \frac{x_0^2}{r_0^2}\right)}{K_1' + K_2' + K_3' + K_4\text{^"}}\right] \tag{6.22}$$

where

$$K_1' = K_1|_{f=1}, K_2' = K_2|_{f=1}, K_3' = K_3|_{f=1}, K_4' = K_4|_{f=1}$$

and

$$r_e = \frac{\omega_{p0} r_0}{c}$$

The laser beam for which the point $(\beta E_{00}^2, r_e)$ lies on the critical curve defined by eq. (6.18), $\frac{d^2 f}{d\xi^2}$ will vanish at $\xi = 0$. This simply means that during the journey of the laser beam through the plasma, there will be no change in the curvature of the wavefront, i.e. $\frac{df}{d\xi}$ will remain constant and value of this constant will be equal to initial value, that I have taken to be zero. Hence, $\frac{d^2 f}{d\xi^2} = \frac{df}{d\xi} = 0$ at $\xi = 0$ indicates that $\frac{df}{d\xi} = 0$ for $\xi > 0$ also. Physically, this means that there will be no change in the spot size of the laser beam during its propagation. This mode of propagation is known as self trapped mode. Thus, the region of space lying on the critical curve corresponds to self channeling of the laser beam.

If the point $(\beta E_{00}^2, r_e)$ lies in the upper region of critical curve, then the initial value of $\frac{d^2 f}{d\xi^2}$ will be positive and hence f will increase monotonically with distance. This mode of propagation is known as self broadening of the beam. If the point $(\beta E_{00}^2, r_e)$ lies below the critical curve then initial value of $\frac{d^2 f}{d\xi^2}$ will be negative and thus f will decrease with distance. This mode is known as self focusing of the laser beam. Thus, the region below the critical curve corresponds to self focusing.

6.7. Self Phase Modulation of Laser Beam

The self phase modulation of the laser beam occurs due to shift in its longitudinal phase occurring from transverse spatial confinement [174]. Due to its finite effective beam width, the laser beam behaves as it is passing through a narrow slit and thus through position-momentum uncertainty $(\Delta x \Delta p_x = \text{constant})$ experiences a spread in its transverse momenta and hence a shift in expectation value of the propagation constant. The r.m.s spectral width σ_k of the laser beam is defined as

$$\sigma_{k,M.G} = \sqrt{\langle k_x^2 \rangle + \langle k_y^2 \rangle} \tag{6.23}$$

$$\langle k_x^2 \rangle = \frac{\int_{-\infty}^{\infty} \int_{-\infty}^{\infty} k_x^2 S(k_x, k_y) dk_x dk_y}{\int_{-\infty}^{\infty} \int_{-\infty}^{\infty} S(k_x, k_y) dk_x dk_y} \tag{6.24a}$$

$$\langle k_y^2 \rangle = \frac{\int_{-\infty}^{\infty}\int_{-\infty}^{\infty} k_y^2\, S(k_x,k_y)dk_x dk_y}{\int_{-\infty}^{\infty}\int_{-\infty}^{\infty} S(k_x,k_y)dk_x dk_y} \tag{6.24b}$$

$$S(k_x,k_y) = \left|\int_{-\infty}^{\infty}\int_{-\infty}^{\infty} A_0\,(x,y)|_{z=0} e^{-i(k_x x+k_y y)}dx\,dy\right|^2 \tag{6.25}$$

The ratio $\sum_k$ of spectral widths of a M.G beam to that of a Gaussian beam $\sigma_{k,G}$ can be written as

$$\sum_k = \frac{\sigma_{k,M.G}}{\sigma_{k,G}} = \left\{\frac{1+e^{-\frac{x_0^2}{2r_0^2}}\left(1-\frac{x_0^2}{r_0^2}\right)}{1+e^{-\frac{x_0^2}{2r_0^2}}}\right\}^{\frac{1}{2}} \tag{6.26}$$

The wave number k_0 of the laser beam is related to transverse and longitudinal components through

$$k_0^2 = k_x^2 + k_y^2 + k_z^2 \tag{6.27}$$

where k_z is the axial wave number, and $k_x$and k_y are the transverse wave numbers, respectively. The effective axial propagation constant of an optical beam is defined in r.m.s sense as

$$\bar{k}_z = \frac{\langle k_z^2\rangle}{k_0} = k_0 - \frac{\langle k_x^2\rangle}{k_0} - \frac{\langle k_y^2\rangle}{k_0} \tag{6.28}$$

The overall on axis phase $\theta(z)$ is related to effective propagation constant as [169]

$$\bar{k}_z = \frac{\partial\theta}{\partial z} \tag{6.29}$$

The first term in Eq. (6.28) gives the phase k_{0z} of an infinite plane wave propagating along z-axis. The second term represents a phase shift of finite beam in comparison to infinite plane wave.

$$\frac{d\theta_p}{dz} = -\frac{1}{k_0}\left(\langle k_x^2\rangle + \langle k_y^2\rangle\right) \tag{6.30}$$

Thus, it can be seen that average value of the transverse momentum of the beam is measure of shift in its longitudinal phase. Using eqs. (6.24) and (6.25) in eq. (6.30) we can obtain

$$\frac{d\theta_p}{dz} = -\left\{\frac{1+e^{-\frac{x_0^2}{2r_0^2}}\left(1-\frac{x_0^2}{r_0^2}\right)}{1+e^{-\frac{x_0^2}{2r_0^2}}}\right\}^{\frac{1}{2}} \frac{1}{f^2} \tag{6.31}$$

6.8 Results and Discussion

In present analysis eqs.(6.12) and (6.31) have been solved with the help of Runge Kutta fourth order method for the following set of parameters: $\omega_0 = 1.78 \times 10^{15}\text{rad/sec}$, $\lambda = 1.06\mu m, r_0 = 15\mu m, \left(\frac{\omega_{p0} r_0}{c}\right)^2 = 12,$ and $\beta E_{00}^2 = 3.$

Before solving the beam width equation, i.e. eq. (6.12), it is important to study the role and origin of the various terms contained in it. The first term on the right hand side (R.H.S) that varies inversely as cube of the beam width, is the spatial dispersive term. It models the spreading of the laser beam in transverse directions occurring as a consequence of diffraction divergence. The second term which is having complex dependence on f, arises due to the relativistic mass nonlinearity of the plasma electrons and is responsible for nonlinear refraction of the laser beam. The relative magnitude of the two terms determines the behaviour of the beam width of the laser beam during its propagation.

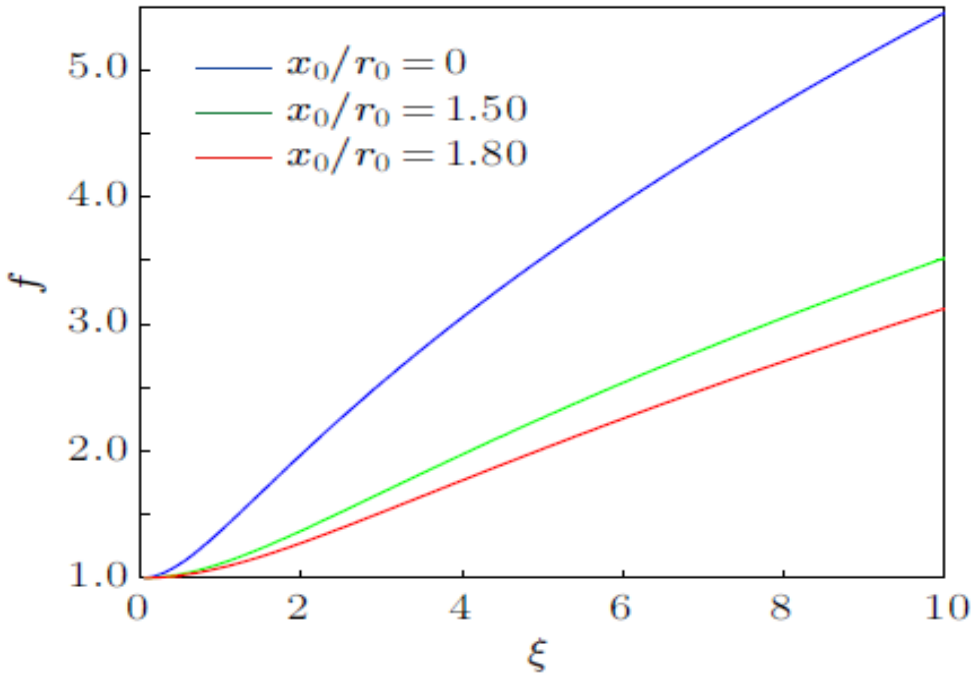

Fig.6.2: Variation of beam width parameter f against the distance of propagation for different values of $\frac{x_0}{r_0}$ viz., $\frac{x_0}{r_0} = 0, 1.50$ and 1.80 in the absence of nonlinear refraction

Firstly, in order to investigate linear characteristics of the laser beam, its propagation in vacuum has been considered. Hence, eq.(6.12) has been solved for different values of $\frac{x_0}{r_0}$

in the absence of nonlinear term. The corresponding variations of beam width with distance are plotted in fig.6.2. It can be easily seen that irrespective of the value of $\frac{x_0}{r_0}$, the beam width of the M.G laser beams diverge monotonically during its propagation in vacuum. This is due to light's natural wave property of diffraction. Due to its finite cross section, the laser beam behaves as it is passing through a slit whose width is equal to the radius of the laser beam. As an optical beam passing through a narrow slit diverge monotonically, similarly the laser beam of finite cross section undergoes monotonic increase in its radius during its propagation through a linear medium. However, the rate of divergence reduces by increasing $\frac{x_0}{r_0}$. Thus, by optimizing the value of $\frac{x_0}{r_0}$, one can control the diffraction broadening of the laser beam. From application point of view this is an important result as the M.G laser beams have smaller divergence compared to that with Gaussian beams.

The increase in the effective radius of the laser beam due to shifting of laser intensity to off axial regions with an increase in the value of $\frac{x_0}{r_0}$. As the phenomenon of diffraction varies inversely with its effective beam width of an optical beam, an increase in the value of $\frac{x_0}{r_0}$ leads to decrease in the divergence of the M.G laser beam due to diffraction divergence. Thus, it can be concluded that the diffraction of an optical beam depends on its effective cross section which is defined by its r.m.s beam width not by geometric radius r_0.

Figs. 6.3 and 6.4 depict the effect of $\frac{x_0}{r_0}$ on the evolution of beam width of the laser beam while propagating through plasma. The plots in these figures depict that during its propagation through the plasma, the beam width of the laser beam varies harmonically. These harmonic variations of the beam width can be explained as shown in fig.6.3-6.4. Due to the intensity gradient along the cross section of the laser beam, there is a nonuniform mass distribution of the plasma electrons. Mass of the plasma electrons is maximum where the laser intensity is maximum and vice versa. Hence, the central part of the beam experiences larger refractive index compared to its tails. The resulting gradient in the phase velocity of the laser beam along its cross section, bends its wave fronts in such a way that the laser beam is passing through a convex lens.

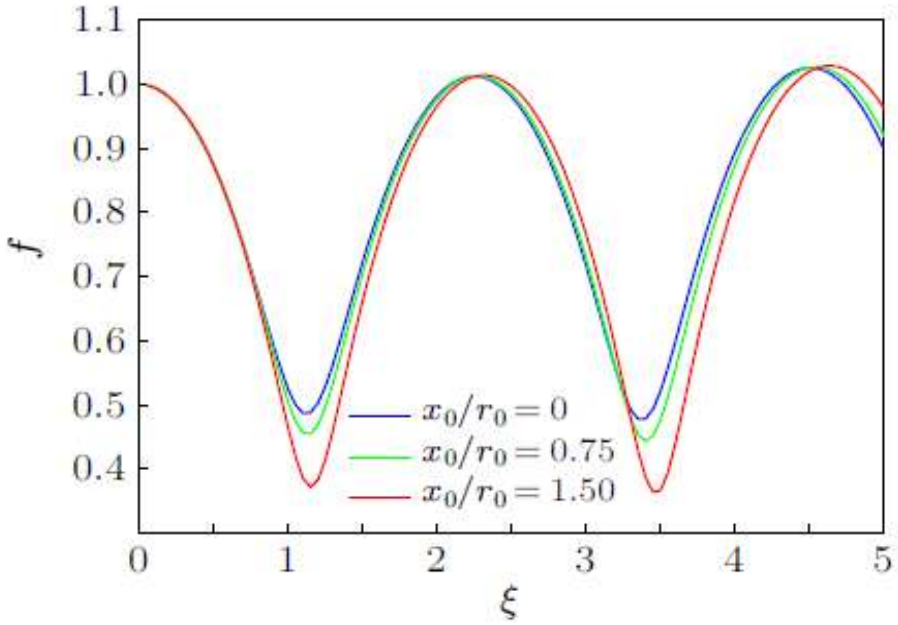

Fig.6.3: Variarion of beam width parameter f with dimensionless distance of propagation ξ for different values of $\frac{x_0}{r_0}$ viz., $\frac{x_0}{r_0} = 0, 0.75$ and 1.50

The nonlinear refraction of the laser beam thus tends to counter balance the effect of diffraction. Thus, during the propagation of the laser beam through the plasma, there is a competition between the two phenomena of diffraction and nonlinear refraction. The winning phenomenon ultimately decides the behaviour of the laser beam, i.e. whether the beam will converge or diverge. Thus, there is a critical value of beam intensity (that can be obtained by equating the right hand side of eq. (6.12) with zero) above which the beam will converge. In the present investigation, the initial beam intensity has been taken greater than the critical intensity, i.e. why the laser spot size of the laser beam is converging initially. As the beam width decreases, its intensity increases. When the laser intensity becomes too high, the nonlinear refractive term in eq. (6.12) disappears, leaving only the diffraction effects to dominate. Hence, after focusing to minimum, the beam width bounces back to its original value. As the beam width of the laser beam starts increasing, the phenomena of diffraction divergence and nonlinear refraction again start competing each other. Now, this competition lasts till maximum value of f is obtained. These processes go on repeating themselves and thus give breather like behaviour to beam width.

Further, it is observed that an increase in the value of $\frac{x_0}{r_0}$ for $0 \leq \frac{x_0}{r_0} \leq 1.5$ results in enhancement of self focusing of the laser beam whereas beyond $\frac{x_0}{r_0} = 1.5$ with an increase in the value of $\frac{x_0}{r_0}$ the extent of self focusing of the laser beam decreases. This is because for $0 \leq \frac{x_0}{r_0} \leq 1.5$ with an increase in the value of $\frac{x_0}{r_0}$ the intensity distribution over the cross section of the laser beam becomes more and more uniform. As a consequence, the laser beam gets equal contribution from the off axial parts for nonlinear refraction as provided by axial part. As the phenomenon of self focusing is a homeostasis of nonlinear refraction, an increase in the value of $\frac{x_0}{r_0}$ in the range $0 \leq \frac{x_0}{r_0} \leq 1.5$ results in the enhancement of self focusing of the laser beam.

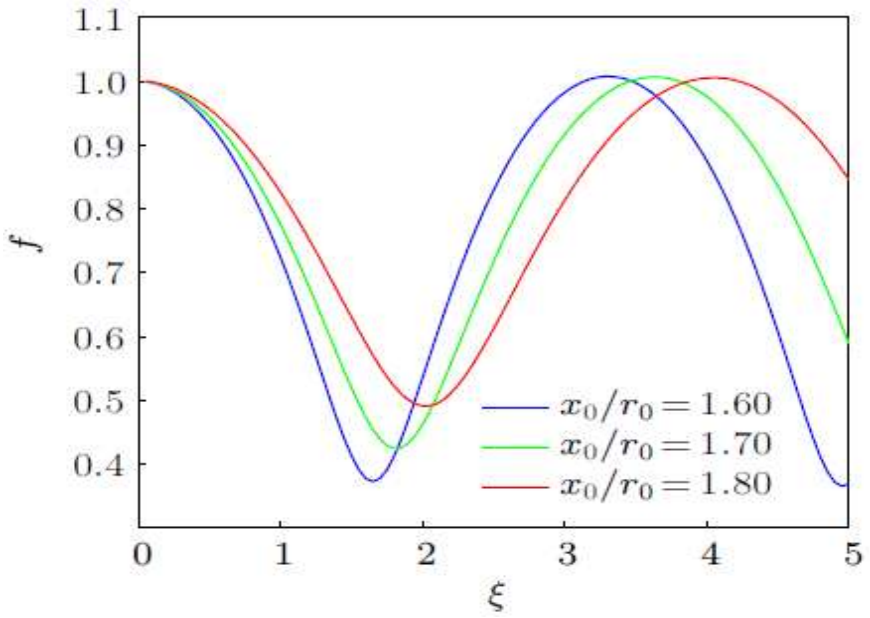

Fig.6.4: Variarion of beam width parameter f with dimensionless distance of propagation ξ for different values of $\frac{x_0}{r_0}$ viz., $\frac{x_0}{r_0} = 1.60, 1.70$ and 1.80

The decrease in the extent of self focusing of the laser beam by increasing $\frac{x_0}{r_0}$ beyond 1.5 is because for $\frac{x_0}{r_0} > 1.5$ the intensity maxima of individual Gaussian laser beams constituting the M.G laser beams are so far away from each other that after superposition the intensity maxima of the resulting beam appear in the off axial parts. This makes paraxial part of the laser beam weaker as compared to off axial part and hence the laser beam gets

a very little contribution from the axial part for nonlinear refraction. This in turn leads to the reduced focusing of the laser beam. Thus, by optimizing the value of $\frac{x_0}{r_0}$, one can control the propagation dynamics of the laser beam in a nonlinear medium.

In order to have insight into the nature of periodicity of the oscillations of beam width of the laser beam I have plotted the phase space trajectories of the laser beam in figs. 6.5 and 6.6. Closed phase space trajectories indicate the stable and periodic harmonic oscillations (i.e., oscillations containing a single resonant frequency) of the beam width whereas, spiral trajectories indicate quasi periodic oscillations (i.e., oscillations containing multiple resonant frequencies). Thus, it is clear from phase space plots that the M.G laser beams possess quasi periodic oscillations in their beam width.

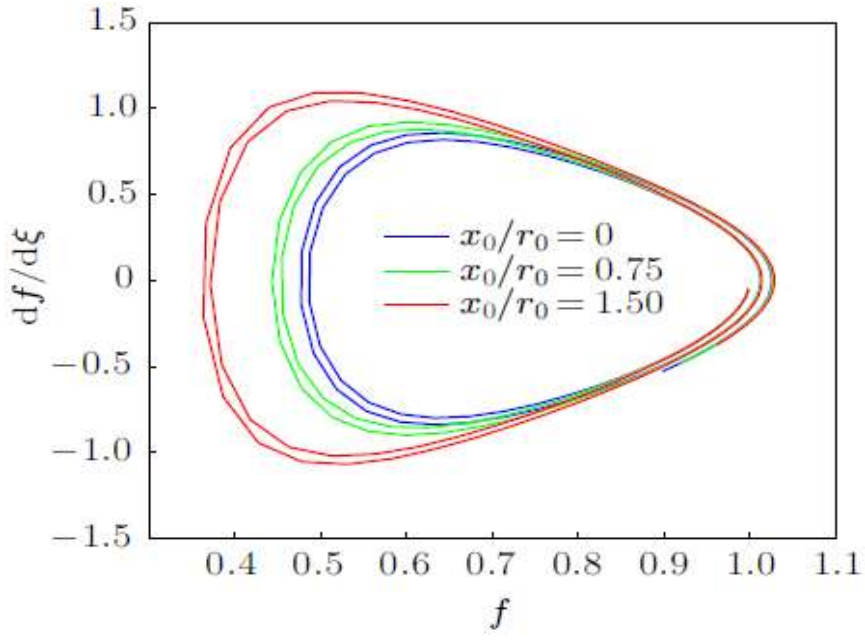

Fig.6.5: Phase space plots for self focused M.G laser beam for different values of $\frac{x_0}{r_0}$ viz., $\frac{x_0}{r_0} = 0, 0.75$ and 1.50

The underlying physics behind this fact can be explained by comparing the evolution equation of beam width with equation of motion of nonlinear oscillator. In case of nonlinear oscillator, resonance does not occur at same frequencies for all amplitudes. Depending on the nature of nonlinearity, the resonance frequency is an increasing or decreasing function of amplitude. Hence, the beam width of the laser beam exhibits quasi periodic behaviour.

Thus, it can be concluded that the beam width of an intense laser beam in a nonlinear medium behave like a nonlinear classical oscillator.

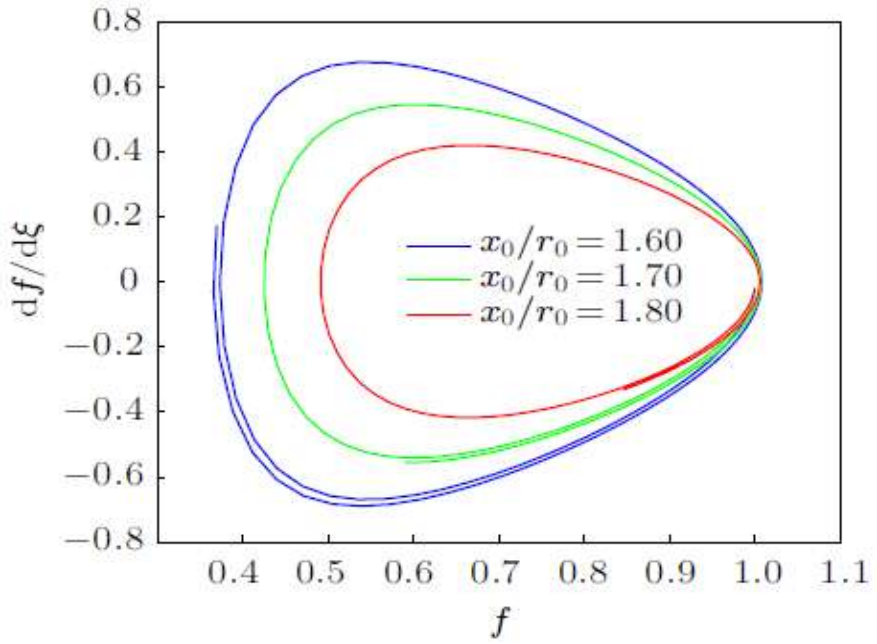

Fig. 6.6: Phase space plots for self focused M.G laser beam for different values of $\frac{x_0}{r_0}$ viz., $\frac{x_0}{r_0} = 1.60, 1.70, 1.80$

The phase space plots also depict that initially the laser beam focuses at a slower rate but as the laser beam gets more and more focused, there is an abrupt increase in the rate of focusing. This is due to the fact that with self focusing of the laser beam, plasma becomes more and more nonlinear. Also, it is observed that the laser beams with higher value of $\frac{x_0}{r_0}$ in the range $0 \leq \frac{x_0}{r_0} \leq 1.5$ span larger phase space area. Whereas, the beams with larger value of $\frac{x_0}{r_0}$ for $\frac{x_0}{r_0} > 1.5$ cover lesser phase space area. This is due to the fact that area of phase space gives the measure of extent of self focusing of the laser beam. Further it can be seen that with an increase in $\frac{x_0}{r_0}$ for $0 \leq \frac{x_0}{r_0} \leq 1.5$, the phase space trajectories become more and more spiral. This is due to an increase in self focusing of the laser beam. An increase in self focusing leads to enhanced amplitude of the oscillations of the beam width that makes them highly nonlinear. Similarly, with an increase in $\frac{x_0}{r_0}$ beyond 1.5, the phase space trajectories tend to become closed one. This is due to the reduction in self focusing

with an increase in $\frac{x_0}{r_0}$ beyond 1.5 that results in more and more stable oscillations of beam width.

Figs. 6.7 and 6.8 illustrate the effect of $\frac{x_0}{r_0}$ on potential function $V(f)$. It is observed that $V(f) \to \infty$ for $f \to 0$. This is because of the domination of diffraction effects for $f \to 0$. For $f \to \infty$, $V(f) \to 0$ because the laser beams with very large spot size are free from diffraction effects as well as they do not produce any nonlinearity in the medium.

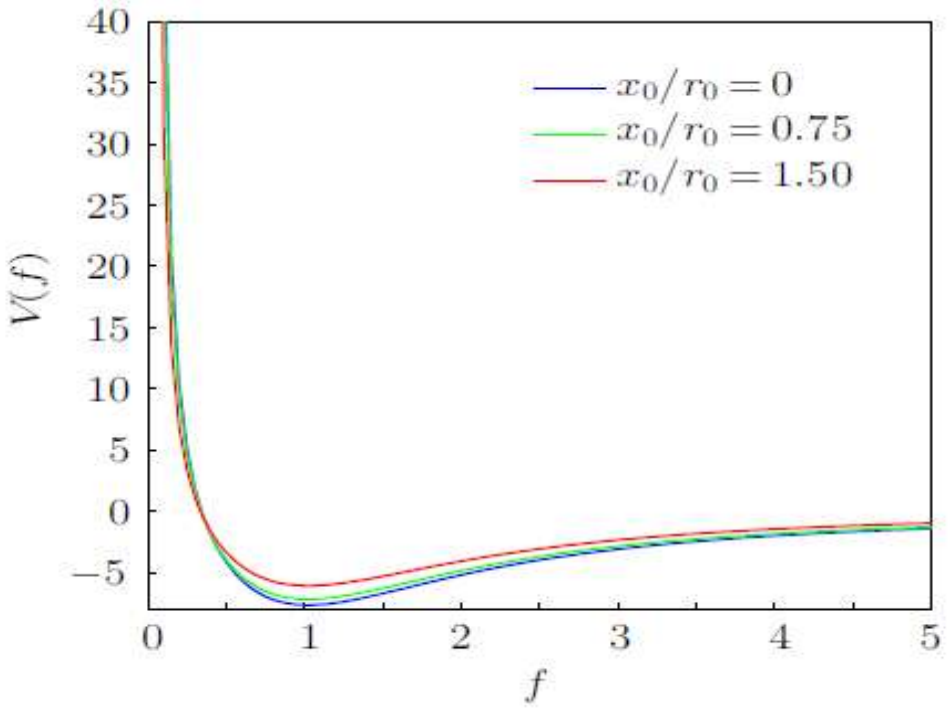

Fig. 6.7: Variation of potential function for self focused M.G laser beam for different values of $\frac{x_0}{r_0}$ viz., $\frac{x_0}{r_0} = 0, 0.75$ and 1.50

It is also observed that with an increase in the value of $\frac{x_0}{r_0}$ for $0 \leq \frac{x_0}{r_0} \leq 1.5$, the bottom of the potential well shifts upwards, and downwards with an increase in the value of $\frac{x_0}{r_0}$ for $\frac{x_0}{r_0} > 1.5$. This indicates that for $0 \leq \frac{x_0}{r_0} \leq 1.5$, the M.G laser beams with higher value of $\frac{x_0}{r_0}$ require lesser intensity to get self focused and for $\frac{x_0}{r_0} > 1.5$, the M.G laser beams with higher value of require higher intensity to get self focused.

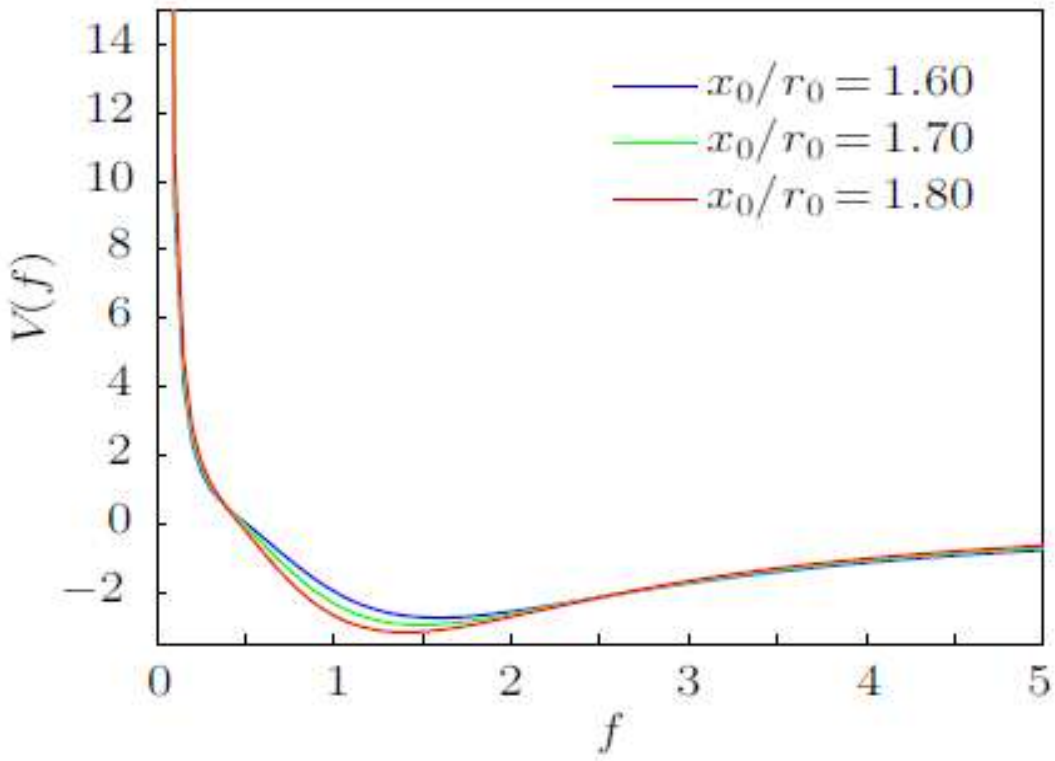

Fig. 6.8: Variation of potential function for self focused M.G laser beam for different values of $\frac{x_0}{r_0}$ viz., $\frac{x_0}{r_0} = 1.60, 1.70$ and 1.80

Figures 6.9 and 6.10 illustrate the effect of $\frac{x_0}{r_0}$ on critical curves of the laser beam. It is observed that at lower laser intensity ($\beta E_{00}^2 \ll 1$), the equilibrium beam width r_e decreases very sharply and at very high laser intensity ($\beta E_{00}^2 \gg 1$), it becomes independent of laser intensity. This is because at very high intensities, in the region of plasma illuminated by the laser beam, all the electrons oscillate at same velocity and thus the relativistic nonlinearity gets saturated and hence the plasma dielectric function becomes independent of laser intensity. Hence, at high intensities, the beam width of the laser beam becomes independent of intensity.

It is also observed that self channeling cannot occur for very narrow laser beams. This is due to the fact that narrow beams possess large diffraction angles. Hence, in order to get self guided, they require larger index differences.

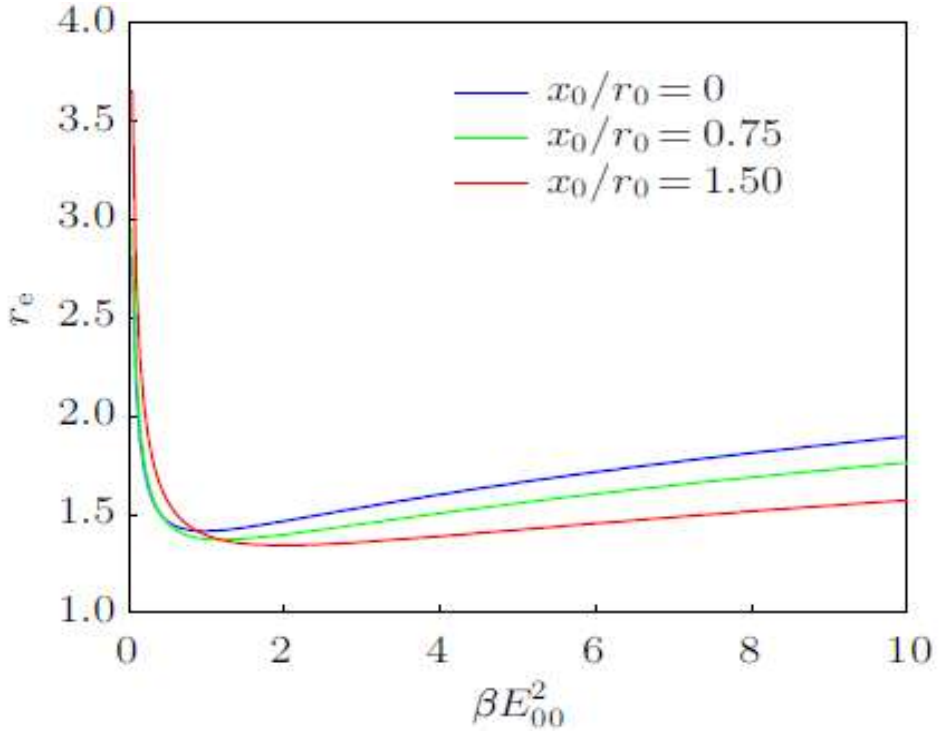

Fig.6.9: Variation of equilibrium beam width r_e against the normalized intensity βE_{00}^2 for different values of $\frac{x_0}{r_0}$ viz., $\frac{x_0}{r_0} = 0, 0.75,$ and 1.50

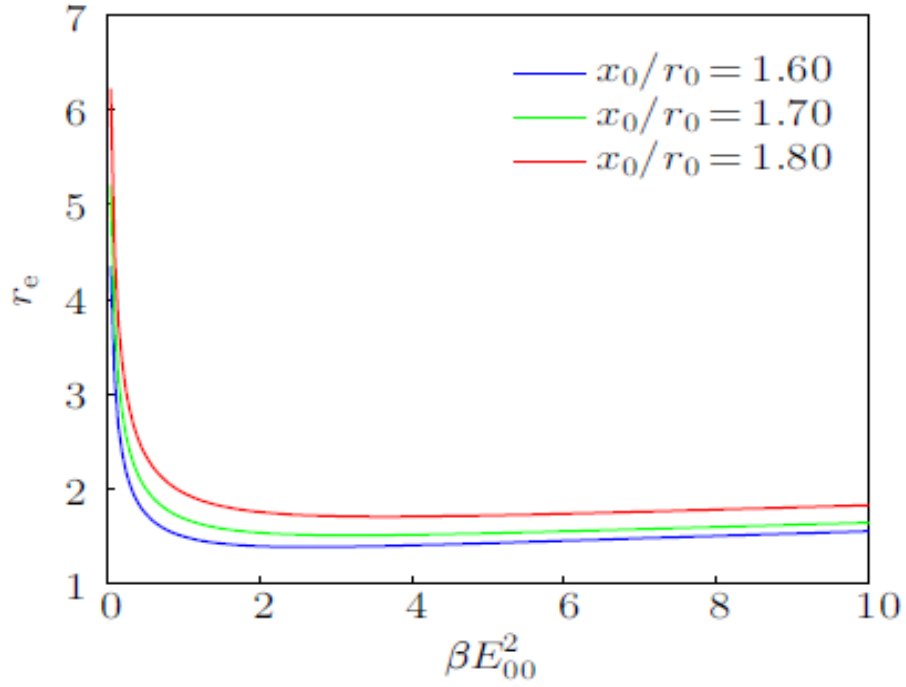

Fig.6.10: Variation of equilibrium beam width r_e against the normalized intensity βE_{00}^2 for different values of $\frac{x_0}{r_0}$ viz., $\frac{x_0}{r_0} = 1.60, 1.70, 1.80$

It is also observed that with an increase in the value of $\frac{x_0}{r_0}$ for $0 \leq \frac{x_0}{r_0} \leq 1.5$, the critical curves shift downwards which means that the laser beams with higher values of $\frac{x_0}{r_0}$ in the range $0 \leq \frac{x_0}{r_0} \leq 1.5$, can be self guided at relatively lower power. This is due to the fact that these laser beams get equal contribution from off-axial rays towards nonlinear refraction.

Figs. 6.11 and 6.12 illustrate that how the value of $\frac{x_0}{r_0}$ affects the evolution of longitudinal phase θ_p. It is observed that longitudinal phase θ_p decreases monotonically with distance of propagation, showing step-like behaviour. This is because self focusing of the laser beam increases its intensity and hence, the laser phase fronts start experiencing larger refractive indices. These results in decreased phase velocity of the phase fronts lead to decreased spacing between them. Hence, the longitudinal phase of the laser beam keep on decreasing with distance.

Step-like behaviour of the longitudinal phase, with each step occurring at positions of minimum beam width is also observed. This indicates that there is slowest decrement in θ_p at points of minimum beam width. This is opposite to the behaviour of phase in graded index fibers, where phase decreases slowest in the positions of minimum intensity, i.e. maximum beam width. This difference in the behaviour of longitudinal phase in plasmas and that in graded index fibers is due to the fact that owing to relativistic nonlinearity, plasmas behave as oscillating linear wave guides. In linear wave guides, the growth rate of longitudinal phase is inversely proportional to the square of beam width (eq. (6.31)).

It can also be seen that there is an increase in the rate of the decrease of longitudinal phase θ_p with an increase in the value of $\frac{x_0}{r_0}$ for $0 < \frac{x_0}{r_0} \leq 1.5$. This is due to the dependence of longitudinal phase on beam width of the laser beam. The smaller is the spot size of the laser beam, the grater is the shift in its longitudinal phase through the position momentum uncertainty ($\Delta x \Delta k_x = \text{constant}$). As, with an increase in the value of $\frac{x_0}{r_0}$ in the range $0 < \frac{x_0}{r_0} \leq 1.5$, there is an increase in the extent of focusing of the laser beam, and there is a corresponding increase in the rate of modulation its longitudinal phase.

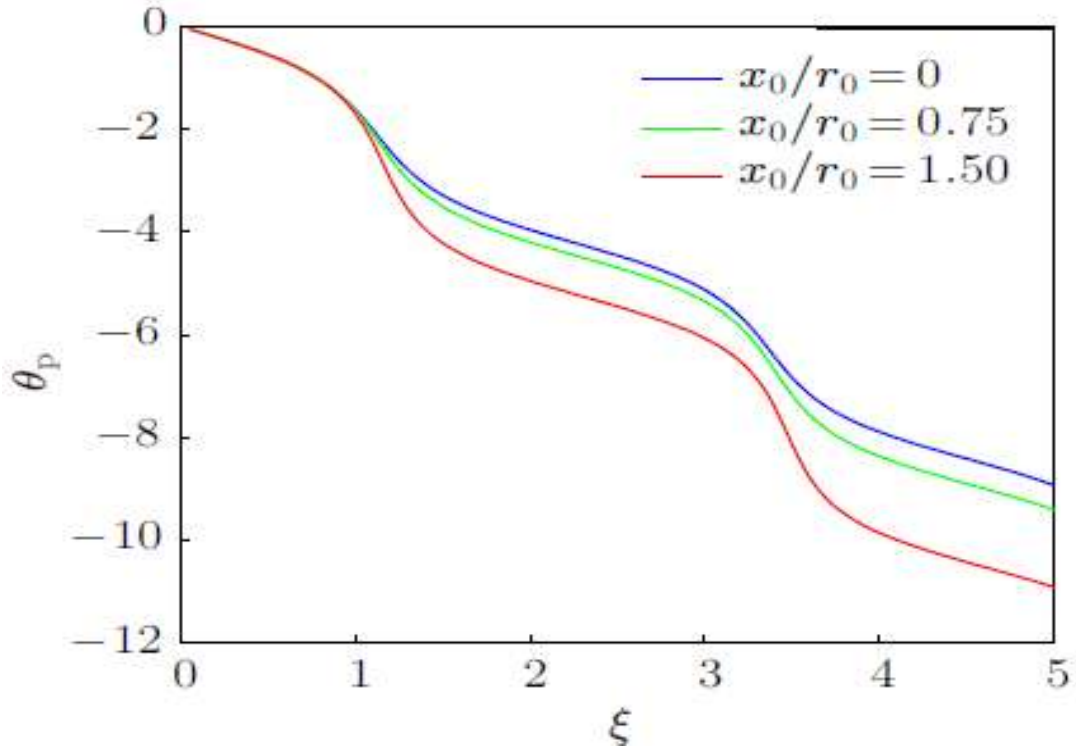

Fig.6.11: Variation of longitudinal phase θ_p with dimensionless distance of propagation ξ for different values of $\frac{x_0}{r_0}$ viz., $\frac{x_0}{r_0} = 0, 0.75$ and 1.50

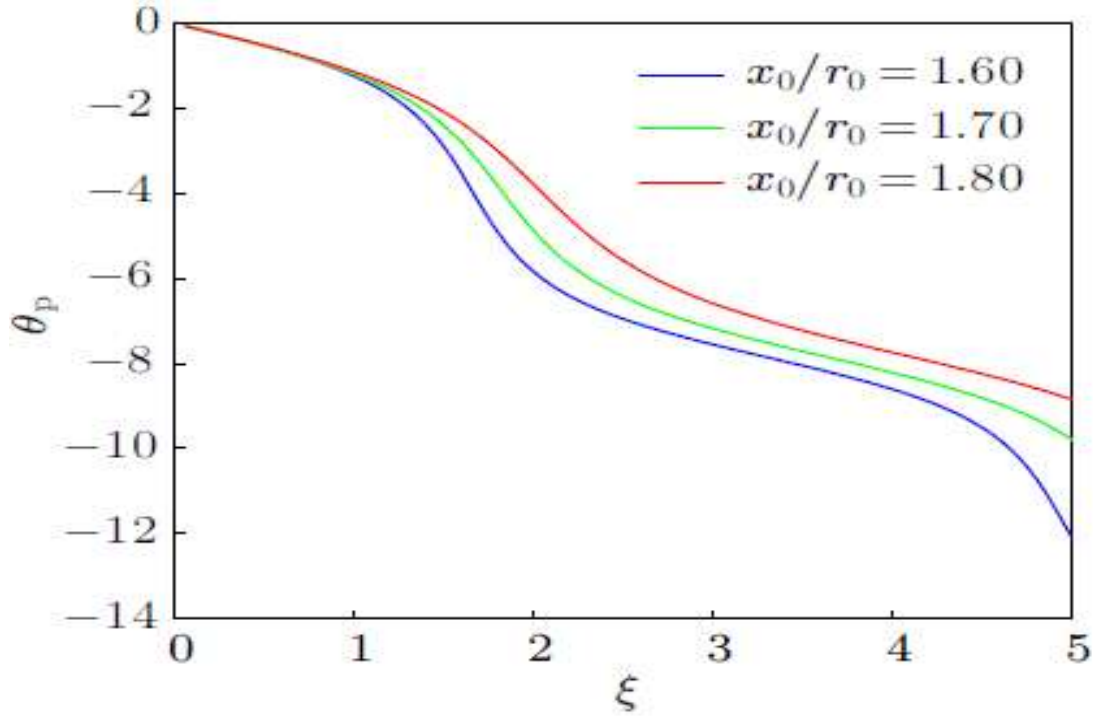

Fig. 6.12: Variarion of longitudinal phase θ_p with dimensionless distance of propagation ξ for different values of $\frac{x_0}{r_0}$ viz., $\frac{x_0}{r_0} = 1.60, 1.70, 1.80$

It is also observed that for $\frac{x_0}{r_0} \geq 1.5$, an increase in the value of $\frac{x_0}{r_0}$ reduces the rate of modulation of longitudinal phase θ_p. This is due to reduced focusing of the laser beam with an increase in the value of $\frac{x_0}{r_0}$ beyond $\frac{x_0}{r_0} = 1.5$.

6.9 Conclusions

In this work, investigation on the linear and nonlinear dynamics of multi-Gaussian laser beam in relativistic plasma has been presented. Comparison between the dynamics of Gaussian and M.G laser beams has also been made. It has been observed that diffraction of Gaussian laser beam is higher than the M.G. laser beam. Whereas, that the diffraction broadening of M.G. laser beam can be controlled by optimizing the value of $\frac{x_0}{r_0}$. The maximum intensity of M.G laser beam can be attained at 1.50 value of $\frac{x_0}{r_0}$ which may be applicable in electron acceleration and uniform heating of fuel pellet in inertial confinement fusion.

Chapter-7

Coherent Terahertz Generation by Cross Focused q-Gaussian Laser Beams in Plasma: Relativistic Effects

7.1 Introduction

The expansion of man's spectrum of observation has led to an explosive increase in his physical knowledge and to unparalleled changes in his way of life. It has brought forth such inventions as radar, radio, television, medical uses of radiation, machines for chemical analyses, automatic factories and so on. It has in fact become our major instrument for investigating the nature of matter and many other mysteries of the universe. The subject of this article is a new frontier region within the spectrum namely, the submillimeter range of radio microwaves known as terahertz (THz) radiations [50]. The THz wavelength lies at the border between microwaves and the infrared. It was the last gap in the spectrum to be closed and is known as THz gap.

The terahertz range refers to frequencies between 0.3 and 10 THz or wavelengths from 1 mm to $30\mu m$. Electromagnetic radiation at these frequencies has some unique properties. Terahertz waves pass through a variety of amorphous substances that are normally considered opaque, such as clothing, paper, or plastics [48]. The underlying principle is scattering: terahertz waves are not scattered as much as those at visible and near-infrared (IR) wavelengths, and reduced scattering means increased penetration depth. However, terahertz radiation is strongly absorbed by water molecules-and liquid water turns out to be a more dominant absorber than water vapor [49], so a single green plant leaf blocks a terahertz beam.

Another attractive scenario is to unite the advantages of imaging and spectral sensitivity characteristic of terahertz radiation. Many chemical compounds have distinct absorption lines at frequencies between 0.5 and 5 THz. Potentially, explosives or illicit drugs could not only be localized within a parcel or an envelope, but also identified unambiguously because of their spectral fingerprint. Other areas that would benefit from

an imaging terahertz spectrometer include quality control of pharmaceutical and the analysis of food stuffs inside air-tight packages [175].

One early terahertz application is quality control of drug tablets [176]. Even for homogeneous tablets (as opposed to time-release or coated tablets), manufacturers need to know whether enough of the active ingredient is in a specific tablet and that it is evenly distributed. Current testing regimes for tablets tend to be destructive a few tablets from a batch are removed, and may be subjected to IR imaging before destructive testing, such as cutting and dissolving the tablet. The beauty of terahertz imaging is that it provides a 3-D chemical and structural map of a tablet in a nondestructive way. The terahertz radiations can scan a tablet, providing several point measurements showing the distribution and concentration of the active ingredient through the tablet. This method could provide nondestructive batch testing potentially through the packaging plastic.

In addition, providing a means to scan the bulk properties of a tablet and THz radiations can also image coatings. Many new tablets have complex coatings or other structures in them that are difficult to probe with other techniques. THz radiations potentially provide a solution to these issues. Tablets and pills are only one example of mixtures that could benefit from THz radiations. THz radiations could be used to examine many other mixtures, including chemicals mixed with a base carrier, metal flakes in paint, or tears in paper products-in paper mills, one of the biggest problems is paper tearing. It's possible that the water absorption of terahertz radiation could be used to identify potential tears before they occur if tears occur where the paper contains more moisture.

Nature has a way of coupling risk and reward so that frequently those processes that have the greatest potential for benefiting mankind are also those that can be achieved only with the greatest difficulty. So it is with THz generation. THz frequencies are too high to be produced by semiconductor devices, yet too low to be produced by solid-state lasers. In this regard a promising hope is given by nonlinear optical phenomenon known as difference frequency generation. When two intense laser beams with slightly different frequencies propagate simultaneously through a medium whose index of refraction is a function of the intensity of the optical beam, the nonlinear coupling between the two beams

result in a third wave whose frequency is equal to the difference of the frequencies of the two beams. There for by suitably tuning the frequencies of the two pump beams one can generate THz radiations in nonlinear media.

There is range of media (dielectrics [177], semiconductors [178] etc.) that can respond nonlinearly to intense laser beams. But due to their susceptibility towards ionization induced damages limits their power handling capacity. Also, their lower conversion efficiency to the THz radiation does not fulfill the requirement of power levels of THz radiations those are required for practical purposes. In contrast to this being already in an ionized state plasma is not susceptible to ionization induced damages. At least in theory it is having almost infinite immunity to ionization induced damages. Also, their highly nonlinear nature and higher conversion efficiency to THz frequency make them an ideal candidate for generation of coherent THz radiations [8].

This chapter presents theoretical investigation on THz generation by cross focused q-Gaussian laser beams in underdense plasma targets.

7.2 Relativistic Nonlinearity of Plasma

The dielectric function of a plasma with electron density n_e, for an electromagnetic beam with frequency ω_j is given by

$$\varepsilon = 1 - \frac{\omega_p^2}{\omega_j^2} \tag{7.1}$$

where,

$$\omega_p^2 = \frac{4\pi e^2 n_0}{m_e} \tag{7.2}$$

is the natural frequency of oscillations of plasma electrons i.e., plasma frequency. When under the effect of intense fields of the incident laser beams the quiver velocity of plasma electrons becomes comparable to that of speed of light in vacuum, then the effective mass m_e of electron in eq. (7.2) need to be replaced by $m_0\gamma$, where, γ is the relativistic Lorentz factor and m_0 is the rest mass of electron. Following Akhiezer and Polovin [31] the relativistic Lorentz factor can be related to the total intensity of the laser beams as

$$\gamma = \left(1 + \sum_j \frac{1}{\omega_j^2} A_j A_j^*\right)^{\frac{1}{2}} \tag{7.3}$$

Where, $\beta_j = \frac{e^2}{m_0^2 c^2 \omega_j^2}$ is the coefficient of relativistic nonlinearity.

Since, the effective dielectric function of plasma depends on effective mass of plasma electrons through the plasma frequency (eq.7.2). Hence, intensity dependence of electron mass in turn affect the optical properties of plasma in a nonlinear manner. The resulting intensity dependence of dielectric function of plasma for q-Gaussian laser beams can be written as

$$\varepsilon_j = 1 - \frac{\omega_{p0}^2}{\omega_j^2}\left(1 + \sum_j \frac{\beta_j E_{j0}^2}{f_j^2}\left(1 + \frac{r^2}{q r_j^2 f_j^2}\right)\right)^{-\frac{1}{2}} \tag{7.4}$$

Where,

$$\omega_{p0}^2 = \frac{4\pi e^2}{m_0} n_e$$

is the plasma frequency in the absence of laser beams. Eq.(7.4) can be written as

$$\varepsilon_j = \varepsilon_{0j} + \Phi_j(A_1 A_1^*, A_2 A_2^*) \tag{7.5}$$

Where

$$\varepsilon_{0j} = 1 - \frac{\omega_{p0}^2}{\omega_j^2} \tag{7.6}$$

are the linear parts of dielectric function and

$$\Phi_j(A_1 A_1^*, A_2 A_2^*) = \frac{\omega_{p0}^2}{\omega_j^2}\left\{1 - \left(1 + \sum_j \frac{\beta_j E_{j0}^2}{f_j^2}\left(1 + \frac{r^2}{q_j r_j^2 f_j^2}\right)^{-q_j}\right)^{\frac{1}{2}}\right\} \tag{7.7}$$

are the nonlinear parts of dielectric function.

7.4 Cross-Focusing of Laser Beams

The evolution of beam envelope of an optical beam through a nonlinear medium is governed by the wave equation [156]

$$i\frac{\partial E_j}{\partial z} = \frac{1}{2k_j}\nabla_\perp^2 E_j + \frac{k_j}{2\varepsilon_{0j}}\Phi_j(A_1A_1^*, A_2A_2^*)A_j \tag{7.8}$$

According to variational method [60-62] eq.(7.8) is a variational problem for action principle based on Lagrangian density

$$\pounds = i\left(A_1\frac{\partial A_1^*}{\partial z} - A_1^*\frac{\partial A_1}{\partial z}\right) + i\left(A_2\frac{\partial A_2^*}{\partial z} - A_2^*\frac{\partial A_2}{\partial z}\right) + |\nabla_\perp A_1|^2 + |\nabla_\perp A_1|^2 - \frac{\omega_1^2}{c^2}\int^{A_1A_1^*}\Phi(A_1A_1^*, A_2A_2^*)d(A_1A_1^*)$$
$$-\frac{\omega_2^2}{c^2}\int^{A_2A_2^*}\Phi(A_1A_1^*, A_2A_2^*)d(A_2A_2^*) \tag{7.9}$$

Substituting the trial function for q-Gaussian beam profile in lagrangian density and integrating over the entire cross section of the laser beam we get the reduced lagrangian as $L = \int \pounds\, d^2r$. The corresponding Euler-Lagrange equations

$$\frac{d}{dz}\left(\frac{dL}{\partial\left(\frac{\partial f_j}{\partial z}\right)}\right) - \frac{\partial L}{\partial f_j} = 0 \tag{7.10}$$

give

$$\frac{d^2f_j}{d\xi^2} + \frac{1}{f_j}\left(\frac{df_j}{d\xi}\right)^2 = \frac{1}{k_j^2 r_j^4 f_j^3}\frac{\left(1-\frac{1}{q_j}\right)\left(1-\frac{1}{q_j}\right)}{\left(1+\frac{1}{q_j}\right)} + \frac{\left(1-\frac{2}{q_j}\right)}{r_j^2\varepsilon_{0j}I_{0j}}\int r^2 A_jA_j^*\frac{\partial\Phi_j}{\partial r}d^2r \tag{7.11}$$

Using eq. (7.7) in (7.11), the set of coupled differential equations for beam widths of the two laser beams are obtained

$$\frac{d^2f_1}{d\xi^2} + \frac{1}{f_1}\left(\frac{df_1}{d\xi}\right)^2 = \frac{\left(1-\frac{1}{q_1}\right)\left(1-\frac{1}{q_1}\right)}{\left(1+\frac{1}{q_1}\right)}\frac{1}{f_1^3} - 2\left(\frac{\omega_{p0}r_1}{c}\right)^2\left(1-\frac{1}{q_1}\right)\left(1-\frac{2}{q_1}\right)J_1 \tag{7.12}$$

$$\frac{d^2f_2}{d\xi^2} + \frac{1}{f_2}\left(\frac{df_2}{d\xi}\right)^2 = \left(\frac{r_1}{r_2}\right)^4\left(\frac{\omega_1}{\omega_2}\right)^2\left(\frac{\varepsilon_{01}}{\varepsilon_{02}}\right)\frac{\left(1-\frac{1}{q_2}\right)\left(1-\frac{1}{q_2}\right)}{\left(1+\frac{1}{q_2}\right)}\frac{1}{f_2^3} - 2\left(\frac{\omega_{p0}r_1}{c}\right)^2\left(1-\frac{1}{q_2}\right)\left(1-\frac{2}{q_2}\right)J_2 \tag{7.13}$$

where, $\xi = \frac{z}{k_1r_1^2}$ is the dimensionless distance of propagation, and

$$J_1 = \frac{\beta_1E_{10}^2}{f_1^3}T_1 + \frac{\beta_2E_{20}^2}{f_1^3}\left(\frac{r_1}{r_2}\right)^2\left(\frac{f_1}{f_2}\right)^4T_2$$

$$J_2 = \frac{\beta_1E_{10}^2}{f_2^3}T_3 + \frac{\beta_2E_{20}^2}{f_2^3}\left(\frac{r_1}{r_2}\right)^2\left(\frac{f_1}{f_2}\right)^4T_4$$

$$T_1 = \int_0^{\infty} x^3 \left(1 + \frac{x^2}{q_1}\right)^{-2q_1-1} G(x)dx$$

$$T_2 = \int_0^{\infty} x^3 \left(1 + \frac{x^2}{q_1}\right)^{-q_1} \left(1 + \frac{x^2}{q_2}\left(\frac{r_1 f_1}{r_2 f_2}\right)^2\right)^{-q_2-1} G(x)dx$$

$$T_3 = \int_0^{\infty} x^3 \left(1 + \frac{x^2}{q_1}\right)^{-q_1-1} \left(1 + \frac{x^2}{q_2}\left(\frac{r_1 f_1}{r_2 f_2}\right)^2\right)^{-q_2} G(x)dx$$

$$T_4 = \int_0^{\infty} x^3 \left(1 + \frac{x^2}{q_2}\left(\frac{r_1 f_1}{r_2 f_2}\right)^2\right)^{-2q_2-1} G(x)dx$$

$$G(x) = e^{-\left\{\frac{\beta_1 E_{10}^2}{f_1^2}\left(1+\frac{x^2}{q_1}\right)^{-q_1} + \frac{\beta_2 E_{20}^2}{f_2^2}\left(1+\frac{x^2}{q_2}\left(\frac{r_1 f_1}{r_2 f_2}\right)^2\right)^{-q_2}\right\}}$$

$$x = \frac{r}{r_1 f_1}$$

Equations (7.12) and (7.13) are the coupled nonlinear differential equations governing the cross focusing of two coaxial q-Gaussian laser beams in collisionless plasma. For initially plane wavefronts these equations are subjected to boundary conditions $f_j = 1$ and $\frac{df_j}{d\xi} = 0\ at\ \xi = 0$. Numerical computational techniques are used to investigate the beam dynamics as analytic solutions of these equations are not possible.

7.4 Excitation of Electron Plasma Wave (EPW)

EPW that results in the generation of THz radiations can be excited into the plasma due to remarkable properties of plasma [179, 180]. Plasma as a whole possesses quasi neutrality i.e., it contains almost equal number of free electrons and ions. But, as the electrons and net positively charged ions are separated, a disturbance can create regions of net negative and regions of positive charges acting like the plates of a charged parallel plate capacitor. Such an uneven distribution of charges results in an electric field running from positive to negative regions. This electric field pulls the electrons and ions towards each other with equal forces. Ions being much heavier than the electrons remain at rest and the electrons move towards the positive regions. As the electrons move towards the ions, they steadily gain velocity and momentum like a pendulum moving towards its mean position from an extreme position. Due to this gain in momentum, the electrons overshoot their

equilibrium positions resulting in reversing the direction of electric field. Now the reversed electric field opposes the motion of electrons and slow them down and then pulling them back again. The process repeats itself, establishing electron oscillations. In the presence of thermal velocities these electrons oscillations form a longitudinal wave of positive and negative regions travelling through the plasma.

The electron oscillators can be set in motion by intense laser beams. As the laser beams enter the plasma region, they exert pressure on plasma electrons and hence the plasma electrons move out of the way. As the laser beams exit, leaving a region deficient of electrons, the plasma electrons rush back to establish equilibrium. This movement of plasma electrons initiates the oscillations and results in a plasma wave.

As the two laser beams with different frequencies are propagating simultaneously through the plasma, the plasma oscillations of the plasma electrons under the fields of the two laser beams also contain a frequency component equal to the difference of the frequencies of the two laser beams. The electron density perturbation n' associated with the excited EPW evolves according to the wave equation [76]

$$\frac{\partial^2 n'}{\partial t^2} - v_{th}^2 \nabla^2 n' + \omega_p^2 n' = \frac{e}{m} n_0 \nabla \Sigma_j E_j \tag{7.14}$$

Taking

$$n' = n_1 e^{i(\omega t - kz)}$$

where, $\omega = \omega_2 - \omega_1$ and $k = k_2 - k_1$, we get the amplitude of density perturbation associated with plasma wave

$$n_1 = \frac{e n_0}{m} \frac{1}{\left(\omega_0^2 - k_0^2 v_{th}^2 - \omega_p^2\right)} \left[\frac{E_{10}}{r_1^2 f_1^3} \left(1 + \frac{r^2}{q_1 r_1^2 f_1^2}\right)^{-\frac{q_1}{2}-1} + \frac{E_{20}}{r_2^2 f_2^3} \left(1 + \frac{r^2}{q_2 r_2^2 f_2^2}\right)^{-\frac{q_1}{2}-1} \right] r \tag{7.15}$$

7.6 THz Generation

The density perturbation associated with excited EPW results in a nonlinear current density at frequency $\omega = \omega_2 - \omega_1$ that acts as source for the THz radiation. The generated current density is given by

$$J_T = \frac{e^2 n_0}{m\omega} \left(\frac{n_1}{n_0}\right) e^{i(\omega t - kz)} \left(E_1 + E_2\right) \tag{7.16}$$

The electric field of the resulting THz evolves according to the wave equation

$$\nabla^2 E_T = \frac{1}{c^2}\frac{\partial^2 E_T}{\partial t^2} + \frac{4\pi}{c^2}\frac{\partial J_T}{\partial t} \tag{7.17}$$

This equation gives the magnitude of electric field of THz radiation as

$$E_T = i\frac{\left(\frac{\omega_{p0}^2}{c^2}\right)}{\left(\frac{\omega^2}{c^2} - k^2\right)}\frac{n_1}{n_0}(E_1 + E_2) \tag{7.18}$$

Defining the normalized power of THz radiation as

$$P_T = \frac{\int_0^\infty E_T E_T^* r dr}{\int_0^\infty A_1 A_1^* r dr} \tag{7.19}$$

We get

$$P_T = \frac{\left(\frac{\omega_{p0}^2}{c^2}\right)^2}{\left(\frac{\omega^2}{c^2} - k^2\right)^2}\frac{\int\left(\frac{n_1}{n_0}\right)^2 (E_1 + E_2)^2 r dr}{\int A_1 A_1^* r dr} \tag{7.20}$$

Equation (7.20) gives the normalized power of the THz radiation produced by the two laser beams while propagating through the plasma.

7.6 Results and Discussion

To analyze the effect of deviation of intensity distribution of laser beams from Gaussian distribution and plasma density on cross focusing of the laser beams eqs.(7.12)-(7.13) have been solved for following set of laser-plasma parameters:

$$\omega_1 = 1.758 \times 10^{14} rad\ s^{-1}, \qquad \omega_2 = 1.75 \times 10^{14} rad\ s^{-1}$$
$$r_1 = 15\mu m, \qquad r_2 = 16\mu m, \qquad \beta_2 E_{20}^2 = 1.5, \qquad T_0 = 10^7 K$$

and for different values of $q_1, q_2, \frac{\omega_{p0}^2 r_1^2}{c^2}$ and $\beta_1 E_{00}^2$viz.,

$$q_1 = q_2 = (3,4,\infty), \frac{\omega_{p0}^2 r_1^2}{c^2} = (9,12,15), \beta_1 E_{10}^2 = (3,3.5,4)$$

Figures 7.1 and 7.2 illustrate the effect of deviation parameter q_1 of beam1 on focusing/defocusing of the two laser beams. It can be seen that during the propagation of the laser beams through plasma their beam width vary harmonically with distance. This behaviour of the beam widths of the laser beams can be explained by examining the role and origin of various terms contained in equations (7.12) and (7.13).

The first terms on the right hand sides (R.H.S) of these equations that vary inversely with the cube of their beam widths, are the spatial dispersive terms that model the spreading

of the laser beams in transverse directions occurring as consequence of light's wave nature of diffraction. The second terms on the R.H.S of these equations that have complex dependence on beam widths f_1 and f_2 of the two laser beams arise as a consequence of relativistic nonlinearity of plasma and nonlinear coupling the laser beams with each other. It can be seen that although two copropagating laser beams through vacuum don't interact with each other, but during their propagation through plasma medium they get coupled with each other. As a consequence of the relativistic nonlinearity of plasma the resulting nonlinear refraction of the laser beams tend to counter balance the effect of diffraction by inducing a convex lens like structure into the plasma. Thus, during the propagation of the laser beams through plasma, there starts a competition between the two phenomena of diffraction and nonlinear refraction. The winning phenomenon ultimately decides the behaviour of the laser beams i.e., whether the beams will converge or diverge. Thus, there exists a critical value of the total beam intensity above which the beams will converge.

In the present investigation the initial beam intensity has been taken to be greater than the critical intensity i.e., why the spot sizes of the two laser beams are converging initially. As the beam widths of the laser beams get reduced, their intensity increases. When the intensity of the laser beams become too high, the mass of plasma electrons and thus the optical nonlinearity of plasma gets saturated. Thus, the laser beams propagate as if they are propagating through a linear medium. Hence, after attaining minimum possible value, the beam widths of the two laser beams bounce back to their initial values. As the beam widths of the laser beams start increasing, the competition between diffraction and nonlinear refraction starts again. Now, the competition lasts till maximum values of $f_1 \; and \; f_2$ are obtained. These processes go on repeating themselves and thus give breather like behaviour to the spot sizes of the laser beams.

The plots in fig.7.1 depict that increase in the value of q_1 leads to decrease in the extent of self focusing of first laser beam. This is due to the fact that as the value of q_1 increases towards higher values, the intensity of the first laser beam shifts towards the axial region of the wavefront. As a result, laser beams with higher q value get lesser contribution from the off axial rays towards nonlinear refraction. As nonlinear refraction of the laser

beam is a homeostasis for self focusing, increase in the value of q_1 results in reduced focusing of beam 1. It is also observed from fig.7.1 that the laser beams with higher q values possess faster focusing. The underlying physics behind this fact is the slower focusing character of the off axial rays.

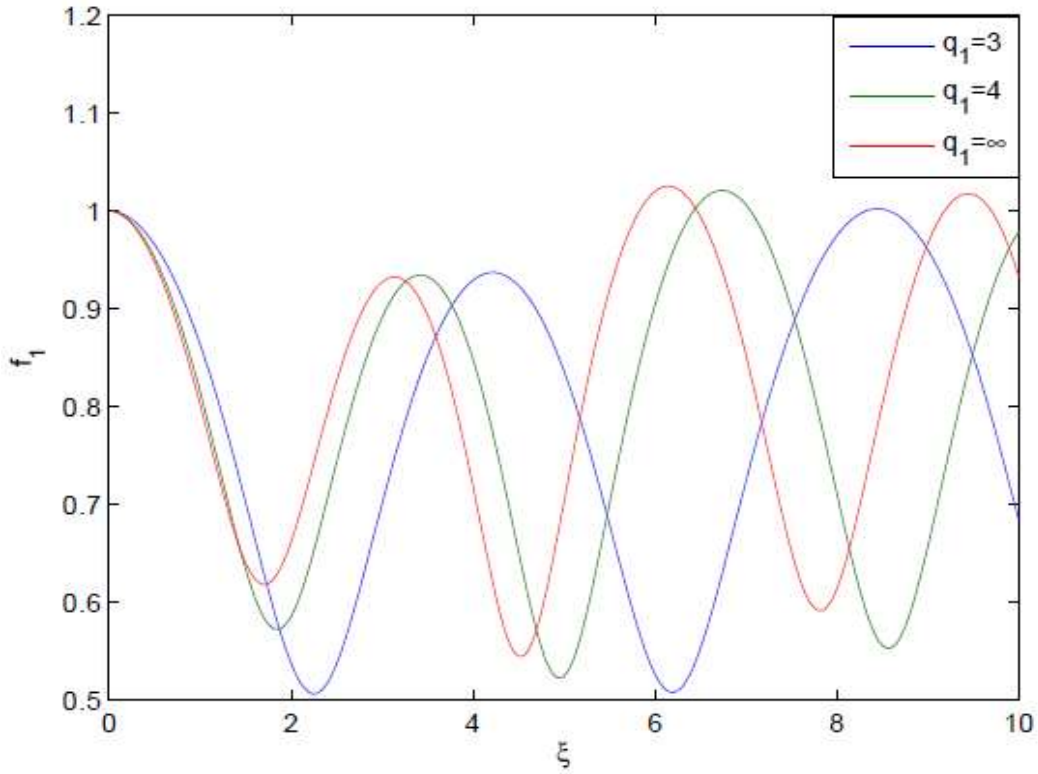

Fig. 7.1: Variation of beam width parameter f_1 of beam 1 with distance of propagation in plasma for different values of q_1 and at fixed values of $q_2 = 3, \frac{\omega_{p0}^2 r_1^2}{c^2} = 9$ and $\beta_1 E_{10}^2 = 3$

The plots in fig. 7.2 depict that increase in the value of q_1 leads to increase in the extent of self focusing of the second laser beam. This is due to the fact that due to nonlinear coupling between the two laser beams the increase in value of $q_1$favours the nonlinear refraction of beam2.

Figs. 7.3 and 7.4 depict the effect of deviation parameter q_2 of beam 2 on evolution of the beam widths of the two laser beams. It can be seen that increase in value of q_2 decreases the self focusing of beam 2 and increases that of beam 1.

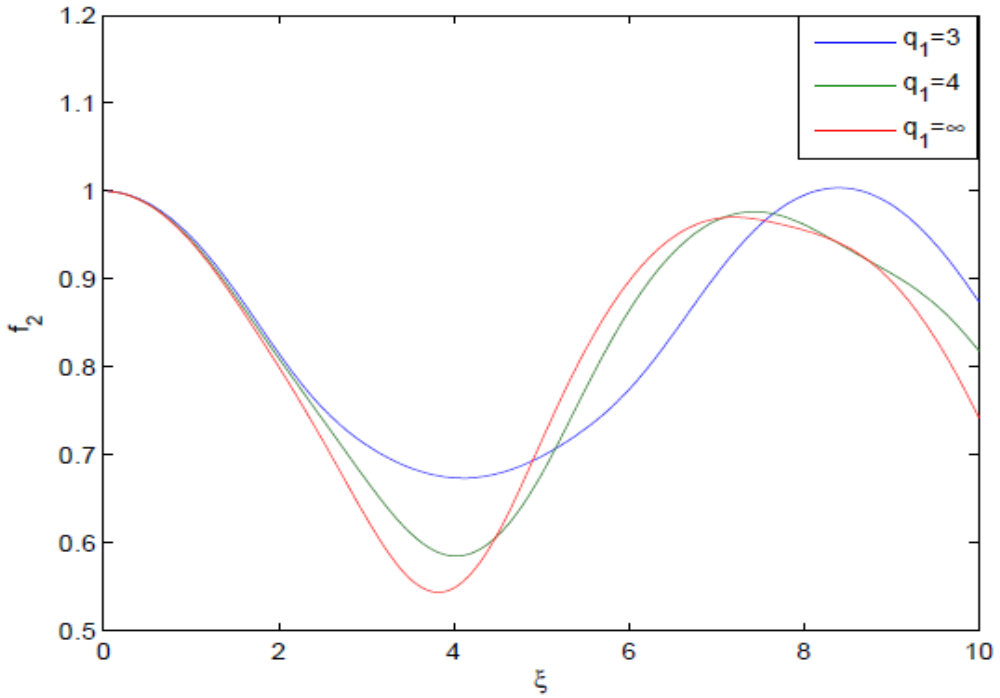

Fig. 7.2: Variation of beam width parameter f_2 of beam 2 with distance of propagation in plasma for different values of q_1 and at fixed values of $q_2 = 3, \frac{\omega_{p0}^2 r_1^2}{c^2} = 9$ and $\beta_1 E_{10}^2 = 3$

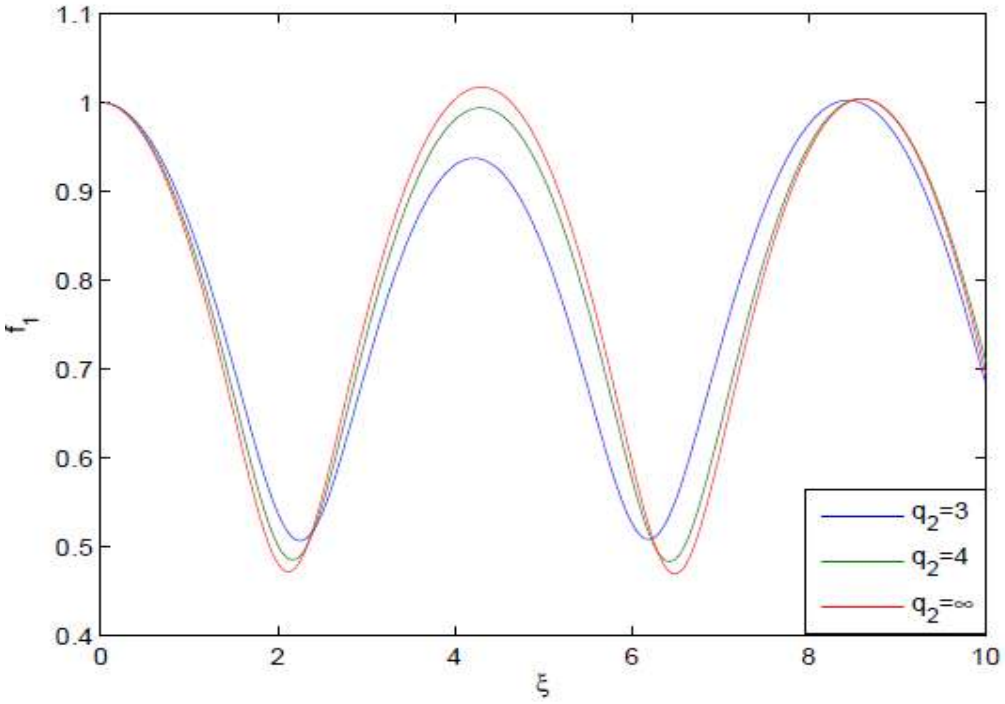

Fig. 7.3: Variation of beam width parameter f_1 of beam 1 with distance of propagation in plasma for different values of q_2 and at fixed values of $q_1 = 3, \frac{\omega_{p0}^2 r_1^2}{c^2} = 9$ and $\beta_1 E_{10}^2 = 3$

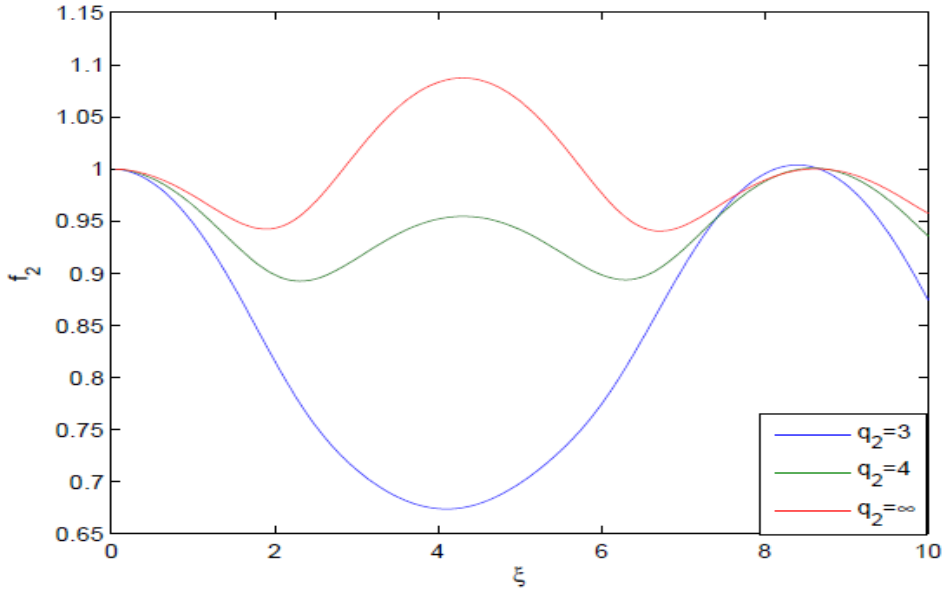

Fig. 7.4: Variation of beam width parameter f_2 of beam 2 with distance of propagation in plasma for different values of q_2 and at fixed values of $q_1 = 3, \frac{\omega_{p0}^2 r_1^2}{c^2} = 9$ and $\beta_1 E_{10}^2 = 3$

Figs.7.5 and 7.6 depict the effect of plasma density on self focusing of the two laser beams. It can be seen that increase in plasma density increases the self focusing of both the laser beams.

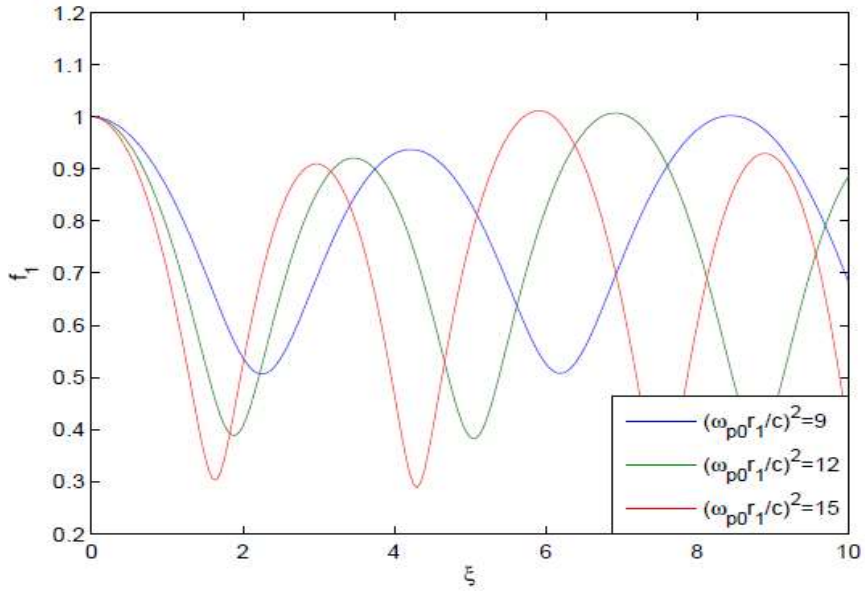

Fig. 7.5: Variation of beam width parameter f_1 of beam 1 with distance of propagation in plasma for different values of $\frac{\omega_{p0}^2 r_1^2}{c^2}$ and at fixed values of $q_1 = q_2 = 3$ and $\beta_1 E_{10}^2 = 3$

This is due to the fact that increase in plasma density increases the number of plasma electrons contributing to the relativistic nonlinearity of plasma. As self focusing of the laser beams results from relativistic nonlinearity, increase in plasma density increases the self focusing of the two laser beams.

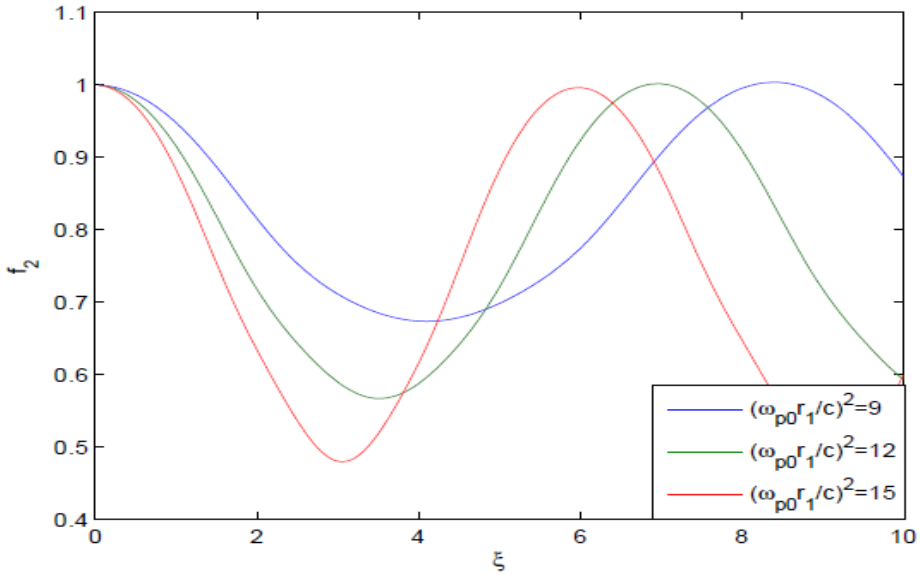

Fig. 7.6: Variation of beam width parameter f_2 of beam 2 with distance of propagation in plasma for different values of $\frac{\omega_{p0}^2 r_1^2}{c^2}$ and at fixed values of $q_1 = q_2 = 3$ and $\beta_1 E_{10}^2 = 3$

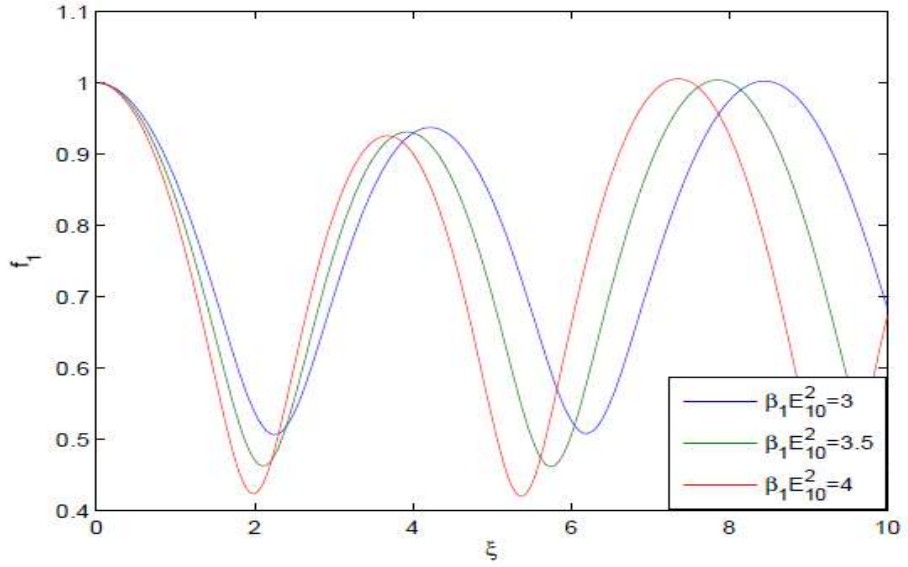

Fig. 7.7: Variation of beam width parameter f_1 of beam 1 with distance of propagation in plasma for different values of $\beta_1 E_{10}^2$ and at fixed values of $q_1 = q_2 = 3$ and $\frac{\omega_{p0}^2 r_1^2}{c^2} = 9$

Figs.7.7 and 7.8 depict the effect of initial intensity of beam 1 on self focusing of the two laser beams. It can be seen that increase in intensity of beam 1 leads to increase in self focusing of the two laser beams. This is again due to the increase in the magnitude of relativistic with increase in initial beam intensity.

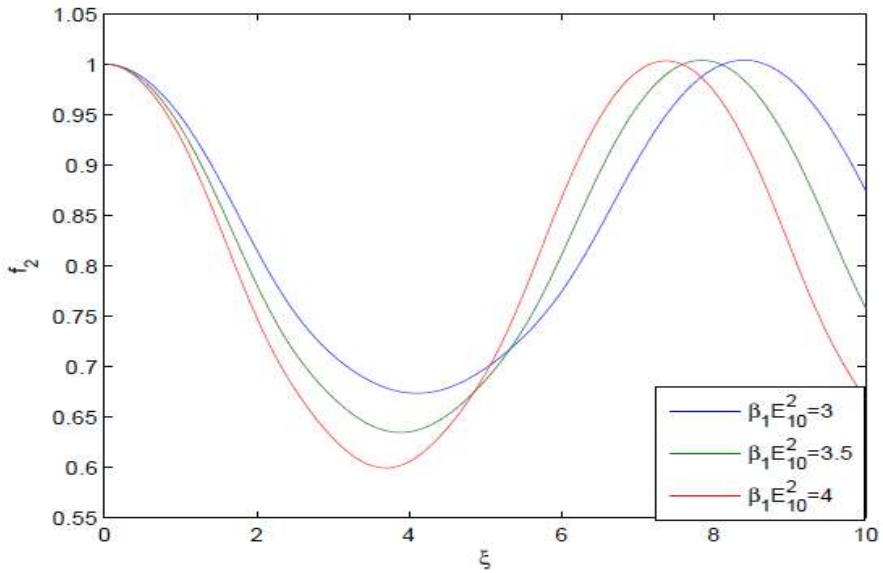

Fig. 7.8: Variation of beam width parameter f_2 of beam 2 with distance of propagation in plasma for different values of $\beta_1 E_{10}^2$ and at fixed values of $q_1 = q_2 = 3$ and $\frac{\omega_{p0}^2 r_1^2}{c^2} = 9$

Further, eq. 7.20 has been solved numerically in association with the beam width equations 7.12 and 7.13 and the corresponding evolutions of the normalized power with distance of propagation for different values of q, plasma density and initial beam intensity have been depicted in figs. 7.9-7.12.

Figs.7.9 and 7.10 depict the effect of q_1 and q_2 on evolution of normalized power of generated THz radiation with distance. It has been observed that the power of THz radiation is a monotonically increasing function of propagation, showing step like behaviour. Each step occurs at the position of the minimum beam width of the two laser beams. This is because as the pump beams get self focused their intensity increases and consequently the oscillation amplitude of the plasma electrons also increases which in turn increases the amplitude of the generated EPW. Since, the density perturbation associated with EPW acts as source for nonlinear current density for THz, there is monotonic increase in the second

harmonic power with distance. The step like behaviour of the power of THz radiation at the positions of the minimum beam width of the pump beams is owing to the fact that these are the regions of highest intensity and hence the current density for THz radiation is maximum there.

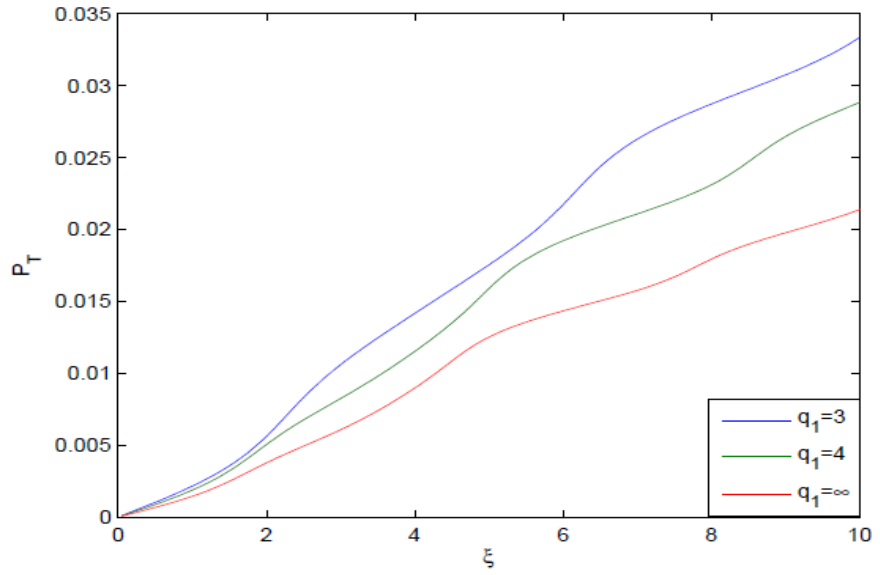

Fig. 7.9 Variation of beam width parameter P_T of THz radiation with distance of propagation in plasma for different values of q_1 and at fixed values of $q_2 = 3$, $\beta_1 E_{10}^2 = 3$ and $\frac{\omega_{p0}^2 r_1^2}{c^2} = 9$

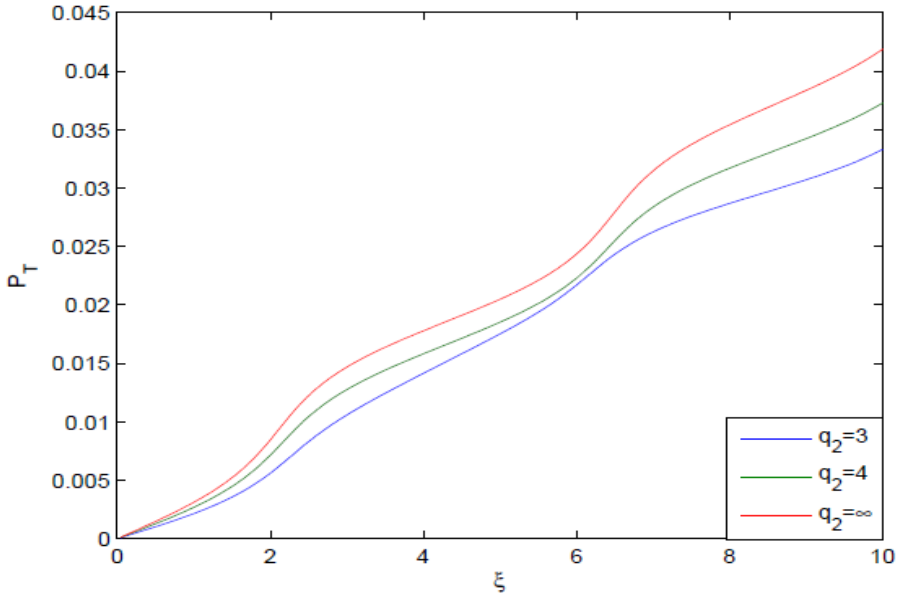

Fig. 7.10: Variation of beam width parameter P_T of THz radiation with distance of propagation in plasma for different values of q_2 and at fixed values of $q_1 = 3$, $\beta_1 E_{10}^2 = 3$ and $\frac{\omega_{p0}^2 r_1^2}{c^2} = 9$

Hence, after attaining its maximum value the power of THz radiation moves towards its next possible higher value at next focal spot. These transitions of THz power form one maximum value to next maximum value give it a step like behaviour.

Reduction in the second THz power P_T with increase in the value of deviation parameter q_1 of beam 1 has also been observed from the plots in fig.7.9. The underlying physics behind this is the one to one correspondence between the power of THz radiation and the degree of self focusing of the pump beams. As increase in the value of q_1 reduces the extent of focusing of the pump beam 1 (beam with higher initial intensity) and increases the focusing of beam 2. However, in producing THz radiation, dominant role is played by beam with higher initial intensity. Hence, there is corresponding decrease in the power of THz radiation with increase in q_1. Same is the reason behind the observed increase in the power of THz radiation with increase in the value of deviation parameter q_2 of beam 2 (fig. 7.10).

Figs. 7.11 and 7.12 depict that by increasing either plasma density or initial pump beam intensity there is increase in the power of THz radiation. This is again due to the fact that with increase in plasma density or initial pump intensity there is increase in the extent of self focusing of both the laser beams.

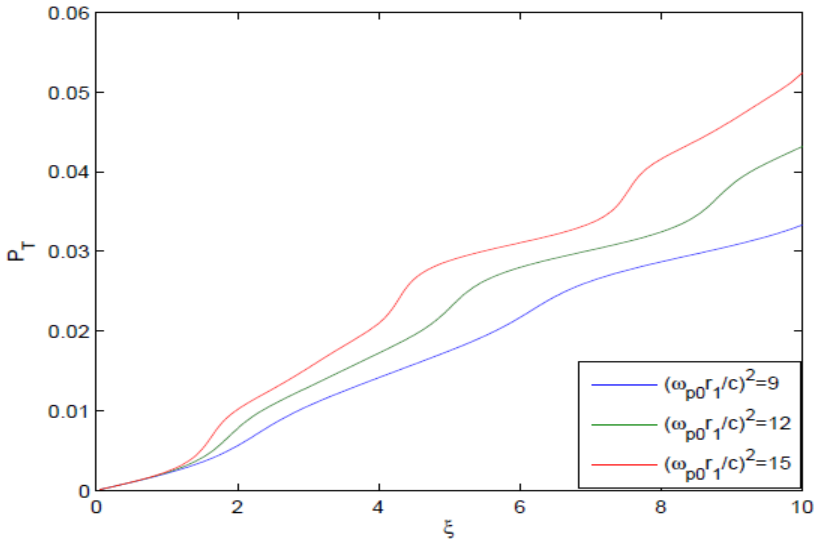

Fig. 7.11: Variation of beam width parameter P_T of THz radiation with distance of propagation in plasma for different values of $\frac{\omega_{p0}^2 r_1^2}{c^2}$ and at fixed values of $q_1 = q_2 = 3$ and $\beta_1 E_{10}^2 = 3$

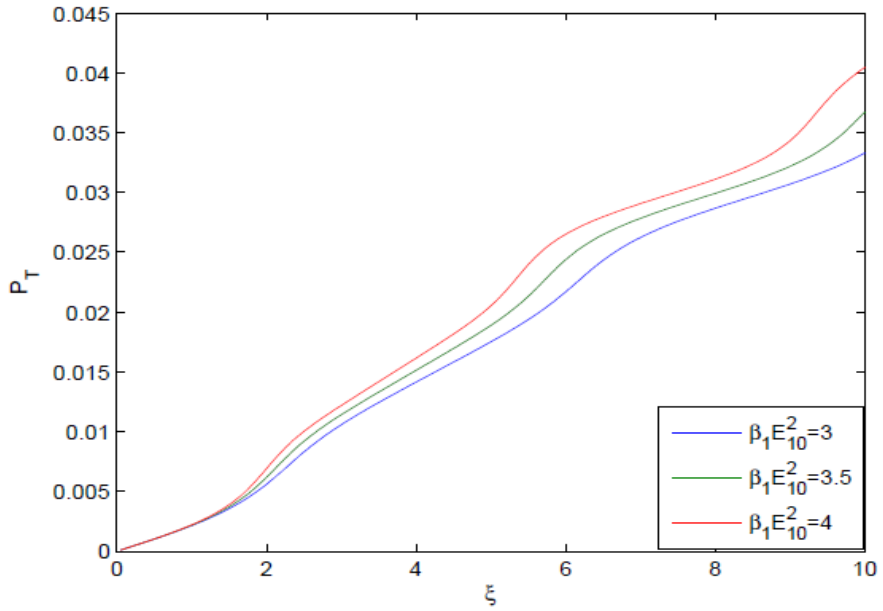

Fig. 7.12: Variation of beam width parameter P_T of THz radiation with distance of propagation in plasma for different values of $\beta_1 E_{10}^2$ and at fixed values of $q_1 = q_2 = 3$ and $\frac{\omega_{p0}^2 r_1^2}{c^2} = 9$

7.7 Conclusions

In conclusion I have investigated the effect of cross focusing of intense laser beams on generation of coherent THz radiations in plasma under the effect of relativistic nonlinearity. Effect of the deviation of amplitude structure of laser beams from ideal Gaussian profile has been incorporated through q-Gaussian distribution. It has been observed that deviation parameters of the laser beams significantly affect the cross focusing and hence the power of generated THz radiations. As the amplitude structure of laser beam with higher initial intensity (i.e., pump beam) converges towards the ideal Gaussian profile, there is decrease in the power of generated THz radiations. However, in case the amplitude structure of laser beam with lower initial intensity (i.e., probe beam) converges towards the ideal Gaussian profile, there is increase in the power of generated THz radiations. Thus, by controlling the deviation parameters of the pump and probe beams one can optimize the power of generated THz radiations for given set of plasma parameters. The results of present study may be helpful for the experimentalists working in the field of LPI.

Chapter-8

THz Generation by Filamentation of q-Gaussian Laser Beams in Narrow Band Semiconductor

8.1 Introduction

The advent of laser in the early 1960's set in motion a train of events that led to a renaissance in the field of light-matter interactions. The past few years have seen two important advances. One was the proposal of initiating fusion reactions [3, 163] for viable energy production that would quench humanity's endless thirst for energy without worsening the global climate change. Another noteworthy advance was the laser driven particle accelerators [7]. Particle acceleration by laser driven plasma wave is an extremely interesting and far-reaching idea that can bring huge particle accelerators to bench top. The efforts to translate these concepts into reality, however, have to surmount two serious problems: (1) the creation of relativistic plasmas requires ultrahigh laser intensities in the excess of $10^{18} - 10^{20} W/cm^2$, and (2) the plasmas have to be extremely homogeneous. These rather daunting requirements have made it difficult even to carry out exploratory experiments to test the proposed ideas.

Therefore, there have been ongoing efforts to find alternatives to standard plasma experiments, where these severe constraints could be mitigated. One could then validate the theoretical frameworks, and shed light on the eventual feasibility of these ideas. Fortunately, such an alternative exists; it is provide by certain special plasmas found in the narrow-band semiconductors [25]. Plasmas contain negative and positive carriers under conditions in which they do not combine. In the fig.(8.1) a red dot is an electron, or negative charge, a blue dot containing a plus sign is a positive charge and neutral atoms are shown green. In a gas there are two kinds of charge carrier: electrons and positive ions (atoms lacking electrons). In a simple metal the only mobile carriers are electrons; positive ions are locked in the crystal lattice. A semiconductor has two kinds of mobile carrier: electrons and positive "holes," or missing electrons. All three plasmas can transmit waves.

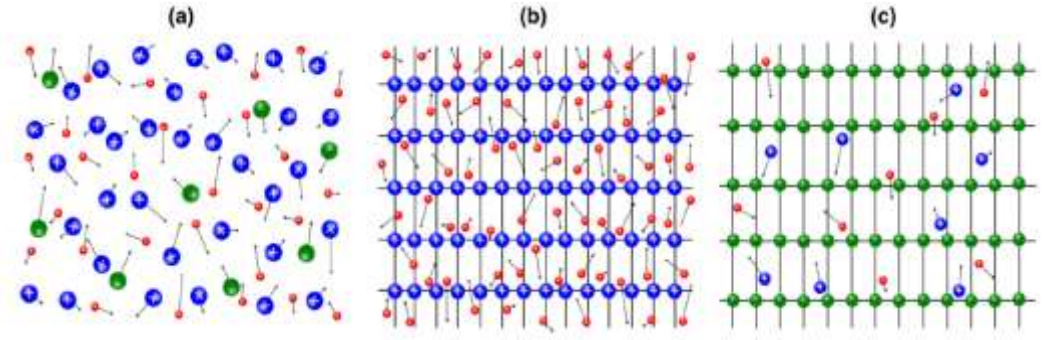

Fig.8.1: Three kinds of plasmas a) gaseous plasma b) metallic plasma c) semiconductor plasma

Interaction of intense laser beams with semiconductor plasmas are rich in copious nonlinear effects. This span a gamut from parametric instabilities to several nonlinear effects such as self focusing, self trapping, HHG, THz generation etc. [25, 42, 97, 98]. Among these nonlinear optical effects, THz radiations have influenced the researchers due to its non-ionizing character and penetrating power. These radiations are broadly applicable in the field of medical imaging, short range communication, surveillance and security scanning [48, 50, 51]. The unique properties of THz radiations further open numerous opportunities in industrial and basics research.

A number of methods have been established for the generation of THz radiation such as optical rectification, gyrotron-method, photo-conductive antennas, conventional accelerator etc. But, due to the limitations of conventional methods, the generation of THz radiation is restricted up to some μJ. Therefore, in this regards the plasma [109, 112] and narrow band semiconductor [178, 181, 182] candidates have appeared which are most suitable for attaining new level of high-power THz radiation. In this chapter generation of THz radiation by two q-Gaussian laser beams and narrow band semiconductor has been investigated.

8.2. Relativistic Dielectric Function of Narrow Band Semiconductor

The temperature of free carriers, in semiconductors at equilibrium, is same as that of crystal so that the net energy exchange between the carriers and the lattice of the crystal is zero. However, in the presence of laser electric field, the free carriers gain energy from the electric field, which causes their temperature to be higher than that of the crystal in the steady state [181]. The exchange of energy between electrons and lattice in a

semiconductor can be explained by hydraulic analogy shown in fig.(8.2). The movement of water through the system shown here is analogous to the flow of energy in a semiconductor. The open tap corresponds to the electric field of the laser beam. Energy is transferred from the field to the electrons (container at the left), which it accelerates. The electrons in turn transfer their energy to the crystal lattice (container at the right). The size of the tube between the two containers represents the strength of the interaction of the electrons with the lattice. Electrons can also transfer energy out of the crystal by electromagnetic radiation, whereas the lattice can lose energy by heat conduction or convection. If the leaks to the outside are small, the containers will fill up when the tap is turned on. This retention of energy results in heating the crystal. If the tap is merely dripping, the water in the two containers will be at the same level, in other words, if the laser beam is sufficiently weak the effective temperature of the electrons and lattice will be same.

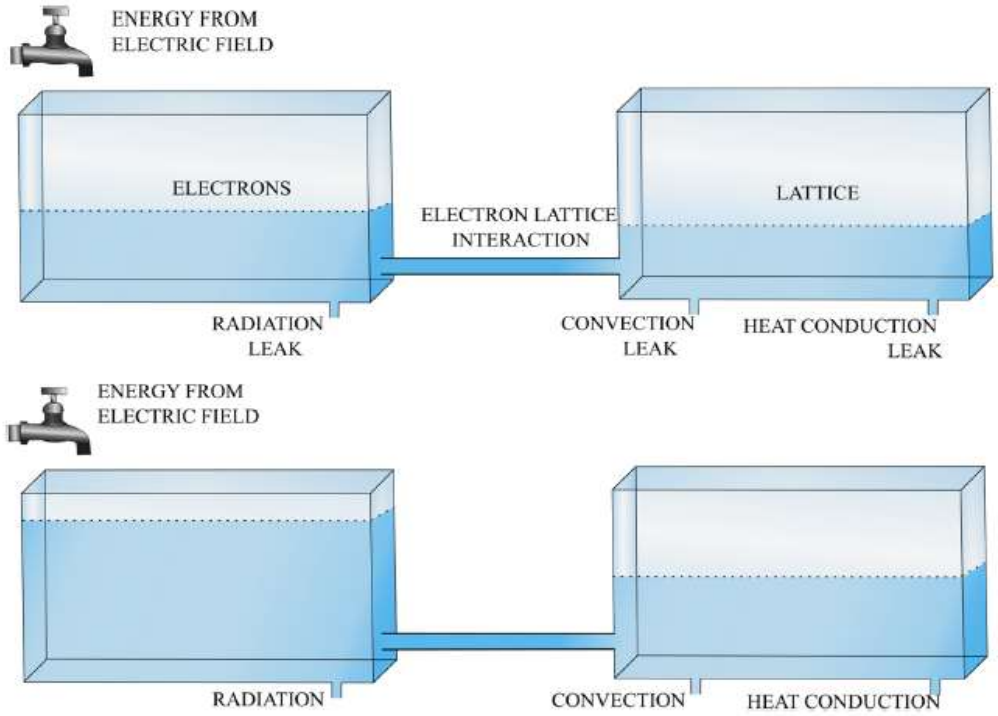

Fig.8.2: Hydraulic analogy of laser interaction with semiconductor

On the other hand, if the laser beam is sufficiently intense i.e., when the tap is opened all the way, the electron-lattice pipe may be too small to keep the water in the two

containers at the same level. The water level in the left container will then be higher and the effective temperature of electrons will be greater than that of lattice.

In narrow band gap semiconductors, for moderate values of the electric field, the increase in temperature of carriers is proportional to the square of the electric field. The change in temperature of carriers leads to corresponding change in the effective mass of carriers. This effect is one of the important mechanisms of self-focusing of laser beams in semiconductors.

In narrow-band semiconductors large non-parabolicity of the conduction band dispersion relation also causes laser self-focusing. This is because, in narrow band semiconductors, the velocity of the conduction electrons can become relativistic even when moderate intensity laser fields are applied. It just so happens that in the two band approximation of Kane's model [182], the Hamiltonian of the conduction band electrons mimics the relativistic form $H = (m_*^2 c_*^2 + c_*^2 p^2)^{\frac{1}{2}}$. Here, $c_* = \left(\frac{E_g}{2m_*}\right)^{\frac{1}{2}}$ plays the part of speed of light, m_* is the effective mass of electrons at the bottom of the conduction band, E_g is the width of forbidden band, and p is the electron quasi momentum. In several semiconductors, the characteristic velocity c_* that enters the Kane's dispersion law is much less than the speed of light e.g., for InSb, $c_* = 3 \times 10^{-3} c$. Because of this, the quiver velocity of the conduction electrons can become relativistic even at moderate laser intensities. A relativistic jitter is possible because the conduction band is partially empty, and as result the electrons can become accelerated under the effect of electric field. The non parabolicity of the conduction band implies a nonlinear electron velocity-momentum dependence which, in turn, leads to a nonlinear dependence of the current density on the electric field. This nonlinearity dominates the nonlinearity due to electron heating, provided the relevant wave frequencies are much higher than the effective collision frequency.

Consider the simultaneous propagation of two circularly polarized laser beam having electric field vector

$$\boldsymbol{E_j}(x, y, z, t) = \frac{1}{2}\left[\psi_j(r) e^{i(\omega_0 t - k_0 z) + c.c}\right](e_x + i e_y) \tag{8.1}$$

through a semiconductor plasma having dielectric function

$$\varepsilon = \varepsilon_0 - \frac{\omega_{p*}^2}{\omega_0^2} \tag{8.2}$$

where, ω_0 and k_0 respectively are angular frequency and vacuum wave number of the laser beam, (x, y) is the slowly varying amplitude of the laser beam and

$$\omega_{p*}^2 = \frac{4\pi e^2 n_0}{\varepsilon_0 m_*} \tag{8.3}$$

is the plasma frequency in the presence of the laser beam. Here, ε_0 is the dielectric constant of the lattice, m_* is the effective mass of the electron at the bottom of the conduction band in the presence of the laser beam.

When circularly polarized laser beam propagates through the semiconductor plasma, the circular polarization of the electric field of the laser beam makes the conduction electrons to move along circular orbits with frequency ω_0 and due to high field associated with the laser beam the jitter velocity of conduction electrons becomes relativistic. Hence, the effective mass m_* of the conduction electrons in eq.(8.3) gets replaced by $m_{0*}\gamma$, where m_{0*} is the effective mass of the conduction electron in the absence of the laser beam and γ is the relativistic Lorentz factor. Following Akhiezer and Polovin [31]

$$-e\sum_j \psi_j = \frac{m_{0*} v}{\sqrt{1 - \frac{v^2}{c_*^2}}}$$

From which, we get

$$\gamma = \sum_j \left(1 + \beta \psi_j \psi_j^*\right)^{\frac{1}{2}} \tag{8.4}$$

Where, $\beta = \frac{e^2}{m_{0*}^2 c_*^2 \omega_0^2}$ is the coefficient of relativistic nonlinearity. Hence, effective dielectric function of semiconductor plasma can be written as

$$\varepsilon = \varepsilon_0 - \frac{\omega_{p0*}^2}{\omega_0^2 \gamma} \tag{8.5}$$

where, $\omega_{p0*}^2 = \left(\frac{4\pi e^2 n_0}{\varepsilon_0 m_{0*}}\right)$ is the plasma frequency in the absence of the laser beam. eq.(8.5) can be written as

$$\varepsilon = \varepsilon_0' + \phi(\psi\psi^*) \tag{8.6}$$

Where

$$\varepsilon_0' = \varepsilon_0 - \frac{\omega_{p0*}^2}{\omega_0^2} \tag{8.7}$$

is the linear part of dielectric function and

$$\phi(\psi\psi^*) = \frac{\omega_{p0*}^2}{\omega_0^2}\left[1 - \frac{1}{\gamma}\right] \tag{8.8}$$

is the nonlinear part of dielectric function. For q-Gaussian amplitude structure, eq.(8.8) can be written as

$$\Phi_j(E_1E_1^*, E_2E_2^*) = \frac{\omega_{p0*}^2}{\omega_0^2}\left\{1 - \left[1 + \sum_j \frac{\beta_j E_{j0}^2}{f_j^2}\left(1 + \frac{r^2}{q_j r_j^2 f_j^2}\right)^{-\frac{q}{2}}\right]^{\frac{1}{2}}\right\} \tag{8.9}$$

8.3 Cross-focusing of Laser Beam

The evolution of beam envelope of an optical beam through a nonlinear medium is governed by the wave equation

$$i\frac{\partial E_j}{\partial z} = \frac{1}{2k_j}\nabla_\perp^2 E_j + \frac{k_j}{2\varepsilon_{0j}}\phi_j(E_1E_1^*, E_2E_2^*)E_j \tag{8.10}$$

According to variational method, eq.(8.10) is a variational problem for action principle based on Lagrangian density [60-62, 64,65]

$$\pounds = i\left(\psi_1\frac{\partial\psi_1^*}{\partial z} - \psi_1^*\frac{\partial\psi_1}{\partial z}\right) + i\left(\psi_2\frac{\partial\psi_2^*}{\partial z} - \psi_2^*\frac{\partial\psi_2}{\partial z}\right) + |\nabla_\perp\psi_1|^2 + |\nabla_\perp\psi_2|^2 - \frac{\omega_1^2}{c^2}\int^{E_1E_1^*}\Phi(E_1E_1^*, E_2E_2^*)d(E_1E_1^*)$$
$$- \frac{\omega_2^2}{c^2}\int^{E_2E_2^*}\Phi(E_1E_1^*, E_2E_2^*)d(E_2E_2^*) \tag{8.11}$$

Substituting the trial function for q-Gaussian beam profile in lagrangian density and integrating over the entire cross section of the laser beam we get the reduced lagrangian as $L = \int \pounds\, d^2r$. The corresponding Euler-Lagrange equations

$$\frac{d}{dz}\left(\frac{dL}{\partial\left(\frac{\partial f_j}{\partial z}\right)}\right) - \frac{\partial L}{\partial f_j} = 0 \tag{8.12}$$

give

$$\frac{d^2f_j}{d\xi^2} + \frac{1}{f_j}\left(\frac{df_j}{d\xi}\right)^2 = \frac{1}{k_j^2 r_j^4 f_j^3}\frac{\left(1 - \frac{1}{q_j}\right)\left(1 - \frac{1}{q_j}\right)}{\left(1 + \frac{1}{q_j}\right)} + \frac{\left(1 - \frac{2}{q_j}\right)}{r_j^2\varepsilon_{0j}I_{0j}}\int r^2\psi_j\psi_j^*\frac{\partial\phi_j}{\partial r}d^2r \tag{8.13}$$

Using eq.(8.9) in (8.13), the set of coupled differential equations for beam widths of the two laser beams are obtained as

$$\frac{d^2f_1}{d\xi^2}+\frac{1}{f_1}\left(\frac{df_1}{d\xi}\right)^2=\frac{\left(1-\frac{1}{q_1}\right)\left(1-\frac{1}{q_1}\right)}{\left(1+\frac{1}{q_1}\right)}\frac{1}{f_1^3}-2\left(\frac{\omega_{p0*}r_1}{c_*}\right)^2\left(1-\frac{1}{q_1}\right)\left(1-\frac{2}{q_1}\right)J_1 \tag{8.14}$$

$$\frac{d^2f_2}{d\xi^2}+\frac{1}{f_2}\left(\frac{df_2}{d\xi}\right)^2=\left(\frac{r_1}{r_2}\right)^4\left(\frac{\omega_1}{\omega_2}\right)^2\left(\frac{\varepsilon_{01}}{\varepsilon_{02}}\right)\frac{\left(1-\frac{1}{q_2}\right)\left(1-\frac{1}{q_2}\right)}{\left(1+\frac{1}{q_2}\right)}\frac{1}{f_2^3}-2\left(\frac{\omega_{p0*}r_1}{c_*}\right)^2\left(1-\frac{1}{q_2}\right)\left(1-\frac{2}{q_2}\right)J_2 \tag{8.15}$$

where, $\xi=\frac{z}{k_1r_1^2}$ is the dimensionless distance of propagation, and

$$J_1=\frac{\beta_1E_{10}^2}{f_1^3}T_1+\frac{\beta_2E_{20}^2}{f_1^3}\left(\frac{r_1}{r_2}\right)^2\left(\frac{f_1}{f_2}\right)^4T_2$$

$$J_2=\frac{\beta_1E_{10}^2}{f_2^3}T_3+\frac{\beta_2E_{20}^2}{f_2^3}\left(\frac{r_1}{r_2}\right)^2\left(\frac{f_1}{f_2}\right)^4T_4$$

$$T_1=\int_0^\infty x^3\left(1+\frac{x^2}{q_1}\right)^{-2q_1-1}G(x)dx$$

$$T_2=\int_0^\infty x^3\left(1+\frac{x^2}{q_1}\right)^{-q_1}\left(1+\frac{x^2}{q_2}\left(\frac{r_1f_1}{r_2f_2}\right)^2\right)^{-q_2-1}G(x)dx$$

$$T_3=\int_0^\infty x^3\left(1+\frac{x^2}{q_1}\right)^{-q_1-1}\left(1+\frac{x^2}{q_2}\left(\frac{r_1f_1}{r_2f_2}\right)^2\right)^{-q_2}G(x)dx$$

$$T_4=\int_0^\infty x^3\left(1+\frac{x^2}{q_2}\left(\frac{r_1f_1}{r_2f_2}\right)^2\right)^{-2q_2-1}G(x)dx$$

$$G(x)=e^{-\left\{\frac{\beta_1E_{10}^2}{f_1^2}\left(1+\frac{x^2}{q_1}\right)^{-q_1}+\frac{\beta_2E_{20}^2}{f_2^2}\left(1+\frac{x^2}{q_2}\left(\frac{r_1f_1}{r_2f_2}\right)^2\right)^{-q_2}\right\}}$$

$$x=\frac{r}{r_1f_1}$$

Equations (8.14) and (8.15) are the coupled nonlinear differential equations governing the cross focusing of two coaxial q-Gaussian laser beams in narrow band semiconductors. For initially plane wavefronts these equations are subjected to boundary conditions $f_j=$

1 and $\frac{df_j}{d\xi} = 0\ at\ \xi = 0$. Numerical computational techniques are used to investigate the beam dynamics as analytic solutions of these equations are not possible.

8.4 Excitation of Electron Plasma Wave (EPW)

The electron density perturbation n' associated with the excited EPW evolves according to the wave equation

$$\frac{\partial^2 n'}{\partial t^2} - v_{th}^2 \nabla^2 n' + \omega_{p0*}^2 n' = \frac{e}{m_{0*}} n_0 \nabla \sum_j E_j \tag{8.16}$$

Taking

$$n' = n_1 e^{i(\omega t - kz)}$$

where, $\omega = \omega_2 - \omega_1$ and $k = k_2 - k_1$, we get the amplitude of density perturbation associated with plasma wave

$$n_1 = \frac{e n_0}{m_{0*}} \frac{1}{\left(\omega_0^2 - k_0^2 v_{th}^2 - \omega_{p*}^2\right)} \left[\frac{E_{10}}{r_1^2 f_1^3} \left(1 + \frac{r^2}{q_1 r_1^2 f_1^2}\right)^{-\frac{q_1}{2}-1} + \frac{E_{20}}{r_2^2 f_2^3} \left(1 + \frac{r^2}{q_2 r_2^2 f_2^2}\right)^{-\frac{q_1}{2}-1} \right] r \tag{8.17}$$

8.5 THz Generation

The density perturbation associated with excited EPW results in a nonlinear current density at frequency $\omega = \omega_2 - \omega_1$ that acts as a source for the THz radiation. The generated current density is given by

$$J_T = \frac{e^2 n_0}{m_{0*}\omega} \left(\frac{n_1}{n_0}\right) e^{i(\omega t - kz)} \left(E_1 + E_2\right) \tag{8.18}$$

The electric field of the resulting THz evolves according to the wave equation

$$\nabla^2 E_T = \frac{1}{c^2} \frac{\partial^2 E_T}{\partial t^2} + \frac{4\pi}{c^2} \frac{\partial J_T}{\partial t} \tag{8.19}$$

This equation gives the magnitude of electric field of THz radiation as

$$E_T = i \frac{\left(\frac{\omega_{p0*}^2}{c_*^2}\right)}{\left(\frac{\omega^2}{c_*^2} - k^2\right)} \frac{n_1}{n_0} (E_1 + E_2) \tag{8.20}$$

Defining the normalized power of THz radiation as

$$P_T = \frac{\int_0^\infty E_T E_T^* r dr}{\int_0^\infty \psi_1 \psi_1^* r dr} \tag{8.21}$$

We get

$$P_T = \frac{\left(\frac{\omega_{p0*}^2}{c_*^2}\right)^2}{\left(\frac{\omega^2}{c_*^2} - k^2\right)^2} \frac{\int \left(\frac{n_1}{n_0}\right)^2 (E_1 + E_2)^2 r dr}{\int \psi_1 \psi_1^* r dr} \tag{8.22}$$

Equation (8.22) has been solved numerically in association with the beam width equations (8.14) and (8.15) and the corresponding evolutions of the normalized power with distance of propagation for different values of q.

8.6 Results and Discussion

To investigate the effect of deviation of intensity distribution of laser beams from Gaussian distribution and plasma density on cross focusing of the laser beams eqs. (8.4)-(8.15) have been solved for following set of laser-plasma parameters:

$$\omega_1 = 1.758 \times 10^{14} rad\ s^{-1}, \quad \omega_2 = 1.75 \times 10^{14} rad\ s^{-1}$$

$$r_1 = 15\mu m, \quad r_2 = 16\mu m, \quad \beta_1 E_{10}^2 = 3, \quad \beta_2 E_{20}^2 = 1.5\,, \quad q_2 = 3, \quad \left(\frac{\omega_{p0*} r_0}{c_*}\right)^2 = 9$$

and for different values of q_1 viz., $q_1 = (3,4,\infty)$. In the present investigation Eq. (26) has been solved numerically for typical parameters of n-InSb plasma. The parameters are:

$$E_g = 0.234eV, \quad T = 77K, \quad m_{0*} = \frac{m_e}{74}, \quad \varepsilon_0 = 16, \quad c^* = \frac{c}{253}, \quad n_0 = 10^{15} cm^{-1}.$$

The plots in figs. 8.3 and 8.4 depict that during their propagation through semiconductor, the laser beam break up into narrow localized structure called as filaments. These filamentation of laser beams occurs due to the periodic focusing/defocusing of the laser beams occurring as a consequence of optical nonlinearity of semiconductor.

The plots in fig.8.3 depict that with increase in the value of deviation parameter q_1 of beam1, the brightness of its filaments decreases, however the number of filaments in a given distance of propagation increases. This is due to the faster but reduced self focusing of beam1 with increase in its deviation parameter.

The plots in fig.8.4 depict that increase in the deviation parameter of beam1, makes the filaments of beam2 more localized, i.e., brightness of the filaments of beam2 increases. This is due to the nonlinear coupling between the two beams. With increase in q_1, the axial part of beam2 becomes stronger that enhances the brightness of the filaments of beam2.

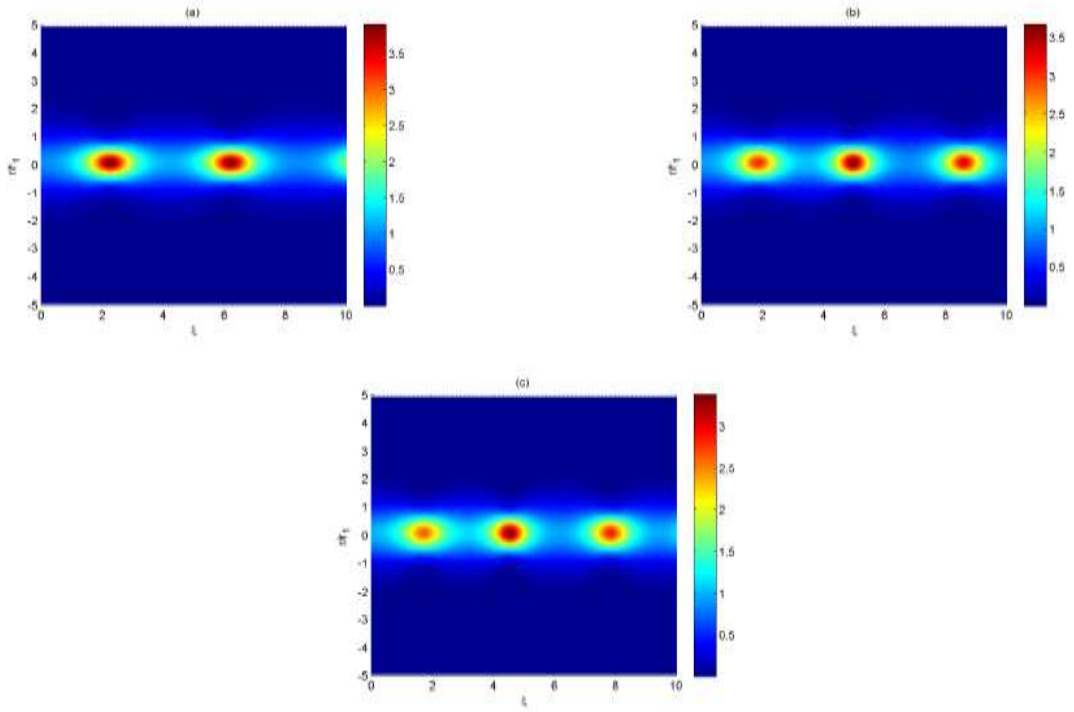

Fig.8.3: Effect of q_1 on filamentation of beam 1 a) $q_1 = 3$, b) $q_1 = 4$, c) $q_1 = \infty$

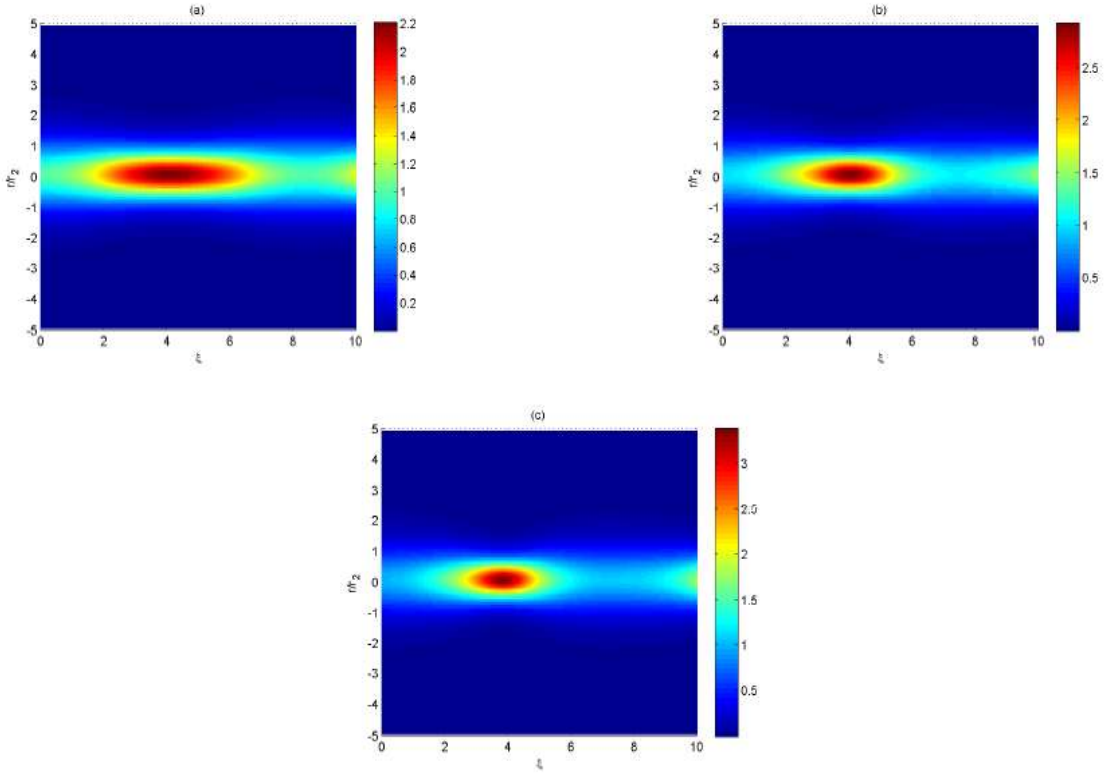

Fig.8.4: Effect of q_1 on filamentation of beam 2 a) $q_1 = 3$, b) $q_1 = 4$, c) $q_1 = \infty$

Fig.8.5 illustrates the impact of deviation parameter of beam1 that is q_1 on evolution of normalized power of produced THz radiation with distance of propagation. It has been investigated that the power of THz radiation is monotonically increasing along the direction of propagation, showing step like behaviour. Each step occurs approximately at the position of filaments of the laser beams. This is because as the pump beam gets self focused their intensity increases and as the result of which the amplitude of oscillations of the plasma electrons also increases. Hence, the amplitude of the generated EPW increases. Since, the density perturbation associated with EPW acts as source for nonlinear current density for THz, there is monotonic increase in the THz power with distance.

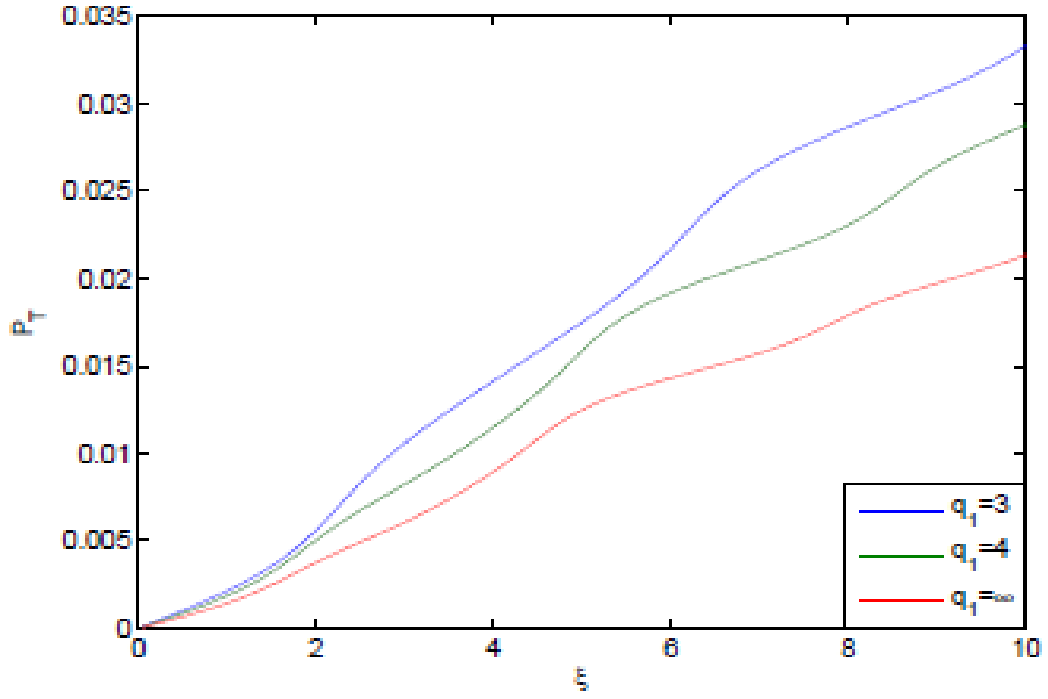

Fig.8.5: Effect of q_1 on power of THz radiation

Decrease in the THz power P_T with increase in deviation parameter q_1 of beam1 has also been depicted from the plots in fig.8.5. The reason behind this is the one to one correspondence between the THz power and the degree of self focusing of the pump beam. As increase in the value of q_1 reduces the extent of focusing of the pump beam1 (beam with higher initial intensity) and increases the focusing of beam 2. However, in producing

THz radiation dominant role is played by beam with higher initial intensity. Hence, there is corresponding decrease in the power of THz radiation with increase in q_1.

8.7 Conclusions

It has been observed that filamentations in narrow band semiconductors are produced due to the self focusing/defocusing of both q-Gaussian laser beams under the effects of each other and the relativistic nonlinearity of narrow band semiconductor. The brightness of filamentations is reduced as the q_1 is increased. It means, the intensities of filaments are decreased due to which the oscillations of electrons are decreased. Consequently, the yield of THz radiation is reduced.

Chapter-9

Generation of Second Harmonics of q-Gaussian Laser Beams in Collisional Plasma with Upward Density Ramp

9.1 Introduction

The quest for short-wavelength coherent radiation sources for medical treatment and diagnostics [183], homeland security [184], plasma diagnostics [185] etc. has a long history. For the past few decades, only two main types of facilities, namely free electron lasers (FELs) [186] and synchrotrons [187], have been considered for this purpose. Such large facilities have provided scientists with the tools to probe and image matter on very small length scales and over very short periods of time, enabling ground breaking work in fields as diverse as biology and archaeology. A large infrastructure involving accelerators, beam lines and massive gantries of more than 1000 tons is required for these facilities. Hence, significant capital investment is required for the construction and maintenance of these so-called third generation (synchrotrons) and fourth generation (FELs) radiation sources. As a result, these facilities are not affordable for less affluent institutes such as universities and hospitals. Therefore, research related to them is not growing very fast.

By producing similar extreme ultraviolet and soft x-ray radiation on a bench top scale, the phenomenon of high harmonic generation (HHG) can serve as a cost-effective means of extending access to and application of light in this part of the spectrum. The reduction in cost is due not only to the replacement of the accelerator but also to the fact that there will be no requirement for large building footprints and massive gantries. HHG can be produced in a number of nonlinear media such as gases [188], dielectrics [41], semiconductors [189] and plasmas [27, 44, 82-88]. Plasmas have several interesting advantages over normal states of matter (i.e. solids, liquids and gases) that make them ideal candidate for HHG. Firstly, being already ionized, plasmas are immune to material damage. Hence, there is no upper limit on the intensity of the pump beam. Secondly, HHG in plasmas is associated with free electrons, and therefore there is no upper bound on the frequency of the generated harmonics either, i.e. higher harmonics of desirable order and intensity can be produced in plasmas.

Several mechanisms such as parametric instabilities [190], resonance absorption [191], ionization absorption [192], photon acceleration [193], density gradients due to filamentation of light [194] and excitation of electron plasma waves (EPW) [88, 109, 179, 180] are thought to be responsible for HHG in plasmas. For second harmonic generation (SHG), excitation of EPWs has been found to be the most efficient mechanism [39]. By interacting nonlinearly with the pump beam, the excited EPW converts it to its second harmonics through the phenomenon of sum frequency generation.

The phenomenon of SHG was first reported by Franken *et al* in 1961 [41], very soon after the invention of laser by Maiman in 1960 [1]. Since then, a number of investigations by several researchers have highlighted theoretical as well as experimental aspects of SHG. The main aim of all these investigations was to increase the efficiency of SHG so that one can get more and more intense short-wavelength coherent radiation sources at moderate pumps. This chapter presents an investigation of SHG of q-Gaussian laser beams in collisional plasma with an upward density ramp. The density ramp will enhance the interaction of the laser beam with plasma, and therefore an enhanced conversion efficiency of second harmonics can be expected.

9.2 Nonlinear Dynamics of Pump Beam

Consider the interaction of a linearly polarized laser beam having electric field

$$\boldsymbol{E}(\boldsymbol{r},\boldsymbol{z},\boldsymbol{t}) = A_0(r,z)e^{i(k_0 z-\omega_0 t)}e_x \tag{9.1}$$

with collisional plasma having an upward density ramp [77]. The Ohmic nonlinearity of the plasma electrons is modelled by the dielectric function

$$\phi(A_0A_0^*) = \frac{\omega_p^2(z)}{\omega_0^2}\left(1-\left(1+\frac{1}{2}\beta A_0A_0^*\right)^{\frac{s}{2}-1}\right) \tag{9.2}$$

where $\omega_p^2 = \frac{4\pi e^2 n(z)}{m}$ is the plasma frequency, $n(z)$ being the axially increasing electron density of plasma, and $\beta = \frac{e^2 M}{6K_0T_0m^2\omega_0^2}$ is the coefficient representing the strength of collisional nonlinearity. The nature of collisions is expressed by the parameter s and $s = 0$ indicates velocity-independent collisions, $s = 2$ corresponds to collisions between

electrons and diatomic molecules and $s = -3$ indicates collisions between electrons and ions.

Laser beam propagation through such a medium is modeled by the wave equation (which can be obtained from Maxwell's equations)

$$2ik_0 \frac{\partial A_0}{\partial z} = \nabla_\perp^2 A_0 + \frac{\omega_0^2}{c^2} \phi(A_0 A_0^*) A_0 \tag{9.3}$$

Equation (9.3) is identical to a well-known wave equation known as the nonlinear Schrödinger equation (NLSE) that governs the transmission of electromagnetic waves through nonlinear media and is a statement of interplay between nonlinearity and spatial dispersion.

Being nonlinear in nature, the superposition principle does not apply to equation (9.3), i.e., a linear combination of two solutions is not a solution. Mathematically this means that the conventional method of solving partial differential equations, i.e. expansion in power series, is not applicable to NLSE. In fact no exact analytical solution exists for this equation. In order to obtain physical insight into the propagation dynamics of the laser beam, I have adopted a semi-analytical technique known as the variational method [38, 60-62, 64, 68]. This method replaces a partial differential equation with a set of coupled ordinary equations for the various parameters of the laser beam. According to this method equation (9.3) is a variational problem for the action principle based on Lagrangian density:

$$£ = i\left(A_0 \frac{\partial A_0^*}{\partial z} - A_0^* \frac{\partial A_0}{\partial z}\right) + |\nabla_\perp A_0|^2 - \frac{\omega_0^2}{c^2} \int^{A_0 A_0^*} \phi(A_0 A_0^*)\, d(A_0 A_0^*) \tag{9.4}$$

In the present analysis, I have assumed that $A_0(r, z)$ takes the form of the function given by

$$A_0(r, z) = \frac{E_{00}}{f}\left(1 + \frac{r^2}{q r_0^2 f^2}\right)^{-\frac{q}{2}} \tag{9.5}$$

where the parameter $f(z)$ is currently undetermined and upon multiplication with initial beam width r_0 it gives the waist size of the laser beam at a particular location inside the medium. Hence, the parameter $f(z)$ can be referred to as a dimensionless beam width parameter. The phenomenological parameter q is related to the deviation of the irradiance, over the cross section of the beam, from the ideal Gaussian profile. Substituting the trial

function (equation (9.5)) in the Lagrangian density and integrating over r, I get the reduced Lagrangian as $L = \int_0^\infty £\, r dr$. The corresponding Euler–Lagrange equation

$$\frac{d}{dz}\left(\frac{\partial L}{\partial\left(\frac{\partial f}{\partial z}\right)}\right) - \frac{\partial L}{\partial f} = 0 \tag{9.6}$$

gives the following ordinary differential equation describing the dynamical variations of beam width with propagation distance:

$$\frac{d^2 f}{d\xi^2} = \frac{\left(1-\frac{1}{q}\right)\left(1-\frac{2}{q}\right)}{\left(1+\frac{1}{q}\right)}\frac{1}{f^3} + \left(\frac{\omega_p(\xi) r_0}{c}\right)^2 \left(1-\frac{1}{q}\right)\left(1-\frac{2}{q}\right)\left(\frac{s}{2}-1\right)\frac{\beta E_{00}^2}{f^3} T \tag{9.7}$$

where

$$T = \int_0^\infty x\left(1+\frac{x}{q}\right)^{-2q-1}\left\{1+\frac{1}{2}\frac{\beta E_{00}^2}{f^2}\left(1+\frac{x}{q}\right)^{-q}\right\}^{\frac{s}{2}-2} dx$$

$$x = \frac{r^2}{r_0^2 f^2}$$

$$\xi = \frac{z}{k_0 r_0^2}$$

Thus, it follows from equation (9.7) that the problem of solving a partial differential equation, i.e. NLSE (equation (9.3)), has reduced to that of solving an ordinary differential equation. Although this reduced equation is also lacking an exact analytical solution due to its non-integrability, its approximate solution can be easily obtained with the help of simple numerical techniques.

Considering the plasma density to be increasing axially as $n(\xi) = n_0(1 + \tan(\xi d))$, where n_0 [172] is the plasma density seen by the laser beam while entering the plasma and d is the measure of the rate of increase of plasma density with distance, one can write the plasma frequency as

$$\omega_p^2(\xi) = \omega_{p0}^2(1 + \tan(\xi d)) \tag{9.8}$$

with

$$\omega_{p0}^2 = \frac{4\pi e^2 n_0}{m_e}$$

9.3 Generation of Second Harmonics

The nonuniform irradiance over the cross section of the laser beam produces a transverse density gradient in the plasma by evacuating electrons from high-intensity regions. This density gradient results in an EPW at pump frequency ω_0, whose amplitude is governed by the wave equation [92]

$$-\omega_0 n' + v_{th}^2 \nabla^2 n' + \omega_p^2(\xi) n' = \frac{e}{m} n(\xi) \nabla A_0 \tag{9.9}$$

From this wave equation we can get the amplitude of the plasma wave as

$$n' = \frac{en(\xi)}{m} \frac{E_{00}}{r_0^2 f^3} \frac{r}{(\omega_0^2 - k_0^2 v_{th}^2 - \omega_p^2(\xi))} \times \frac{\left(1 + \frac{r^2}{q r_0^2 f^2}\right)^{-\frac{q}{2}-1}}{\left\{1 + \frac{\beta E_{00}^2}{f^2}\left(1 + \frac{r^2}{q r_0^2 f^2}\right)^{-q}\right\}^{\frac{s}{2}-1}} \tag{9.10}$$

The generated EPW interacts nonlinearly with the incident beam to produce its second harmonics. The electric field vector E_2 of the second harmonics satisfies the wave equation

$$\nabla^2 E_2 + \frac{\omega_2^2}{c^2} \varepsilon_2(\omega_2) E_2 = \frac{4\pi e^2}{c^2} n' A_0 \tag{9.11}$$

which gives

$$E_2 = \frac{4\pi e^2}{mc^2} n' \frac{A_0}{k_2^2 - 4k_0^2} \tag{9.12}$$

Defining the yield Y_2 of second harmonics as

$$Y_2 = \frac{P_2}{P_0} \tag{9.13}$$

where

$$P_2 = \int_0^\infty E_2 E_2^* r dr$$

$$P_0 = \int_0^\infty A_0 A_0^* r dr$$

we can get

$$Y_2 = \frac{8}{9} \frac{K_0 T_0}{mc^2} \left(\frac{\omega_0^2 r_0^2}{c^2}\right) \frac{\beta E_{00}^2}{f^4} \left(1 - \frac{1}{q}\right) H \tag{9.14}$$

$$H = \int_0^\infty \frac{\left(1 + \frac{x}{q}\right)^{-2q-2}}{\left[\left(\frac{\omega_0^2 r_0^2}{c^2}\right) - \frac{\omega_0^2 r_0^2}{c^2} \frac{\varepsilon_0 v_{th}^2}{c^2} - \frac{\omega_{p0}^2 r_0^2}{c^2} (1 + \tan(\xi d)) \left(1 + \frac{\beta E_{00}^2}{f^2}\left(1 + \frac{x}{q}\right)^{-q}\right)^{\frac{s}{2}-1}\right]^2} x dx$$

Equation (9.14) governs the evolution of second harmonic yield Y_2 with distance of propagation.

9.4 Results and Discussion

In the present analysis solution of equation (9.7) in association with equation (9.8) has been obtained with the help of the Runge–Kutta fourth order method for the following set of laser and medium parameters

$$\omega_0 = 1.78 \times \frac{10^{15} rad}{sec}, \qquad r_0 = 15\mu m, \qquad s = -3, \quad \frac{\omega_{p0}^2(z) r_0^2}{c^2} = 6\,, \qquad T_0 = 10^6 K.$$

In solving equation (9.7) it has been assumed that initially the beam is collimated, i.e., it satisfies the initial conditions $f = 1$ and $\frac{df}{d\xi} = 0$ at $\xi = 0$.

The corresponding evolution of the beam width with distance through the plasma is shown in fig.9.1. Breather-like behaviour, i.e. harmonic variations in the beam width with distance of propagation through the medium, can be clearly seen from the plots in fig.9.1.

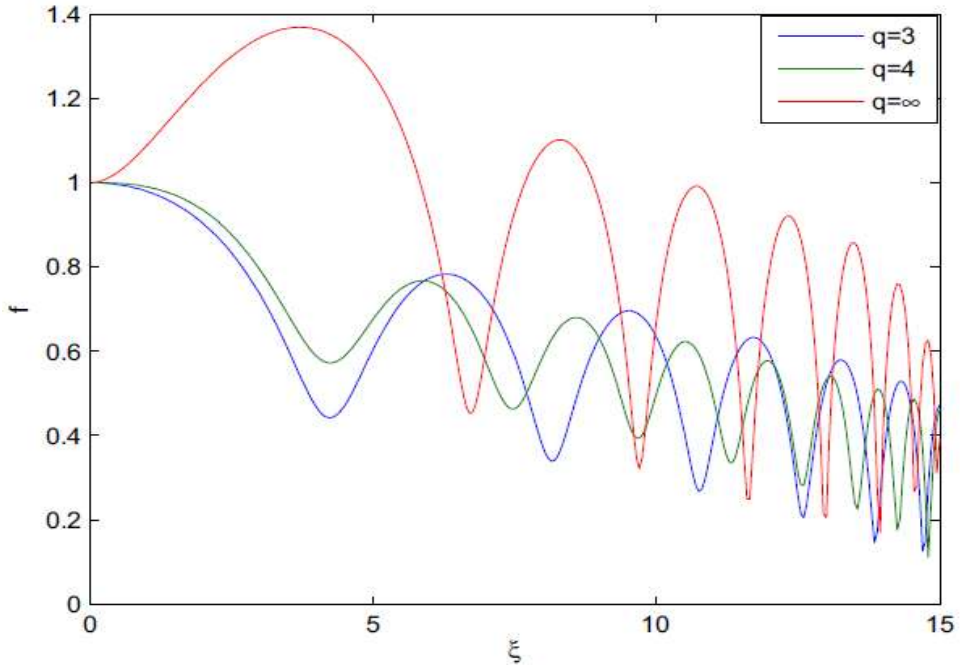

Fig.9.1: Effect of q, i.e. the deviation of the intensity profile of the laser beam from a Gaussian profile, on the evolution of the width of the laser beam with distance of propagation.

These harmonic variations of the beam width can be explained by examining the role and origin of various terms in equation (9.7). The first term on the right-hand side, which is

proportional to f^{-3}, is the spatial dispersive term, which models the spreading of the laser beam in transverse directions that occurs as a consequence of diffraction divergence. The second term, which has a complex dependence on f, arises due to the nonuniform Ohmic heating of plasma and is responsible for the nonlinear optical response of the plasma to the pump beam. As a consequence of this optical nonlinearity of the plasma the resulting nonlinear refraction of the laser beam tends to counter balance the effect of diffraction. Thus, during the propagation of the laser beam through collisional plasma, a competition arises between the two phenomena of diffraction and nonlinear refraction. The winning phenomenon ultimately decides the behaviour of the laser beam, i.e. whether it will converge or diverge. Thus, there exists a critical value of beam intensity (which can be obtained by balancing the two terms on the right-hand side of equation (9.7)) above which the beam will converge. In the present investigation the initial beam intensity has been taken to be greater than the critical intensity, i.e. why the laser spot size of the laser beam is converging initially. As the beam width decreases, its intensity increases. When the laser intensity becomes too high then the Ohmic nonlinearity gets saturated and thus the nonlinear refraction vanishes, leaving only the diffraction effects to dominate. Hence, after focusing to a minimum, the beam width bounces back to its original value. As the width of the laser beam starts increasing, the competition between diffraction and nonlinear refraction starts again. This competition now lasts until a maximum value of f is obtained. These processes go on repeating themselves and thus give breather-like behaviour to the spot size of the laser beam. Furthermore, it has been observed that after every focal spot the maximum as well as the minimum of the beam width shifts downwards. This is owing to the fact that the equilibrium electron density is an increasing function of longitudinal distance. Hence, the plasma index of refraction keeps on decreasing with the penetration of the laser beam into the plasma. Consequently, the self focusing effect gets enhanced and the maximum as well as minimum of the beam width goes on shifting downwards after every focal spot. It is also seen that the frequency of oscillations of the beam width increases with distance. The physics behind this fact is that the denser the plasma, the

higher will be the phase velocity of the laser beam through it. Hence, in denser plasma a laser beam takes less time to get self focused.

Reduced focusing of laser beams with a higher value of q can also be seen from fig.9.1. The reason behind this effect is that for laser beams with higher value of q most of the intensity is concentrated in a narrow region around the axis of the beam. Hence, these beams receive a much reduced contribution from the off-axial part in order to produce nonlinearity in the medium. As the phenomenon of self focusing is a homeostasis of nonlinear refraction of the laser beam due to optical nonlinearity of the medium, an increase in the value of q reduces the extent of self focusing.

The plots in fig.9.1 also indicate that instead of their reduced focusing, laser beams with a higher value of q possess a faster focusing character. This is due to the faster focusing character of axial rays. Being away from the axis, off-axial rays take longer duration to get self focused. There are more off-axial rays in laser beams with lower q values, and hence the focusing of the laser beam becomes faster with increasing q. Hence, by optimizing the value of q, one can control the extent of self focusing as well as the location of the focal spot of a laser beam.

In order to see the effect of initial plasma density on the behaviour of the envelope of the pump beam, equation (9.7) has been solved for different values of normalized plasma density $\frac{\omega_{p0}^2(z)r_0^2}{c^2}$ at fixed values of q and beam intensity βE_{00}^2. The resulting behaviour of the beam width has been shown in fig.9.2. The substantial increase in the extent of self focusing is a consequence of the increase in initial plasma density. It is because of this increase in plasma density that the mean free path of plasma electrons decreases. As a result, their collisions with other species become more frequent, leading to the enhancement of optical nonlinearity of the plasma. As self focusing of the laser beam is a homeostasis of optical the nonlinearity of the medium, an increase in plasma density results in an increase in the extent of self focusing of the laser beam.

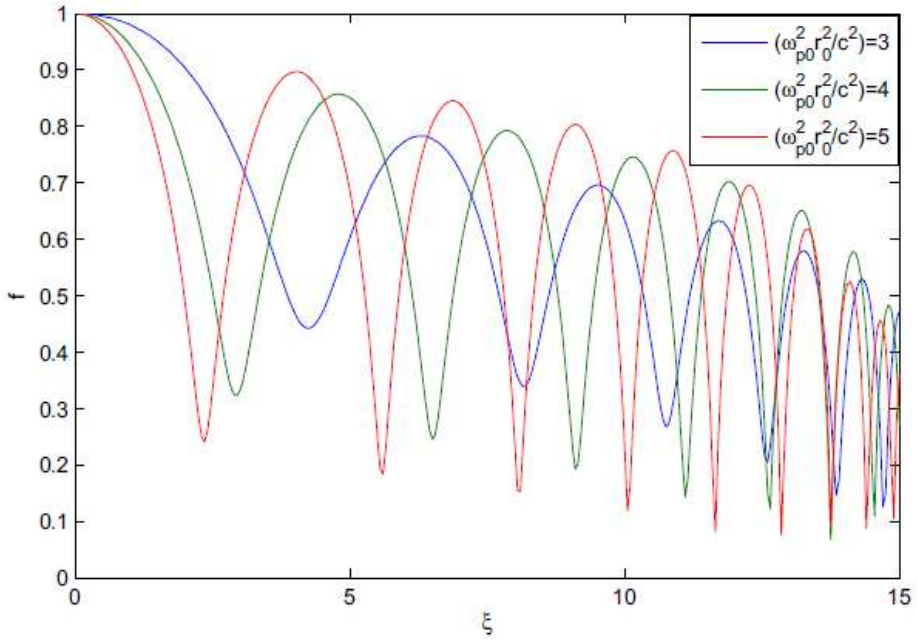

Fig.9.2: Effect of normalized plasma density on the evolution of the width of the laser beam with distance of propagation

Fig.9.3 illustrates the effect of initial beam intensity on self focusing of the laser beam. It can be seen that with increasing initial intensity of the laser beam, there is enhancement in the extent of its self focusing and also it becomes faster. This occurs because with increasing intensity of the pump beam, the kinetic energy of the plasma

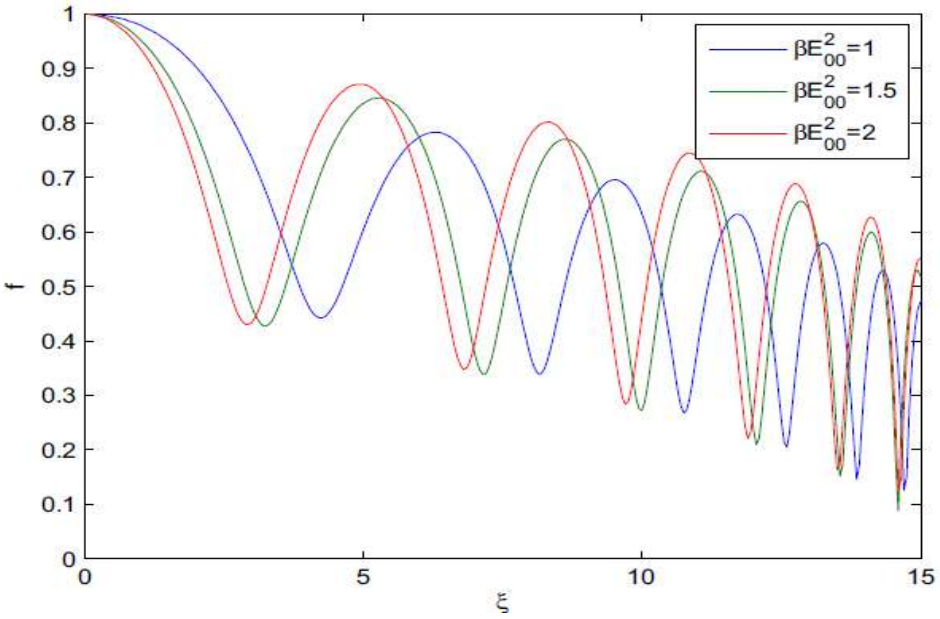

Fig.9.3: Effect of normalized laser intensity on evolution of the width of the laser beam with distance of propagation.

electrons increases, which in turn increases the collisional nonlinearity via nonuniform Ohmic heating. Thus an increase in the laser intensity enhances the amount of focusing of the laser beam.

Further, equation (9.14) has been solved numerically in association with equation (9.7) in order to envision how the power of generated second harmonics evolves with longitudinal distance through the plasma. The corresponding variation of Y_2 with distance ξ is depicted in fig.9.4.

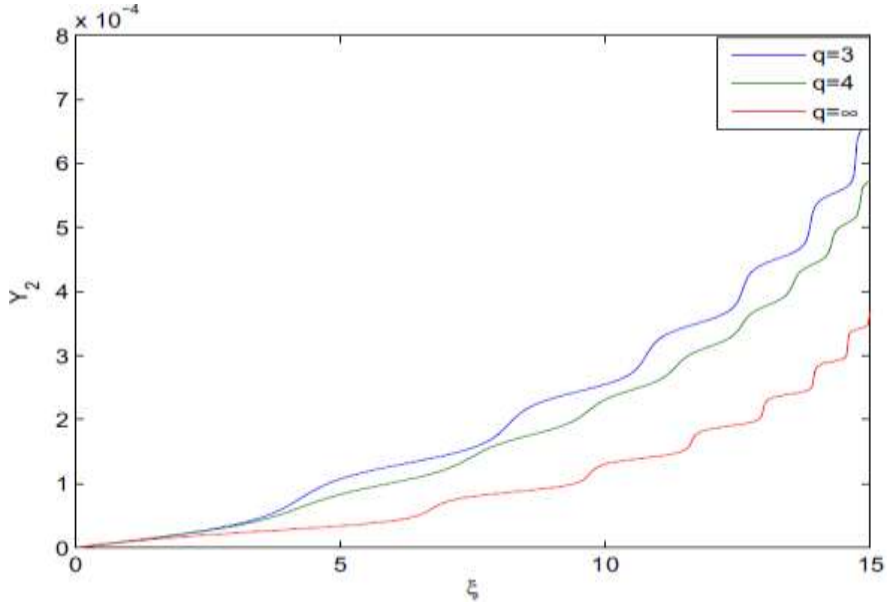

Fig 9.4: Effect of q, i.e. deviation of the intensity profile of the laser beam from a Gaussian profile, on the evolution of the yield of second harmonics with distance of propagation.

It has been observed that the power of second harmonic radiation is a monotonically increasing function of propagation, showing step-like behaviour. Each step occurs at a position of minimum beam width. This is because as the pump beam gets self focused its intensity increases, and consequently the oscillation amplitude of the plasma electrons also increases, which in turn increases the amplitude of the generated EPW. Since the density perturbation associated with an EPW acts as a source for nonlinear current density for SHG, there is a monotonic increase in the conversion efficiency of second harmonics with distance.

The step-like behaviour of the power of harmonic radiation at the positions of minim

-um width of the pump beam is owing to the fact that these are the regions of highest intensity and hence the current density for SHG is maximum there. Hence, after attaining its maximum value the harmonic power moves towards its next possible higher value at the next focal spot. These transitions of harmonic power from one maximum value to the next give it a step-like behaviour.

Further, it is observed that with longitudinal distance the steepness of the steps goes on increasing whereas their size decreases. This is due the fact that the steepness of the steps is proportional to the extent of self focusing, and the step size is inversely proportional to the frequency of oscillations of the beam width. Since, the extent as well as the frequency of self focusing increase with distance, r_e is an increase in the steepness of the steps of the curve of Y_2 versus ξ whereas the size of steps goes on decreasing.

A reduction in the efficiency Y_2 of conversion to second harmonics with increasing q has also been observed from the plots in fig.9.4. The underlying physics behind this is the one-to-one correspondence between the conversion to higher harmonics and the degree of self focusing of the pump beam. An increase in the value of q reduces the extent of focusing of the pump beam, hence there is a corresponding decrease in the conversion efficiency of second harmonics.

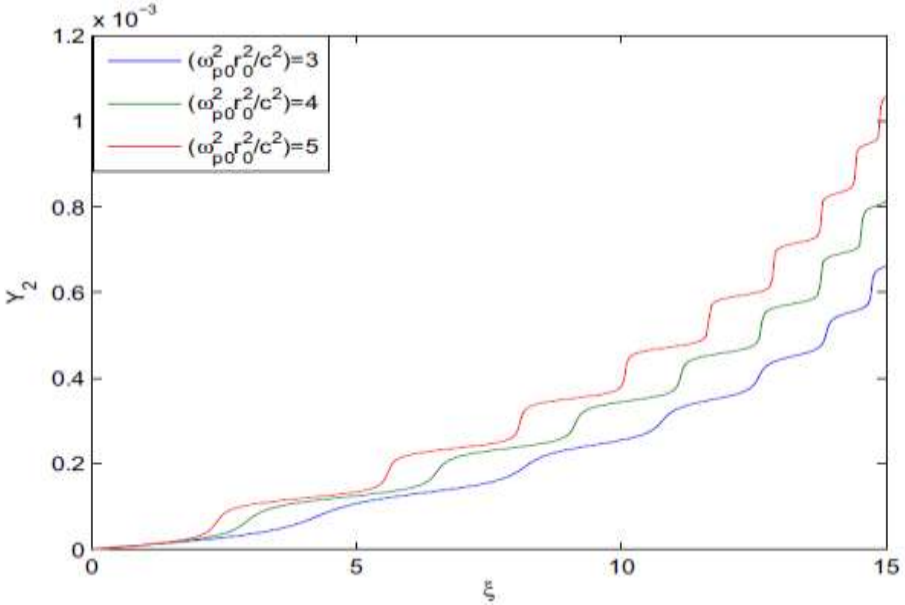

Fig 9.5: Effect of normalized plasma density on the evolution of the yield of second harmonics with distance of propagation.

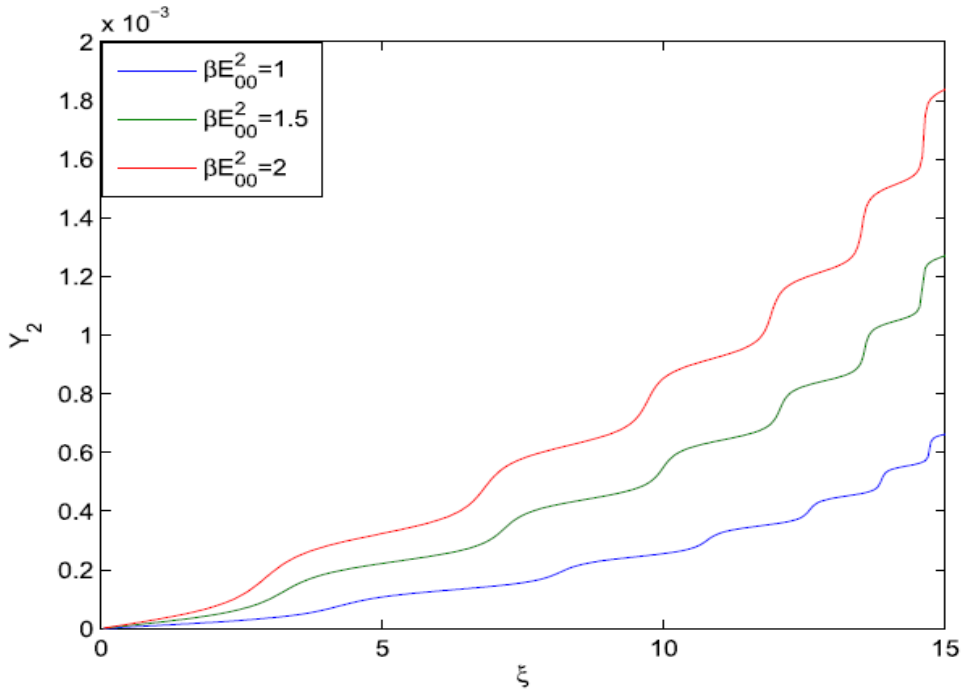

Fig.9.6: Effect of normalized laser intensity on the evolution of the yield of second harmonics with distance of propagation

The plots in figs.9.5-9.6 indicate that an increase in initial plasma density or intensity of the pump results in enhancement of the conversion efficiency of second harmonics. This is due to the increase in the extent of self focusing with increasing plasma density or intensity of the pump beam.

9.5 Conclusions

In the present investigation, study on the effect of self focusing on SHG of q-Gaussian laser beam in collisional plasma with ramped density. It has been observed that the self focusing and yield of SHG of q-Gaussian laser beam can be increased by including the off-axial contribution of the cross section of the laser beam. In addition, the self focusing and SHG can also be enhanced with increase in initial intensity of q-Gaussian laser beam and density of plasma. The obtained results of self focusing and SHG can be fruitful in plasma diagnostics, inertial confinement fusion (ICF) and other investigations on laser plasma interactions.

Chapter-10

Generation of Second Harmonics of Self focused Quadruple-Gaussian Laser Beams in Collisional Plasmas with Density Ramp

10.1 Introduction

The revolution in the field of laser has made it useful in interdisciplinary fields of research. Among these fields, generation of harmonics of electromagnetic radiation in plasma is a hot topic of research due to its vast applications such as plasma based electron accelerator [7, 16], inertial confinement fusion [6], medical diagnostics [183], plasma diagnostics [185] etc. The deep penetration of laser beams in plasma is preliminary requirement for all these applications. The propagation of laser beam through nonlinear medium reveals different nonlinear self-actions effects e.g. self focusing, self trapping, X-ray laser and harmonics generation [22, 24, 60-63]. In the absence of these self-action effects, due to diffraction property, laser beam only propagate a Rayleigh length. Among different nonlinear mechanisms, higher harmonics generation play vital role as these can penetrate deep into the plasma and provide plasma diagnostics such as local plasma density, temperature of plasma, opacity, electrical conductivity of plasma etc.

Due to the applications of harmonics of laser beam, the researchers are busy in producing higher harmonics generation. It is well-known fact that laser beams differing in intensity profile behave differently in nonlinear media. Literature review reveals the fact that most of the earlier theoretical investigations on nonlinear optical phenomena of laser beams have been directed toward revealing the propagation characteristics of laser beams with ideal Gaussian profile. However, in context of ICF [16, 163] there is growing interest in class of laser beams those are having uniform irradiance over wider area of their cross sections.

In comparison to Gaussian beams, laser beams with uniform irradiance possess low divergence and thus can improve the efficiency of laser plasma coupling during ICF. Also, these beams can deliver high power densities to the fuel pellet without crossing the threshold for other parametric instabilities. Mathematically, such beam profiles are

modeled by super Gaussian or Q.G beam profiles. To the best of authors knowledge no earlier theoretical investigation on S.H.G of Q.G laser beams in plasmas has been reported in the past. This article aims to investigate for the first time generation of second harmonics of Q.G laser beams in collisional plasmas with density ramp.

10.2 Thermal Nonlinearity of Plasma with Density Ramp

Propagation of a laser beam with amplitude A_0 through a plasma dominated with collisional nonlinearity is governed by the wave equation

$$2ik_0\frac{\partial A_0}{\partial z}=\nabla_\perp^2 A_0+\frac{\omega_p^2(z)}{c^2}\left(1-\left(1+\frac{1}{2}\beta A_0A_0^*\right)^{\frac{s}{2}-1}\right)A_0 \tag{10.1}$$

Where, the symbols have the usual meaning as defined in chapter-1. The Lagrangian density corresponding to eq.(10.1) is

$$\pounds=i\left(A_0\frac{\partial A_0^*}{\partial z}-A_0^*\frac{\partial A_0}{\partial z}\right)+|\nabla_\perp A_0|^2-\frac{\omega_p^2(z)}{c^2}\int^{A_0A_0^*}\left(1-\left(1+\frac{1}{2}\beta A_0A_0^*\right)^{\frac{s}{2}-1}\right)d(A_0A_0^*) \tag{10.2}$$

In the present analysis we assume that the trial function $A_0(x,y,z)$ takes the form of quadruple-Gaussian ansatz

$$A_0A_0^\star=\frac{E_{00}^2}{f^2}\left[e^{-\frac{(x-x_0f)^2+y^2}{2r_0^2f^2}}+e^{-\frac{(x+x_0f)^2+y^2}{2r_0^2f^2}}+e^{-\frac{x^2+(y-x_0f)^2}{2r_0^2f^2}}+e^{-\frac{x^2+(y+x_0f)^2}{2r_0^2f^2}}\right]^2 \tag{10.3}$$

Substituting the above anstz in Lagrangian density and using variational analysis and upward ramp density $n=n_0(1+\tan(z/d))$ [172] (explained in chapter-4), the equation of motion of beam width of laser beam has been obtained as

$$\frac{d^2f}{d\xi^2}=\frac{1}{4f^3}\left[\frac{1+e^{-\frac{x_0^2}{r_0^2}}\left(1-\frac{x_0^2}{r_0^2}\right)+e^{-\frac{x_0^2}{2r_0^2}}\left(2-\frac{x_0^2}{r_0^2}\right)}{\left(2+2\frac{x_0^2}{r_0^2}\right)+\left(2+2\frac{x_0^2}{r_0^2}\right)e^{-\frac{x_0^2}{2r_0^2}}+2e^{-\frac{x_0^2}{r_0^2}}}\right]+\left[\frac{\frac{1}{2\pi}\left(\frac{\omega_{p0}r_0}{c}\right)^2\left(\frac{s}{2}-1\right)\frac{\beta E_{00}^2}{f^3}\left(1+tan\left(\frac{z}{d'}\right)\right)}{\left(2+2\frac{x_0^2}{r_0^2}\right)+\left(2+2\frac{x_0^2}{r_0^2}\right)e^{-\frac{x_0^2}{2r_0^2}}+2e^{-\frac{x_0^2}{r_0^2}}}\right](K_1+K_2+K_3+K_4) \tag{10.4}$$

Where,

$$K_1=\int_0^\infty\int_0^\infty t_1\left(t_1-\frac{x_0}{r_0}\right)e^{-\frac{\left(t_1-\frac{x_0}{r_0}\right)^2+t_2^2}{2}}\times G_1^3(t_1,t_2)G_2(t_1,t_2)dt_1dt_2$$

$$sK_2=\int_0^\infty\int_0^\infty t_1\left(t_1+\frac{x_0}{r_0}\right)e^{-\frac{\left(t_1+\frac{x_0}{r_0}\right)^2+t_2^2}{2}}\times G_1^3(t_1,t_2)G_2(t_1,t_2)dt_1dt_2$$

$$K_3=\int_0^\infty\int_0^\infty t_1^2e^{-\frac{t_1^2+\left(t_2-\frac{x_0}{r_0}\right)^2}{2}}\times G_1^3(t_1,t_2)G_2(t_1,t_2)dt_1dt_2$$

$$K_4 = \int_0^{\infty}\int_0^{\infty} t_1^2 e^{-\frac{t_1^2+\left(t_2+\frac{x_0}{r_0}\right)^2}{2}} \times G_1^3(t_1,t_2)G_2(t_1,t_2)dt_1dt_2$$

$$G_1(t_1,t_2) = e^{-\frac{\left(t_1-\frac{x_0}{r_0}\right)^2+t_2^2}{2}} + e^{-\frac{\left(t_1+\frac{x_0}{r_0}\right)^2+t_2^2}{2}} + e^{-\frac{t_1^2+\left(t_2-\frac{x_0}{r_0}\right)^2}{2}} + e^{-\frac{t_2^2+\left(t_2+\frac{x_0}{r_0}\right)^2}{2}}$$

$$G_2(t_1,t_2) = \left[1+\frac{\beta AA^*}{f^2}G_1^2(t_1,t_2)\right]^{-\frac{3}{2}}$$

$$t_1 = \frac{x}{r_0 f},\quad t_2 = \frac{y}{r_0 f}, \xi = \frac{z}{k_0 r_0^2}, d' = \frac{d}{k_0 r_0^2}$$

10.3 Current Density for SHG

In hydrodynamic model of plasma, the evolution of density perturbation of plasma associated with EPW excited by the laser beam evolves according to wave equation

$$\frac{\partial^2 n'}{\partial t^2} - v_{th}^2\nabla^2 n' + \omega_p^2 n' = \frac{e}{m}n_0\nabla \boldsymbol{E} \tag{10.5}$$

taking

$$n' = n'' e^{i(\omega_0 t - k_0 z)}$$

where n'' is the amplitude of EPW, one can obtain

$$-\omega_0^2 n' + k_0^2 v_{th}^2 n' + \omega_p^2 n' = \frac{e}{m}n_0\nabla E \tag{10.6}$$

Using eq. (10.3) in eq. (10.6), the source term for SHG of Q.G laser beam in collisional plasma is obtained as

$$n'' = \frac{en_0}{m}\frac{F(x,y)}{\left(\omega_0^2 - k_0^2 v_{th}^2 - \omega_{p0}^2\left(1+\tan\left(\frac{z}{d}\right)\right)\left(1+\frac{1}{2}\beta AA^*\right)^{\frac{S}{2}-1}\right)} \tag{10.7}$$

where

$$F(x,y) = \left[\frac{(x-x_0f)}{r_0^2f^2}e^{-\frac{(x-x_0f)^2+y^2}{2r_0^2f^2}} + \frac{(x+x_0f)}{r_0^2f^2}e^{-\frac{(x+x_0f)^2+y^2}{2r_0^2f^2}} + \frac{x}{r_0^2f^2}e^{-\frac{x^2+(y-x_0f)^2}{2r_0^2f^2}} + \frac{x}{r_0^2f^2}e^{-\frac{x^2+(y+x_0f)^2}{2r_0^2f^2}}\right.$$
$$+\frac{y}{r_0^2f^2}e^{-\frac{(x-x_0f)^2+y^2}{2r_0^2f^2}} + \frac{y}{r_0^2f^2}e^{-\frac{(x+x_0f)^2+y^2}{2r_0^2f^2}} + \frac{(y-x_0f)}{r_0^2f^2}e^{-\frac{x^2+(y-x_0f)^2}{2r_0^2f^2}}$$
$$\left.+\frac{(y+x_0f)}{r_0^2f^2}e^{-\frac{x^2+(y+x_0f)^2}{2r_0^2f^2}}\right]$$

The interaction of pump beam with EPW results in a nonlinear current density at frequency double of that of pump beam as

$$J_2 = \frac{e^2n_0A}{m\omega_0}\left(\frac{n''}{n_0}\right)e^{i(\omega_2 t - k_2 z)} \tag{10.8}$$

10.4 Generation of Second Harmonics

The current density given by eq.(10.8) act as a source of second harmonics of the incident beam. The generated harmonics are governed by eq.

$$\nabla^2 E_2 + \frac{\omega_2^2}{c^2}\varepsilon_2(\omega_2)E_2 = \frac{4\pi}{c^2}\frac{\partial J_2}{\partial t} \tag{10.9}$$

Using Eq. (10.8) in (10.9), the amplitude of the second harmonics is obtained as from above equation, the expression for field E_2 of second harmonic is obtained as

$$E_2 = \frac{\omega_p^2}{c^2}\frac{n''}{n_0}\frac{E_0}{(k_2^2 - 4k_0^2)} \tag{10.10}$$

Defining normalized power η of second harmonics in the same way as defined in chapter-9. We can get

$$\eta = \frac{4}{3}\frac{m}{M}\left(\frac{K_0 T_0}{mc^2}\right)\frac{\beta E_{00}^2}{f^4}H \tag{10.11}$$

where

$$H = \int_0^\infty \int_0^\infty \frac{F_2(t_1,t_2)}{\left[\frac{\omega_0^2 r_0^2}{c^2} - \frac{\varepsilon_0 v_{th}^2}{c^2}\frac{\omega_0^2 r_0^2}{c^2} - \frac{\omega_{p0}^2 r_0^2}{c^2}\left(1+\tan\left(\frac{\xi}{d'}\right)\right)\left(1+\frac{\beta E_{00}^2}{2f^2}G_1^2(t_1,t_2)\right)^{\frac{s}{2}-1}\right]^2} dt_1 dt_2$$

$$F_2(t_1,t_2) = \left[\left(t_1 - \frac{x_0}{r_0}\right)e^{-\frac{\left(t_1-\frac{x_0}{r_0}\right)^2+t_2^2}{2}} + \left(t_1+\frac{x_0}{r_0}\right)e^{-\frac{\left(t_1+\frac{x_0}{r_0}\right)^2+t_2^2}{2}} + t_1 e^{-\frac{t_1^2+\left(t_2-\frac{x_0}{r_0}\right)^2}{2}} + t_1 e^{-\frac{t_1^2+\left(t_2+\frac{x_0}{r_0}\right)^2}{2}}\right.$$

$$\left. + t_2 e^{-\frac{\left(t_1-\frac{x_0}{r_0}\right)^2+t_2^2}{2}} + t_2 e^{-\frac{\left(t_1+\frac{x_0}{r_0}\right)^2+t_2^2}{2}} + \left(t_2 - \frac{x_0}{r_0}\right)e^{-\frac{t_1^2+\left(t_2-\frac{x_0}{r_0}\right)^2}{2}} + \left(t_1 - \frac{x_0}{r_0}\right)e^{-\frac{t_1^2+\left(t_2+\frac{x_0}{r_0}\right)^2}{2}}\right]^2$$

10.5 Results and Discussion

Approximate solution of equation (10.4) has been obtained with the help of Runge Kutta fourth-order method for the following set of parameters:

$$\omega_0 = 1.78\times 10^{15} rad\, s^{-1}, \quad \lambda = 1.06\mu m, \qquad r_0 = 15\mu m, \; s = -3, \qquad d' = 10$$

by assuming that initially the beam is collimated, i.e., it satisfies the initial conditions $f = 1$ and $\frac{df}{d\xi} = 0$ at $\xi = 0$.

Figs. 10.1 and 10.2 depict the effect of $\frac{x_0}{r_0}$ on the evolution of beam width of the laser beam while propagating through collisional plasma. It is observed that increase in the value of $\frac{x_0}{r_0}$ for $0 \le \frac{x_0}{r_0} \le 1.5$ results in enhancement of self-focusing of the laser beam whereas

beyond $\frac{x_0}{r_0} = 1.5$ with increase in the value of $\frac{x_0}{r_0}$ the extent of self-focusing of the laser beam decreases. This is because for $0 \leq \frac{x_0}{r_0} \leq 1.5$ with increase in the value of $\frac{x_0}{r_0}$ the intensity distribution over the cross section of the laser beam becomes more and more uniform. As a consequence of which the laser beam gets equal contribution from the off axial parts for nonlinear refraction as provided by axial part. As the phenomenon of self focusing is a homeostasis of nonlinear refraction, increase in the value of $\frac{x_0}{r_0}$ in the range $0 \leq \frac{x_0}{r_0} \leq 1.5$ results in the enhancement of self-focusing of the laser beam.

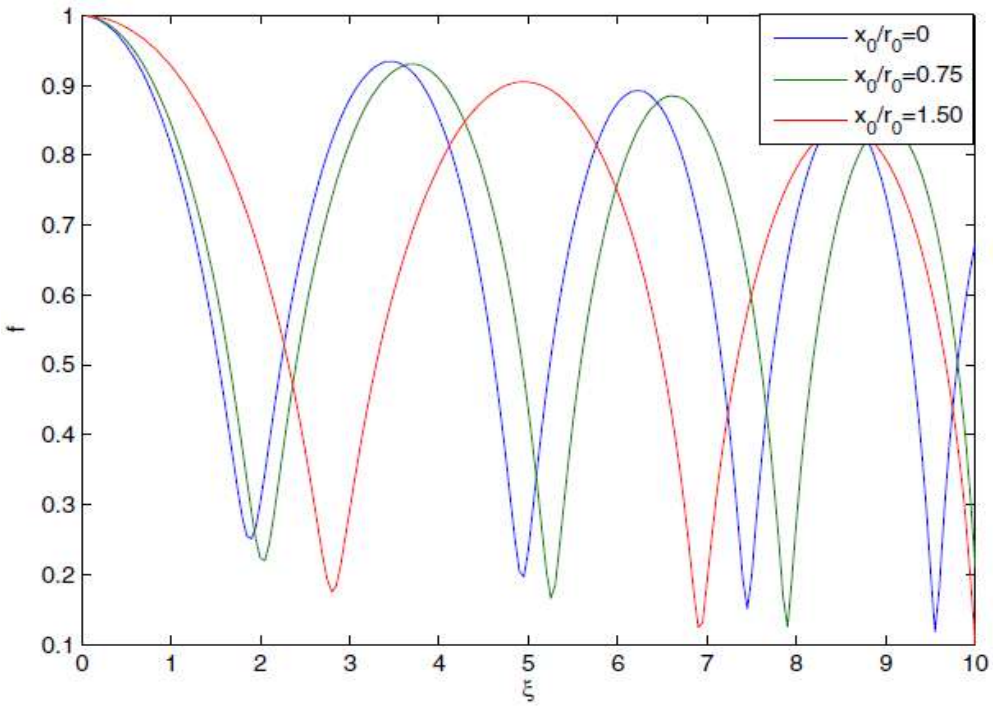

Fig. 10.1: Variation of beam width against the distance of propagation for different values of $\frac{x_0}{r_0}$ viz. $\frac{x_0}{r_0} = 0, 0.75, 1.50$ in plasma with density ramp

Decrease in the extent of self-focusing of the laser beam by increasing $\frac{x_0}{r_0}$ beyond 1.5 is because of the reason that for $\frac{x_0}{r_0} > 1.5$ the intensity maxima of individual Gaussian laser beams constituting the Q.G laser beams are so far away from each other that after superposition the intensity maxima of the resulting beam appear in the off axial parts. This makes paraxial part of the laser beam weaker as compared to off axial part and hence the

laser beam gets a very little contribution from the axial part for nonlinear refraction. This in turn leads to reduced focusing of the laser beam as shown in fig.10.2.

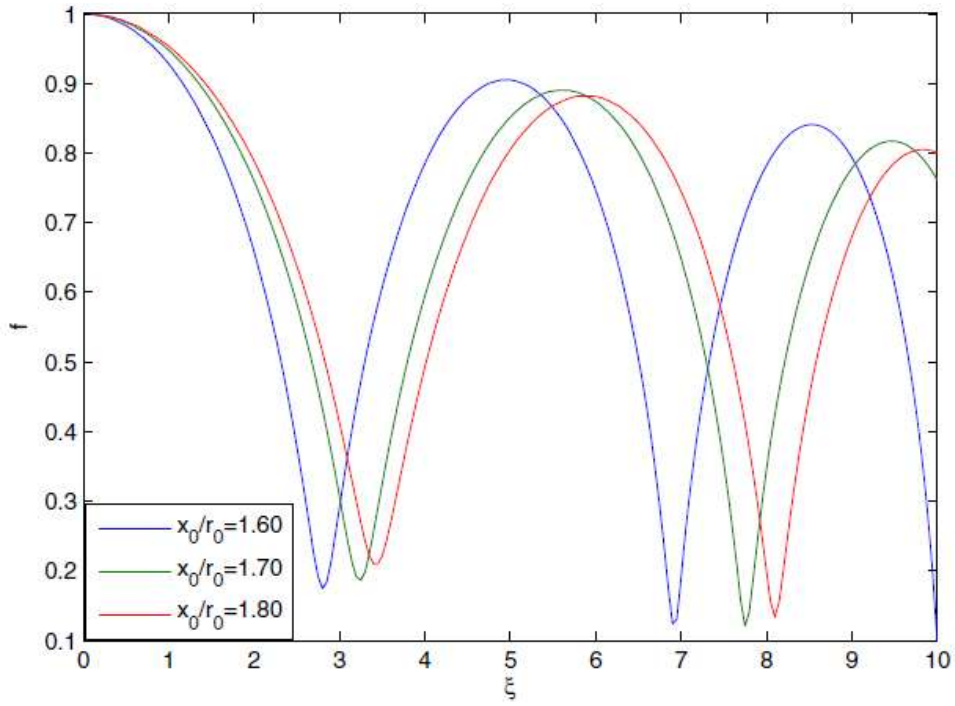

Fig. 10.2: Variation of beam width against the distance of propagation for different values of $\frac{x_0}{r_0}$ viz. $\frac{x_0}{r_0} = 1{:}60;\ 1{:}70;\ 1{:}80$ in plasma with density ramp

Fig. 10.3 illustrates the effect of initial beam intensity on self-focusing of the laser beam. It can be seen that with increase in the initial intensity of the laser beam, there is enhancement in the extent of self-focusing of the laser beam and also it becomes faster. This occurs because with increase in the intensity of pump beam, the kinetic energy of the plasma electrons increases that in turn increases the collisional nonlinearity via nonuniform Ohmic heating. Thus, increase in the laser intensity enhances the amount of focusing of the laser beam.

Equation (10.11) describes the evolution of normalized power of second harmonic power η with distance and has been solved numerically in association with eq. (10.4). The corresponding variations of the power of second harmonics have been depicted in figs.10.4, 10.5 and 10.6.

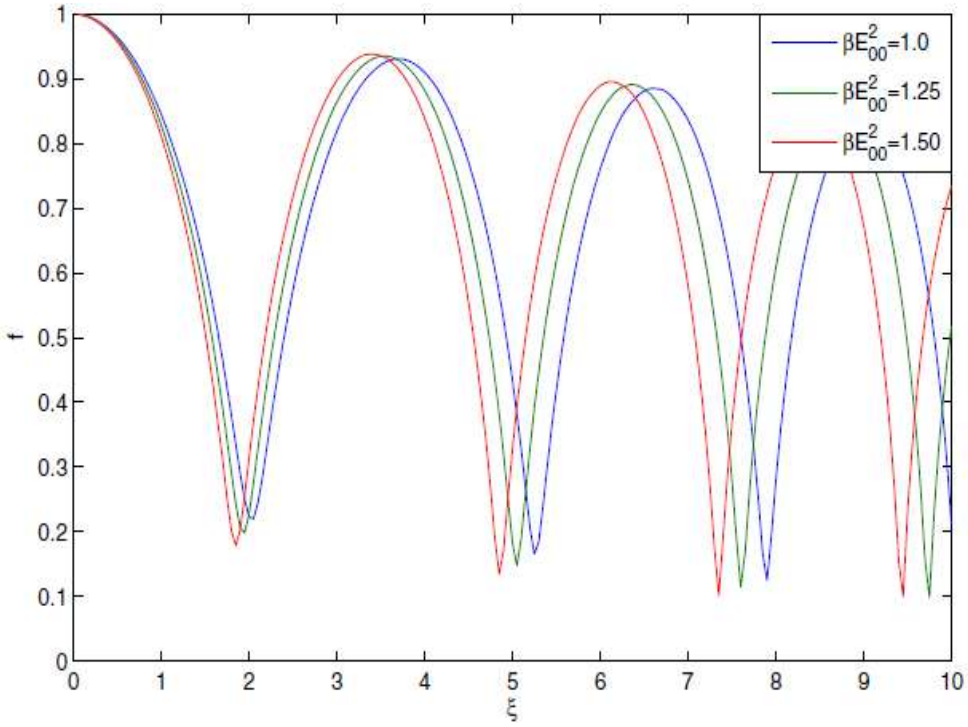

Fig. 10.3: Variation of beam width against the distance of propagation for different values of laser intensity viz. $\boldsymbol{\beta E_{00}^2 = 1;\ 1{:}25;\ 1{:}50}$ in plasma with density ramp

From the plots in fig. 10.4 it is observed that the laser beams with higher value of $\frac{x_0}{r_0}$ in the range $0 \leq \frac{x_0}{r_0} \leq 1.5$ produce second harmonics with higher power as compared to that produced by beams with lower value of $\frac{x_0}{r_0}$. This is due to one to one correspondence between extent of focusing and power of generated harmonics. As the pumps with larger value of $\frac{x_0}{r_0}$ in the range $0 \leq \frac{x_0}{r_0} \leq 1.5$ possess enhanced self-focusing, thus they produce harmonics with higher power. Similarly, as the extent of focusing of Q.G decreases (fig.10.5) with increasing the value of $\frac{x_0}{r_0}$ for $\frac{x_0}{r_0} > 1.5$, hence reduction in the power of second harmonics with increase in the value of $\frac{x_0}{r_0}$ for $\frac{x_0}{r_0} > 1.5$ is observed from fig. 10.5.

Figure 10.6 illustrates that with increase in the intensity of the pump beam the intensity of generated second harmonics increases. This is due to enhanced focusing of the pump beam by increasing its intensity.

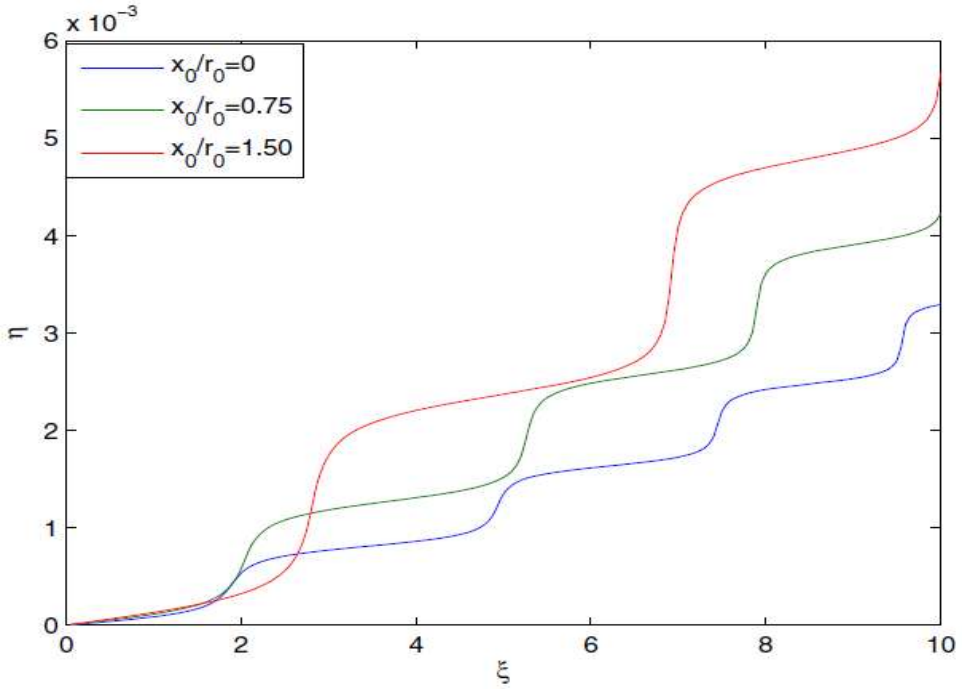

Fig.10.4: Variation of normalized power η of second harmonics against the distance of propagation for different values of $\frac{x_0}{r_0}$ viz. $\frac{x_0}{r_0} = 0, 0.75, 1.5$ in the plasma with density ramp.

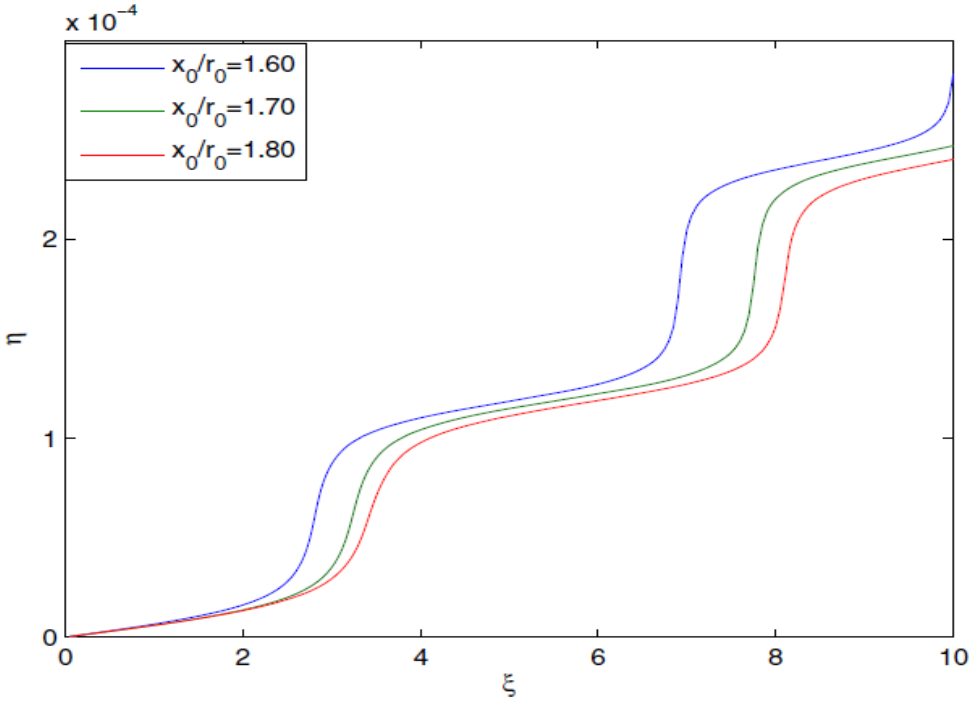

Fig. 10.5: Variation of normalized power η of second harmonics against the distance of propagation for different values of $\frac{x_0}{r_0}$ viz. $\frac{x_0}{r_0} = 1.60, 1.70, 1.80$ in the plasma with density ramp.

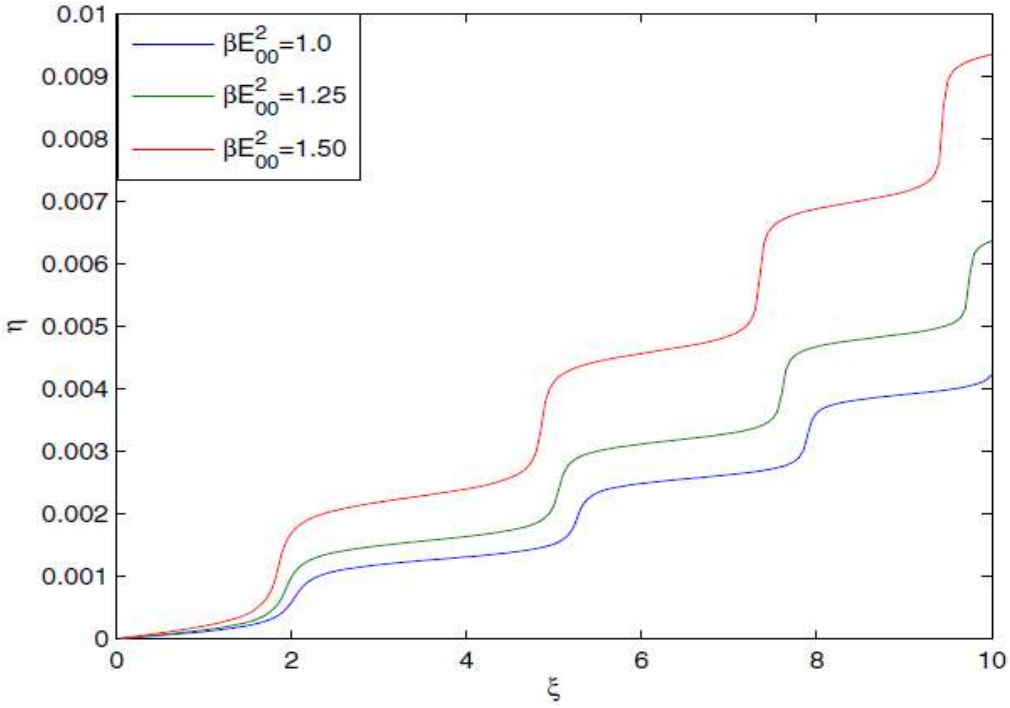

Fig. 10.6: Variation of normalized power η of second harmonics against the distance of propagation for different values of laser intensity viz. $\beta E_{00}^2 = 1, 1.25, 1.50$ in plasma with density ramp

10.6 Conclusions

In the present work, we have revealed the nonlinear characteristics of propagation of Q.G. laser beam in collisional plasma. It has been observed that one can control the self focusing by optimizing the laser and plasma parameters. Further, the effects of self focusing on second harmonic generation of Q.G. laser beam have been reported. It has been noted that the self focusing and efficiency of SHG can be maximum at normalized value 1.50 of the decentering parameter $\frac{x_0}{r_0}$. The results of this chapter can be applied in plasma diagnostics and inertial confinement fusion (ICF).

Chapter 11

THz Generation by Cross Focused Surface Plasma Waves

11.1 Introduction

The planar interface of two dissimilar materials plays a vital role in many optical phenomena [121, 122, 127]. In elementary optics, for instance, the interface between two optically rarer and denser media forms the principle of total internal reflection. Optical fibers based on this total internal reflection are now spanning the entire globe. Round the clock optical fibers are guiding light signals that convey voluminous streams of voice communications and vast amounts of data. Due to this gargantuan data carrying capacity of optical fibers some researchers believe that someday photonic devices (i.e., the devices based on manipulation of light or other electromagnetic waves) will entirely replace electronic devices i.e., transistors in microprocessors and other chips [195]. However, unfortunately the inherent wave property of light to get diffract puts a constraint on the size and performance of photonic devices. Due to the possibility of inference between two closely spaced light waves, the diameter of an optical fiber carrying them must be at least half the wavelength of light inside that material. The chips based on optical circuits, for example, most probably will be based on near infrared wavelength (1500 nm). Thus, the minimum width of the photonic device (750 nm) will be much larger than the smallest transistor (100 nm) those are currently in use.

During past few decades a new technique of transmitting electromagnetic waves known as surface plasma waves [120-126], through nanoscale structures has gained significant interest among researchers. Such a wave travels in a direction parallel to the interface but, on either side of the interface, its amplitude is minuscule after a certain distance from the interface. This localization is a propitious quality that is exploited, for example, in some extremely sensitive bio/chemical sensors. The present chapter is focused on the investigation on terahertz generation by two cross focused surface plasma waves propagating over semiconductor free space interface.

11.2 Cross Focusing of Surface Plasma Waves

Consider an interface formed between free space ($x > 0$) and a narrow band semiconductor ($x < 0$). The simultaneous propagation of two surface plasma waves over this interface is governed by equation [196]

$$2\iota k_j \frac{\partial A_j}{\partial z} + \frac{\partial^2 A_j}{\partial y^2} + \beta \phi_j (A_1 A_1^*, A_2 A_2^*) A_j \; ; j = 1,2 \tag{11.1}$$

where, A_1 and A_2 are the amplitudes of the two waves and ϕ_j is the nonlinear dielectric function of the interface for the j^{th} wave and

$$\beta = \frac{\int_{-\infty}^{0} e^{\alpha_2 x} dx}{\int_{0}^{\infty} e^{-\alpha_1 x} dx + \int_{-\infty}^{0} e^{\alpha_2 x} dx} \tag{11.2}$$

Here, α_1 and α_2 are the attenuation coefficients for the surface plasma waves above the interface and beneath the interface respectively.

is given by

$$\Phi_j (A_1 A_1^*, A_2 A_2^*) = \frac{\omega_{p0*}^2}{\omega_j^2} \left\{ 1 - \left(1 + \sum_j \frac{\beta_j E_{j0}^2}{f_j^2} \left(1 + \frac{r^2}{q_j r_j^2 f_j^2} \right)^{-q_j} \right)^{\frac{1}{2}} \right\} \tag{11.3}$$

The Lagrangian density for equation 11.1 is

$$\begin{aligned} £ = {} & i \left(A_1 \frac{\partial A_1^*}{\partial z} - A_1^* \frac{\partial A_1}{\partial z} \right) + i \left(A_2 \frac{\partial A_2^*}{\partial z} - A_2^* \frac{\partial A_2}{\partial z} \right) + |\nabla_\perp A_1|^2 + |\nabla_\perp A_1|^2 \\ & - \beta \frac{\omega_1^2}{c^2} \int^{A_1 A_1^*} \Phi (A_1 A_1^*, A_2 A_2^*) d(A_1 A_1^*) \\ & - \beta \frac{\omega_2^2}{c^2} \int^{A_2 A_2^*} \Phi (A_1 A_1^*, A_2 A_2^*) d(A_2 A_2^*) \end{aligned} \tag{11.4}$$

Substituting the trial function for q-Gaussian beam profile

$$A_j = \frac{E_{0j}}{\sqrt{f_j}} \left(1 + \frac{y^2}{q_j r_j^2 f_j^2} \right)^{-\frac{q_j}{2}} \tag{11.5}$$

in lagrangian density and integrating over the entire cross section of the laser beam we get the reduced lagrangian as $L = \int £ \, d^2 r$. The correspondingEuler-Lagrange equations

$$\frac{d}{dz} \left(\frac{dL}{\partial \left(\frac{\partial f_j}{\partial z} \right)} \right) - \frac{\partial L}{\partial f_j} = 0 \tag{11.6}$$

the set of coupled equations governing the evolution of beam width of surface plasma waves has been obtained as follows:

$$\frac{d^2f_1}{d\xi^2}+\frac{1}{f_1}\left(\frac{df_1}{d\xi}\right)^2=\frac{\left(1-\frac{1}{q_1}\right)\left(1-\frac{1}{q_1}\right)}{\left(1+\frac{1}{q_1}\right)}\frac{1}{f_1^3}-2\left(\frac{\omega_{p0*}r_1}{c}\right)^2\left(1-\frac{1}{q_1}\right)\left(1-\frac{2}{q_1}\right)J_1 \quad (11.7)$$

$$\frac{d^2f_2}{d\xi^2}+\frac{1}{f_2}\left(\frac{df_2}{d\xi}\right)^2=\left(\frac{r_1}{r_2}\right)^4\left(\frac{\omega_1}{\omega_2}\right)^2\left(\frac{\varepsilon_{01}}{\varepsilon_{02}}\right)\frac{\left(1-\frac{1}{q_2}\right)\left(1-\frac{1}{q_2}\right)}{\left(1+\frac{1}{q_2}\right)}\frac{1}{f_2^3}-2\left(\frac{\omega_{p0*}r_1}{c}\right)^2\left(1-\frac{1}{q_2}\right)$$
$$\times\left(1-\frac{2}{q_2}\right)J_2 \quad (11.8)$$

Where,

$$J_1=\frac{\beta_1E_{10}^2}{f_1^3}T_1+\frac{\beta_2E_{20}^2}{f_1^3}\left(\frac{r_1}{r_2}\right)^2\left(\frac{f_1}{f_2}\right)^4T_2$$

$$J_2=\frac{\beta_1E_{10}^2}{f_2^3}T_3+\frac{\beta_2E_{20}^2}{f_2^3}\left(\frac{r_1}{r_2}\right)^2\left(\frac{f_1}{f_2}\right)^4T_4$$

$$T_1=\int_0^\infty x^3\left(1+\frac{x^2}{q_1}\right)^{-2q_1-1}G(x)dx$$

$$T_2=\int_0^\infty x^3\left(1+\frac{x^2}{q_1}\right)^{-q_1}\left(1+\frac{x^2}{q_2}\left(\frac{r_1f_1}{r_2f_2}\right)^2\right)^{-q_2-1}G(x)dx$$

$$T_3=\int_0^\infty x^3\left(1+\frac{x^2}{q_1}\right)^{-q_1-1}\left(1+\frac{x^2}{q_2}\left(\frac{r_1f_1}{r_2f_2}\right)^2\right)^{-q_2}G(x)dx$$

$$T_4=\int_0^\infty x^3\left(1+\frac{x^2}{q_2}\left(\frac{r_1f_1}{r_2f_2}\right)^2\right)^{-2q_2-1}G(x)dx$$

$$G(x)=e^{-\left\{\frac{\beta_1E_{10}^2}{f_1^2}\left(1+\frac{x^2}{q_1}\right)^{-q_1}+\frac{\beta_2E_{20}^2}{f_2^2}\left(1+\frac{x^2}{q_2}\left(\frac{r_1f_1}{r_2f_2}\right)^2\right)^{-q_2}\right\}}$$

$$x=\frac{y}{r_1f_1}$$

11.3 Excitation of Electron Plasma Wave (EPW)

As the two SPWs with different frequencies are propagating simultaneously over the semiconductor free space interface, the electron oscillations of the plasma electrons under

the fields of the two waves also contain a frequency component equal to the difference of the frequencies of the two waves. The electron density perturbation n' associated with the excited EPW evolves according to the wave equation

$$\frac{\partial^2 n'}{\partial t^2} - v_{th}^2 \nabla^2 n' + \omega_p^2 n' = \frac{e}{m} n_0 \nabla \Sigma_j E_j \tag{11.9}$$

Taking

$$n' = n_1 e^{i(\omega t - kz)}$$

where, $\omega = \omega_2 - \omega_1$ and $k = k_2 - k_1$, we get the amplitude of density perturbation associated with plasma wave

$$n_1 = \frac{e n_0}{m} \frac{1}{\left(\omega_0^2 - k_0^2 v_{th}^2 - \omega_p^2\right)} \left[\frac{E_{10}}{r_1^2 f_1^3} \left(1 + \frac{r^2}{q_1 r_1^2 f_1^2}\right)^{-\frac{q_1}{2}-1} + \frac{E_{20}}{r_2^2 f_2^3} \left(1 + \frac{r^2}{q_2 r_2^2 f_2^2}\right)^{-\frac{q_1}{2}-1} \right] r \tag{11.10}$$

11.4 THz Generation

The density perturbation associated with excited EPW results in a nonlinear current density at frequency $\omega = \omega_2 - \omega_1$ that acts as source for the THz radiation. The generated current density is given by

$$J_T = \frac{e^2 n_0}{m_0^* \omega} \left(\frac{n_1}{n_0}\right) e^{i(\omega t - kz)} \left(E_1 + E_2\right) \tag{11.11}$$

The electric field of the resulting THz evolves according to the wave equation

$$\nabla^2 E_T = \frac{1}{c^2} \frac{\partial^2 E_T}{\partial t^2} + \frac{4\pi}{c^2} \frac{\partial J_T}{\partial t} \tag{11.12}$$

This equation gives the magnitude of electric field of THz radiation as

$$E_T = i \frac{\left(\frac{\omega_{p0}^2}{c^2}\right)}{\left(\frac{\omega^2}{c^2} - k^2\right)} \frac{n_1}{n_0} \left(E_1 + E_2\right) \tag{11.13}$$

Defining the normalized power of THz radiation as

$$P_T = \frac{\int_0^\infty E_T E_T^* r dr}{\int_0^\infty A_1 A_1^* r dr} \tag{11.14}$$

We get

$$P_T = \frac{\left(\frac{\omega_{p0}^2}{c^2}\right)^2}{\left(\frac{\omega^2}{c^2} - k^2\right)^2} \frac{\int \left(\frac{n_1}{n_0}\right)^2 (E_1 + E_2)^2 r dr}{\int A_1 A_1^* r dr} \tag{11.15}$$

Equation (11.15) gives the normalized power of the THz radiation produced by the SPWs while propagating through the plasma.

11.5 Results and Discussion

To analyze the effect of deviation of intensity distribution of laser beams from Gaussian distribution and plasma density on cross focusing of the laser beams eqs.(11.7), (11.8), (11.15) have been solved for following set of parameters:

$$\omega_1 = 1.758 \times 10^{14} rad\ s^{-1}, \quad \omega_2 = 1.75 \times 10^{14} rad\ s^{-1}, q_2 = 3$$

$$r_1 = 15\mu m, \quad r_2 = 16\mu m, \quad \beta_1 E_{10}^2 = 2, \quad \beta_2 E_{20}^2 = 1.5, \quad T_0 = 10^3 K, \frac{\omega_{p0}^2 r_1^2}{c^2} = 9$$

and for different values of $q_1$viz., $q_1 = (3,4,\infty)$

Fig.11.1 shows the effect of $q_1$on the power of THz radiation. It can be seen that the effect of increase in q_1 is to reduce the power of THz radiation. This means ideal Gaussian SPW are not suitable for the efficient generation of THz radiations.

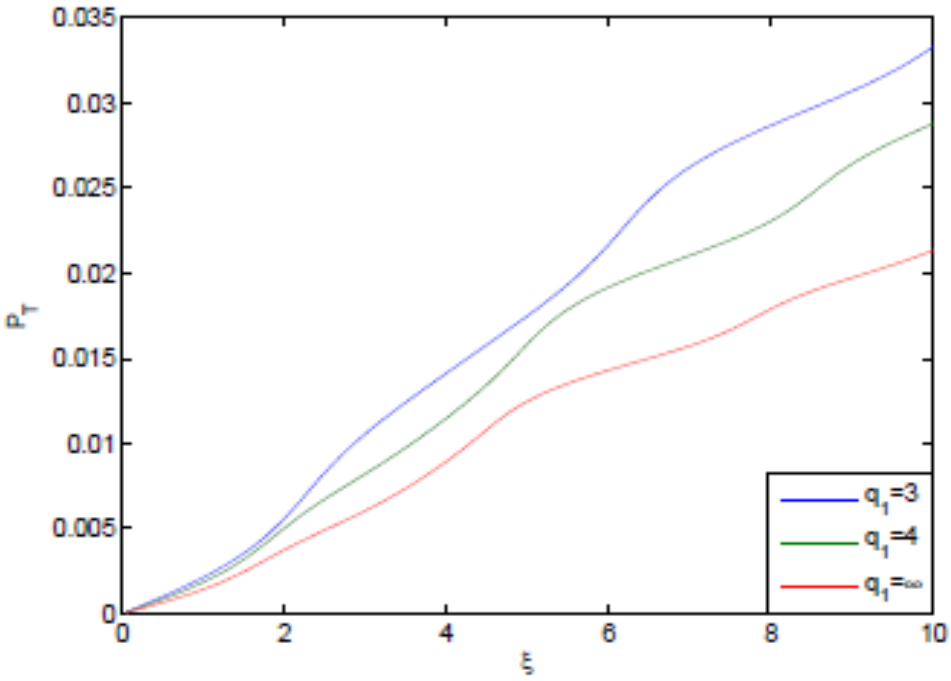

Fig.11.1: Effect of q_1 on power of THz radiation generated by SPW

11.6 Conclusions

The generation of THz radiation has been obtained with the help of surface plasma waves propagating over the semiconductor-free space interface. Firstly, the cross focusing of q-Gaussian SPW has been developed. The cross-focusing results in nonlinear current at difference frequency which act as a source of THz radiation. It has been observed that the power of generated THz radiation has been increased for $q_1 = q_2 = 3$ parameters. It indicates that an ideal Gaussian SPW are not suitable for the efficient generation of THz radiations.

Chapter-12

Conclusion and Future Scopes

12.1 Conclusion

In present work, I have investigated analytically and numerically (i) self-action effects of various laser beams such as q-Gaussian, Quadruple-Gaussian (Q.G) and Cosh-Gaussian laser beams through different nonlinear media (ii) Impacts of self-action effects of different laser beams on the higher harmonics and THz generations. The main emphasis is given to enhance the intensity of laser, HHG and THz generation. I have explored the chances to enhance the yield of HHG and THz generation by optimizing laser and plasma parameters.

1) Conclusions of self-action effects of the present thesis work is summarized as:
   It has been depicted that self focusing of laser beam can be enhanced by including the contribution of off-axial intensity of laser beam and ramped density plasma.
   a) In case of q-Gaussian laser beam, the maximum self focusing is achieved for $q = 3$ by considering the off-axial rays into account which enhances the nonlinearities of plasma. Whereas, for elliptical q-Gaussian laser beam, it has been revealed that with increase in the ellipticity, diffraction effect starts dominating. Therefore, the self focusing is decreased for higher ellipiticity of elliptical q-Gaussian laser beam.
   b) In case of Cosh-Gaussian laser beam, self focusing of laser beam can be enhanced by optimizing the decentered parameter of the laser beam. The self focusing of Cosh-Gaussian laser beam can be maximized by increasing the decentered parameter (b) from 0 to 1. The collisions of the constituents of plasma with each other decreases the self focusing of Cosh-Gaussian laser beam in collisional plasma, even collisions of electrons with diatomic molecules $(s = 2)$ vanishes the self focusing of Cosh-Gaussian laser beam.

c) In case of Q.G. laser beam, the diffraction broadening of Q.G. laser beam can be controlled as compare to Gaussian laser beam. The self focusing of the Q.G. laser beam can be maximized by controlling the $\frac{x_0}{r_0}$ values. As the value of $\frac{x_0}{r_0}$ is increased from 0 to 1.50 the self focusing is enhanced and when we increase the values from 1.60 to 1.80 the self focusing starts decreasing. The phase shift of the Q.G. laser beam decreases monotonocally as the values of $\frac{x_0}{r_0}$ is increased from 0 to 1.50. Whereas, reverse nature of self focusing and phase shift is observed when $\frac{x_0}{r_0}$ is increased from 1.50 to 1.80. The phase shift plots show the step like behavior at the minimum beam width distance.

2) In the present thesis work on THz generation, beating of two laser beams scheme has been adopted. To obtain efficient THz radiation, relativistic plasma and narrow band gap semiconductor have been chosen. It is concluded that
   a) Resonant THz generation is highly dependent on the relativistic self focusing. It is observed that the relativistic self focusing is increased with increase in plasma density, therefore yield of THz generation is increased.
   b) THz radiation with good efficiency can be achieved by beating of two laser beams under the effect of relativistic nonlinearity of the plasma.
   c) Excitation of electron plasma wave is a remarkable property of plasma that is used for THz generations.
   d) Enhancement in brightness of filamentation of q-Gaussian laser beam increases the THz generation.
   e) It has been observed that the ideal Gaussian SPWs are not suitable for the efficient generation of THz radiations.
3) Conclusions of HHG of the present thesis work is summarized as:
   a) The second harmonics generation can be achieved by propagating q-Gaussian laser beam in collisional plasma with density ramp. The density ramp of plasma participate to enhance the self focusing of q-Gaussian laser beam. Therefore, the intensity of laser beam is increased which enhances the conversion efficiency of

SHG. The yield of SHG is increased monotonically as we include the off-axial rays of cross section of laser beam because the off-axial intensity increases the nonlinearity of plasma. The increase in initial intensity or initial density the yield of SHG is enhanced.

b) In the case of Quadruple-Gaussian laser beam, the self focusing and yield of the SHG is maximum at normalized value 1.50 of the $\frac{x_0}{r_0}$. Further, the self focusing and yield of SHG is enhanced as the density of the plasma is increased.

12.2 Future Scopes

Different projects such as plasma-based electron accelerator [7], inertial confinement plasma (ICF) [3, 6], tabletop THz source [18], etc. are going on for serving society. These projects are dependent on (i) lasers having uniform irradiance over cross-sections of their spot size (ii) highly intense laser beam. In the present research work, I have provided different models for (a) q-Gaussian laser beam (b) cosh-Gaussian laser beam (c) quadruple-Gaussian laser beams for achieving these two main prerequisites for different laser beams.

I have reported theoretically and numerically that the intensity and region for uniform intensity can be enhanced for q-Gaussian, cosh-Gaussian, and Q.G. laser beams. I have reported that wide uniform intensity regime over cross-section for parameters $b = 1$ and $\frac{x_0}{r_0} =$ 1.5 of cosh-Gaussian and Q.G. laser beam respectively. In achieving ICF, among different challenges, the primary one is delivering uniform energy to the target for which laser beams must be precise and smooth laser. The outcomes of the present work may help in achieving the uniform heating of the target.

Nowadays, THz radiation is of great experimental and theoretical interest because of its non-ionizing character and penetrating power. The present work can generate THz with yield nearly 0.045 for $q_1 = 3$ and $q_2 = \infty$. The off-axial intensity of the beams play vital role which enhance the THz yield. These radiations can be further useful for THz spectroscopy, security, and communication purposes.

I have reported the generation of EPW for q-Gaussian and Q.G. laser beams in collisional plasma with ramp density. It has been reported that maximum electric field can be

obtained for $q = 3$ and $\frac{x_0}{r_0} = 1.5$ of q-Gaussian and Q.G. laser beams. The plasma based electron acceleration project depends upon the electric field of EPW. Hence, the achieved results of EPW may be used for electron trapping mechanism.

References

1] Maiman, T.H., 1960. Stimulated optical radiation in ruby. *Nature*, 493-494.

2] Steinmeyer, G., Sutter, D. H., Gallmann, L., Matuschek, N., & Keller, U. (1999). Frontiers in ultrashort pulse generation: pushing the limits in linear and nonlinear optics. Science. *Frontier in optics*, **286**, 1507-1512.

3] Haines, M. G. (1997). Review of inertial confinement fusion. *Astrophysics and space science,* **256**, 125-139.

4] Singh, V. K., & Rai, A. K. (2011). Prospects for laser-induced breakdown spectroscopy for biomedical applications: a review. *Lasers in medical science,* **26,** 673-687.

5] Mourou, G. (1997). The ultrahigh-peak-power laser: present and future. *applied Physics B*, **65**, 205-211.

6] Tabak, M., Hammer, J., Glinsky, M.E., Kruer, W.L., Wilks, S.C., Woodworth, J., Campbell, E.M., Perry, M.D. and Mason, R.J. (1994). Ignition and high gain with ultrapowerful lasers. *Physics of Plasmas,* **1**, 1626-1634.

7] Tajima, T., & Dawson, J. M. (1979). Laser electron accelerator. *Physical Review Letters,* **43,** 267.

8] Jaroszynski, D.A., Bingham, R., Brunetti, E., Ersfeld, B., Gallacher, J., van Der Geer, B., Issac, R., Jamison, S.P., Jones, D., De Loos, M. and Lyachev, A. (2006). Radiation sources based on laser–plasma interactions. *Philosophical Transactions of the Royal Society A: Mathematical, Physical and Engineering Sciences,* **364,** 689-710.

9] Strickland, D., & Mourou, G. (1985). Compression of amplified chirped optical pulses. *Optics communications*, **55**, 447-449.

10] Pessot, M., Squier, J., Mourou, G., & Harter, D. J. (1989). Chirped-pulse amplification of 100-fsec pulses. *Optics letters*, **14**, 797-799.

11] Danson, C., Hillier, D., Hopps, N., & Neely, D. (2015). Petawatt class lasers worldwide. *High power laser science and engineering,* **3**, 1-14.

12] Danson, C.N., Haefner, C., Bromage, J., Butcher, T., Chanteloup, J.C.F., Chowdhury, E.A., Galvanauskas, A., Gizzi, L.A., Hein, J., Hillier, D.I. and Hopps, N.W. (2019). Petawatt and exawatt class lasers worldwide. *High Power Laser Science and Engineering*, **7**,1-54.

13] Tajima, T., & Mourou, G. (2002). Zettawatt-exawatt lasers and their applications in ultrastrong-field physics. *Physical Review Special Topics-Accelerators and Beams*, **5**, 031301.

14] Umstadter, D. P., Barty, C., Perry, M., & Mourou, G. A. (1998). Tabletop, ultrahigh-intensity lasers: dawn of nonlinear relativistic optics. *Optics and Photonics News*, **9**, 40.

15] Akhmanov, S. A., Sukhorukov, A. P., & Khokhlov, R. V. (1968). Self-focusing and diffraction of light in a nonlinear medium. *Soviet physics USPEKHI*, **10**, 609.

16] HORA, H., HOELSS, M., SCHEID,W.,WANG, J.W., HO, Y.K., OSMAN, F. &CASTILLO, R. (2000). Principle of high accuracy for the nonlinear theory of the acceleration of ICFs in a vacuum by lasers at relativistic intensities. *Laser Part. Beams* **18**, 135–144.

17] MacGowan, B.J., Maxon, S., Hagelstein, P.L., Keane, C.J., London, R.A., Matthews, D.L., Rosen, M.D., Scofield, J.H. and Whelan, D.A. (1987). Demonstration of soft x-ray amplification in nickel-like ions. *Physical review letters*, **59**, 2157.

18] Liao, G.Q., Li, Y.T., Li, C., Liu, H., Zhang, Y.H., Jiang, W.M., Yuan, X.H., Nilsen, J., Ozaki, T., Wang, W.M. and Sheng, Z.M. (2016). Intense terahertz radiation from relativistic laser–plasma interactions. *Plasma Physics and Controlled Fusion*, **59**,014039.

19] Ganeev, R. A. (2007). High-order harmonic generation in a laser plasma: a review of recent achievements. *Journal of Physics B: Atomic, Molecular and Optical Physics*, **40**, R213.

20] Teubner, U., & Gibbon, P. (2009). High-order harmonics from laser-irradiated plasma surfaces. *Reviews of Modern Physics*, **81**, 445.

21] Sodha, M. S., & Kaw, P. K. (1966). Nonlinear Sum and Difference Frequency Generation in an Inhomogeneous Plasma. *The Physics of Fluids*, ***9***, 603-614.

22] Askaryan, G.A. (1962). Effects of the gradient of strong electromagnetic beam on electrons and atoms. *Soviet Phys.JETP* **15**, 1088–1092

23] Hafez, H. A., Chai, X., Ibrahim, A., Mondal, S., Férachou, D., Ropagnol, X., & Ozaki, T. (2016). Intense terahertz radiation and their applications. *Journal of Optics*, **18**, 093004.

24] Chiao, R. Y., Garmire, E., & Townes, C. H. (1965). Self-Trapping of Optical Beams. *Physical Review Letters*, 14, 1056.

25] Sodha, M.S., Ghatak, A.K. & Tripathi, V.K. (1976). Self focusing of laser beams in plasmas and semiconductors. *Progress in Optics. Amsterdam: North Holland,Amsterdam*, **13**, 169–265.

26] Max, C. E. (1976). Strong self-focusing due to the ponderomotive force in plasmas. *The Physics of Fluids*, 19, 74-77.

27] Wang, Y., Liang, Y., Yao, J., Yuan, C., & Zhou, Z. (2018). Nonlinear propagation characteristics of multi-Gaussian beams in collisionless plasmas. *JOSA B*, **35**, 3088-3093.

28] Perkins, F. W., & Valeo, E. J. (1974). Thermal self-focusing of electromagnetic waves in plasmas. *Physical Review Letters*, **32**, 1234.

29] El Sayed, A., El Badawy, N., Mohamed, S., El Halafawy, F.Z.: Self-focusing of powerful CO2-laser beams in collisional plasmas. *J. Opt. Soc. Am.* **72**, 1393–1397 (1982)

30] Gupta, D. N., Islam, M. R., Jang, D. G., Suk, H., & Jaroszynski, D. A. (2013). Self-focusing of a high-intensity laser in a collisional plasma under weak relativistic-ponderomotive nonlinearity. *Physics of Plasmas*, ***20***, 123103.

31] Akhiezer, A.I. & Polovin, R.V. (1956). Theory of wave motion of an electron plasma. *Sov. Phys.–JETP* **, 3**, 696–705.

32] Singh, A., & Walia, K. (2010). Relativistic self-focusing and self-channeling of Gaussian laser beam in plasma. *Applied Physics B*, **101,** 617-622.

33] Hora, H. (1975). Theory of relativistic self-focusing of laser radiation in plasmas. *JOSA*, **65**, 882-886.

34] Stegeman, G. I., & Segev, M. (1999). Optical spatial solitons and their interactions: universality and diversity. *Science*, **286**, 1518-1523.

35] Brandi, H. S., Manus, C., Mainfray, G., Lehner, T., & Bonnaud, G. (1993). Relativistic and ponderomotive self-focusing of a laser beam in a radially inhomogeneous plasma. I. Paraxial approximation. *Physics of Fluids B: Plasma Physics*, **5**, 3539-3550.

36] Gupta, R., Sharma, P., Rafat, M., & Sharma, R. P. (2011). Cross-focusing of two hollow Gaussian laser beams in plasmas. *Laser and Particle Beams*, ***29***, 227-230.

37] Lam, J. F., Lippmann, B., & Tappert, F. (1977). Self-trapped laser beams in plasma. *The Physics of Fluids*, **20**, 1176-1179.

38] Anderson, D. (1978). Stationary self-trapped laser beams in plasma. *Physica Scripta*, **18**, 35.

39] Sodha, M. S., Sharma, J. K., Tewari, D. P., Sharma, R. P., & Kaushik, S. C. (1978). Plasma wave and second harmonic generation. *Plasma Physics*, **20**, 825.

40] Helk, T., Berger, E., Jamnuch, S., Hoffmann, L., Kabacinski, A., Gautier, J., Tissandier, F., Goddet, J.P., Chang, H.T., Oh, J. and Pemmaraju, C.D. (2021). Table-top extreme ultraviolet second harmonic generation. *Science Advances*, **7**, 2265.

41] Franken, E. P., Hill, A. E., Peters, C. W., & Weinreich, G. (1961). Generation of optical harmonics. *Physical Review Letters*, **7**, 118.

42] Franken, P. A., & Ward, J. F. (1963). Optical harmonics and nonlinear phenomena. *Reviews of Modern Physics*, **35**, 23.

43] Bloembergen, N., & Pershan, P. S. (1962). Light waves at the boundary of nonlinear media. *Physical review*, ***128***, 606.

44] Gibbon, P. (1997). High-order harmonic generation in plasmas. *IEEE Journal of Quantum Electronics*, **33**, 1915-1924.

45] Chen, F. F. (2012). Introduction to plasma physics. *Springer Science & Business Media.*

46] Engers, T., Fendel, W., Schüler, H., Schulz, H., & Von der Linde, D. (1991). Second-harmonic generation in plasmas produced by femtosecond laser pulses. *Physical Review A*, **43,** 4564.

47] Hu, K., Yi, L., & Fülöp, T. (2021). Multimillijoule terahertz radiation from laser interactions with microplasma waveguides. *Plasma Physics and Controlled Fusion*, **63**, 035028.

48] Nikitkina, A.I., Bikmulina, P.Y., Gafarova, E.R., Kosheleva, N.V., Efremov, Y.M., Bezrukov, E.A., Butnaru, D.V., Dolganova, I.N., Chernomyrdin, N.V., Cherkasova, O.P. and Gavdush, A.A. (2021). Terahertz radiation and the skin: a review. *Journal of Biomedical Optics*, **26**, 043005.

49] Gente, R., & Koch, M. (2015). Monitoring leaf water content with THz and sub-THz waves. *Plant methods*, **11**, 1-9.

50]. Son, J. H., Oh, S. J., & Cheon, H. (2019). Potential clinical applications of terahertz radiation. *Journal of Applied Physics*, **125**, 190901.

51] Yang, X., Zhao, X., Yang, K., Liu, Y., Liu, Y., Fu, W., & Luo, Y. (2016). Biomedical applications of terahertz spectroscopy and imaging. *Trends in biotechnology*, **34**, 810-824.

52] Tripathi, V. K., & Liu, C. S. (1990). Plasma effects in a free electron laser. *IEEE transactions on plasma science*, *18*, 466-471.

53] Sharifian, M., Sharifinejad, H. R., & Golbakhsi, H. (2014). Terahertz wave generation by beating of two spatial-Gaussian lasers in collisional plasma. *Journal of Plasma Physics*, **80**, 453-463.

54] Askari, H. R., & Zarezadeh, J. (2011). Effect of a wiggler magnetic field on the sum frequency generation in laser–plasma interactions. *Optics & Laser Technology*, **43,** 173-178.

55] Kelley, P. L. (1965). Self-focusing of optical beams. *Physical Review Letters*, **15,** 1005.

56] Piekara, A. H., Moore, J. S., & Feld, M. S. (1974). Analysis of self-trapping using the wave equation with high-order nonlinear electric permittivity. *Physical Review A*, **9**, 1403.

57] Hora, H. (1969). Self-focusing of laser beams in a plasma by ponderomotive forces. *Zeitschrift für Physik A Hadrons and nuclei*, **226**, 156-159.

58] Sodha, M. S., Sinha, S. K., & Sharma, R. P. (1979). The self-focusing of laser beams in magnetoplasmas: the moment theory approach. *Journal of Physics D: Applied Physics*, **12**, 1079.

59] Mori, W. B., Joshi, C., Dawson, J. M., Forslund, D. W., & Kindel, J. M. (1988). Evolution of self-focusing of intense electromagnetic waves in plasma. *Physical review letters*, **60**, 1298.

60] Anderson, D., & Bonnedal, M. (1979). Variational approach to nonlinear self-focusing of Gaussian laser beams. *The Physics of Fluids*, **22,** 105-109.

61] Anderson, D., Bonnedal, M., & Lisak, M. (1979). Self-trapped cylindrical laser beams. *The Physics of Fluids*, **22,** 1838-1840.

62] Anderson, D. (1981). Self-trapping of intense laser beams. *The Physics of Fluids*, **24,** 2345-2347.

63] Chen, Y. (1991). Self-trapped light in saturable nonlinear media. *Optics letters*, ***16***, 4-6.

64] Desaix, M., Anderson, D., & Lisak, M. (1991). Variational approach to collapse of optical pulses. *JOSA B*, **8,** 2082-2086.

65] Karlsson, M., & Anderson, D. (1992). Super-Gaussian approximation of the fundamental radial mode in nonlinear parabolic-index optical fibers. *JOSA B*, **9**, 1558-1562.

66] Karlsson, M. (1992). Optical beams in saturable self-focusing media. *Physical Review A*, **46,** 2726.

67] Dimitrevski, K., Reimhult, E., Svensson, E., Öhgren, A., Anderson, D., Berntson, A., Lisak, M. and Quiroga-Teixeiro, M.L.(1998). Analysis of stable self-trapping of laser beams in cubic-quintic nonlinear media. *Physics Letters A*, **248**,369-376.

68] Chen, R.P. and Wang, H.T. (2010). Propagation of Laguerre–Gaussian beams in cubic–quintic nonlinear media by variational approach. *Optics & Laser Technology*, **42**, 1318-1322.

69] Nanda, V., Kant, N., & Wani, M. A. (2013). Sensitiveness of decentered parameter for relativistic self-focusing of Hermite-cosh-Gaussian laser beam in plasma. *IEEE Transactions on Plasma Science*, **41**, 2251-2256.

70] Ianetz, D., Kaganovskii, Y., Wilson-Gordon, A. D., & Rosenbluh, M. (2010). Propagation of an asymmetric Gaussian beam in a nonlinear absorbing medium. *Physical Review A*, **81**, 053851.

71] Wani, M. A., & Kant, N. (2016). Self-Focusing/Defocusing of Chirped Gaussian Laser Beam in Collisional Plasma with Linear Absorption. *Communications in Theoretical Physics*, ***66***, 349.

72] Gupta, N. and Singh, A. (2019). Dynamics of quadruple laser beams in collisionless plasmas. *Waves in Random and Complex Media*, **29**, 1-18.

73] Gupta, N. (2018). Self-action effects of quadruple-Gaussian laser beam in media possessing cubic–quintic nonlinearity. *Journal of Electromagnetic Waves and Applications*, **32**, 2350-2366.

74] Purohit, G., Gaur, B., Rawat, P. (2016). Propagation of two intense cosh-Gaussian laser beams in plasma in the relativistic-ponderomotive regime. *J. Opt. Soc. Am. B*, **33**, 1716–1722.

75] Kaur, S., Kaur, M., Kaur, R. and Gill, T.S. (2017). Propagation characteristics of Hermite-cosh-Gaussian laser beam in a rippled density plasmas. *Laser and Particle Beams*, **35**, 100-107.

76] Yadav, M., Gupta, D. N., & Sharma, S. C. (2020). Electron plasma wave excitation by a q-Gaussian laser beam and subsequent electron acceleration. *Physics of Plasmas,* **27,** 093106.

77] Walia, K., & Singh, A. (2021). Non-linear interaction of Cosh-Gaussian beam in thermal quantum plasma under combined influence of relativistic-ponderomotive force. *Optik*, **247**, 167867.

78] Kant, N., & Thakur, V. (2021). Enhanced self-focusing of Laguerre-Gaussian laser beam in relativistic plasma under exponential plasma density transition. *Chinese Journal of Physics*, ***70,*** 182-187.

79] Bobin, J. L., Decroisette, M., Meyer, B., & Vitel, Y. (1973). Harmonic generation and parametric excitation of waves in a laser-created plasma. *Physical Review Letters*, ***30***, 594.

80] Burnett, N. H., Baldis, H. A., Richardson, M. C., & Enright, G. D. (1977). Harmonic generation in CO2 laser target interaction. *Applied Physics Letters*, ***31***, 172-174.

81] Sprangle, P., Esarey, E. and Ting, A., 1990. Nonlinear theory of intense laser-plasma interactions. *Physical review letters*, 64, 2011.

82] Rax, J. M., & Fisch, N. J. (1992). Third-harmonic generation with ultrahigh-intensity laser pulses. *Physical review letters*, ***69,*** 772.

83] Parashar, J., & Pandey, H. D. (1992). Second-harmonic generation of laser radiation in a plasma with a density ripple. *IEEE transactions on plasma science*, **20**, 996-999.

84] Esarey, E., Ting, A., Sprangle, P., Umstadter, D., & Liu, X. (1993). Nonlinear analysis of relativistic harmonic generation by intense lasers in plasmas. *IEEE transactions on plasma science*, **21**, 95-104.

85] Malka, V., Modena, A., Najmudin, Z., Dangor, A.E., Clayton, C.E., Marsh, K.A., Joshi, C., Danson, C., Neely, D. and Walsh, F.N. (1997). Second harmonic generation and its interaction with relativistic plasma waves driven by forward Raman instability in underdense plasmas. *Physics of Plasmas*, **4**, 1127-1131.

86] Jha, P., Mishra, R. K., Raj, G., & Upadhyay, A. K. (2007). Second harmonic generation in laser magnetized–plasma interaction. *Physics of plasmas*, **14,** 053107.

87] Rajput, J., Kant, N., Singh, H., & Nanda, V. (2009). Resonant third harmonic generation of a short pulse laser in plasma by applying a wiggler magnetic field. *Optics communications*, ***282***, 4614-4617.

88] Singh, A., & Walia, K. (2011). Self-focusing of Gaussian laser beam through collisionless plasmas and its effect on second harmonic generation. *Journal of fusion energy*, **30**, 555-560.

89] Singh, A., & Walia, K. (2011). Self-focusing of laser beam in collisional plasma and its effect on Second Harmonic generation. *Laser and Particle Beams*, ***29,*** 407-414.

90] Singh, A., & Gupta, N. (2014). Higher harmonic generation by self-focused q-Gaussian laser beam in preformed collisionless plasma channel. *Laser and Particle Beams*, ***32***, 621-629.

91] Singh, A., & Gupta, N. (2015). Second harmonic generation by relativistic self-focusing of q-Gaussian laser beam in preformed parabolic plasma channel. *Physics of Plasmas*, ***22***, 013102.

92] Singh, A., & Gupta, N. (2016). Second-harmonic generation by relativistic self-focusing of cosh-Gaussian laser beam in underdense plasma. *Laser and Particle Beams*, **34,** 1-10.

93] Gupta, N., Singh, N., & Singh, A. (2015). Second harmonic generation of q-Gaussian laser beam in preformed collisional plasma channel with nonlinear absorption. *Physics of Plasmas*, ***22***, 113106.

94]Singh, N., Gupta, N., & Singh, A. (2016). Second harmonic generation of Cosh-Gaussian laser beam in collisional plasma with nonlinear absorption. *Optics Communications*, ***381***, 180-188.

95] Bhatia, A., Walia, K., & Singh, A. (2021). Second harmonic generation of intense Laguerre-Gaussian beam in relativistic plasma having an exponential density transition. *Optik*, **244**, 167608.

96] Pathak, N., Agarwal, P. C., Gill, T. S., & Kaur, S. (2021). Dynamics of resonant self-focusing on second harmonic generation of Gaussian laser beam in a rippled density plasma. *Contributions to Plasma Physics*, ***61***, e202100031.

97] Hamster, H., Sullivan, A., Gordon, S., White, W., & Falcone, R. W. (1993). Subpicosecond, electromagnetic pulses from intense laser-plasma interaction. *Physical review letters*, **71**, 2725.

98] Hamster, H., Sullivan, A., Gordon, S., & Falcone, R. W. (1994). Short-pulse terahertz radiation from high-intensity-laser-produced plasmas. *Physical Review E*, **49**, 671.

99] Leemans, W.P., Van Tilborg, J., Faure, J., Geddes, C.G.R., Tóth, C., Schroeder, C.B., Esarey, E., Fubiani, G. and Dugan, G. (2004). Terahertz radiation from laser accelerated electron bunches. *Physics of plasmas*, **11,** 2899-2906.

100] Antonsen Jr, T. M., Palastro, J., & Milchberg, H. M. (2007). Excitation of terahertz radiation by laser pulses in nonuniform plasma channels. *Physics of plasmas*, 14, 033107.

101] Bhasin, L., Tripathi, D., Uma, R., & Tripathi, V. K. (2011). Laser beat wave terahertz generation in a clustered plasma in an azimuthal magnetic field. *Physics of Plasmas*, **18,** 053109.

102] Malik, A. K., Malik, H. K., & Nishida, Y. (2011). Terahertz radiation generation by beating of two spatial-Gaussian lasers. *Physics Letters A*, **375**, 1191-1194.

103] Malik, A. K., Malik, H. K., & Stroth, U. (2012). Terahertz radiation generation by beating of two spatial-Gaussian lasers in the presence of a static magnetic field. *Physical Review E*, **85**, 016401.

104] Malik, H. K., & Malik, A. K. (2012). Strong and collimated terahertz radiation by super-Gaussian lasers. *EPL (Europhysics Letters)*, **100,** 45001.

105] Varshney, P., Sajal, V., Singh, K. P., Kumar, R., & Sharma, N. K. (2013). Strong terahertz radiation generation by beating of extra-ordinary mode lasers in a rippled density magnetized plasma. *Laser and Particle Beams*, **31,** 337-344.

106] Sharma, R. P., & Singh, R. K. (2014). Terahertz generation by two cross focused laser beams in collisional plasmas. *Physics of Plasmas*, **21**, 073101.

107] Singh, D., & Malik, H. K. (2014). Terahertz generation by mixing of two super-Gaussian laser beams in collisional plasma. *Physics of Plasmas*, 21, 083105.

108] Singh, D., & Malik, H. K. (2015). Enhancement of terahertz emission in magnetized collisional plasma. *Plasma Sources Science and Technology*, **24,** 045001.

109] Hussain, S., Singh, M., Singh, R. K., & Sharma, R. P. (2014). THz generation by self-focusing of hollow Gaussian laser beam in magnetised plasma. *EPL (Europhysics Letters)*, ***107***, 65002.

110] Hussain, S., Singh, R. K., & Sharma, R. P. (2016). Terahertz radiation generation by beating of two super Gaussian lasers in plasma having static dc electric field. *Physics of Plasmas*, **23**, 073120.

111] Sobhani, H., Dehghan, M., & Dadar, E. (2017). Effect of pump depletion and cross-focusing on twisted terahertz radiation generation. *Physics of Plasmas*, **24**, 023110.

112] Abedi-Varaki, M., & Jafari, S. (2018). Enhanced THz radiation from beating of two Cosh–Gaussian laser beams in a wiggler-assisted collisional magnetized plasma. *JOSA B*, **35,** 1165-1172.

113] Varshney, P., Upadhayay, A., Madhubabu, K., Sajal, V., & Chakera, J. A. (2018). Strong terahertz radiation generation by cosh-Gaussian laser beams in axially magnetized collisional plasma under non-relativistic ponderomotive regime. *Laser and Particle Beams*, 36, 236-245.

114] Safari, S., Niknam, A. R., Jahangiri, F., & Jazi, B. (2018). Terahertz radiation generation through the nonlinear interaction of Hermite and Laguerre Gaussian laser beams

with collisional plasma: field profile optimization. *Journal of Applied Physics*, **123**, 153101.

115] Hematizadeh, A., Jazayeri, M., & Ghafary, B. (2018). Generation of terahertz radiation via cosh-Gaussian and top-hat laser beams in a collisional magnetized plasma. *Contributions to Plasma Physics*, **58**, 904-916.

116] Arefnia, M., Sharifian, M., & Ghorbanalilu, M. (2021). Terahertz Radiation Generation by Beating of Two Chirped Laser Pulses In a Warm Collisional Magnetized Plasma. *Chinese Physics B*, **30**, 094101.

117] Wood, R. W. (1902). XLII. On a remarkable case of uneven distribution of light in a diffraction grating spectrum. *The London, Edinburgh, and Dublin Philosophical Magazine and Journal of Science*, **4**, 396-402.

118] Rayleigh, L. (1907). III. Note on the remarkable case of diffraction spectra described by Prof. Wood. *The London, Edinburgh, and Dublin Philosophical Magazine and Journal of Science*, **14**, 60-65.

119] Fano, U. (1941). The theory of anomalous diffraction gratings and of quasi-stationary waves on metallic surfaces (Sommerfeld's waves). *JOSA*, **31**, 213-222.

120] Stern, E. A., & Ferrell, R. A. (1960). Surface plasma oscillations of a degenerate electron gas. *Physical Review*, **120**, 130.

121] Ritchie, R. H. (1957). Plasma losses by fast electrons in thin films. *Physical review*, **106**, 874.

122] Otto, A. (1968). Excitation of nonradiative surface plasma waves in silver by the method of frustrated total reflection. *Zeitschrift für Physik A Hadrons and nuclei*, **216**, 398-410.

123] Kretschmann, E., & Raether, H. (1968). Radiative decay of non radiative surface plasmons excited by light. *Zeitschrift für Naturforschung A*, **23**, 2135-2136.

124] Raether, H. (1988). Surface plasmons on smooth surfaces. In *Surface plasmons on smooth and rough surfaces and on gratings*, 4-39. Springer, Berlin, Heidelberg.

125] Lee, H. J., & Cho, S. H. (1999). Parametric coupling of a light wave and surface plasma waves. *Physical Review E*, **59**, 3503.

126] Yasumoto, K. (1981). Electromagnetic decay into a surface plasma wave and an ion acoustic surface wave in a semi-infinite plasma. *Journal of Applied Physics*, **52,** 3238-3244.

127] Singh, D. B., & Tripathi, V. K. (2007). Laser beat wave excitation of surface plasma wave and material ablation. *Physics of Plasmas*, **14**, 103115.

128] Aliev, Y. M., & Brodin, G. (1990). Instability of a strongly inhomogeneous plasma. *Physical Review A*, ***42***, 2374.

129] Macchi, A., Cornolti, F., Pegoraro, F., Liseikina, T. V., Ruhl, H., & Vshivkov, V. A. (2001). Surface oscillations in overdense plasmas irradiated by ultrashort laser pulses. *Physical review letters*, **87**, 205004.

130] Parashar, J., Pandey, H. D., & Tripathi, V. K. (1998). Laser excitation of surface waves over a dense plasma. *Journal of plasma physics*, **59**, 97-102.

131] Raynaud, M., Héron, A., & Adam, J. C. (2020). Excitation of surface plasma waves and fast electron generation in relativistic laser–plasma interaction. *Scientific Reports*, **10**, 1-10.

132] Kaur, K. G., Kumar, P., Kant, N., & Rajput, J. (2020). Non linear surface plasma wave assisted electron acceleration in metal structure. In *Journal of Physics: Conference Series* **1531**, 012021.

133] Marini, S., Kleij, P. S., Amiranoff, F., Grech, M., Riconda, C., & Raynaud, M. (2021). Key parameters for surface plasma wave excitation in the ultra-high intensity regime. *Physics of Plasmas*, **28**, 073104.

134] Kaw, P., Schmidt, G., & Wilcox, T. (1973). Filamentation and trapping of electromagnetic radiation in plasmas. *The Physics of Fluids*, **16**, 1522-1525.

135] Salimullah, M., Hossain, M. A., Alam, M. N., & Salahuddin, M. (1987). Filamentation instability of an Alfvén wave in a compensated semiconductor. *Physical Review B*, **35**, 2303.

136] Stenflo, L., & Shukla, P. K. (1989). Filamentation instability of electromagnetic waves in compensated magnetoactive semiconductors. *Physical Review B*, **39**, 12941.

137] Young, P. E. (1991). Experimental study of filamentation in laser–plasma interactions. *Physics of Fluids B: Plasma Physics*, **3**, 2331-2336.

138] Shukla, P. K. (1992). The modulational and filamentational instabilities of two coupled electromagnetic waves in plasmas. *Physica Scripta*, **45**, 618.

139] Braun, A., Korn, G., Liu, X., Du, D., Squier, J., & Mourou, G. (1995). Self-channeling of high-peak-power femtosecond laser pulses in air. *Optics letters*, 20(1), 73-75.

140] Vidal, F., & Johnston, T. W. (1996). Electromagnetic beam breakup: Multiple filaments, single beam equilibria, and radiation. *Physical review letters*, **77**, 1282.

141] Johnston, T. W., Vidal, F., & Fréchette, D. (1997). Laser-plasma filamentation and the spatially periodic nonlinear Schrödinger equation approximation. *Physics of Plasmas*, **4**, 1582-1588.

142] Brodeur, A., Chien, C. Y., Ilkov, F. A., Chin, S. L., Kosareva, O. G., & Kandidov, V. P. (1997). Moving focus in the propagation of ultrashort laser pulses in air. *Optics Letters*, **22**, 304-306.

143] Bergé, L., Skupin, S., Lederer, F., Méjean, G., Yu, J., Kasparian, J., Salmon, E., Wolf, J.P., Rodriguez, M., Wöste, L. and Bourayou, R. (2004). Multiple filamentation of terawatt laser pulses in air. *Physical Review Letters*, ***92***, 225002.

144] Singh, M., Mahmoud, S. T., & Sharma, R. P. (2012). Generation of THz radiation from laser beam filamentation in a magnetized plasma. *Contributions to Plasma Physics*, **52**, 243-250.

145] Hassan, M. B., Abd-Ali, I. J., & Soary, A. O. (2019). The filamentation instability of nonparaxial laser beam inside magnetized plasma. *Results in Physics*, **14**, 102386.
146] Lee, D., & Mazumder, J. (2016). Effects of laser beam spatial distribution on laser-material interaction. *Journal of Laser Applications*, **28**, 032003.
147] Vhanmore, B. D., Patil, S. D., Valkunde, A. T., Urunkar, T. U., Gavade, K. M., Takale, M. V., & Gupta, D. N. (2018). Effect of q-parameter on relativistic self-focusing of q-Gaussian laser beam in plasma. *Optik*, 158, 574-579.

148] Patel, P.K., Key, M.H., Mackinnon, A.J., Berry, R., Borghesi, M., Chambers, D.M., Chen, H., Clarke, R., Damian, C., Eagleton, R. and Freeman, R. (2005). Integrated laser–target interaction experiments on the RAL petawatt laser. *Plasma physics and controlled fusion*, **47,** B833-B840.

149] Nakatsutsumi, M., Davies, J.R., Kodama, R., Green, J.S., Lancaster, K.L., Akli, K.U., Beg, F.N., Chen, S.N., Clark, D., Freeman, R.R. and Gregory, C.D. (2008). Space and time resolved measurements of the heating of solids to ten million kelvin by a petawatt laser. *New Journal of Physics*, **10**, 043046.

150] Kaur, M., Agarwal, P. C., Kaur, S., & Gill, T. S. (2018). Relativistic effects on propagation of q-Gaussian laser beam in a rippled density plasma: Application of higher order corrections. *Laser and Particle Beams*, ***36***, 246-253.

151] Sharma, A., & Kourakis, I. (2010). Spatial evolution of a q-Gaussian laser beam in relativistic plasma. *Laser and Particle Beams*, **28**, 479-489.
152] Mahajan, R., Gill, T. S., Kaur, R., & Aggarwal, M. (2018). Stability and dynamics of a cosh-Gaussian laser beam in relativistic thermal quantum plasma. *Laser and Particle Beams*, **36**, 341-352.
153] Hoffnagle, J. A., & Jefferson, C. M. (2000). Design and performance of a refractive optical system that converts a Gaussian to a flattop beam. *Applied optics*, **39**, 5488-5499.
154] Casperson, L. W., Hall, D. G., & Tovar, A. A. (1997). Sinusoidal-Gaussian beams in complex optical systems. *JOSA A*, **14**, 3341-3348.

155] Gill, T. S., Kaur, R., & Mahajan, R. (2011). Relativistic self-focusing and self-phase modulation of cosh-Gaussian laser beam in magnetoplasma. *Laser and Particle Beams*, **29**, 183-191.

156] Vij, S., Kant, N., & Thakur, V. (2019). Cross-focusing of a quadruple Gaussian laser beam in plasma in the relativistic regime. *Laser Physics*, **29**, 095404.

157] Sati, P., Sharma, A., & Tripathi, V. K. (2012). Self focusing of a quadruple Gaussian laser beam in a plasma. *Physics of Plasmas*, **19**, 092117.

158] Khalkhal, E., Tavirani, M.R., Zali, M.R., Akbari, Z. (2019). The evaluation of laser application in surgery: a review article. *J. Lasers Med. Sci*. **10**, S104–S111

159] Deutsch, C., Furukawa, H., Mima, K., Murakami, M., Nishihara, K. (1996). Interaction physics of the fast ignitor concept. *Phys. Rev. Lett*. **77**, 2483–2486

160] Roso, N.A., Moreira, R.C., Oliveira, J.B. (2014). High power laser weapons and operational implications. *J. Aerosp. Technol. Manag*. **6**, 231–236.

161] Kurniawan, K.H., Tjia, M., Kagawa, K. (2014). Review of laser-induced plasma, its mechanism, and application to quantitative analysis of hydrogen and deuterium. *Appl. Spectrosc. Rev*. **49**, 323–434.

162] Leduc, M., Dugue, J., Simone, J. (2018). Laser cooling, trapping, and Bose–Einstein condensation of atoms and molecules. *Phys. Today*.**71**, 37–42.

163] Spiers, B.T., Hill, M.P., Brown, C., Ceurvorst, L., Ratan, N., Savin, A.F., Allan, P., Floyd, E., Fyrth, J., Hobbs, L., James, S., Luis, J., Ramsay, M., Sircombe, N., Skidmore, J., Aboushelbaya, R., Mayr, M.W., Paddock, R., Wang, R.H.W., Norreys, P.A.(2021) Whole-beam self-focusing in fusion-relevant plasma. *Philos. Trans. R. Soc. A.* **379**, 20200159.

164] Konar, S., Sengupta, A. (1994). Propagation of an elliptic Gaussian laser beam in a medium with saturable nonlinearity. *J. Opt. Soc. Am. B*. **11**, 1644–1646.

165] Singh, T., Kaul, S.S. (1999). Self-focusing and self-phase modulation of elliptic Gaussian laser beam in a graded Kerr-medium. *Indian J. Pure Appl. Phys*. **37**, 794–797

166] Taniuti, T., & Washimi, H. (1968). Self-trapping and instability of hydromagnetic waves along the magnetic field in a cold plasma. *Physical review letters*, **21**, 209.

167] Ablowitz, M. J., & Segur, H. (1979). On the evolution of packets of water waves. *Journal of Fluid Mechanics*, **92,** 691-715.

168] Hariharan, P., Robinson, P.A. (1996). The gouy phase shift as a geometrical quantum effect. *J. Mod. Opt*. **43**, 219– 221.

169] Feng, S., Winful, H.G. (2001).Physical origin of the Gouy phase shift. *Opt. Lett*. **26**, 485–487.

170] Boyd, R. W. (1980). Intuitive explanation of the phase anomaly of focused light beams. *JOSA*, **70,** 877-880.

171] Yang, J., & Winful, H. G. (2006). Generalized eikonal treatment of the Gouy phase shift. *Optics letters*, **31**, 104-106.

172] Gupta, D. N., Hur, M. S., & Suk, H. (2007). Additional focusing of a high-intensity laser beam in a plasma with a density ramp and a magnetic field. *Applied Physics Letters*, **91**, 081505.

173] Gustafson, T. K., Taran, J. P., Haus, H. A., Lifsitz, J. R., & Kelley, P. L. (1969). Self-modulation, self-steepening, and spectral development of light in small-scale trapped filaments. *Physical Review*, **177,** 306.

174] Habibi, M., & Ghamari, F. (2012). Stationary self-focusing of intense laser beam in cold quantum plasma using ramp density profile. *Physics of Plasmas*, **19**, 103110.

175] Davies, A. G., Burnett, A. D., Fan, W., Linfield, E. H., & Cunningham, J. E. (2008). Terahertz spectroscopy of explosives and drugs. *Materials today*, **11**, 18-26.

176] Kawase, K. (2004). Terahertz imaging for drug detection and large-scale integrated circuit inspection. *Optics and photonics news*, **15**, 34-39.

177] Dey, I., Jana, K., Fedorov, V.Y., Koulouklidis, A.D., Mondal, A., Shaikh, M., Sarkar, D., Lad, A.D., Tzortzakis, S., Couairon, A. and Kumar, G.R.(2017). Highly efficient broadband terahertz generation from ultrashort laser filamentation in liquids. *Nature communications*, **8**, 1-7.

178] Shan, J., & Heinz, T. F. (2004). Terahertz radiation from semiconductors. *Ultrafast Dynamical Processes in Semiconductors, Topics Appl. Phys*. **92,** 1-56.

179] Sodha, M. S., Sharma, J. K., Tewari, D. P., Sharma, R. P., & Kaushik, S. C. (1978). Plasma wave and second harmonic generation. *Plasma Physics*, **20,** 825.

[180] Parashar, J., & Sharma, A. K. (1998). Second-harmonic generation by an obliquely incident laser on a vacuum-plasma interface. *EPL (Europhysics Letters)*, **41**, 389.

181] Gupta, D. N., & Suk, H. (2007). Enhanced focusing of laser beams in semiconductor plasmas. *Journal of applied physics*, **101,** 043109.

182] Dubey, P. K., & Paranjape, V. V. (1973). Self-Action of Laser Beams in Semiconductors. *Physical Review B*, ***8***, 1514.

183] Antonov, V. M., Mamilayev, R. M., Nalimov, I. P., & Shakirov, A. H. (1981). 3-D holographic pictures of human lungs. *Optics Communications*, **38**, 81-84.

184] Song, Q., Zhao, Y., Redo-Sanchez, A., Zhang, C., & Liu, X. (2009). Fast continuous terahertz wave imaging system for security. *Optics Communications*, **282**, 2019-2022.

185] DeSilva, A. W. (2000). The evolution of light scattering as a plasma diagnostic. *Contributions to Plasma Physics*, **40**, 23-35.

186] McNeil, B. W., & Thompson, N. R. (2010). X-ray free-electron lasers. *Nature photonics*, **4,** 814-821.

187] Bohon, J., D'Mello, R., Ralston, C., Gupta, S., & Chance, M. R. (2014). Synchrotron X-ray footprinting on tour. *Journal of synchrotron radiation*, **21**, 24-31.

188] Vampa, G., & Brabec, T. (2017). Merge of high harmonic generation from gases and solids and its implications for attosecond science. *Journal of Physics B: Atomic, Molecular and Optical Physics*, **50**, 083001.

189] Orlando, G., Wang, C. M., Ho, T. S., & Chu, S. I. (2018). High-order harmonic generation in disordered semiconductors. *JOSA B*, ***35***, 680-688.

190] Bobin, J. L. (1985). High intensity laser plasma interaction. *Physics Reports*, *122*, 173-274.

191] Erokhin, N. S., Zakharov, V. E., & Moiseev, S. S. (1969). Second harmonic generation by an electromagnetic wave incident on inhomogeneous plasma. *Sov. Phys. JETP*, **29**, 101.

192] Brunel, F. (1990). Harmonic generation due to plasma effects in a gas undergoing multiphoton ionization in the high-intensity limit. *JOSA B*, **7,** 521-526.

193] Wilks, S. C., Dawson, J. M., Mori, W. B., Katsouleas, T., & Jones, M. E. (1989). Photon accelerator. *Physical review letters*, **62**, 2600.

194] Stamper, J. A., Lehmberg, R. H., Schmitt, A., Herbst, M. J., Young, F. C., Gardner, J. H., & Obenschain, S. P. (1985). Evidence in the second-harmonic emission for self-focusing of a laser pulse in a plasma. *The Physics of fluids*, **28**, 2563-2569.

195] Konar, S., Jana, S., & Mishra, M. (2005). Induced focusing and all optical switching in cubic quintic nonlinear media. *Optics communications*, **255**, 114-129.

196] Kumar, A. (2013). Ponderomotive self-focusing of surface plasma wave. *Plasmonics*, **8**, 1135-1139.

List of Publications and Conferences/School Attended

Published Papers

1. Gupta, N., & Kumar, S. (2021). Generation of second harmonics of q-Gaussian laser beams in collisionless plasma with axial density ramp. *Nonlinear Optics, Quantum Optics: Concepts in Modern Optics*, *54*.
2. Gupta, N., & Kumar, S. (2021). Nonlinear interaction of elliptical q-Gaussian laser beams with plasmas with axial density ramp: effect of ponderomotive force. *Optical and Quantum Electronics*, *53*(5), 1-20.
3. Gupta, N., & Kumar, S. (2021). Generation of second harmonics of relativistically self-focused q-Gaussian laser beams in underdense plasma with axial density ramp. *Optical and Quantum Electronics*, *53*(4), 1-15.
4. Gupta, N., & Kumar, S. (2021). Self-action effects of quadruple-Gaussian laser beams in collisional plasmas and their resemblance to Kepler's central force problem. *Pramana*, *95*(2), 1-14.
5. Gupta, N., & Kumar, S. (2021). All optical switching by two co-propagating q-Gaussian laser beams in nonlinear optical media. *Nonlinear Optics, Quantum Optics: Concepts in Modern Optics*, *54*.
6. Gupta, N., Kumar, S., Bhardwaj, S. B., Kumar, S., & Choudhry, S. (2021). Nonlinear interaction of quadruple Gaussian laser beams with narrow band gap semiconductors. *Journal of Optics*, 1-14.
7. Gupta, N., Kumar, S., Gnaneshwaran, A., Kumar, S., & Choudhry, S. (2021). Self-focusing of cosh-Gaussian laser beam in collisional plasma: effect of nonlinear absorption. *Journal of Optics*, 1-11.
8. Gupta, N., Choudhry, S., Bhardwaj, S. B., Kumar, S., & Kumar, S. (2021). Relativistic effects on stimulated brillouin scattering of self-focused q-Gaussian laser beams in plasmas with axial density ramp. *Journal of Russian Laser Research*, *42*(4), 418-429.

9. Gupta, N., & Kumar, S. (2020). Linear and nonlinear propagation characteristics of multi-Gaussian laser beams. *Chinese Physics B*, *29*(11), 114210.
10. Gupta, N., & Kumar, S. (2020). Generation of second harmonics of self-focused quadruple-Gaussian laser beams in collisional plasmas with density ramp. *Journal of Optics*, *49*(4), 455-468.
11. Gupta, N., & Kumar, S. (2020). Generation of second harmonics of q-Gaussian laser beams in collisional plasma with upward density ramp. *Laser Physics*, *30*(6), 066003.
12. Gupta, N., & Kumar, S. (2020). Self-focusing of multi-Gaussian laser beams in nonlinear optical media as a Kepler's central force problem. *Optical and Quantum Electronics*, *52*(3), 1-17.

Accepted Papers

1. Naveen Gupta, Rohit Johari, Shivani Sharma, Senthil Kumaran, Sandeep Kumar, Phase space dynamics of self-focusing of dark hollow Gaussian laser beam, (Accepted: *Nonlinear Optics, Quantum Optics*)
2. Naveen Gupta, Sandeep Kumar, Gnaneshwaran A, Rohit Johari, Senthil Kumaran, Alex Aand Sagar Channabasappa Angadi, Free electron laser and its applications: a review, (Accepted: *Nonlinear Optics, Quantum Optics*)
3. Sandeep Kumar, Naveen Gupta, Self-focusing and self trapping of cosh-Gaussian laser beam in thermal quantum plasmas, (Accepted: *Nonlinear Optics, Quantum Optics)*
4. Naveen Gupta, Sanjeev Kumar, Suman Choudhry, S.B. Bhardwaj and Sandeep Kumar, Potential well dynamics of self focusing of quadruple Gaussian laser beams in thermal quantum plasma, **(**Accepted: *Nonlinear Optics, Quantum Optics)*
5. Naveen Gupta, Suman Choudhry, Sanjeev Kumar, S. B. Bhardwaj, Sandeep Kumar, Gnaneshwaran A., Siddhanth Shishodia and Kishore B, Scattering of laser light in dielectrics and plasmas: a review, (Accepted: *Nonlinear Optics, Quantum Optics*)

6. Naveen Gupta, Rohit Johari and Sandeep Kumar, Excitation of Electron Plasma Wave by Beating Two Copropagating q-Gaussian Laser Beams in Thermal Quantum Plasma: Relativistic Effects, (Accepted: *Nonlinear Optics, Quantum Optics*)

Conferences/ School Attended

1. 17th International conference on optics, laser & photonics, Tokyo, Japan (Virtual) from 26-27 June.2021. Keynote Presentation: Nonlinear dynamics of non-Gaussian laser beam semiconductor plasma. **(Got Best Young Scientist Award)**
2. "47th IEEE International conference on plasma sciences (Virtual)" organized at Singapore, from 6-10 Dec,2020. Oral talk title: Self action effects of multi Gaussian laser beams in thermal quantum plasma.
3. 15th Kudowa School towars "Fusion Energy" (Virtual Edition) organized by IPPLM, Poland, from 30th June-2nd July,2020. Oral talk title: Enhancement of self-focusing of q-gaussian laser beam by ramped density plasma. **(Got Excellent Talk Award)**
4. Webinar on "GHz to THz Antennas: Trends Techniques and next generation Requirements in Wireless communication" organized by Manipal University, Jaipur on 10 June, 2020.
5. SERB School on "Nonlinear Dynamics" at IIT Patna (Bihar) from Dec3-Dec30, 2019.
6. 12th International conference on "Plasma Science and Applications- 2019" at Lucknow university (AIP Proceeding). Poster Title: Self-Focusing and Self Phase Modulation of q- Gaussian Laser Beam in Collisionless Plasma with Exponential Density Ramp
7. National Conference on "Students Conference on Optics and Photonics" at Physical Research Laboratory, Ahmedabad (Gujarat). Poster Title: Self Focusing of q-Gaussian Laser Beams in Collisional Plasma with Ramped Density
8. National conference on "Innovations in Applied Sciences and Engineering" at NIT Jalandhar. Poster Title: Third Harmonic Generation of q-Gaussian Laser Beams in Cubic-Quintic Nonlinear Media"

9. National Conference on “Nonlinear Optics” at GNDU Amritsar. Poster Title: Self-Focusing of Multi-Gaussian laser beam in narrow band semiconductor. **(Got Best Poster Award)**
10. SERB School on “Ultrahigh intensity laser produced plasma: Physics and Applications” at RRCAT, Indore (MP)